

Development of a diagnostic microarray for the rapid  
detection of Extended Spectrum Beta-Lactamases  
for the use in clinical microbiology

Entwicklung eines diagnostischen Mikroarrays zum  
Nachweis von Beta-Laktamasen mit erweitertem  
Wirkungsspektrum für den Einsatz in der klinischen  
Mikrobiologie

Von der Fakultät Geo- und Biowissenschaften der Universität Stuttgart  
genehmigte Abhandlung  
zur Erlangung der Würde eines  
Doktors der Naturwissenschaften (Dr. rer. nat.)

Vorgelegt von

**Verena Ulrike Grimm**

aus Herten in Westfalen

Hauptberichter: Prof. Dr. R. D. Schmid

Mitberichter: Prof. Dr. P. Scheurich

Tag der mündlichen Prüfung: 06.12.2005

Institut für Technische Biochemie der Universität Stuttgart  
2005



---

<b>ZUSAMMENFASSUNG .....</b>	<b>3</b>
BETA-LAKTAMASEN MIT ERWEITERTEM WIRKUNGSSPEKTRUM (ESBLs) .....	3
<i>Phänotypischer Nachweis von ESBLs</i> .....	3
<i>Genotypischer Nachweis von ESBLs</i> .....	4
NACHWEIS VON ESBLs PER DNS-MIKROARRAYANALYSE .....	4
<i>Entwicklung des Systems</i> .....	4
<i>Entwicklung einer neuen Methode des Sondendesigns</i> .....	5
<i>Validierung mit Referenzstämmen und klinischen Isolaten</i> .....	5
<i>Nachweis gemischter Resistenzmerkmale</i> .....	5
<i>Optimierung der Hybridisierung</i> .....	6
<i>Einfluss von Eigenschaften der Ziel-DNS</i> .....	6
WEITERFÜHRENDE ENTWICKLUNGEN .....	7
<i>Kombination des Resistenznachweises mit einer Kultur-unabhängigen Isolation</i> .....	7
<i>Ausweitung des Nachweisspektrums</i> .....	7
<i>Entwicklung eines marktreifen Systems</i> .....	8
FAZIT .....	8
<b>ABSTRACT .....</b>	<b>9</b>
<b>1 INTRODUCTION .....</b>	<b>10</b>
1.1 ANTIBIOTIC RESISTANCE .....	10
1.1.1 <i>Beta-lactam resistance</i> .....	11
1.1.2 <i>Extended Spectrum Beta-Lactamases (ESBLs)</i> .....	14
1.1.3 <i>Prevalence of ESBLs</i> .....	15
1.1.4 <i>Phenotypic ESBL detection</i> .....	16
1.1.5 <i>Genotypic ESBL detection</i> .....	18
1.2 GENOTYPING OF SINGLE NUCLEOTIDE POLYMORPHISMS .....	19
1.2.1 <i>SNP discrimination methods</i> .....	19
1.2.2 <i>SNP detection methods</i> .....	20
1.3 DNA MICROARRAYS .....	21
1.3.1 <i>Development</i> .....	21
1.3.2 <i>Principle</i> .....	21
1.3.3 <i>Array based genotyping methods</i> .....	24
1.3.4 <i>Microarray preparation</i> .....	25
1.3.5 <i>Transfer to a marketable array format</i> .....	29
1.3.6 <i>Link of the resistance to the pathogenic bacteria</i> .....	31
1.4 OBJECTIVES .....	32
<b>2 MATERIAL AND METHODS .....</b>	<b>33</b>
2.1 MATERIAL .....	33
2.1.1 <i>Biological reagents</i> .....	33
2.1.2 <i>Chemical reagents</i> .....	33
2.1.3 <i>Equipment</i> .....	33
2.1.4 <i>Consumables</i> .....	34
2.1.5 <i>Clinical isolates</i> .....	34
2.1.6 <i>Software</i> .....	36
2.2 SOLUTIONS .....	36
2.3 METHODS .....	37
2.3.1 <i>Identification of SNP positions</i> .....	37
2.3.2 <i>Probe design</i> .....	37
2.3.3 <i>Oligonucleotide array fabrication on poly-L-lysine-sides</i> .....	38
2.3.4 <i>Oligonucleotide array fabrication on epoxy slides</i> .....	38
2.3.5 <i>Controls</i> .....	40
2.3.6 <i>Bacterial strains</i> .....	41
2.3.7 <i>Preparation of target DNA</i> .....	41
2.3.8 <i>Hybridization</i> .....	42
2.3.9 <i>Data acquisition and processing</i> .....	44
2.3.10 <i>DNA sequencing</i> .....	45

---

<b>3</b>	<b>RESULTS</b> .....	<b>46</b>
3.1	RESULTS TEM-ARRAY .....	46
3.1.1	<i>Probe design</i> .....	46
3.1.2	<i>Setting up the system on poly-L-lysine slides</i> .....	51
3.1.3	<i>Setting up the system on epoxy slides</i> .....	53
3.1.4	<i>Proof of concept</i> .....	54
3.1.5	<i>Probe performance analysis</i> .....	56
3.1.6	<i>Reproducibility of the perfect match/mismatch discrimination</i> .....	57
3.1.7	<i>Testing of clinical isolates and reference strains</i> .....	59
3.1.8	<i>Influence of target DNA properties</i> .....	64
3.1.9	<i>Reduction of assay time and test of hybridization devices</i> .....	71
3.1.10	<i>Mixed resistances</i> .....	85
3.1.11	<i>Validation of the TEM-array with clinical samples from the NRCA</i> .....	87
3.2	RESULTS SHV-ARRAY .....	90
3.2.1	<i>Probe design I</i> .....	90
3.2.2	<i>Probe performance analysis I</i> .....	93
3.2.3	<i>Probe design II</i> .....	96
3.2.4	<i>Probe performance analysis II</i> .....	100
3.2.5	<i>Proof of concept</i> .....	105
3.2.6	<i>Identification of SHV variants</i> .....	108
3.3	VALIDATION OF THE SHV- AND TEM-ARRAY WITH CLINICAL ISOLATES COLLECTED IN CROATIA .....	112
3.3.1	<i>TEM-array</i> .....	112
3.3.2	<i>SHV-array</i> .....	113
3.4	ONGOING DEVELOPMENTS .....	122
3.4.1	<i>Transfer of the TEM-array to a marketable array format</i> .....	122
3.4.2	<i>Link of the resistance to the pathogenic bacteria</i> .....	124
<b>4</b>	<b>DISCUSSION</b> .....	<b>125</b>
4.1	PHENOTYPIC RESISTANCE TESTS .....	125
4.2	GENOTYPIC RESISTANCE TESTS .....	127
4.3	METHODS FOR MOLECULAR ESBL DETECTION .....	127
4.4	DNA MICROARRAYS FOR MOLECULAR RESISTANCE DETECTION .....	129
4.5	IMPLEMENTATION OF THE SYSTEM .....	130
4.6	PROBE DESIGN AND PERFORMANCE .....	131
4.6.1	<i>Sequence analysis</i> .....	131
4.6.2	<i>Performance analysis</i> .....	132
4.6.3	<i>New probe design strategy</i> .....	134
4.7	ARRAY PERFORMANCE .....	135
4.7.1	<i>Discrimination efficiency</i> .....	135
4.7.2	<i>Reproducibility</i> .....	136
4.7.3	<i>Sensitivity</i> .....	137
4.8	PARAMETERS INFLUENCING THE HYBRIDIZATION .....	139
4.8.1	<i>Fragmentation</i> .....	139
4.8.2	<i>Assay time and hybridization devices</i> .....	140
4.9	DETECTION OF MIXED RESISTANCES .....	141
4.10	TEST OF CLINICAL ISOLATES .....	142
4.11	ONGOING DEVELOPMENTS .....	143
4.11.1	<i>Transfer to a marketable format</i> .....	143
4.11.2	<i>Link of the resistance to the pathogenic bacteria</i> .....	143
4.11.3	<i>Extension of the detection spectrum of the ESBL chip</i> .....	144
4.12	CONCLUSION .....	145
<b>5</b>	<b>REFERENCES</b> .....	<b>146</b>
<b>6</b>	<b>APPENDIX</b> .....	<b>162</b>
6.1	LIST OF ABBREVIATIONS .....	162
6.2	ACKNOWLEDGEMENTS .....	164
6.3	CURRICULUM VITAE .....	166
6.4	DECLARATION .....	167



## Zusammenfassung

### ***Beta-Laktamasen mit erweitertem Wirkungsspektrum (ESBLs)***

Das Auftreten von Resistenzen gegen Beta-Laktam Antibiotika ist ein Problem von zunehmender Bedeutung weltweit. Das Vorkommen von Beta-Laktamasen mit erweitertem Wirkungsspektrum (*Extended Spectrum Beta-Lactamases*, ESBL) ist hierbei besonders problematisch. Die am häufigsten vertretenen Enzyme dieser Art in klinischen Isolaten sind Varianten von TEM-1 oder SHV-1 Beta-Laktamasen. Diese zahlreichen Varianten unterscheiden sich von den Urtypen durch Aminosäureaustauschmutationen, die zu einer Erweiterung des Substratspektrums führen und auch Resistenzen gegen neuere Generationen der Beta-Laktam Antibiotika (Cephalosporine der 3. und 4. Gruppe) vermitteln. Sie werden durch so genannte Beta-Laktamase Inhibitoren (z. B. Clavulansäure oder Tazobactam) gehemmt. Es treten aber auch Varianten der TEM- oder SHV-Familie auf, die Resistenzen gegen eben diese Inhibitoren vermitteln, jedoch nicht gegen Cephalosporine der neueren Generation. Diese Enzyme gehören daher nicht zur Gruppe der ESBLs und werden als IRTs (ursprünglich für *Inhibitor Resistant TEM*) bezeichnet. Sequenzen von über 120 TEM- und 50 SHV-Varianten sind bisher veröffentlicht. ESBLs und IRTs sind plasmidkodiert und treten in vielen verschiedenen Spezies der Gattung Enterobacteriaceae, hauptsächlich in *Klebsiella pneumoniae* und *Escherichia coli*, aber auch in *Pseudomonas aeruginosa*, *Haemophilus influenzae*, und *Neisseria gonorrhoe* auf (16). In den letzten Jahren hat die Häufigkeit von Enterobacteriaceae mit Resistenz gegen Cephalosporine der 3. Gruppe deutlich zugenommen (181). Laut einer von 1997-1999 durchgeführten Studie treten resistente Stämme inner- und außerhalb des Krankenhauses mit einem für ESBL charakteristischen Phänotyp bei *K. pneumoniae* zu 45 % in Lateinamerika, zu 25 % in der Region des westlichen Pazifik, zu 23 % in Europa und zu 8 % in den USA auf (180).

### ***Phänotypischer Nachweis von ESBLs***

ESBL produzierende Organismen stellen ein besonderes Problem im klinischen Alltag dar, da sie mit herkömmlichen phänotypischen Screening-Methoden schwierig nachzuweisen sind. Die bisher aufgetretenen Enzymvarianten unterscheiden sich durch eine Vielfalt von Mutationspositionen, die zu stark unterschiedlichen Substratspektren führen. Die Auswahl des zu testenden Antibiotikums ist daher kritisch, z.B. kann ein Enzym Ceftazidim gut hydrolysieren mit einer Minimalen Hemmkonzentration (MHK) von bis zu 256 µg/ml, während es Cefotaxim nur unzureichend umsetzt, mit einer MHK von nur 4 µg/ml (95). Um einen zuverlässigen Nachweis aller ESBLs zu gewährleisten, muss die Empfindlichkeit der Isolate daher gegen eine Auswahl verschiedener Antibiotika getestet werden. Eine nicht nachgewiesene Resistenz kann zum Therapiemisserfolg führen und außerdem zu einer Verbreitung der Resistenz beitragen. Ein weiterer Grund für die Unzuverlässigkeit der bisherigen Methoden zum Nachweis von ESBLs ist die Abhängigkeit der Minimalen Hemmkonzentration von der eingesetzten Startmenge der Bakterien im Test, dem so genannten Inokulum-Effekt (108,132,168). Eine unzureichende Menge eingesetzter Bakterien kann somit zu falsch-negativen Ergebnissen führen. Hinweis darauf, dass dieser Inokulum-Effekt auch bei klinischen Infektionen auftritt, geben Berichte über Therapiemisserfolge und suboptimale klinische Ergebnisse, sowie eine erhöhte Sterblichkeitsrate von Patienten bei der

## **Zusammenfassung**

---

Behandlung von ESBL-Infektionen mit Cephalosporinen, obwohl die festgestellten MHK-Werte im empfindlichen Bereich lagen (89,124,142,149).

Um die Zuverlässigkeit der Ergebnisse des ESBL Screenings zu erhöhen, ist die Durchführung von zusätzlichen phänotypischen Tests zur Bestätigung des ESBL-Verdachts unerlässlich (115). Da die üblichen phänotypischen Testverfahren auf dem Nachweis der Hemmung des Wachstums von Bakterien in Anwesenheit verschiedener Antibiotikakonzentrationen beruhen, sind diese Verfahren sehr zeitaufwendig (98). Es kann bis zu drei Tagen dauern, bis der Verdacht auf Infektion mit einem ESBL-produzierenden Organismus bestätigt werden kann. Da eine effiziente Antibiotikatherapie jedoch so früh wie möglich einsetzen muss, wird die bisherige Resistenzdiagnostik eher retrospektiv denn prediktiv eingesetzt. Um Therapiemisserfolge zu vermeiden, werden daher mehr Breitbandantibiotika als notwendig verschrieben. Dies fördert die Verbreitung neuer Resistenzen. Infektionen mit ESBL produzierenden *E. coli* und *K. pneumoniae* werden mit längeren Krankenhausaufenthalten und höheren Behandlungskosten in Verbindung gebracht (85). Daher ist die Entwicklung präziserer und schnellerer Testmethoden zum Nachweis von ESBLs notwendig.

### ***Genotypischer Nachweis von ESBLs***

Die Mikroarray Technologie erlaubt die genotypische Identifizierung von Resistenzen innerhalb einer Analysezeit von weniger als einem Tag. Hierbei können, im Gegensatz zur phänotypischen Diagnostik und auch zu vielen anderen genotypischen Nachweisverfahren, alle relevanten Mutationspositionen erkannt und somit auch verschiedene ESBL-Typen differenziert nachgewiesen werden. Für viele ESBL-Varianten wurde bereits ein spezifisches Substratspektrum definiert (21,130), welches nach der eindeutigen Identifizierung auf der molekularen Ebene zu Rate gezogen werden kann, um eine spezialisierte, prediktive Diagnostik zu ermöglichen. Weiterhin kann die genotypische Identifizierung, im Gegensatz zum phänotypischen Nachweis, für eine zuverlässige Überwachung der Verbreitung bestimmter Resistenzmerkmale oder multiresistenter Bakterien im klinischen Umfeld eingesetzt werden.

### ***Nachweis von ESBLs per DNS-Mikroarrayanalyse***

In dieser Arbeit wurde ein diagnostischer Mikroarray entwickelt für den schnellen und spezifischen Nachweis der Mutationen der meisten zurzeit bekannten TEM und SHV Beta-Laktamase Varianten, die verantwortlich für die Ausprägung eines ESBL oder IRT Phänotyps sind. Die Allel-spezifische Hybridisierung auf dem DNS-Mikroarray erlaubt nun den Nachweis und die Identifizierung von 41 Mutationspositionen der TEM Beta-Laktamase Familie (entspricht 99 % der veröffentlichten Positionen) und 37 Mutationspositionen (entspricht 100 % der veröffentlichten Positionen) relevant für SHV. Dies ermöglicht die Identifizierung von 96 % der bis jetzt bekannten TEM Varianten und 100 % der SHV Varianten. Konsensus-Primer, die homolog zu den veröffentlichten Sequenzen der Varianten sind, wurden entwickelt und erlaubten die Vervielfältigung der Resistenzgene per PCR.

### ***Entwicklung des Systems***

Anfänglich wurde der Array auf einer Poly-L-Lysin Oberfläche hergestellt, welche jedoch unzureichende Ergebnisse lieferte in Bezug auf Sensitivität und

Reproduzierbarkeit der Analyse. Durch Einsatz einer Epoxid-Oberfläche zur Immobilisierung der Sonden und eines phosphatsalzhaltigen Druckpuffers, sowie durch Optimierung des Druckprozesses konnte die anfänglich festgestellte hohe Varianz zwischen Signalintensitäten von Replika von 68 % im Mittel (für vier Replika innerhalb eines Arrays auf Poly-L-Lysin) auf durchschnittlich 18 % (für 9 Replika innerhalb von drei Arrays auf Epoxid) reduziert werden. Diese Varianz liegt innerhalb der technischen Grenzen für durch Kontaktdruckverfahren hergestellte Mikroarrays (157,185). Weiterhin konnten die erhaltenen Fluoreszenzsignalintensitäten um mindestens den Faktor 3 gesteigert werden und somit die Sensitivität des Systems durch den Einsatz der neuen Oberfläche erhöht werden. Dies kann entweder auf eine bessere Immobilisierungseffizienz (55) oder auf bessere Zugänglichkeit der Sonden auf der Epoxid-Oberfläche zurückgeführt werden.

### *Entwicklung einer neuen Methode des Sondendesigns*

Für fünf SHV-Polymorphismen konnten keine üblichen Sondensets zur Allel-spezifischen Hybridisierung entwickelt werden, da die zur getesteten Ziel-DNS komplementären Sonden starke Sekundärstrukturen aufwiesen. Dies kann zu Unzugänglichkeit der Sonden für die Hybridisierung der Ziel-DNS führen (111,112). Für diese Positionen wurden neue Sonden entwickelt, bei denen die vorhandene Sekundärstruktur durch Einfügen einer ungepaarten Base geschwächt, bzw. aufgehoben wurde. Für vier der fünf Positionen konnte auf diese Art ein spezifischer Nachweis der korrekten Mutationspositionen ermöglicht werden.

### *Validierung mit Referenzstämmen und klinischen Isolaten*

Die Sensitivität, Reproduzierbarkeit und die Spezifität der Identifizierung der unterschiedlichen Varianten per Mikroarrayanalyse wurde anhand von Referenzstämmen (für TEM: *bla*<sub>TEM-3,-7,-8,-116</sub>; für SHV: *bla*<sub>SHV-1,-2,-3,-4,-5,-7,-8</sub>) nachgewiesen. Hierbei wurden alle untersuchten Mutationspositionen eindeutig und reproduzierbar identifiziert. Weiterhin wurde der TEM-Array validiert durch die Mikroarrayanalyse von 72 klinischen Isolaten, die aus unterschiedlichen Institutionen in Deutschland, Kroatien und Russland stammten. Zur Validierung des SHV-Arrays wurden 30 klinische Isolate aus Kroatien getestet. Siebzig TEM-Varianten und 29 SHV-Varianten konnten bei diesen Tests eindeutig identifiziert werden. Drei Proben wurden aufgrund von Fehlern bei der Vorbereitung der Ziel-DNS von der Analyse ausgeschlossen. Die Ergebnisse der Mikroarray-Analyse wurden durch Resultate einer Standard-DNS-Sequenzierung bestätigt.

### *Nachweis gemischter Resistenzmerkmale*

Das Vorkommen unterschiedlicher Beta-Laktamase Varianten derselben Familie innerhalb eines einzigen Stammes wurde sowohl im Fall von TEM (17), als auch von SHV (43) Beta-Laktamasen schon nachgewiesen. Die nicht-ESBL Varianten TEM-1 (95) und SHV-1 (8) sind weit verbreitete Enzyme und es kann nicht ausgeschlossen werden, dass eine nicht-ESBL Variante und eine ESBL Variante koexistieren (64). Ein genotypischer Test muss daher in der Lage sein zwei Varianten simultan zu identifizieren. Die Möglichkeit zwei Varianten (*bla*<sub>TEM-116</sub> und *bla*<sub>TEM-8</sub>) der gleichen Laktamase-Familie nachzuweisen, wurde für TEM in einem Modell-System bis zu einem Verhältnis von 1 zu 10 gezeigt. Für SHV wurde das gleichzeitige Vorkommen unterschiedlicher Varianten (*bla*<sub>SHV-1</sub> in Kombination mit *bla*<sub>SHV-5</sub> oder *bla*<sub>SHV-12</sub>) in den getesteten klinischen Isolaten nachgewiesen. Die genotypische Identifizierung mittels DNS-Mikroarrays einer ESBL Variante in Gegenwart einer nicht-ESBL Variante

wurde somit sowohl im Modellsystem, als auch in realen klinischen Proben nachgewiesen.

### *Optimierung der Hybridisierung*

Für den klinischen Einsatz eines Testverfahrens spielt der Zeitaspekt eine große Rolle. Die entscheidenden Zeit verbrauchenden Schritte der DNS-Mikroarrayanalyse nach der DNS-Isolation sind hierbei die Vervielfältigung der Ziel-DNS mit zwei Stunden, der Hybridisierungsschritt mit anfangs drei Stunden, sowie die Waschschrte mit insgesamt 30 Minuten. Die Vervielfältigung der Ziel-DNS erfolgte bisher nach der Isolation des Krankheitserregers durch eine Vorkultur, was im Zuge weiterer Entwicklungen jedoch durch ein zeitsparendes Kultur-unabhängiges Anreicherungsverfahren ersetzt werden soll. Die Optimierung des Vervielfältigungsschrittes sollte daher in Adaption an das Anreicherungsverfahren erfolgen. Da die Kombination beider Schritte sich jedoch noch in der Entwicklungsphase befindet, wurde das Augenmerk in dieser Arbeit zunächst auf eine Optimierung des Hybridisierungsverfahrens, sowie der Waschschrte gerichtet. Hierfür wurden umfangreiche Testreihen mit vier verschiedenen Geräten (ArrayBooster, Lucidea Slide Pro, Tecan HS400, Thermomixer mit Hybridisierungsaufsatz) durchgeführt, die durch Agitation der Hybridisierungslösung eine Verbesserung der Hybridisierungskinetik (151) und Homogenität der Signalverteilung versprochen, wobei die Geräte neben verschiedenen Verfahren zur Agitation auch unterschiedliche Automatisierungsgrade der einzelnen Schritte boten. Die Beurteilungskriterien umfassten die Steigerung der Fluoreszenzsignalintensitäten, die Spezifität der Identifizierung der Mutationen, die Reproduzierbarkeit der Daten, sowie niedrige und einheitliche Hintergrundsignalintensitäten. Die Sensitivität und die Reproduzierbarkeit konnten durch Automatisierung der Hybridisierung und des Waschvorgangs gesteigert werden. Die überzeugendsten Verbesserungen der Qualität und Reproduzierbarkeit der Hybridisierungsergebnisse, sowie den höchsten Grad an Automatisierung lieferte hierbei die Tecan HS400, mit der eine Reduktion der Hybridisierungszeit von anfänglich drei Stunden auf bis zu 15 Minuten gezeigt werden konnte. Das verkürzte die Analysezeit nach der DNS-Isolation von ehemals sechs Stunden auf weniger als 3.5 Stunden. Da jedoch bei allen getesteten Verfahren eine starke Verkürzung der Hybridisierungszeit auch eine Verminderung der Spezifität und Sensitivität der Identifizierung zur Folge hatte, wurde als Kompromiss zwischen optimalen Analyseergebnissen und möglichst kurzer Testdauer eine Hybridisierungszeit von einer Stunde für alle folgenden Versuche festgelegt. Somit betrug die Analysezeit nach der DNS-Isolation etwa vier Stunden.

### *Einfluss von Eigenschaften der Ziel-DNS*

Weiterhin wurde der Einfluss von Eigenschaften der Ziel-DNS, wie der Fragmentlänge und der Einbaurrate der Fluoreszenzmarkierung untersucht. Die Fragmentierung der Ziel-DNS wurde durchgeführt, um eine Verminderung der Sekundärstrukturen zu erreichen, die die Zugänglichkeit der Ziel-DNS für die Hybridisierung an die Oligonukleotid-Sonden erschweren. Außerdem erlaubt eine Fragmentierung die unabhängige Hybridisierung verschiedener Abschnitte der Ziel-DNS an unterschiedliche Sonden (78). Hierbei wurde festgestellt, dass die Hybridisierungseffizienz abhängig ist von der Länge der Ziel-DNS Fragmente und von der Position der Sonde in Bezug auf die Ziel-DNS Sequenz. Je länger das zu hybridisierende Ziel-Fragment war, desto schwächer waren die

Hybridisierungsergebnisse für Sonden, die komplementär zu dem 3' Ende des Ziel-DNS-Strangs waren. Mögliche Erklärungen hierfür waren eine niedrige Zugänglichkeit des 3' Endes des Ziel-DNS-Strangs wegen vorhandener Sekundärstrukturen, oder eine Verminderung der Hybridisierungseffizienz durch Interaktionen zwischen den komplementären Ziel-DNS-Strängen (127), da doppelsträngige DNS zur Hybridisierung eingesetzt wurde. Wie erwartet wurden die besten Hybridisierungsergebnisse bezüglich Spezifität und Sensitivität der Identifizierung der Mutationsposition mit Fragmentlängen erreicht, bei denen laut festgestellter Einbaurrate die Mehrzahl der Fragmente eine Fluoreszenzmarkierung trägt (etwa 25 - 500 bp). Obwohl noch kleinere Fragmente eine bessere Zugänglichkeit ermöglichen, konnte für kleinere Fragmentlängen (< 50 bp) eine Verminderung der Sensitivität der Mutationsidentifizierung festgestellt werden. Dies wurde auf eine erhöhte Anzahl an unmarkierten Fragmenten zurückgeführt, welche in Konkurrenz mit den markierten Fragmenten stehen und somit die Sensitivität der Analyse negativ beeinflussen.

### **Weiterführende Entwicklungen**

#### *Kombination des Resistenznachweises mit einer Kultur-unabhängigen Isolation*

Die Identifizierung der TEM und SHV Varianten erfolgte in dieser Arbeit aus klinischen Isolaten, d.h. es wurde eine Isolierung des Krankheitserregers durch eine Vorkultur vorgenommen, bevor die DNS-Extraktion und danach die DNS-Mikroarrayanalyse stattfand. Dieser Schritt ist bisher notwendig, um die Resistenz eindeutig dem Krankheitserreger zuzuordnen, ansonsten könnte ein nichtpathogener Resistenzträger zu falsch positiven Ergebnissen führen. Diese Isolation ist der zeitaufwendigste Schritt bei der kompletten Analyse. Um die Ausschöpfung des vollen Potenzials eines genotypischen Resistenznachweises zu ermöglichen, insbesondere des Zeitvorteils, ist eine Kultur-unabhängige Methode notwendig. An der Technischen Universität München wurde ein Verfahren entwickelt bei dem eine speziesspezifische Anreicherung durch den Einsatz von Polynukleotidsonden stattfindet. In Zusammenarbeit wurde festgestellt, dass nach einer Anreicherung von *E. coli* Bakterien aus einer klinischen Urinprobe das vorhandene *bla<sub>TEM</sub>* - Resistenzgen durch die Mikroarrayanalyse identifiziert werden konnte. Somit wurde der Nachweis erbracht, dass die Entwicklung eines komplett Kultur-unabhängigen genotypischen Resistenznachweises möglich ist.

#### *Ausweitung des Nachweisspektrums*

Der Vorteil der phänotypischen Analyse bleibt, dass ein großes Spektrum unterschiedlicher Resistenzdeterminanten nachweisbar ist. Um einen zu dieser Standardmethode konkurrenzfähigen Test zu entwickeln, muss daher die große Mehrheit der klinisch relevanten Resistenzmerkmale für ESBL und ähnlicher Resistenzphänotypen nachweisbar sein. Die Ergänzung der bisher entwickelten TEM und SHV-Arrays zu einem Komplettsystem zum Nachweis aller Merkmale klinisch relevanter Laktamasefamilien (z.B. auch CTX-M (13) und AmpC (169)) ist möglich und derzeit in Arbeit. Ein Prototyp-Array, der unter den für den TEM- und SHV-Array festgelegten Versuchsparametern eine Auswahl von CTX-M-Varianten nachweisen kann, wurde bereits von M. Rubtsova (*National Research Center for Antibiotic Resistance*, Moskau, Russland) entwickelt.

### *Entwicklung eines marktreifen Systems*

Die Entwicklung eines marktreifen Systems aus den in dieser Studie entwickelten Prototypen ist nur in Verbindung mit einer patentrechtlich zugänglichen Methodik möglich. Da das Standard Arrayformat von kovalent immobilisierten Oligonukleotidsonden von Patenten von Oxford Gene Technology (u. a. Patentnummer EP0373203B1) abgedeckt ist, kann es nicht lizenzfrei angewendet werden. Durch die Kooperation mit einem Industriepartner (Eppendorf Array Technology) war ein alternatives (jedoch nicht offen gelegtes) Immobilisierungsverfahren zugänglich. In einem ersten Anwendungsversuch konnte gezeigt werden, dass die Identifizierung der relevanten Mutationspositionen auch in diesem Format erfolgen kann, aber noch der weiteren Optimierung bedarf.

### **Fazit**

Die entwickelten DNS-Mikroarrays zur Identifizierung von TEM und SHV ESBL und IRT Varianten bieten ein viel versprechendes System für den Einsatz in der klinischen Mikrobiologie dar. Der schnelle Nachweis von resistenten Bakterien durch genotypische Resistenztestung zu einem kompetitiven Preis sollte das Auftreten neuer Resistenzen vermindern. Durch die frühzeitige und spezifische Identifizierung des Resistenzmerkmals kann die Verschreibung von Antibiotika spezialisierter und somit effektiver erfolgen, da bekannte Substratspektren vom genotypischen Profil abgeleitet und vor Therapiebeginn berücksichtigt werden können. Der Einsatz von Breitbandantibiotika könnte eher auf schwere Infektionen beschränkt werden und eine weitere Verbreitung der Resistenzen durch frühzeitige Erkennung und Isolierung von betroffenen Patienten erschwert werden. Weiterhin kann die Verbreitung von bestimmten Resistenzmerkmalen im klinischen Umfeld verfolgt werden, was die Sammlung bedeutender epidemiologischer Daten zur Resistenzentwicklung ermöglicht. Die Entwicklung von genotypischen Methoden zur Resistenztestung kann daher große Auswirkungen haben auf die klinische Behandlung von Infektionskrankheiten und deren Kosten.

## Abstract

Among the most important types of resistances to be detected are the extended spectrum beta-lactamases (ESBLs). ESBLs are found in many different species of the family Enterobacteriaceae. Most ESBLs are mutants of TEM- or SHV-type beta-lactamases. The TEM- and SHV- subtypes are derived from parental sequences (TEM-1, SHV-1) and differ from them by a variable number of amino acid substitutions. These mutations lead to an extended spectrum of activity against newer lactams, especially against 3<sup>rd</sup> generation cephalosporins. Other derivatives of the classical TEM or SHV enzymes also show an inhibitor resistant TEM (IRT) phenotype conferring resistance to beta-lactamase inhibitors. ESBL producing organisms are difficult to detect in standard phenotypic screening tests, mainly because of their widely varying levels of activity against various cephalosporins. For an improved accuracy confirmatory susceptibility tests have to be performed resulting in a response time of three days until the ESBL phenotype can be identified unequivocally. Since infections with ESBL producing organisms are registered with increased prevalence and are associated with significantly longer hospital stays and higher costs, more accurate tests to detect ESBLs in clinical isolates are necessary. The microarray technology allows the genotypic identification of resistance traits in less than one day of analysis time. Furthermore, the identification of the beta-lactamase variant on a molecular level will define for most ESBL isolates a specific substrate pattern, which can be considered for the determination of the appropriate antibiotic treatment. Additionally, the genotyping of resistances can be used for the reliable surveillance of multiresistant bacteria in wards or hospitals.

In the present study a diagnostic microarray was developed for the rapid identification of mutations of the majority of the currently known TEM or SHV beta-lactamase variants, which are related to the ESBL and/or IRT phenotype. The assay enabled the detection and identification of 99 % of the relevant polymorphisms for TEM beta-lactamases and 100 % of the mutations of SHV beta-lactamases. This allows the detection of 96 % of the currently known TEM-variants and 100 % of the known SHV-variants. Consensus primers were developed and used for target amplification covering the majority of the known variant sequences. The sensitivity, reproducibility and identification capability of the developed arrays was determined with a set of reference samples. Furthermore, the TEM-array was validated by testing 72 clinical isolates collected in diverse institutions in Germany, Croatia and Russia. The SHV-array was validated by testing 30 clinical isolates collected in Croatia. The simultaneous detection of an extended spectrum-variant in presence of a narrow spectrum-variant was shown in a model system for TEM up to a ratio of 1:10, as well as in clinical isolates for SHV. Starting from the isolated DNA, the assay could be performed in less than 3.5 hours. The discrimination level, the sensitivity and the reproducibility were enhanced by automation of the hybridization procedure. The development of a marketable diagnostic ESBL microarray based on the presented prototypes and the extension of the developed system towards the detection of other relevant beta-lactamase families is in progress. In conclusion, the diagnostic test developed in this study offers a promising approach for the rapid identification and epidemiologic monitoring of TEM or SHV ESBL and IRT beta-lactamases.

# 1 Introduction

## **1.1 Antibiotic Resistance**

The discovery of penicillin by Alexander Fleming in 1928 was a first step towards the development of modern antibiotics and is still one of the most outstanding achievements of modern medicine. Since the world war II era these drugs became widely used, allowing the treatment of the most serious infections by pathogenic microorganisms. However, over fifty years of extensive use of antibiotics have led to the emergence of multiple defense mechanisms developed by the targeted bacteria. Although the sort, action and number of currently available antibiotics is astounding, the options for treatment of serious infections within the clinical setting become more and more limited, and at the beginning of the 21<sup>st</sup> century the current methods of applying existing and developing new antibiotics have to be reviewed (91).

Drug resistance is especially problematic in hospitals, since patients with serious diseases are impaired regarding their immune defense system and present an easy target for pathogenic organisms. The extensive use of antibiotics to treat those infections increases the selective pressure for the development of new mutations promoting bacterial survival. Therefore, the hospital environment is the major point of origin of the spread of multiple resistant organisms. According to statistics from the Centers for Disease Control and Prevention in the US nearly two million patients get an hospital acquired infection each year. About 90,000 of these patients die because of this cause. The risk to acquire such an infection has risen steadily in recent decades. The incidence of blood and tissue infections (sepsis) has almost tripled from 1979-2000. More than 70 % of the bacteria causing infections in hospitals are resistant to at least one of the antibiotics most commonly used to treat them (<http://www.niaid.nih.gov/factsheets/antimicro.htm>). The infections with drug resistant organisms prolong the hospital stays and increase health care costs. Even organisms which are resistant to the most powerful antibiotics available (methicillin and vancomycin) are emerging presenting physicians and patients with serious problems (141).

The mode of action of antibiotics is targeted towards different components of the bacterial life cycle and organism. The antibiotics can interfere with the biosynthesis and function of the genetic material, proteins and the cell wall. Bacteria are single cell organisms with a compact genetic material and short reproduction times. Therefore, new mutations with an impact on bacterial survival can evolve rapidly. Three major defense mechanisms against antibiotics emerged: (i) inhibition of the import or fast export of the antibiotic by change of the membrane permeability, (ii) modification of the binding domain of the target structure or (iii) enzymatic inactivation of the antibiotic (177). These defense mechanism are often transmittable between microorganisms, because they can be encoded on transferable genetic elements, such as plasmids (34) or transposons (6), or are propagated by phages.



### 1.1.1 Beta-lactam resistance

Beta-lactams account for approximately 50 % of the global antibiotic consumption (96). They interact with enzymes responsible for the final step of the bacterial cell wall synthesis: the cross-linking of the peptidoglycan layer. Loss or damage of this peptidoglycan layer destroys the rigidity of the bacterial cell wall, resulting in death of the cell in a hypertonic environment. The peptidoglycan layer consists of a carbohydrate backbone of alternating units of N-acetyl glucosamine and N-acetyl muramic acid. The N-acetyl muramic acid residues are cross-linked via a transpeptidase reaction: by cleavage of a terminal D-alanyl-D-alanine bond the C-terminus of a peptide side chain is linked to a free amino group of another peptide chain (see figure 1). This reaction is inhibited by  $\beta$ -lactam antibiotics (177).

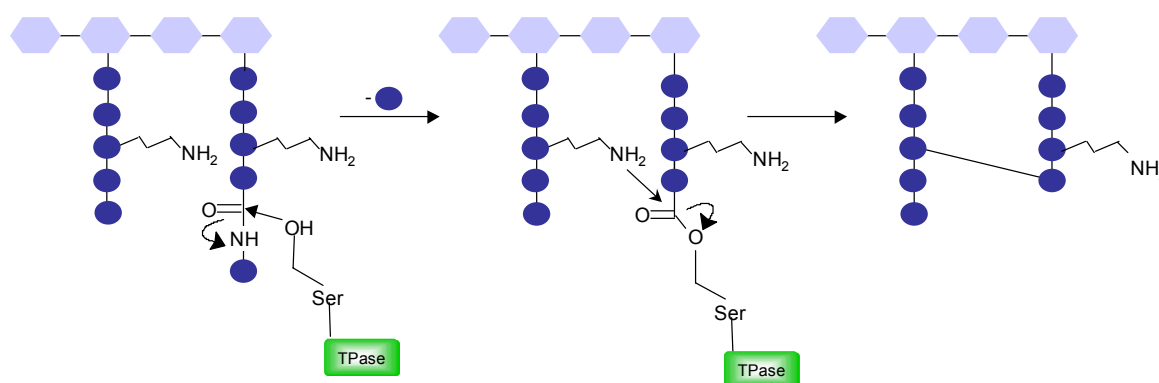


**Figure 1.** Schematic view of the transpeptidase (TPase) reaction for cross-linking of the peptidoglycan layer. By cleavage of a terminal D-alanyl-D-alanine bond the C-terminus of a peptide side chain is linked to a free amino group (e.g. from L-lysine) of a neighboring peptide chain.

The four-membered beta-lactam ring is the common basic structure of all beta-lactam antibiotics. Beta-lactams applied in human medicine are derived from natural products generated by fungi, such as *Penicillium chrysogenum* or *Acremonium chrysogenum*. The different groups of  $\beta$ -lactam antibiotics are the penicillins, cephalosporins (including oxacephems and cephamycins), thienamycins (carbapenems), and aztreonam (monobactam) (see figure 2). Penicillins and cephalosporins are widely used to inhibit gram-positive and gram-negative bacilli. Monobactams inhibit only aerobic gram-negative bacilli, clavulanic acid acts as a beta-lactamase inhibitor and thienamycin inhibits a wide range of aerobic and anaerobic species (10).

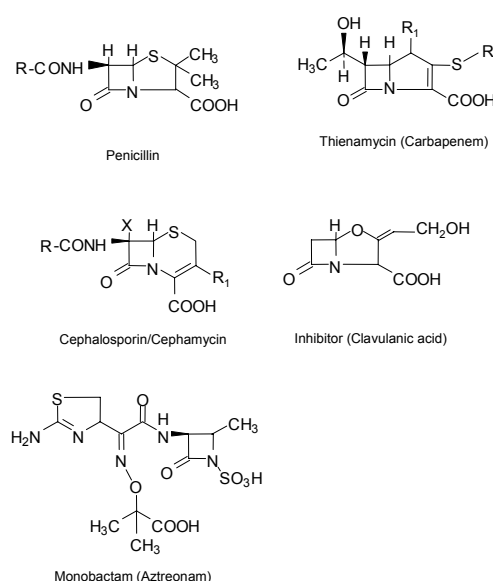


**Figure 2.** Basic structures of beta-lactam antibiotics. R and R<sub>1</sub> represent various carbon groups. X can be either a hydrogen or a methoxy group.

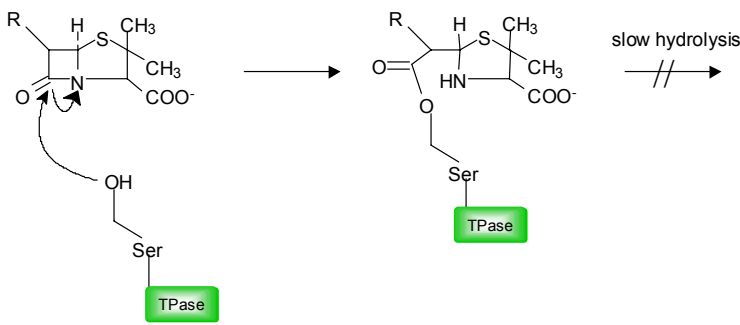


**Figure 3.** Schematic representation of the inactivation reaction of the transpeptidase by penicillin. The hydrolysis of the lactam-bound transpeptidases is a very slow process.

The beta-lactam ring is a structural analog to the D-alanyl-D-alanine terminal peptide bond, so that it undergoes an acylation reaction with the transpeptidases (also called Penicillin Binding Proteins PBPs) that cross-link the peptidoglycan layer (see figure 3). The hydrolysis of the lactam-bound transpeptidases is very slow, so that the cross-linking reaction is inhibited resulting in a mechanically labile cell wall (47).

The resistance mechanisms to beta-lactam antibiotics are various. One mechanism consists of an alteration of the target site of the agent, the transpeptidase PBPs. In gram-positive bacteria a preexisting low affinity of the targeted transpeptidase towards the antibiotic (e.g. for Enterococci) was observed. In gram positive and gram negative bacteria an alteration of the transpeptidase structure (e.g. Streptococcus, Neisseria) or the coexpression of an alternative enzyme with a decreased affinity for the antibiotic (e.g. PBP2a for Staphylococcus) can be a cause of this resistance type. In gram-negative bacteria deletion of a porin protein can cause the impermeability of the membrane for the beta-lactam antibiotic (47,60,156).

In gram-negative and -positive bacteria the expression of beta-lactamases, which inactivate the beta-lactam antibiotic by cleavage of the beta-lactam ring, is one of the clinically most relevant resistance mechanisms (95).

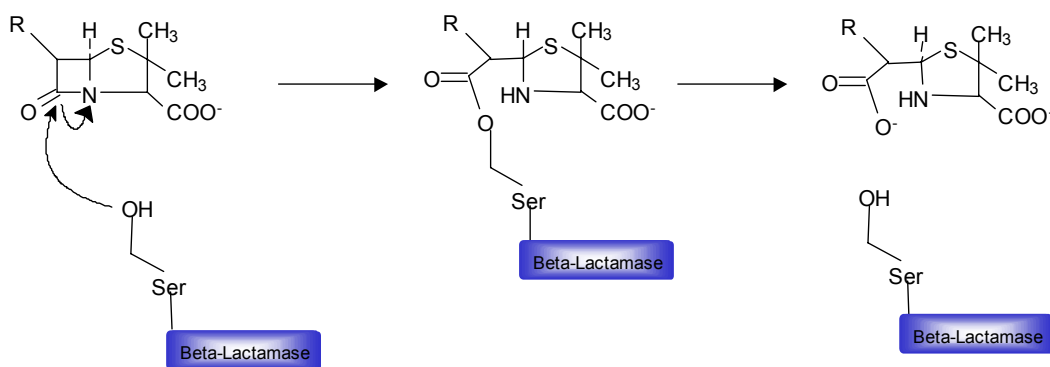


**Figure 4.** Mechanism of the hydrolysis of penicillin by a beta-lactamase. One beta-lactamase molecule can hydrolyze app. 1000 penicillin molecules per second (177).

A few beta-lactamases utilize Zinc ions to disrupt the beta-lactam ring (metallo-beta-lactamases of molecular class B (2)), but the far greater number of class A (2), C (73), and D (67) enzymes bear a serine residue at the active site. The enzyme first associates noncovalently with the antibiotic to yield a noncovalent Michaelis complex. The beta-lactam ring is then attacked by the free hydroxyl of the serine residue,

yielding a covalent acyl ester. Hydrolysis of the ester finally liberates the active enzyme and the inactivated drug, since the opened beta-lactam ring can no longer be recognized by the transpeptidases as a substrate (176) (see figure 4). This mechanism is very effective, since one beta-lactamase molecule can hydrolyze about 1000 penicillin molecules per second (177).

**Table 1.** Classes of beta-lactam antibiotics<sup>a</sup>

Cephalosporins	Antibiotic
1 <sup>st</sup> Generation	Cefazolin Cephalexin Cephalothin Cephadrine
2 <sup>nd</sup> Generation	Cefuroxime Cefamandole Cefaclor
2 <sup>nd</sup> Generation (cephamycines)	Cefoxitin Cefotetan
3 <sup>rd</sup> Generation	Cefotaxime Ceftriaxone Ceftazidime Cefpodoxime
4 <sup>th</sup> Generation	Cefepime
<b>Penicillins</b>	
Beta-lactamase sensitive penicillins	Benzylpenicillin Phenoxymethylpenicillin Propicillin Azidocillin
Beta-lactamase resistant penicillins	Flucloxacillin Dicloxacillin Oxacillin
Extended-spectrum penicillins	Amoxicillin Ampicillin Bacampicillin Mezlocillin Piperacillin
<b>Other beta-lactams</b>	
Thienamycins/Carbapenems	Imipenem Meropenem
Monobactam	Aztreonam
Beta-lactamase inhibitors	Clavulanic acid Sulbactam Tazobactam

<sup>a</sup>Only a selection of the most common antibiotics of the displayed groups is listed.

### 1.1.2 Extended Spectrum Beta-Lactamases (ESBLs)

In 2001 more than 340 different beta-lactamase types were known (20). A major part of these enzymes constitute plasmid mediated serine beta-lactamases in gram-negative bacilli. The most common of these enzymes in Enterobacteriaceae is TEM-1, which has been reported in about 50-80 % of plasmid mediated lactam resistances (106,134,146). SHV-1 is also a prevalent enzyme and was first described as a chromosomally encoded beta-lactamase in members of the genus *Klebsiella*. Subsequent work demonstrated that SHV-1 is also encoded by transposons or plasmids (62).

TEM-1, TEM-2 and SHV-1 are the point of origin of a vast number of TEM- and SHV-variants, which differ from the parental TEM and SHV beta-lactamases by a variable number of amino acid substitutions. The classical TEM-1, TEM-2 or SHV-1 enzymes attack the narrow spectrum cephalosporins and all the anti-gram-negative penicillins except temocillin, but they have minimal activity against newer cephalosporins (other than cefamandole and cefoperazone) and monobactams or carbapenems (69,72). A major number of the new enzyme variants mediate resistance to extended spectrum (third generation) cephalosporins and monobactams, as well as narrow spectrum (first or second generation) cephalosporins and anti-gram negative penicillins (71) (see table 1). These enzymes are designated Extended Spectrum Beta-Lactamases (ESBLs) in reference to their extended spectrum of activity against newer beta-lactam antibiotics. They do not affect cephamycins or carbapenems and are usually susceptible to inhibitors of beta-lactamases like clavulanic acid. There are also derivatives of the classical TEM or SHV enzymes showing an IRT (which originally stands for Inhibitor Resistant TEM) phenotype, conferring resistance to inhibitors of beta-lactamases like clavulanic acid, but which do not confer an ESBL type phenotypic resistance pattern (95).

ESBLs are found in many different species of the family Enterobacteriaceae, predominantly in *Klebsiella pneumoniae* and *Escherichia coli*, but also in *Pseudomonas aeruginosa*, *Haemophilus influenzae*, and *Neisseria gonorrhoe*. Most ESBLs are mutants of TEM-1, TEM-2 or SHV-1, but there are also derivatives belonging to the CTX-M- or OXA-family of beta-lactamases. Few ESBLs are not closely related to the established families, these lactamases are designated PER, VEB, GES, TLA, FEC, CME, SFO and BES (16). The nomenclature of these enzymes is not standardized: The TEM-1 enzyme was originally found in a single *E. coli* strain isolated from a patient named Temoniera (33), hence the designation TEM. SHV denotes a variable response to sulfhydryl inhibitors (107). OXA is derived from oxacillin resistant (20), CTX-M was designated in reference to its hydrolytic activity against cefotaxime (13).

The TEM- and SHV- subtypes are derived from parental sequences (TEM-1, TEM-2, SHV-1) and differ from them by a variable number of amino acid substitutions (for amino acid sequences of TEM and SHV beta-lactamases see <http://www.lahey.org/Studies/>). Their degree of activity against different beta-lactam antibiotics is depending on the combination of different amino acid substitutions surrounding the active site of the enzyme. The amino acid positions are numbered in the literature according to a beta-lactamase alignment proposed by Ambler in 1991 (3). The most important substitution positions for an extension of the substrate spectrum are situated for TEM beta-lactamase at Ambler position 164, for SHV at position 179 and for both families in position 238, which result in an expansion of the

substrate binding site. Amino acid substitutions in position 104 and 240 in TEM and SHV enhance the interaction with oxyimino side-chains of ceftazidim and aztreonam. Mutation in amino acid 237 in TEM enzymes reduces the activity toward ceftazidime and aztreonam, while increasing it towards cefotaxime and cephalotin. In some TEM and SHV enzymes ESBL-type mutations have been found together with those that determine resistance to inhibitors (positions 69, 130, 275, 276). Some positions are considered as neutral (e.g. position 21 in TEM), however it is possible, that some of these mutations could reveal a modulation in enzyme activity in context of other mutations (51,82). Neutral mutations can also constitute genetic markers for specifying genealogic lineages of ESBL genes and their analysis is very useful in evolutionary as well as epidemiologic investigations. Up to date there are more than 120 different TEM and more than 50 different SHV variants known.

### 1.1.3 Prevalence of ESBLs

The occurrence of plasmid encoded resistance against 3<sup>rd</sup> generation cephalosporins is reported since 1983 (80,81). Epidemic outbreaks of those resistances within the clinical setting were observed in France (148), the US (109) and other European countries (52,160,174) since then continuously. Whether these outbreaks were caused by ESBLs or AmpC-type enzymes was not investigated consistently. The existing epidemiologic data up to date suggests that the prevalence and type of ESBL resistance is highly variable and depends on the geographic area and the investigated institution. However, a trend of an increase of the resistance against 3<sup>rd</sup> generation cephalosporins can be observed (181). In the Sentry antimicrobial surveillance program the prevalence of ESBL producing isolates of *E. coli*, *P. mirabilis*, *Salmonella* spp. and *K. pneumoniae* was evaluated originating from institutions situated in the US, Canada, Europe, Latin America and the Western Pacific region. As displayed in figure 5 the highest percentage of ESBL phenotypes was detected among *K. pneumoniae* isolates from Latin America (45 %) followed by those from the Western pacific region (25 %) and Europe (23 %), the US (8 %) and Canada (5 %) (180).

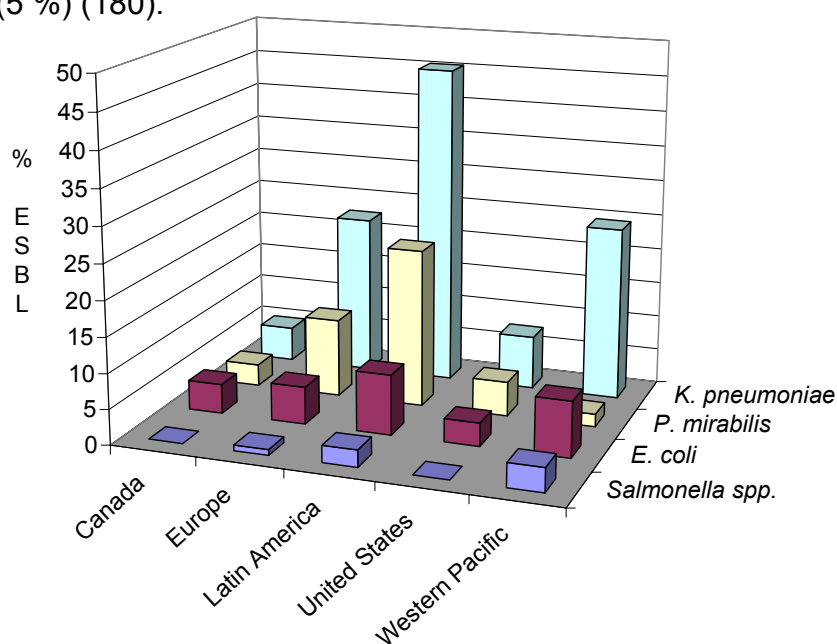


**Figure 5.** Percentage of ESBL phenotypes detected among *K. pneumoniae*, *E. coli*, *P. mirabilis* and *Salmonella* species isolated in Europe, the Americas and the Western Pacific Region as a part of the Sentry project from 1997-1999 (180).

A study conducted in 1994 in 35 different intensive care units (ICUs) situated in 10 southern and western European countries reported an ESBL prevalence of 22.8 % of all tested isolates and of 28.6 % for *K. pneumoniae* (7). In a study from 2001 evaluating the resistance situation in Germany, Austria and Switzerland (accomplished by the Paul Ehrlich Gesellschaft) among 1.3 % of *K. oxytoca* and 0.8 % of *E. coli* isolates an ESBL-type resistance was detected. In comparison to a study from 1998 the rate of ESBL producing *K. pneumoniae* increased from 4.7 to 8.2 %. The prevalence of different genetic variants was only investigated in selected studies. The most reported ones belong to the TEM and SHV beta-lactamase families, in terms of variant numbers and number of producer strains (51). In a recent publication from 2003 a considerable increase in the occurrence of CTX-M producing strains was reported: in 455 bloodstream isolates of *K. pneumoniae* collected in the US, Taiwan, Australia, South Africa, Turkey, Belgium and Argentina 67.1 % of the ESBL producers carried an SHV-type, 23.3 % of CTX-M type and 16.4 % of TEM-type lactamase (123).

### 1.1.4 Phenotypic ESBL detection

Clinical standard procedures for resistance detection are based on growth inhibition in dilution or disc diffusion tests. For the detection of the minimum inhibitory concentration (MIC) a dilution series of the investigated antibiotic in a culture medium is prepared, the isolated bacteria are inoculated and the samples are incubated for a defined time period. The lowest concentration inhibiting bacterial growth is defined as the MIC. The MIC itself has no therapeutic relevance, because it is detected under *in vitro* conditions and does not reflect the pharmacological properties of the tested agent. Therefore, breakpoint concentrations are defined, corresponding to serum levels obtainable at the half time of the application interval. Considering these benchmark parameters a prediction whether the organism is susceptible to a certain agent can be made. In disc diffusion testing an agar plate is inoculated with the tested isolate and paper discs containing defined concentrations of antibiotics and/or inhibitors are applied and the discs are incubated overnight. The zones of bacterial growth inhibition are measured and interpreted.

The detection of ESBL producing organisms is especially difficult, because of their widely varying levels of activity against various cephalosporins. The choice of the right antibiotic to test is critical, e.g. one enzyme may actively hydrolyze ceftazidime with an MIC of 256 µg/ml, while having a poor activity on cefotaxime with MICs of only 4 µg/ml (95). Therefore, the NCCLS (National Committee for Clinical Laboratory Standards) has defined broth microdilution and disk diffusion screening tests with several selected antibiotics and low MICs of 2 µg/ml to be tested to determine a potential ESBL producer (see table 2). If an ESBL is detected, all penicillins, cephalosporins and aztreonam should be reported as resistant, except the cephamycins, which should be reported according to their test results (115). Even though these tested MICs are still in the susceptible range as defined by the breakpoint analysis ( $\leq 8$  µg/ml), it was shown that they are clinically important, because treatment failures can occur, if they are not considered before treatment (124). Another problem of phenotypic ESBL detection is the occurrence of an inoculum effect. *In vitro*, the MICs of cephalosporins rise as the inoculum increases (108,132,168). Thus ESBL producing organisms might remain undetected, if the inoculum is not sufficient. The occurrence of this inoculum effect in clinical infections is indicated by reports of treatment failures, suboptimal clinical outcome and the

increased mortality of patients infected with ESBL-producing strains, that have MICs in the susceptible range and were treated with cephalosporins (89,124,142,149).

**Table 2.** NCCLS screening parameters for ESBL detection (115)

Disk diffusion		MICs	
cefepodoxime	< 22 mm	cefepodoxime	> 2 µg/ml
ceftazidime	< 22 mm	ceftazidime	> 2 µg/ml
aztreonam	< 27 mm	aztreonam	> 2 µg/ml
cefotaxime	< 27 mm	cefotaxime	> 2 µg/ml
ceftriaxone	< 25 mm	ceftriaxone	> 2 µg/ml

According to recommendations issued by the NCCLS a phenotypic confirmatory test for potential ESBL producing isolates of *K. pneumoniae*, *K. oxytoca* and *E. coli* should be performed by testing cefotaxime and ceftazidime alone and in combination with clavulanic acid. A decrease of > 3 doubling dilutions in an MIC for either agent tested in combination with clavulanic acid versus its MIC when tested alone confirms an ESBL producer. For disc diffusion testing a > 5 mm increase in the zone diameter for cefotaxime or ceftazidime with clavulanic acid versus its zone diameter when tested alone confirms the presence of an ESBL producing organism (115).

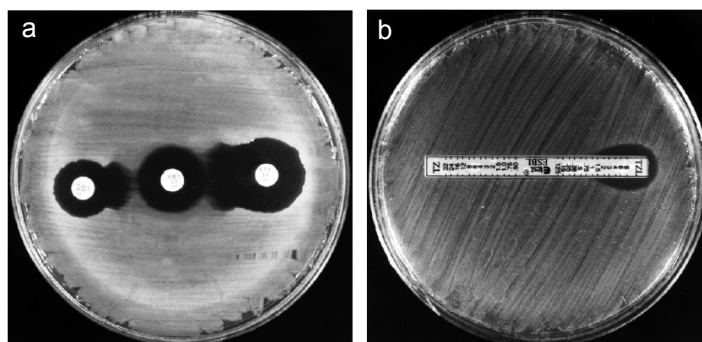


**Figure 6.** Detection of ESBL production in an *E. coli* producing TEM-5 enzyme (a) in a double disc test. Left, ceftazidime, 30 µg; centre, amoxicillin + clavulanate, 20 + 10 µg; right cefotaxime 30 µg, (b) in a Etest ESBL. The strip has a ceftazidime gradient at both ends, with clavulanate in the right hand gradient only (97).

A standard confirmatory test for ESBL detection is also the double disc test. Discs containing ceftazidime and cefotaxime and amoxicillin/clavulanate are placed on inoculated agar plates. An ESBL is detected, when the cephalosporin zone is expanded by the clavulanate. Etest ESBL strips use a strip containing a ceftazidime gradient at the one end and a ceftazidime plus clavulanate gradient at the other end (see figure 6). The MICs can be directly read off the paper strip scale: if the ratio of the MIC of ceftazidime to the MIC of ceftazidime/clavulanate is  $\geq 8$ , ESBL production is inferred. The combined discs method depends on comparing the zones given by discs containing an extended spectrum cephalosporin with and without clavulanic acid. If an ESBL is produced, the zones are enlarged for the discs containing the inhibitor (97). To read out the inhibition zones in all these tests is not always straightforward and interpretation of the test results can be highly subjective.

Furthermore, these phenotypic confirmatory tests can not detect all ESBLs. In organisms with multiple beta-lactamases the phenotype of for example an AmpC or IRT type beta-lactamase can mask a present ESBL phenotype and lead to a false negative test result. Currently the presence of multiple lactamases can only be confirmed by isoelectric focusing or DNA sequencing, which is labor intensive and time consuming. ESBLs can also occur in other Enterobacteriaceae, such as *Salmonella* species, *Proteus mirabilis* or *Pseudomonas aeruginosa*, but the methods defined by the NCCLS for ESBL producing isolates of *K. pneumoniae*, *K. oxytoca* and *E. coli* are not applicable for those species. So far no phenotypic screening and confirmatory tests were defined by the NCCLS for those kind of isolates (143).

In summary, the phenotypic screening tests are, though cost-effective, time consuming (app. 2 days) (99). Furthermore, serious difficulties in interpretation of the test results are associated with treatment failures (95,97). For an improved accuracy and confirmation of the ESBL detection it is indispensable to test isolates on multiple antibiotics in combination with beta-lactamase inhibitors (115). This prolongs the specific response time to 3 days, so that treatment often has to start before the phenotype is determined unequivocally. The fast and accurate identification of the resistance is crucial for the outcome of the antimicrobial therapy and significantly influences following procedures, such as isolation of patients for preventing the spread of antibiotic resistances.

### 1.1.5 Genotypic ESBL detection

Genotypic analysis of putative ESBL strains is a promising alternative for ESBL detection. The genetic testing can be performed directly from the clinical sample as it is drawn from the patient (e.g. blood, urine) without preisolation or cultivation. This shortens the response time considerably and makes a specified antibiotic therapy possible. Unambiguous identification of the ESBL variant, as determined by genotyping, will define for most ESBL isolates a specific substrate pattern, which can be considered for the choice of antibiotic treatment. Furthermore, the time of contact between hospital staff and potentially infective organisms is minimized in comparison to phenotypic methods, so that the risk of cross contamination could be diminished. Genetic testing is much less prone to subjective interpretation, as for example the analysis of growth inhibition zones in phenotypic tests, so that more user-independent test results can be generated. Also resistances from organisms not targeted by NCCLS ESBL confirmatory tests, or from uncultivable organisms, or resistances, which are not detected *in vitro*, can be determined by genetic resistance testing. Additionally, the genotyping of resistances can be used for the reliable surveillance of the multiresistant bacteria within wards or hospital. For genotypic ESBL detection the genetic traits characterizing the diverse ESBL variants have to be detected. The ESBL subtypes are derived from different beta-lactamase families. Within certain families multiple mutations (mostly single nucleotide polymorphisms (SNPs)) in the otherwise highly conserved sequences characterize the different subtypes. Therefore, a method for the parallel analysis of multiple genes, SNPs and other mutations has to be chosen.

A number of molecular methods for determining ESBL resistances have already been developed (48). Biotinylated oligonucleotide probes (167) or radiolabeled primers (5) were used to discriminate between a limited number of ESBL variants. Restriction fragment length polymorphism analysis (PCR-RFLP) (4) and single strand conformation polymorphism analysis (PCR-SSCP) (100), real time PCR (129), ligase



chain reaction (117) or minisequencing (64) have also been used to identify some of the relevant point mutations. The major drawback of all these assays is that they distinguish just between a few variants of the TEM and SHV beta-lactamases due to limited multiplexing capability, so that the full potential of the genotypic analysis is still not exploited. Multiple more advanced methods for SNP detection have already been developed, but have not been applied so far for the detection of ESBL or IRT polymorphisms.

## **1.2 Genotyping of single nucleotide polymorphisms**

The analysis of DNA sequence variations is of major interest, in particular since the sequencing of the human genome was completed. The high frequency of SNPs and their use as genetic markers for genome mapping studies, medical diagnostics and identity testing has driven the development of multiple methods for detection and identification of SNPs.

### *1.2.1 SNP discrimination methods*

SNP assay methods usually apply hybridization to specific oligonucleotides to discriminate between perfectly matched and non-perfectly matched duplexes. Assays based on direct hybridization use complementary oligonucleotide sequences, which are annealed under stringent conditions to differentiate between sequence variations. Enzymatic reactions can be used to enhance the specificity and sensitivity of the reaction. Hereby DNA ligase, nucleases or DNA polymerase can be applied (75). In DNA ligase based assays SNPs are discriminated by the enzymatic joining of two oligonucleotides, if they are both complementary to the template at the position of the joining (136).

Site-specific endonucleases are used in restriction fragment length polymorphism analysis (RFLP) to produce DNA fragments of different length, due to presence or absence of specific restriction sites at polymorphism positions (152). To achieve better sensitivity PCR amplified products are used in PCR-RFLP as the sample. The Flap endonuclease used in the Invader assay (Third Wave Technologies, Madison, WI) recognizes and cleaves specific overhang structures formed by the tandem hybridization of a signal probe and an Invader probe. The cleaved off overhang is used to drive a universal cleavage reaction for fluorescence signal generation (65). The 5' to 3' exonuclease activity of DNA polymerase and allele specific reporter probes are employed in a PCR reaction for SNP discrimination in the TaqMan assay. The allele specific reporter probes are labeled with a fluorescence dye and a quencher and anneal during PCR to the complementary polymorphism site. During the extension step the 5' reporter dye and the quencher are cleaved off, so that the energy transfer from the reporter to the quencher is stopped and fluorescence is generated (77).

The primer extension assay utilizes an oligonucleotide primer annealing immediate upstream from the polymorphic site of a PCR amplified fragment. The primer is extended in presence of appropriate dNTPs or ddNTPs (159). The products can be distinguished through fragment size determination or fluorescence detection, if labeled nucleotides are used. In allele specific PCR primers with discriminating bases at the 3' ends are employed, they are only extended if they are fully complementary to the template sequence (116). One amplification reaction is run for each allele to be tested and the generation of PCR products can be analyzed by gel electrophoresis.

In the Amplifluor system (Serologicals Corp., Norcross, GA) the discriminating primers are labeled with two different fluorescent dyes, which are quenched initially by close proximity to a quencher molecule in a hairpin structure. The hairpin structure of the primer is unfolded during PCR and a fluorescent signal is generated depending on the present allele (172).

Direct sequencing of polymorphic regions by incorporation of fluorescently labeled nucleotides and analysis of reaction products by gel or capillary electrophoresis in an automated process is still viewed as the gold standard for SNP genotyping, since the presence and identity of any polymorphism can thus be confirmed (84). However, the process is still laborious, expensive and speed as well as throughput are still low for the analysis of multiple samples and multiple polymorphic regions. A minimized sequencing process was developed by Pyrosequencing (Pyrosequencing AB, Uppsala, Sweden). The successful incorporation of a nucleotide is visualized through a chemiluminescent reaction. The process allows the sequencing of up to 20 bases for 96 samples in 10 minutes (133).

### ***1.2.2 SNP detection methods***

The detection of SNPs is based in most aforementioned assays either on size differentiation or on the detection of generated fluorescence signal. The identification of molecular size be performed by gel or capillary electrophoresis, mass spectrometry or high performance liquid chromatography (HPLC). Gel electrophoresis can be used as a detection method for RFLP, PCR, sequencing, primer extension and ligation-based SNP assays. However, gel electrophoresis is laborious and generally not applicable for high-throughput analysis (75). Capillary electrophoresis significantly shortens hands-on time and enhances throughput, but is still labor intensive and expensive compared to other methods.

Mass spectrometry based SNP detection can be done through matrix assisted laser desorption/ionization and time-of-flight detectors (MALDI-TOF). The analytes are deposited with a matrix on a metal plate and are desorbed into the gas phase by a laser pulse. After the analytes are ionized by collision, allele specific products are discriminated by recording the time of flight of a product towards a detector, which can be related to its mass (59). Fully automated MALDI-TOF systems allowing a high-throughput of samples are available, but the need of expensive equipment and highly purified DNA analytes is disadvantageous for a clinical application.

Fluorescence-based genotype detection in solution can be performed in microtiter plates using fluorescence readout systems. These systems are for example applicable for ligation or primer extension, TaqMan, molecular beacons, Amplifluor or Invader assay. This detection format allows higher throughput of samples, however, the number of simultaneously analysable features remains limited, because for multiple analysable polymorphism usually multiple separate reactions have to be performed.

An alternative method based on the detection of SNPs by flow cytometry increasing the number of simultaneously analysable features was developed by Luminex (Austin, TX). Two different fluorescent dyes combined at ten different concentration ratios integrated in microspheres provide a set of 100 distinguishable markers, which can be coupled to capture probes. Single-base extension, allele-specific primer extension (ASPE), oligonucleotide ligation, and direct hybridization have been used

in this format for SNP detection (87). Flow cytometry is already used in the clinical environment for immuno-based analysis, so that the equipment would be available for genotypic analyses. However, although the number of parallel analysable features is significantly enhanced compared to other methods, it's number is still limited, so that depending on the necessary number of SNPs, which need to be analysed, it can still be insufficient. Furthermore, the sensitivity of the method is limited, since a certain population size of present microspheres is necessary for a reliable detection.

A promising genotyping method with a high multiplexing power is provided by DNA microarray technology. DNA microarrays for the detection and identification of ESBL and IRT gene variants have not been reported so far.

### **1.3 DNA microarrays**

#### **1.3.1 Development**

DNA microarrays allow a highly parallel analysis of genetic information. Since microarray technology was first described in the 1990s the number of technical developments and the fields of application of microarray technology have exploded. The underlying principle of a nucleic acid hybridization assay are reported since the 1960s. The vast potential of this principle could only be exploited through the development of solid-phase synthesis of nucleic acids and the introduction of the use of a solid support, which allowed a site-specific attachment and arraying of multiple nucleic acids (153). The first assays reported of this kind were designated dot blots (76) or reverse dot blots (135) using immobilized targets or probes on porous supports respectively. The term probe is used for nucleic acids of known sequence which are applied to analyze the unknown target sequences. The first arrays using *in situ* synthesized short oligonucleotides on impervious supports were described by Maskos and Southern in 1993 (103,104). These experiments established the basis of the current DNA microarray analysis technology. One of the major applications of DNA microarray analysis is the analysis of gene expression (19,40) as first reported by Schena et al. in 1995 (140). The other major application is the analysis of the genetic background, so called genotyping, for identification of species (12,57) or genetic variations (55,58) or to identify the phenotypic effect of genetic variations (24).

#### **1.3.2 Principle**

The basic principle of the DNA microarray analysis consists of DNA probes immobilized on an impermeable carrier in a highly parallel addressable format. Labeled target nucleic acids are synthesized and hybridized on the immobilized probe DNA. Unbound target DNA is washed off and the hybrids are detected via the label. The basic principle of a genotyping microarray analysis is displayed in figure 7. Probes can include synthetic oligonucleotides, amplicons or larger DNA/RNA fragments, as well as peptide nucleic acids. The probes are immobilized covalently or non-covalently on the support consisting of e.g. glass, silicon or plastic substrates usually coated with reactive groups. The microarray can have from a hundred up to  $10^6$  test sites with a size range from 10-500  $\mu\text{m}$  in a 1-2  $\text{cm}^2$  area. The test sites can be constructed by *in situ* synthesis of oligonucleotides or by deposition of presynthesized oligonucleotides or other probe molecules on the solid support by contact printing or by inkjet or microjet deposition technology. Devices allowing

electronic addressing, immobilization and hybridization at specific test sites have also been developed (61). The target nucleic acid to be analyzed can be RNA or DNA, which should preferably be labeled, so that hybrids can be directly detected. It can be synthesized by Polymerase Chain Reaction or *in vitro* transcription. For labeling fluorescent dyes, radioactive markers (153), silver precipitation on gold conjugates (1), etc. can be used. The hybridization can be carried out under standard cover slips or in flow cells or specially designed hybridization chambers. Also hybridization stations for automation of the hybridization and washing steps are available. Commercial scanners for fluorescence image acquisition apply either photomultipliers (PMTs) or charged coupled device (CCD) cameras for detection. Most current systems include two lasers for Cy3 or Cy5 excitation and two filters for the separate detection of the emitted fluorescence signals.

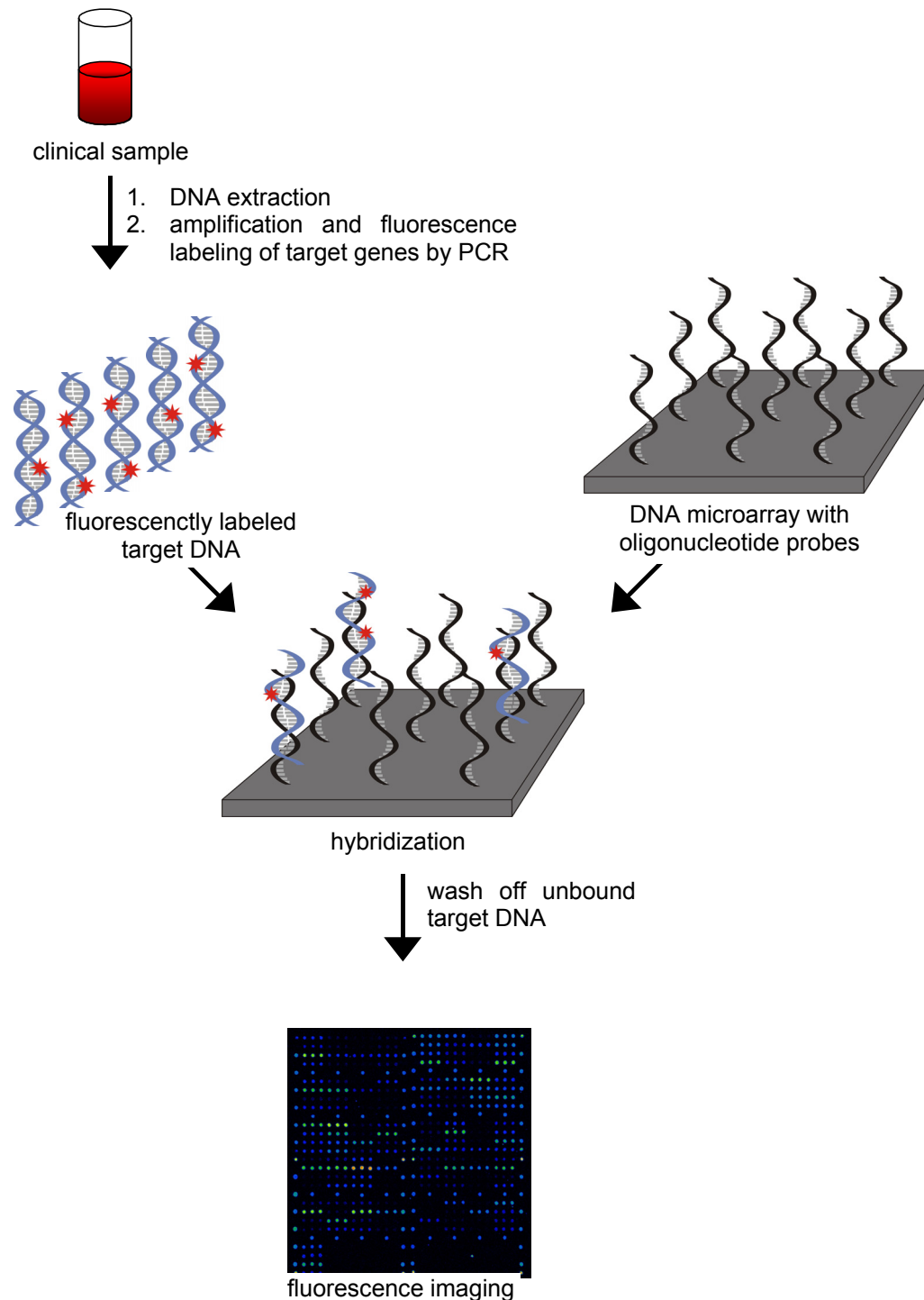


**Figure 7.** Schematic representation of a genotypic DNA microarray method. After DNA isolation from the sample the targeted genes are amplified and fluorescently labeled by PCR. The target DNA is then hybridized on the immobilized target-specific oligonucleotide probes. After washing off unbound target DNA the probe/target duplex are detected via fluorescence imaging.

### ***1.3.3 Array based genotyping methods***

In case of the detection of TEM or SHV extended spectrum beta-lactamases the single nucleotide polymorphisms (SNPs) relevant for the identification of the different variants have to be detected. Therefore, a discrimination between a perfectly matched hybrid and a non-perfectly matched hybrid between a probe and target molecule has to be achieved. For array based genotyping of single nucleotide polymorphisms (SNPs) three major reaction principles were derived for this purpose: primer extension, ligation reaction and allele specific hybridization. For the primer extension and ligation reaction enzymatic reaction steps for discrimination of the different allelic variants are performed.

Multiple array based primer extension methods have been developed. The underlying principle is the extension of an immobilized primer in a primer/target duplex by DNA Polymerase. In the single nucleotide extension assays the discriminating base is located one base upstream of the 3' end of the immobilized primer. The incorporation of a single labeled ddNTP complementary to the base present in the target DNA at the concerned position is used for allele discrimination (83,92,121). Single nucleotide primer extension in solution followed by capturing of extended primers using tag microarrays has also been described (44,63). In the array based allele specific primer extension at least two immobilized primers (one wild type, one mutation specific) are used, because the discriminating base is located at the 3' end of the immobilized primer. The primer strand is only elongated if the 3' end base is perfectly complementary to the target DNA strand (122). The possible incorporation of several labeled dNTPs during extension leads to an increased sensitivity of the assay compared to the single nucleotide extension assay.

Ligation reactions are exploited for allelic discrimination in a microarray format using immobilized oligonucleotide probes (54) or stem loop ligation probes (18). In other methods the ligation is performed in solution followed by hybridization and detection of the ligation products on tag or zipcode microarrays (37,50). Circularisable oligonucleotide ligation probes, so called padlock probes have also been used in a tag microarray format for SNP analysis and enhanced signal amplification (9,32).

Differential hybridization with allele specific oligonucleotide probes is the most commonly used reaction principle in microarray format (122). In the allele specific hybridization the discrimination is achieved by exploiting the destabilizing effect of the mismatched base in the DNA duplex. Usually four probes (termed A, G, C, and T probes) are designed to interrogate a single position in the target sequence. One is designed to be perfect complementary to the investigated sequence stretch (so called perfect match (PM) probe), the other three are identical to the first, except at the interrogated position, where one of the other three bases are substituted (so called mismatch (MM) probes). Upon hybridization with the labeled reference sequence, the probe perfectly complementary to the reference sequence will obtain the highest signal intensity. If a sample with a different base (a substitution variant) at the interrogated position is hybridized, the probe complementary to this variant will obtain the highest fluorescence intensity (94). The probes are designed with the polymorphism in the center-most position for optimal perfect match mismatch discrimination, since the destabilizing effect of the mismatched base is enhanced the more centralized the polymorphism position is in the probe/target duplex (58). The degree of the discrimination is strongly influenced by the hybridization conditions, such as pH, temperature, ionic strength, as well as the position of the polymorphism

in the probe sequence, the sequence surrounding the SNP position, and probe and target secondary structures (154). Therefore, the probe design and the reaction conditions for this method have to be thoroughly optimized. In the experimental approach of this work the allele specific hybridization method was applied for the development of the diagnostic microarray for resistance detection.

### 1.3.4 Microarray preparation

#### 1.3.4.1 Probe design

For the development of an array of allele specific hybridization probes the probes have to be selected and tested for an application under the same hybridization conditions allowing a specific identification of all tested polymorphisms. One option is to use oligos with identical length in combination with hybridization buffers, which diminish the effect of diverging melting temperatures of the oligonucleotide probes (105). Problematic is that the thermodynamic background of these effects is missing, making it impossible to predict the effects of further factors on the behavior of a given oligo probe (12).

The approach used in this work consists of a calculation of the melting temperatures of the central oligonucleotide duplexes and to design sets of oligonucleotides with similar melting temperatures but different length. Furthermore, probe secondary structures such as hairpins or dimers, which decrease the accessibility of the probe for the target DNA, were if possible excluded or minimized by *in silico* probe design analysis. There is a variety of programs on the market, which allow the automated calculation of T<sub>m</sub>s and all oligonucleotide secondary structures facilitating the choice of the appropriate oligonucleotide probe.

#### 1.3.4.2 In situ synthesis and printing

*In situ* synthesis of oligonucleotides allows the production of high density oligonucleotide arrays with a high and consistent yield of probe molecules over the surface of the support and permits the fabrication of large arrays of oligonucleotide probes in few coupling steps. The Affymetrix *in situ* process combines DNA synthesis chemistry with photolithography techniques from the microelectronic industry. Oligonucleotide probes are synthesized attached to a glass substrate. Light is directed through a mask to remove photolabile reactive groups at selected sites. Subsequently chemical building blocks are added, which form the nascent DNA strand (94). The use of micromirrors for light directed synthesis (147) or ink jet delivery of nucleotide precursors (11) to the surface have also been described.

A more generally applicable procedure of manufacturing of oligonucleotide microarrays is to deposit presynthesized oligonucleotides on the surface. This can be done by mechanical printing using pins with a capillary slot or a pin-and-ring system or by non-contact printing using an inkjet dispensing system comparable to traditional inkjet printers. In this work a Microgrid II (Biorobotics) high throughput printer was used for contact printing of presynthesized oligonucleotide probes on a chosen surface. To print the oligonucleotide probes, wolfram pins with a capillary slot were applied. The probes are dissolved in spotting buffer and the solution is drawn into the split of the submerged pin by capillary force. The force generated from the downward movement and the surface tension of the slide draws a small amount of the solution out of the split (27). The printing process involving the pins, the slide surface, the spotting buffer as well as spotting parameters such as the surrounding humidity has to be optimized empirically. Hereby the following effects have to be considered: The

spot size and shape as well as the regularity is depending on the pin specifications, the acceleration of the pin towards the slide, the surface tension of the deposited solution and the slide surface. The surrounding humidity during the printing process is especially important for a uniform drying of the spot, otherwise a concentration gradient inside the drying spot might occur, causing a not uniform probe and thus signal distribution after hybridization (e.g. donut shaped signal patterns). Different pins exhibit mostly diverging printing characteristics. To minimize variation inherent in the spotting process a set of multiple pins should be tested empirically for almost equal performance and replicate spots should be spotted with the same pin.

### 1.3.4.3 Surface and binding chemistry

Today there is a variety of carriers for microarray applications commercially available, differing in the kind of active groups used for covalent or non-covalent coupling of the probe DNA, as well as the nature and structure of the surface. For an accurate location, a precise spot shape in a  $\mu\text{m}$  size range and a facilitated automated image acquisition and processing, dimensional stable and rigid glass or plastic supports are mostly used today. Furthermore, such a flat and impermeable surface permits a good accessibility of the probe, so that the diffusion limitation due to steric hindrances in the hybridization process is decreased (153).

Glass as a solid support is easy to derivatize for immobilization of chemically modified or unmodified oligonucleotides. The most commonly used surface chemistries for DNA microarrays are planar poly-L-lysine, aldehyde or epoxy groups. The probe DNA is bound covalently to these surfaces via reactive groups of the bases itself or via additionally synthesized exposed reactive groups (e.g.  $\text{NH}_2$ ), which allow a directed immobilization (see figure 8). Tethering one end of the probe to the surface is especially advantageous for short oligonucleotide probes, since the base involved in the coupling to the surface can not take part in base pairing and thus the full-length probe sequence is not accessible for target hybridization. The effect is naturally the more pronounced the shorter the probe sequence is. In case of an allele specific hybridization, where the duplex destabilizing effect of a single base mismatch is determined, these effects have to be considered. Generally, the bases nearest to the surface are less accessible for hybridization of the target (151). Therefore, spacer molecules can be introduced between the probe sequence and the surface, so that the probe molecules are more exposed to the target molecules in solution. Spacers can be made of of polynucleotide strands (e.g. polyT (55)) or different chemical building blocks attached to the probe sequence. Hybridization yields can be increased up to two orders of magnitude by introduction of spacers (144). In this work poly-L-lysine and epoxy coated glass slides with unmodified oligonucleotide probes or oligonucleotide probes with a 5' amino group and a polyT spacer were used.



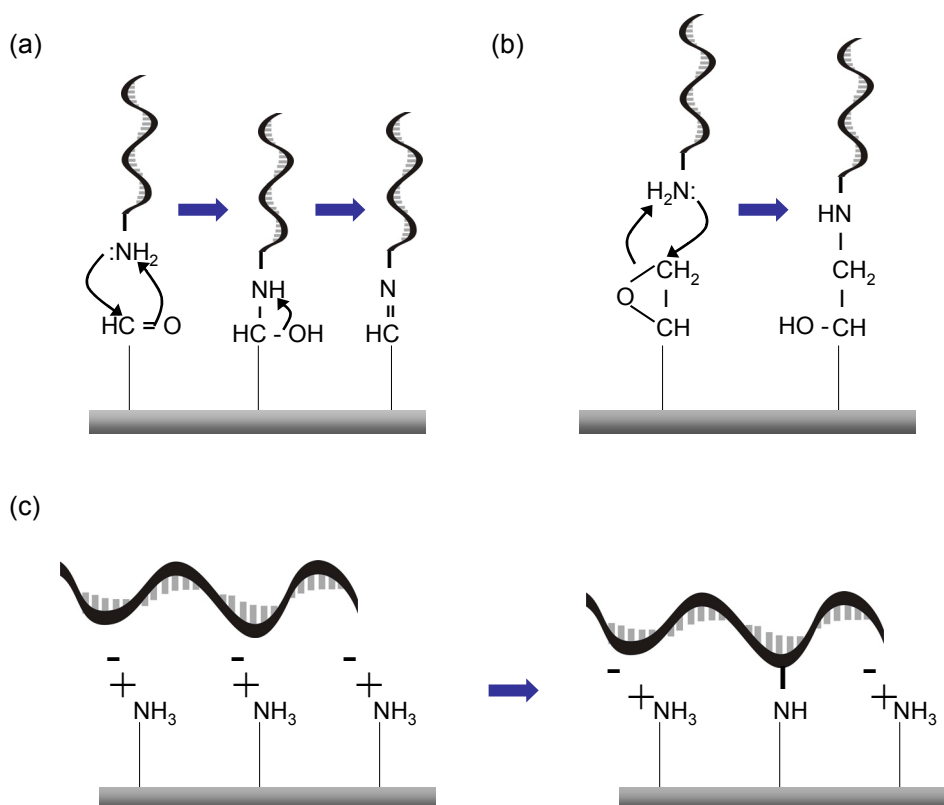


**Figure 8.** Immobilization chemistries for microarray surfaces. The (a) aldehyde or (b) epoxy groups are covalently attached to the glass surface. The DNA probes are bound via exposed amino-groups coupled at the 5' or 3' end or amino groups of the bases itself. (c) On poly-L-lysine surfaces the DNA probes are absorbed electrostatically. The probes are bound via an UV-induced radical reaction between a thymine and an amino group of the surface.

### 1.3.4.4 Target preparation

In general, for reduced sequence complexity and improved sensitivity of the assay an amplification of the target sequence is necessary. Amplification by PCR is therefore a standard part of the target preparation. The target DNA can be produced single stranded or double stranded. A commonly used method to produce single stranded targets from PCR products is to include a promoter for RNA Polymerase in one of the primers, from which RNA is transcribed. Single stranded DNA can be produced either in an asymmetric PCR or one strand of the double stranded amplicon is removed by exonuclease treatment, while the other strand is protected from exonuclease digestion by a resistant group (phosphorothioates (118) or dendritic caps (145)) annealed to one of the primers (153).

During amplification by PCR also the labeling for signal detection can be performed. Fluorescence labels are utilized in the majority of microarray experiments, because they allow high resolution imaging and a sensitive detection. Such dyes absorb light energy at a higher energetic (short) wave length and reemit light at a lower energetic (longer) wavelength. The use of fluorescent labels with differing absorption and emission spectra enables the simultaneous detection of different dyes, which is applied in microarray experiments using comparative analysis (e.g. gene expression analysis (19), loss of signal analysis (58)). The most commonly used fluorescent dyes are Cy3 or Cy5 (see figure 9). The labeling of the target DNA can be carried out via direct incorporation of fluorescently labeled nucleotides during PCR amplification or via indirect coupling: the incorporated nucleotides bear reactive groups, which can be used to couple the fluorescent label in a subsequent reaction (e. g. streptavidin-biotin or amino-allyl coupling). The labeling can also be performed during fragmentation of the target DNA (78).

For microarrays with oligonucleotide probes with a size range between 15-30 nt, it is important to apply randomly fragmented nucleic acid targets (12). This minimizes steric hindrance during hybridization due to target secondary structures and increases the diffusion rate of the targets. Furthermore different regions of the target molecule can hybridize independently from each other to each of the immobilized oligonucleotides (78). Therefore, an enhanced sensitivity and specificity of the analysis especially for SNP detection can be achieved. The random fragmentation can be performed enzymatically (by DNaseI) (31,54) or chemically (78).

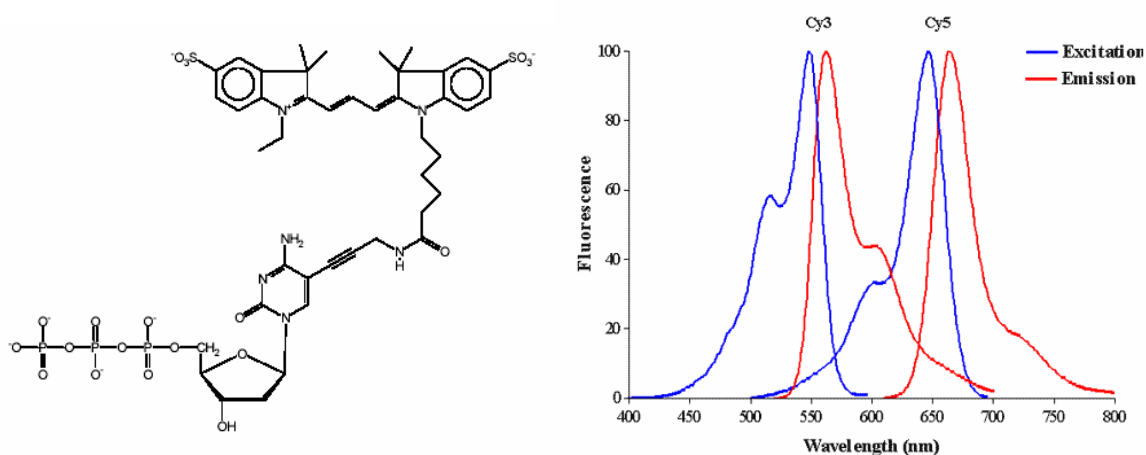


**Figure 9.** Structure of Cy3-dCTP and excitation- and emissions spectra of Cy3 and Cy5.  
Cy3:  $EX_{max}$ : 550 nm,  $Em_{max}$ : 570 nm, Molar extinction coefficient:  $150\ 000\ M^{-1}\cdot cm^{-1}$ ,  
Cy5:  $EX_{max}$ : 649 nm,  $Em_{max}$ : 670 nm, Molar extinction coefficient:  $250\ 000\ M^{-1}\cdot cm^{-1}$ ,  
[Amershambiosciences].

#### 1.3.4.5 Hybridization

Duplex formation is a multistep process that is believed to begin with an initial pairing of a small number of bases in a transient intermediate. If the two strands are complementary, duplex formation propagates from the initiation site in a process known as zippering (151). Whether a labeled target DNA fragment finds an immobilized complementary probe molecule, is depending on the diffusion of the molecule through the solution phase. In the allele specific hybridization format the discrimination between a perfectly matched probe/target duplex and a non-perfectly matched duplex has to be achieved. For maximal PM/MM discrimination the hybridization reaction has to reach an equilibrium state. This is strongly dependent on the number of probe/target meeting events and therefore the hybridization time. To accelerate this process, shorter target DNA fragments, which are less affected by diffusion limitation, and additional agitation of the solution phase can be applied. Further already mentioned factors influencing the discrimination level include ionic strength, pH,  $T_m$  of the duplexes and the hybridization temperature as well as the stringency of the following washing steps. All these parameters have to be optimized empirically.

Hybridization should be carried out in a closed compartment or a humid environment to avoid evaporation and drying of the hybridization solution resulting in high background signal intensities. Furthermore hybridization should be carried out in the dark for avoiding photobleaching of the fluorescent dyes. Multiple manual and automated methods exist for carrying out the hybridization and washing steps. In this work the major focus was to develop a highly reproducible and sensitive assay, therefore a variety of hybridization devices offering different strategies to address the aforementioned problems was tested.

#### 1.3.5 *Transfer to a marketable array format*

The application of microarray technology for diagnostic purposes and the development of marketable array formats is rapidly advancing. Here only few examples for the fast growing number of arrays, which are currently developed for diagnostic applications will be given.

In January 2005 Roche announced that its first microarray-based test, the AmpliChip CYP450 Test (36), has been cleared by the US Food and Drug Administration (FDA) for diagnostic use in the United States. The microarray is based on Affymetrix microarray technology (high density *in situ* synthesized oligonucleotide probe chips) and analyses a patient's Cytochrome P450 2D6 and 2C19 genotypes from genomic DNA extracted from a blood sample. The test results allow physicians to consider genetic information from patients for the selection of medications and doses of medications for a wide variety of common conditions such as cardiac diseases, pain and cancer.

Nanogen developed in 1999 an automated electronic microchip for fast detection of single nucleotide polymorphisms (SNPs), short tandem repeats (STRs), insertions, deletions and other mutation analyses (45). The chip allows the electronic addressing of biotinylated amplicons to selected pads, where they remain embedded through interaction with streptavidin in the permeation layer. The DNA at each test site is then hybridized to a mixture of fluorescently labeled wild-type or mutant probes. This platform has already been applied for the automated detection of mutations involved in beta-thalassemia disease (49) or in familial Mediterranean fever (FMF) (113).

## ***Introduction***

---

Furthermore, the simultaneous *in situ* amplification and genotyping of single nucleotide polymorphism involved in Factor V Leiden (FVL) disease has been shown (66). This method combines strand displacement amplification (SDA) with electrophoretic movement and concentration of DNA on an electronic microarray to provide a single platform for DNA amplification and analysis.

The Austrian Research Center Seibersdorf concentrates on the development of microbial diagnostic microarrays. A prototype microarray has been developed for the detection and community analysis of methanotrophic bacteria (12). The method involves oligonucleotide probes based on 16S rRNA or other genes, which can be used as phylogenetic markers. These probes are applied in a standard hybridization microarray format.

Since specific features of the DNA microarray technology are covered by patents, alternative strategies for the development of a marketable diagnostic array have to be found. The standard array format of oligonucleotide probes immobilized on coated glass slides is currently covered by the patent filed by Edwin Southern and Oxford Gene Technology covering the application of oligonucleotide probes immobilized on impermeable substrates (patent number EP0373203B1). Through the cooperation with Eppendorf Array Technology (EAT, Namur, Belgium) an alternative immobilization method was provided, which is not covered by this patent. Furthermore, this company provides a post-hybridization labeling technique based on the precipitation of silver on gold particles, which are bound to the target DNA via incorporation of biotinylated nucleotides. A streptavidin-gold conjugate is used in the signal development step (1). The applicability of this format for the developed arrays should be evaluated in this study.

### 1.3.6 Link of the resistance to the pathogenic bacteria

For a complete clinical application of the genotypic resistance detection the assignment of the resistance to the pathogenic bacteria is a crucial step, since the human body harbors a wide variety of non-pathogenic microorganisms, which might also carry resistance determinants. Only if the resistance can be linked to the pathogenic bacteria, a proposition for an effective antimicrobial therapy is possible. Currently this was achieved by a culture dependent preisolation of the pathogenic organism, but this is time consuming and hinders the exploitation of the full advancement potential of a genotypic diagnostic. A new approach, which was developed by coworkers at the TU-Munich, uses genetic markers for designing polynucleotide probes for a species-specific enrichment of pathogenic bacteria in microtiterplate wells (46). Afterwards a PCR with resistance gene specific primers can be carried out and the amplicon is analyzed by the resistance microarrays. The proof of principle of the method (as shown in figure 10) for the detection of resistances by microarray analysis should be shown in this work.

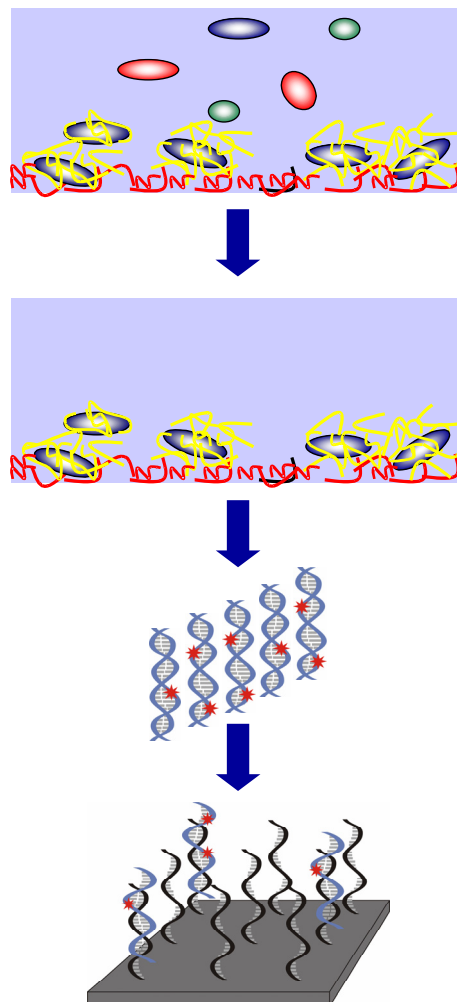


**Figure 10.** Schematic representation of species-specific enrichment and microarray analysis of resistance genes. The bacteria (in clinical samples such as urine, blood,..) are pretreated with detergents, so that the cell walls are permeabilized for probe hybridization to the targeted 16S or 23S rRNA or DNA structures. The hybridization to species-specific polynucleotide probes is carried out in solution. Afterwards the hybridized cells are separated from non-target cells via binding to microtiter cavities coated with complementary nucleic acids (46). After denaturation, the resistance gene is amplified by PCR performed in the microwells and is identified by microarray analysis.

### **1.4 Objectives**

This work was accomplished within the scope of the GenoMik (Genome research on microorganisms) project funded by the BMBF (Bundesministerium für Bildung und Forschung). This project promotes research targeting the genomic and metabolic features of bacteria important for agriculture, environmental protection, biotechnology and the health care sector. The focus of our group at the Institute of Technical Biochemistry (University of Stuttgart, Germany) is the development of rapid genotypic assays for antibiotic resistance detection in pathogenic bacteria. This work was done in cooperation with academic and industry partners. At the Robert-Bosch Hospital in Stuttgart the phenotypic testing was performed, the strain collection was supported and advice concerning the clinical microbiology point of view was provided. The Wernigerode branch of the Robert Koch Institute (the central federal institution responsible for disease control and prevention in Germany) delivered reference strains and knowledge regarding importance and prevalence of diverse antibiotic resistance traits. In a cooperation with the TU-Munich a method for the species-specific enrichment of pathogenic bacteria was provided for a combination with the resistance arrays. The industry partner Eppendorf AG supported this work with technical equipment and promotes the transfer of the developments to a marketable format. Our group also cooperates with the National Research Center for Antibiotics in Moscow, Russia for an early monitoring of emerging antibiotic resistances in eastern Europe.

The ultimate goal in this project was the development of an ESBL-Chip for the rapid, sensitive and reliable detection and identification of the clinically relevant ESBL and IRT producing beta-lactamases for application in clinical microbiology diagnostics as well as epidemiologic studies. Since their first appearance, the most reported ESBL genes belong to the TEM and SHV beta-lactamase families regarding variant numbers and producer strains. Therefore, the focus of this work was directed towards the establishment of an assay system for the detection of these variants, which is still extendable towards other beta-lactamase families (e.g. CTX-M, OXA). In summary, the major objectives of this work were (i) the ability of the assay system to detect relevant single nucleotide polymorphisms and other mutations, (ii) the unambiguous identification of all parental, ESBL and IRT variants of the TEM and SHV beta-lactamase family, (iii) the use of consensus primers for target amplification, (iv) maximal sensitivity and (v) reproducibility of the procedure, (vi) minimal assay time, (vii) validation of the assay system using clinical samples compared to clinical standard procedures, (viii) the possibility to extend the developed system for detection of other ESBL causing gene variants.

## 2 Material and Methods

### 2.1 Material

#### 2.1.1 Biological reagents

Supplier	Product
Amersham Pharmacia Biotech (Freiburg, Germany)	FluoroLink Cy3-dCTP, Cy5-dCTP
Applied Biosystems (Darmstadt, Germany)	Big-dye Terminator Cycle Sequencing Kit
Eppendorf (Hamburg, Germany)	Taq DNA-Polymerase
Gibco BRL Life Technologies (Eggenstein, Germany)	1Kb DNA Ladder, 1Kb Plus DNA Ladder
Invitrogen (Karlsruhe, Germany)	dNTPs
Promega (Mannheim, Germany)	RQ1 RNase-free DNase Kit
Qiagen (Hilden, Germany)	QIAquick PCR Purification Kit

#### 2.1.2 Chemical reagents

Supplier	Product
Gibco BRL Life Technologies Technologies (Eggenstein, Germany)	Agarose
Merck (Darmstadt, Germany)	LiChrosolv ( HPLC Water)
Sigma-Aldrich (Deisenhofen, Germany)	acetic acid, bromphenol blue, DMSO, EDTA, ethanol (100% or 95%), ethidium bromide, ethylene glycol, glycerol, HCl, KCl, 1-methyl-2-pyrrolidinon, SDS, sodium acetate, sodium borate, sodium citrate·2H <sub>2</sub> O, NaCl, Na <sub>2</sub> EDTA, NaH <sub>2</sub> PO <sub>4</sub> , NaOH, succinic acid, Tris , Triton X-100,

#### 2.1.3 Equipment

Supplier	Designation	Equipment
Advantix (Brunnthal, Germany)	hybridization compartment	arraybooster
Affymetrix (Santa Clara, US)	array-scanner	GMS 418 Array Scanner
Applied Biosystems (Darmstadt, Germany)	DNA-sequencer	ABI Prism 377-DNA-Sequencer
Amersham Pharmacia Biotech (Freiburg, Germany)	hybridization station	Lucidea Slide Pro
Biometra (Göttingen, Germany)	hybridization oven UV-crosslinker	OV5 hybridization oven Stratalinker UV Crosslinker 1800
Biorobotics (Cambridge, England)	spotter	Microgrid II Microarrayer
Corning (New York, US)	hybridization chamber	Corning Hybridization Chamber
Eppendorf (Hamburg, Germany)	centrifuge thermomixer thermomixer slide adapter PCR Cycler Automatic Pipette	5417R, 5810R and MiniSpin Thermomixer Comfort Thermomixer Slide Adapter MasterCycler Gradient, Research, Research Pro
Fujifilm (Düsseldorf, Germany)	gel documentation system	Image Reader Las-1000 Plus
Memmert (Schwabach, Germany)	drying compartment	Universal Oven (Model U)
NanoDrop Technologies	spectrophotometer	ND-1000 Spectrophotometer
Scientific Industries (New York, US)	vortex	Vortex-Genie 2
Tecan (Crailsheim, Germany)	hybridization station	HS 400 Hybridization Station
WTW (Weiheim, Germany)	pH-meter	pH500

## Material and Methods

### 2.1.4 Consumables

Supplier	Product
Eppendorf (Hamburg, Germany)	CreativeChip® Oligo Slides, in situ frames (65 µl), safe-lock tubes
Greiner bio-one (Frickenhausen, Germany)	384 well polystyrol (PS)-microtiterplates (U-form), pipette tips
Invitrogen (Karlsruhe, Germany)	oligonucleotide probes for TEM-array (desalted purity grade), PCR primers (desalted)
Metabion (Planegg-Martinsried, Germany)	5' C <sub>6</sub> -amino-modified oligonucleotide probes for SHV-array, oligonucleotide probes with 5' Cy3/Cy5-modification (controlled by MALDI_TOF)
Sigma-Aldrich (Deisenhofen, Germany)	oligonucleotide probes for TEM-array (desalted purity grade), PCR primers (desalted)

### 2.1.5 Clinical isolates

Isolate No.	Identifier Number	Sample	Species	Phenotype	Hospital
<b>Samples collected in Germany</b>					
1	421196	swab	<i>E. cloacae</i>	ESBL	Robert Bosch Hospital
2	474273	urine	<i>E. cloacae</i>	ESBL	Robert Bosch Hospital
3	477997	swab	<i>E. cloacae</i>	ESBL	Robert Bosch Hospital
4	479803	blood	<i>E. amnigenus</i>	ESBL	Robert Bosch Hospital
5	405339	swab	<i>E. cloacae</i>	ESBL	Robert Bosch Hospital
6	406551	urine	Enterobacter spp.	ESBL	Robert Bosch Hospital
7	410147	vaginal swab	<i>E. cloacae</i>	ESBL	Robert Bosch Hospital
8	431859	dialysate	<i>E. cloacae</i>	ESBL	Robert Bosch Hospital
9	431196	BAL	<i>E. cloacae</i>	ESBL	Robert Bosch Hospital
10	431389	urine	<i>E. cloacae</i>	ESBL	Robert Bosch Hospital
11	432697	urine	<i>E. cloacae</i>	ESBL	Robert Bosch Hospital
12	435727	tracheal swab	Klebsiella spp.	ESBL	Robert Bosch Hospital
13	445421	vaginal swab	<i>E. coli</i>	ESBL	Robert Bosch Hospital
14	445437	cervix swab	<i>E. cloacae</i>	ESBL	Robert Bosch Hospital
15	429457	urine	<i>K. pneumoniae</i>	ESBL	Robert Bosch Hospital
16	456789	decubitus swab	Klebsiella spp.	ESBL	Robert Bosch Hospital
17	442766	tracheal swab	<i>E. sakazakii</i>	ESBL	Robert Bosch Hospital
<b>Samples collected in Russia</b>					
25	361	n.s.	<i>E. coli</i>	ESBL	Moscow City Clinic
26	932	n.s.	<i>E. coli</i>	ESBL	Moscow City Clinic
31	n.s	n.s.	<i>P. mirabilis</i>	ESBL/ AmpC	Moscow City Clinic
37	14451	n.s.	<i>K. pneumoniae</i>	ESBL	Moscow City Clinic
39	47a	n.s.	Klebsiella spp.	ESBL	Moscow City Clinic
41	241	n.s.	<i>E. coli</i>	no ESBL	Moscow City Clinic
43	1140	n.s.	<i>E. coli</i>	ESBL	Moscow City Clinic
50	15935	n.s.	<i>K. pneumoniae</i>	ESBL	Central Russian Military Hospital
52	18721	n.s.	<i>E. aerogenes</i>	ESBL	Central Russian Military Hospital
55	20426	n.s.	<i>E. coli</i>	ESBL	Central Russian Military Hospital
57	20585/2	n.s.	<i>E. coli</i>	ESBL	Central Russian Military Hospital
59	129	n.s.	<i>K. pneumoniae</i>	ESBL	Moscow City Clinic
64	1949/2	n.s.	<i>K. pneumoniae</i>	ESBL	Moscow City Clinic
67	361	n.s.	<i>C. freundii</i>	ESBL/ AmpC	Tomsk City Hospital
68	n.s	n.s.	<i>M. morgani</i>	ESBL	Tomsk City Hospital



75	52	n.s.	<i>K. pneumoniae</i>	ESBL	National Research Center for Pediatric Diseases
77	212	n.s.	<i>E. coli</i>	not pure	Moscow City Clinic
79	161	n.s.	<i>E. coli</i>	ESBL	Moscow City Clinic
83	571	n.s.	<i>E. coli</i>	ESBL	Tomsk City Hospital
86	622	n.s.	<i>C. freundii</i>	ESBL/ AmpC	Tomsk City Hospital
87	533	n.s.	<i>E. coli</i>	ESBL	Tomsk City Hospital
90	271	n.s.	<i>P. vulgaris</i>	ESBL	Tomsk City Hospital
92	73	n.s.	<i>K. pneumoniae</i>	ESBL	National Research Center for Pediatric Diseases
93	771	n.s.	<i>E. coli</i>	ESBL/ AmpC	Tomsk City Hospital
94	358	n.s.	<i>E. coli</i>	ESBL	Tomsk City Hospital
95	358	n.s.	<i>K. pneumoniae</i>	ESBL	Tomsk City Hospital
96	797	n.s.	<i>C. freundii</i>	ESBL/ AmpC	Tomsk City Hospital
98	896	n.s.	<i>C. freundii</i>	ESBL	Tomsk City Hospital
99	761	n.s.	<i>C. freundii</i>	ESBL	Tomsk City Hospital
100	813	n.s.	<i>E. coli</i>	no ESBL	Tomsk City Hospital
<b>Samples collected in Croatia</b>					
1	32193/03	urine	<i>K. pneumoniae</i>	ESBL	Zadar Hospital
2	31300/03	wound swab	<i>K. ornithinolytica</i>	CTX-M	Zadar Hospital
3	37254/03		<i>E. coli</i>	ESBL	Zadar Hospital
4	30164/03	urine	<i>K. pneumoniae</i>	ESBL	Zadar Hospital
5	30903/03	urine	<i>K. pneumoniae</i>	ESBL	Zadar Hospital
6	28505/03	urine	<i>K. pneumoniae</i>	ESBL	Zadar Hospital
7	19445/03	urine	<i>K. pneumoniae</i>	ESBL	Zadar Hospital
8	34136/03	n.s.	<i>K. pneumoniae</i>	ESBL	Zadar Hospital
9	28390/03	urine	<i>K. terrigena</i>	ESBL	Zadar Hospital
10	20214/03	urine	<i>E. coli</i>	ESBL	Zadar Hospital
11	18945/03	n.s.	<i>K. pneumoniae</i>	ESBL	Zadar Hospital
12	31015/03	wound swab	<i>K. pneumoniae</i>	ESBL	Zadar Hospital
13	30953	n.s.	<i>K. pneumoniae</i>	no ESBL	Zadar Hospital
14	19586/03	blood	<i>K. pneumoniae</i>	ESBL	Zadar Hospital
15	34640/03	urine	<i>E. coli</i>	ESBL	Zadar Hospital
16	32199/03	urine	<i>K. pneumoniae</i>	ESBL	Zadar Hospital
18	15	urine	<i>E. coli</i>	ESBL	Zadar Hospital
19	34601/03	urine	<i>K. pneumoniae</i>	ESBL	Zadar Hospital
20	33913/03	urine	<i>K. pneumoniae</i>	ESBL/ AmpC	Zadar Hospital
21	35710/03	urine	<i>E. coli</i>	no ESBL	Zadar Hospital
22	14	blood	<i>E. coli</i>	ESBL	Zadar Hospital
23	28	vaginal swab	<i>E. coli</i>	ESBL	Zadar Hospital
24	16	n.s.	<i>E. coli</i>	ESBL	Zadar Hospital
25	32929/03	urine	<i>K. pneumoniae</i>	ESBL	Zadar Hospital
26	31696/03	urine	<i>K. oxytoca</i>	K1	Zadar Hospital
27	2	n.s.	<i>E. coli</i>	ESBL	Zadar Hospital
28	32198/03	urine	<i>K. pneumoniae</i>	ESBL	Zadar Hospital
29	34078/03	urine	<i>K. pneumoniae</i>	ESBL	Zadar Hospital
30	35646/03	n.s.	<i>K. pneumoniae</i>	ESBL	Zadar Hospital
31	28504/03	urine	<i>K. pneumoniae</i>	ESBL	Zadar Hospital
32	29933/03	urine	<i>K. pneumoniae</i>	no ESBL	Zadar Hospital
33	30350/03	urine	<i>K. pneumoniae</i>	ESBL	Zadar Hospital
34	29332/03	n.s.	<i>K. pneumoniae</i>	ESBL	Zadar Hospital

## Material and Methods

35	29843/03	n.s.	<i>K. pneumoniae</i>	ESBL	Zadar Hospital
36	19415/03	n.s.	<i>E. coli</i>	not clear	Zadar Hospital

n.s. = no specification

### 2.1.6 Software

Supplier	Product
Biodiscovery (Los Angeles, USA)	ImaGene™ (Version 3.0)
DNASTar (Madison, USA)	SeqMan™ II (Version 5.0)
Molecular Biology Insights (Cascade, USA)	Oligo (Version 6.65)
PREMIER Biosoft International (Palo Alto, Canada)	Array Designer (Version 2.0)
freeware ( <a href="ftp://ftp-igbmc.u-strasbg.fr/pub/ClustalX/">ftp://ftp-igbmc.u-strasbg.fr/pub/ClustalX/</a> )	ClustalX (Version 1.81)
freeware ( <a href="http://www.ncbi.nlm.nih.gov/BLAST">http://www.ncbi.nlm.nih.gov/BLAST</a> )	nucleotide - nucleotide BLAST (blastn)

### 2.2 Solutions

Name	Composition
Blocking solution for poly-L-lysine-slides	0.18 M succinic acid anhydride, 44 mM sodium borate (pH 8.0) in methyl-pyrrolidinone
Spotting buffer for poly-L-lysine-slides	50 % DMSO (v/v) in ddH <sub>2</sub> O
Spotting buffer for epoxy slides	160 mM Na <sub>2</sub> SO <sub>4</sub> , 130 mM Na <sub>2</sub> HPO <sub>4</sub> in ddH <sub>2</sub> O
Betaine spotting buffer	3 x SSC, 1 M betaine
Rinse solution 1 for epoxy slides	0.1 % (v/v) Triton x 100 in ddH <sub>2</sub> O
Rinse solution 2 for epoxy slides	0.5 µl conc. HCl per ml ddH <sub>2</sub> O
Rinse solution 3 for epoxy slides	100 mM KCl
Blocking solution for epoxy slides	25 % (v/v) ethylene glycol, 0.5 µl conc. HCl per ml ddH <sub>2</sub> O
20 X SSPE	175.3 g NaCl, 88.2 g NaH <sub>2</sub> PO <sub>4</sub> ·1H <sub>2</sub> O, 7.4 g Na <sub>2</sub> EDTA, 800 ml H <sub>2</sub> O, 10 M NaOH (pH 7.4) ad 1l ddH <sub>2</sub> O
20 X SSC	175.3 NaCl, 88.2 g Na <sub>3</sub> Citrat·2H <sub>2</sub> O, HCl (pH 7.0) ad 1l ddH <sub>2</sub> O
Wash solution 1 for PLL-slides	2 x SSC, 0.1% SDS
Wash solution 2 for PLL-slides	0.2 x SSC
Wash solution 1 for epoxy slides	2 x SSC, 0.2% SDS
Wash solution 2 for epoxy slides	2 x SSC
Wash solution 3 for epoxy slides	0.2 x SSC

## **2.3 Methods**

### *2.3.1 Identification of SNP positions*

To identify the SNP (single nucleotide polymorphism) positions data was extracted from web resources containing published amino acid exchanges (<http://www.lahey.org/Studies/>) and a multisequence alignment of all available *bla<sub>SHV</sub>* and *bla<sub>TEM</sub>* nucleotide sequences was established using ClustalX (Version 1.81, freeware).

### *2.3.2 Probe design*

#### *2.3.2.1 TEM-array*

For 41 SNP positions (ESBL, IRT, or both; see table 3) oligonucleotide probes were designed with variable lengths (17 - 27 bases) (see table 4 and 5). For maximum perfect match/mismatch discrimination during hybridization the probes were designed with the SNP at the central base within the probe sequence. For each SNP a probe set of 4 probes was designed with identical sequence except the central base, which is either A, T, G, or C. The SNP probes are named after the position of the amino acid substitution within the TEM sequence, that means probe number 161 defines the polymorphism at position 161 in the TEM amino acid sequence. For seven amino acid substitution positions there are two polymorphisms within one triplet. For these, two SNP probe sets (2 x 4 probes) were designed (e. g. 162, 162.2).

The probe length, the melting temperature ( $T_m$  °C), GC content (GC %), free energy of hairpin bonds (hairpin  $\Delta G$  kcal/mol), the number of bases forming the hairpin bond (hairpin bond), free energy of dimers (dimer  $\Delta G$  kcal/mol), the number of bases forming the dimer bond (dimer bond) as displayed in table 4 were calculated by ArrayDesigner 2.0 software (Premier Biosoft International, Palo Alto, US) using default values: 0.25 nM DNA, 50 mM monovalent ions, 1.5 mM free  $Mg^{2+}$ , temperature for free energy calculation: 25°C. In this program  $T_m$  is calculated based on nearest neighbor thermodynamic theory using SantaLucia values. Entropy and enthalpy calculations are based upon the thermodynamic library of all 10 Watson-Crick DNA nearest-neighbor interactions determined by SantaLucia et al. (139).

#### *2.3.2.2 SHV-array*

For 37 mutation positions (ESBL, IRT, table 8) oligonucleotide probes were designed with variable lengths (15 - 25 bases) (see tables 9 - 12). Secondary structure's  $\Delta G$  values and the melting temperatures were calculated by ArrayDesigner 2.0 software (see above). As for the TEM-array the probes were designed with the mutation at the central position within the probe sequence. For each SNP a probe set of 4 probes was designed with identical sequence except the central base, which is either A, T, G, or C. The probes are named for the position of the amino acid substitution within the SHV sequence, that means probe No 03 defines the polymorphism at position 03 in the SHV amino acid sequence. For amino acid substitution position 175 there are two polymorphisms within one triplet. For this, two SNP probe sets (2 x 4 probes) were designed (e. g. 175.1, 175.1). For the neighboring amino acid position 234 and 235 multiple amino acid exchanges occur. For each naturally occurring SHV-mutant sequence one perfect match probe was designed. These probes are designated by the targeted amino acids at position 234/5 (GE, SE, SK, AE, AK) and the nucleotide at the third codon position for amino acid 235 (GEa or GEg). At three amino acid positions more than one neighboring nucleotide differs in the mutant sequence from

the wildtype sequence (for amino acid position 135/6: GGCC to CCGG, 188/9: GC to CG, 163: insertion of 15 nucleotides), here for each position one probe ( $136_{\text{WILDTYPE}}$ ,  $188/9_{\text{WILDTYPE}}$ ,  $163_{\text{WILDTYPE}}$ ) matching the wildtype sequence (SHV-1) and one probe ( $136_{\text{MUTANT}}$ ,  $188/9_{\text{MUTANT}}$ ,  $163_{\text{MUTANT}}$ ) matching the mutant sequence were designed.

### 2.3.3 Oligonucleotide array fabrication on poly-L-lysine-slides

The array layout (shown in figure 11) was spotted in 4 replicates, each one with a different pin. The probes were dissolved in spotting buffer (50 % DMSO) to a final concentration of 20  $\mu\text{M}$  and spotted with a MicroGrid II using MicroSpot 2500 pins (BioRobotics, Cambridge, UK) on poly-L-Lysine-slides (Sigma-Aldrich, Deisenhofen, Germany). For covalent immobilization the oligonucleotide array was irradiated with 120  $\text{mJ}/\text{m}^2$  in a UV crosslinker (Stratalinker, Biometra, Göttingen, Germany). For blocking, the slides were incubated in blocking solution (0.18 M succinic acid anhydride, 44 mM sodium borate (pH 8.0) in methyl-pyrrolidinone) for 15 min under agitation in a glass container. For cleaning, the slides were rinsed shortly in ddH<sub>2</sub>O and 95 % ethanol and then dried by nitrogen flow. The spot size was estimated to be 150  $\mu\text{m}$  and the spot to spot distance was 320  $\mu\text{m}$ . The processed slides were stored for maximally 20 days dry at room temperature in the dark until further use.

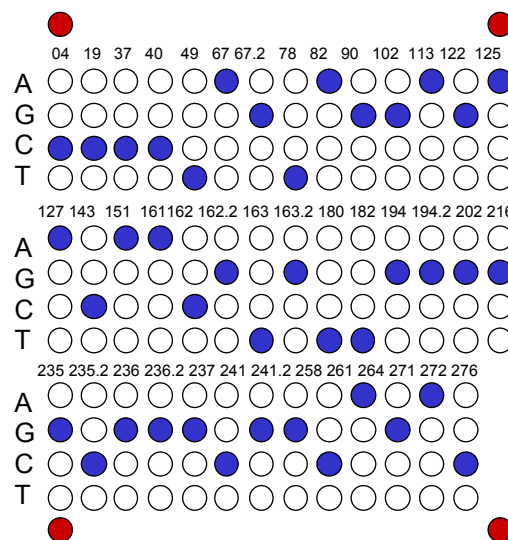


**Figure 11.** One probe set layout of the TEM-microarray on poly-L-lysine slides is displayed. The TEM-array was spotted in 4 identical replicate layouts with four different pins. In the layout the SNP position is indicated above each probe set. The central base in the probe sequence is indicated on the left side of the row as A, G, C or T. Blue spots designate perfect match positions for *bla*<sub>TEM-116</sub> gene, white spots refer to mismatch positions. The spotting controls (indicated in red) frame each replicate layout spotted by a different pin.

### 2.3.4 Oligonucleotide array fabrication on epoxy slides

#### 2.3.4.1 Setting up the system

In the initial spot test a spotting control and a probe set were spotted with a MicroGrid II using MicroSpot 2500 pins (BioRobotics, Cambridge, UK) at a final concentration of 20  $\mu\text{M}$  in DMSO- (50 % DMSO), betaine- (3 x SSC, 1 M betaine) or phosphate-based (160 mM Na<sub>2</sub>SO<sub>4</sub>, 130 mM Na<sub>2</sub>HPO<sub>4</sub>) spotting buffer on epoxy slides. The spotting control was spotted in 32 replicates, the probe set in four replicates for each of eight pins. For covalent immobilization the oligonucleotide array was incubated at 120 °C for 30 min in a drying compartment (Mettler, Schwabach, Germany). For blocking,

the slides were rinsed for 5 min in 0.1 % (v/v) Triton x 100 in ddH<sub>2</sub>O, 4 min in 0.5 μl conc. HCl per ml ddH<sub>2</sub>O, for 10 min in 100 mM KCl solution while constantly stirring. Subsequently, the slides were incubated in blocking solution (25 % (v/v) ethylenglycol, 0.5 μl conc. HCl per ml ddH<sub>2</sub>O) with the spotted side upwards at 50 °C in a heating compartment (OV5, Biometra, Göttingen, Germany). For cleaning, the slides were rinsed in ddH<sub>2</sub>O for 1 min and then dried by nitrogen flow.

### 2.3.4.2 TEM-array

Oligonucleotide arrays were constructed with 168 oligonucleotide capture probes. The oligonucleotides were purchased from Invitrogen (Karlsruhe, Germany) at a desalted purity grade. The capture and control probe sequences are given in table 5. Each SNP probe was spotted in triplicate. The array layout is shown in figure 12. The probes were dissolved in spotting buffer (160 mM Na<sub>2</sub>SO<sub>4</sub>, 130 mM Na<sub>2</sub>HPO<sub>4</sub>) to a final concentration of 20 μM and spotted with a MicroGrid II using MicroSpot 2500 pins (BioRobotics, Cambridge, UK) on epoxy coated glass slides (Elipsa, Berlin, Germany). The immobilization and blocking procedure was identical to the parameters described in section 2.3.4.1. The spot size was estimated to be 150 μm and the spot to spot distance was 320 μm. The processed slides were stored for maximally 20 days dry at room temperature in the dark until further use.

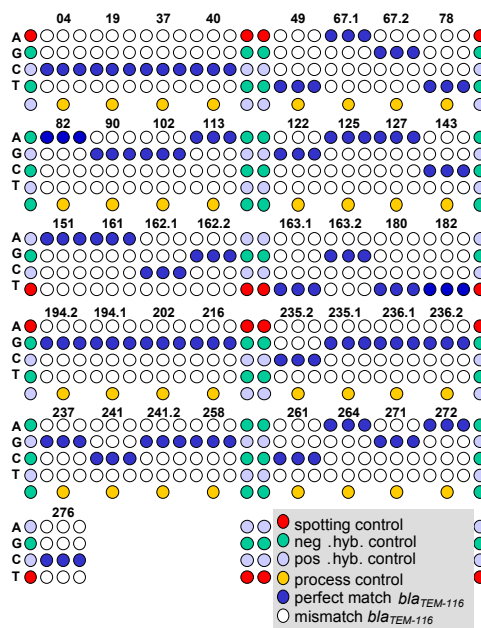


**Figure 12.** The SNP capture probe layout of the TEM microarray on epoxy-coated slides is shown. All SNP capture probes were spotted in triplicates. The SNP position is indicated above each triplicate. The central base in the probe sequence is indicated on the left side of each row as A, G, C or T. Blue spots indicate perfect match positions for *bla*<sub>TEM-116</sub> gene, white spots indicate mismatch positions. Negative and positive hybridization controls are indicated as neg. hyb. and pos. hyb. controls respectively.

2.3.4.3 SHV-array

Oligonucleotide arrays for SHV were constructed with 151 oligonucleotide capture probes. The array layout is shown in figure 13. The oligonucleotides were purchased from Metabion (München, Germany) with a desalted purity grade. The capture and control probe sequences are given in table 12, all probes were equipped with a 13 thymidine spacer and a C<sub>6</sub>-aminomodification. Further production parameters were identical to fabrication of the TEM-array.

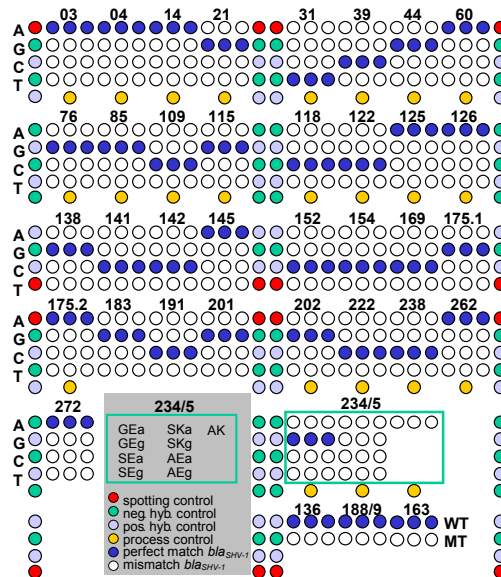


**Figure 13.** The spotting layout of the mutation capture probes of the SHV microarray is displayed. All mutation specific capture probes were spotted in triplicate. The mutation position is indicated above each triplicate. For the SNP specific probes the nucleotide at the central base is indicated on the left side of each row as A, G, C or T. For probe No. 234/5 the probes are designated by the targeted amino acids at position 234/5 (GE, SE, SK, AE, AK) and the nucleotide at the third codon position for amino acid 235 (GEa or GEG) as indicated in the legend. For position 136, 188/9, 163 one probe triplet (WT) matching the wild type sequence (*bla<sub>SHV-1</sub>*) and one probe triplet (MT) matching the mutant sequence (*bla<sub>SHV-X</sub>*) are spotted. Negative and positive hybridization controls are indicated as neg. hyb. and pos. hyb controls respectively.

2.3.5 Controls

Several controls were included on the array: a spotting control (5'-tttttttttttctagacagccactcata-Cy3/Cy5 3'), a positive hybridization control (5'-tttttttttttgattggacgagtcaggagc-3') complementary to a labeled oligonucleotide target (5'-Cy3/5-gctcctgactcgtccaatc-3'), which was spiked in during hybridization, and a negative hybridization control (5'-tttttttttttctagacagccactcata-3'). All these controls consisted of sequences unrelated to bacterial species and were equipped with a C<sub>6</sub>-aminomodification at the 5' end. The process control (5'-NH<sub>2</sub>-ttttttttttttaaagtagtctgctctgcggc-3' for *bla<sub>SHV</sub>*; and 5'-agaaacgctggtgaaagt-3' for *bla<sub>TEM</sub>*) corresponded to a conserved sequence within the *bla<sub>SHV</sub>* or *bla<sub>TEM</sub>* gene family. The spotting controls were set at the corner positions of each subgrid, which was spotted by a different pin. The positive and negative hybridization controls appeared alternately at the side borders of each subgrid. The process controls were spotted in two lines bordering the central SNP probe sets of each subgrid (figure 12 and 13).

### 2.3.6 Bacterial strains

As TEM reference samples two EARSS (European Antibiotic Resistance Surveillance System) reference strains and two strains carrying ESBL-type TEM variants were provided by the Robert Koch Institute in Wernigerode. As SHV reference samples *E. coli* DH5 $\alpha$  transformed with *bla*<sub>SHV</sub> target genes in a pCCR9 target vector were used, which were kindly provided by H. Hächler (Institute of Medical Microbiology, University of Zurich, Switzerland). The bacterial strains were inoculated in 5 ml LB with 50  $\mu$ g ampicillin per ml and incubated overnight at 37°C. Clinical samples were taken during the daily routine of the cooperating hospitals (see section 2.1.5) and processed following standard operation procedures. Prior to microarray analysis, the isolated bacterial strains were inoculated on Müller-Hinton agar plates at 37°C over night. Plasmid DNA was extracted according to the QIAprep Spin Miniprep Kit protocol (Qiagen, Hilden, Germany).

After isolation, bacterial strain identification was performed according to NCCLS standard operation procedures at the Robert Bosch Hospital (RBK) in Stuttgart. Antibiotic resistance determination and confirmation of ESBL phenotypes was also performed at the RBK by agar diffusion testing with ceftazidime, cefotaxime and cefpodoxime with and without clavulanic acid, as well as ceftioxin and aztreonam according to NCCLS standard operation procedures. Automated species identification and ESBL screening were performed at the RBK using an automated microdilution test system (WalkAway 5105, Neg Breakpoint Combo Panel Type 30, Dade MicroScan, West Sacramento, US) according to the manufacturer's protocol.

### 2.3.7 Preparation of target DNA

#### 2.3.7.1 Amplification and labeling

##### **TEM**

The target DNA for hybridization on the oligonucleotide arrays was synthesized by PCR. The sequences of the amplification primers for the *bla*<sub>TEM</sub> gene (with an expected amplicon length of 861 bp) were for the forward primer "temforw": (5'-atgagtattcaacatttccg-3') and reverse "temrev" (5'-ttaatcagtgaggcacctat-3'). For PCR amplification and labeling 1 – 75 ng of plasmid DNA was supplemented with 0.4  $\mu$ M forward and reverse primer, PCR-buffer (2.5 mM Mg(OAc)<sub>2</sub>, 50 mM KCl, 10 mM Tris-HCl pH 8.3) containing 50  $\mu$ M dATP, dGTP, dTTP, 30  $\mu$ M dCTP, 20  $\mu$ M Cy5- or Cy3-dCTP (Amersham Biosciences, Freiburg, Germany) and 10 U Taq DNA Polymerase (Eppendorf, Hamburg, Germany) in a total volume of 100  $\mu$ l. The amplification was performed in a Mastercycler Gradient (Eppendorf, Hamburg, Germany). An initial denaturation step (94°C for 1 min) was followed by 30 cycles (94°C for 30 s, 55°C for 30 s, 72°C for 1 min) and a final extension step at 72°C for 4 min.

##### **SHV**

The sequences of the amplification primers for the *bla*<sub>SHV</sub> gene (with an expected amplicon length of 932 bp) were for the forward primer "shvforw": (5'-gcaaaacgccgggttattc -3') and reverse "shvrev" (5'-ggtagcgttgccagtgc-3'). For PCR amplification and labeling 30-80 ng of plasmid DNA was supplemented with 0.4  $\mu$ M forward and reverse primer, PCR-buffer (2 % DMSO, 2.5 mM Mg(OAc)<sub>2</sub>, 50 mM KCl, 10 mM Tris-HCl pH 8.3) containing 50  $\mu$ M dATP, dGTP, dTTP, 30  $\mu$ M dCTP, 20  $\mu$ M Cy3-dCTP (Amersham Biosciences, Freiburg, Germany) and 10 U Taq DNA Polymerase (Eppendorf, Hamburg, Germany) in a total volume of 100  $\mu$ l. The

## Material and Methods

---

amplification was performed in a Mastercycler Gradient (Eppendorf, Hamburg, Germany). An initial denaturation step (94°C for 1 min) was followed by 30 cycles (94°C for 1min, 54°C for 1 min, 72°C for 1 min) and a final extension step at 72°C for 4 min.

### 2.3.7.2 Purification

The PCR product was purified with the Qiaquick® Spin PCR Purification Kit (Qiagen, Hilden, Germany) according to the manufacture's protocol. The DNA was eluted in 30 µl ddH<sub>2</sub>O.

### 2.3.7.3 Determination of incorporation ratio

The concentration of DNA and fluorescent dye was determined using 1 µl purified target DNA by measuring the absorption of DNA at 260 nm, Cy3 at 550 nm and Cy5 at 650 nm with the ND-1000 Spectrophotometer (NanoDrop Technologies, Rockland, USA) and by calculating the concentrations by Lambert Beer's law. The incorporation ratio of Cy3- or Cy5-dCTP, expressed as number of nucleotides/incorporated fluorescent dye (NT/F) was determined by the following formula:

$$R = \frac{C_{DNA} \times 1000}{M_A \cdot C_F}$$

R: incorporation ratio of Cy3 or Cy5 in NT/Cy3 or NT/Cy5

C<sub>DNA</sub>: DNA concentration in ng/µl

C<sub>F</sub>: Cy3 or Cy5 concentration in pmol/µl

M<sub>A</sub>: average molecular weight of one nucleotide in g/mol (app. 330g/mol)

### 2.3.7.4 Fragmentation

The amplified and labeled target DNA was diluted to a concentration of 30 ng/µl in reaction buffer (40mM Tris-HCl, pH 8, 10 mM MgSO<sub>4</sub>, 1 mM CaCl<sub>2</sub>) and fragmented with DNaseI (11.5 mU/µl) (Promega, Mannheim, Germany) at room temperature for 5 min to fragment sizes of about 15 to 150 bp. The reaction was stopped by the addition of 3 mM EGTA and incubation at 65°C for 10 min.

### 2.3.7.5 Determination of fragment sizes

Fragment sizes were estimated by *lab-on-a-chip* electrophoresis (Bioanalyzer 2100 and DNA 1000 LabChip kit, Agilent, Böblingen, Germany) using 1 µl of fragmented target DNA. The analysis was performed according to the manufacture's protocol.

## 2.3.8 Hybridization

### 2.3.8.1 Preparation

If not stated otherwise, the hybridization solution consisted of fragmented target DNA with addition of control DNA (5'-Cy3- or Cy5-gctcctgactcgtccaatc-3', 0.05 pmol) in 6 x SSPE. All hybridizations were carried out at 45°C. The amount of target DNA (25-400 ng) was depending on the experiment and the incorporation ratio (50 - 150 NT/F). The duration of the hybridization (10 min - 3 h) and the total volume (30 - 65 µl) of the hybridization sample depended on the experiment and the applied hybridization method.



#### 2.3.8.2 Hybridization without agitation

##### **Cover glass hybridization**

The hybridization sample was hybridized with the DNA microarray under a 18 x 18 mm cover glass (Knittel Gläser, Braunschweig, Germany) in a total volume of 30 µl, while incubating in hybridization chambers (Corning, New York, USA), which were placed in a hybridization oven (OV5, Biometra, Göttingen, Germany) for 3 hours.

##### **Hybridization in sealing frames**

The hybridization sample was hybridized with the DNA microarray in *in situ frames* (Eppendorf, Hamburg, Germany) in a total volume of 65 µl, while incubating in a hybridization oven (OV5, Biometra, Göttingen, Germany) for 15 min - 1 hour.

#### 2.3.8.3 Hybridization with agitation

##### **ArrayBooster**

The hybridization sample was hybridized with the DNA microarray in the ArrayBooster (Advalytix, Brunthal, Germany) under a special cover glass (AdvaCard™-micro agitation chip card for 40 µl) with 50-65 ng DNA in a total volume of 40 µl for 30 min - 3 hours with a medium agitation intensity as defined by the manufacturer.

##### **Thermomixer**

The hybridization sample was hybridized with the DNA microarray in *in situ frames* (Eppendorf, Hamburg, Germany) in a total volume of 65 µl, while incubating in a thermomixer slide adapter for 15 min - 1 hour at 45 °C under agitation at 1200 rpm.

##### **Wash and dry**

When a non-automated hybridization was carried out, the washing steps were as follows: After hybridization the poly-L-lysine-slides were washed for 15 min in wash solution 1 (2 X SSC, 0.1 % SDS) and 3 min in wash solution 2 (0,2 x SSC) with agitation in a glass container. For epoxy slides: the slides were washed with 2 x SSC, 0.2 % SDS then 2 x SSC and finally 0.2 x SSC, each time for 10 minutes at room temperature with agitation in a glass container. Finally the slides were dried with N<sub>2</sub>.

#### 2.3.8.4 Automated hybridization and washing

##### **HS4800 or HS400**

These hybridizations were carried out with the hybridization station HS 400 or HS 4800 (Tecan, Crailsheim, Germany) with an initial wash step at 45°C with 6 x SSPE for 30 s, followed by the injection of the hybridization sample in a total volume of 65 µl and hybridization under medium agitation intensity (as defined by the manufacturer) for 15 min - 3 hours. The slides were then washed at room temperature 2 times for 2 min in 2 x SSC, 0.2% SDS and for 1.5 min in 0.2 x SSC. The slides were dried with N<sub>2</sub> for 2 min.

##### **Lucidea Slide Pro**

These hybridizations were carried out with the hybridization station Lucidea Slide Pro (Amersham Pharmacia Biotech, Freiburg, Germany) starting with the injection of the hybridization sample containing 75 ng DNA in a total volume of 250 µl and hybridization for 15 min (mixing cycles: 5 cycles of 3 min); 30 min (mixing cycles: 10 cycles of 3 min); 1h (mixing cycles: 10 cycles of 6 min) (mixing cycles as defined by

the manufacturer). The slides were then washed at room temperature for 2 min in 2 x SSC, 0.2 % SDS, 2 min in 2 x SSC and for 2min in 0.2 x SSC. The slides were dried with N<sub>2</sub> for 2 min.

### **2.3.9 Data acquisition and processing**

Data from oligonucleotide arrays after the hybridization reaction were extracted by acquisition of fluorescence signals with a 418 Array Scanner (Affymetrix, Santa Clara, US) at laser power and gain settings to 100 %. The image processing and calculation of signal intensities was performed using Imagene, Version 3.0 (Biodiscovery, Los Angeles, US). For the calculation of the individual net signal intensities the local background was subtracted from the raw spot intensity. To calculate the mean net signal intensity of one oligo probe on all arrays tested under identical conditions (each carrying three replicate spots of one oligo probe), n replicates of one spot were used (n = number of analyzed spots), herein referred to as "net signal intensity" (NI) (see figure 14a).

Within each oligo set related to one SNP, the highest signal intensity was taken as potential perfect match (PM). The remaining three oligo probes having a lower signal were considered as mismatch (MM). For comparison of inter array variation, mean intensity ratios were calculated by forming the ratio of the mismatch or perfect match signal intensity to the perfect match signal intensity within one SNP probe set and calculating the mean between n probe sets, herein referred to as "relative intensity" (RI) of one oligo probe [ $RI_{MM} = NI_{MM}/NI_{PM}$  and  $RI_{PM} = NI_{PM}/NI_{PM}$ ] (n = number of analyzed spots) (see figure 14b). Accordingly, the perfect match relative intensities  $RI_{PM}$  should correspond to a value of 1, the mismatch relative intensities  $RI_{MM}$  should be below 1. The efficiency of the mismatch to perfect match discrimination was analyzed in detail by reviewing the distribution of all mismatches in dependency of the mismatch to perfect match ratio.

The efficiency of the mismatch to perfect match discrimination was estimated in total by calculating the average of the specific intensities of all probe sets. The "specific intensity" (SI) was hereby defined as the ratio of the perfect match signal intensity over a mean of the three mismatch signal intensities (see figure 14c).

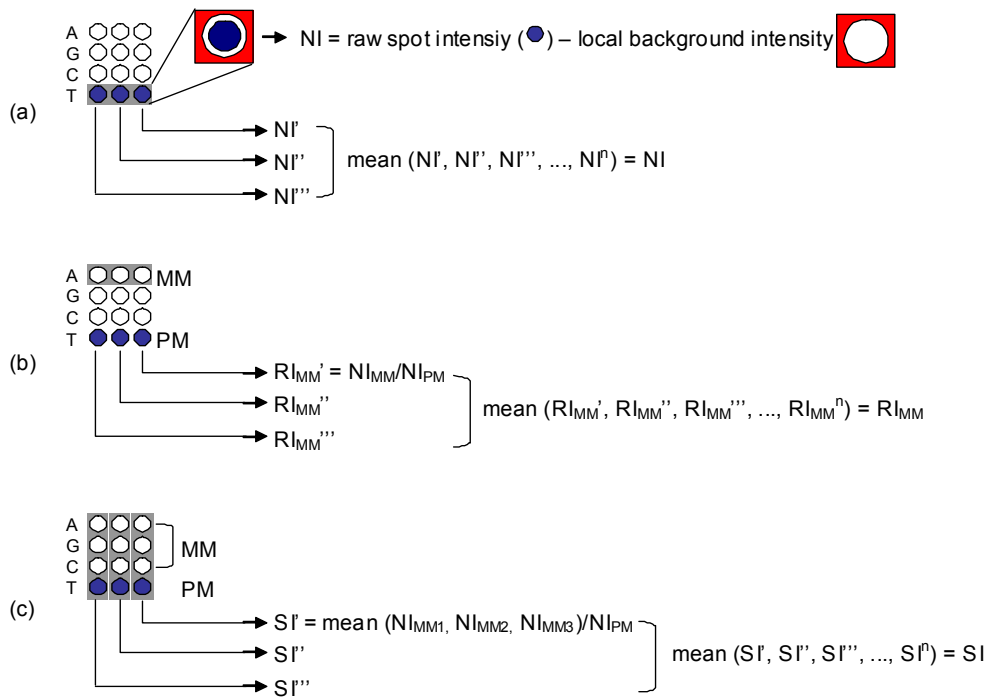


**Figure 14.** (a) To calculate the "net signal intensity" (NI) - the local background is subtracted from the raw spot intensity. The mean signal intensity of one oligo probe is calculated by averaging the individual intensities of  $n$  replicates ( $n$  = number of replicate spots analyzed under the same conditions). (b) Individual relative intensities (RI) of one oligo probe were calculated by forming the ratio of the net mismatch or perfect match signal intensity to the net perfect match signal intensity within one SNP probe set. The "specific intensity" (SI) was defined as the ratio of the net perfect match signal intensity over a mean of the three net mismatch signal intensities. The probes or probe sets, for which an example of calculating a mean (NI, RI, or SI) value is displayed, are shaded in gray.

### 2.3.10 DNA sequencing

The *bla<sub>TEM</sub>* (861 bp) and *bla<sub>SHV</sub>* (932 bp) amplicons were produced by PCR as described in section 2.3.7.1 with two exceptions: instead of the denoted dNTP-mix containing Cy3- or Cy5-dCTP, 50  $\mu$ M dNTPs (Invitrogen (Karlsruhe, Germany)) were used and only 5 U of Taq DNA polymerase instead of 10 U. After purification (as described in "purification of target DNA") 200 ng of the purified DNA were used in a sequencing reaction containing 10 pmol of either a forward or a reverse primer (the same primers as used for amplification reaction) and 4  $\mu$ l of a premix solution from the big-dye terminator cycle sequencing kit (Applied Biosystems, Darmstadt, Germany) in a total volume of 20  $\mu$ l. The premix comprises the AmpliTaq DNA polymerase, dNTPs, as well as the fluorescently labeled ddNTPs. The sequencing reaction was performed in a Mastercycler Gradient (Eppendorf, Hamburg, Germany). An initial denaturation step (95°C for 4 min) was followed by 25 cycles (95°C for 40 s, 55°C for 30 s, 60°C for 4 min) and a final extension step at 60°C for 4 min. The sequencing was carried out in an ABI Prism 377A-DNA-sequencer. The data were analyzed by SeqMan II software.

### 3 Results

#### 3.1 Results TEM-array

##### 3.1.1 Probe design

In the present study an oligonucleotide microarray was developed for genotyping of TEM beta-lactamases from bacteria isolated from real clinical samples. A first subset of probes for the TEM-array was designed by Satoshi Ezaki at the Institute of Technical Biochemistry, University of Stuttgart. Based on this, the complete probe set for the TEM microarray was developed and validated in this study. The whole probe set used for the array design covers 99 % of the amino acid substitution positions published up to date (see table 3) except the end-standing positions of amino acids number 2, 3 and 285 of TEM beta-lactamase. Probes for amino acid position 4 were included, but the probe sequence was partially overlapping the primer sequence, so that the polymorphism detection at this position was not possible with the used primer set. The design of a different primer set outside the open reading frame (ORF) to circumvent the problematic of the detection of end-standing SNPs was currently not advisable, since for a considerable part of the published TEM variants no ORF flanking sequences were available.

In table 4 the results of the probe design for the probes complementary for *bla*<sub>TEM-1</sub> and the mutant *bla*<sub>TEM-X</sub> are displayed. The probe length was between 17-27 bases, the T<sub>m</sub> values varied from 46.4 to 64.7 °C and the GC content between 27.3 to and 76.5 %. Due to the necessity to exclude unfavorable probe secondary structures and to gain sufficient perfect match net signal intensity for analysis, it was determined in first experiments, that a narrow T<sub>m</sub> range could not be realized for the complete probe set (data not shown). Probes with stable secondary structures should be excluded, because of non-optimal accessibility. The applied probe design parameters of the software excluded probes with a hairpin  $\Delta G$  value of less than - 3 kcal/mol and self dimer  $\Delta G$  values of < - 6 kcal/mol. All probes met these criteria for the hairpin secondary structures with  $\Delta G$  values between 0 and - 2.5 kcal/mol. Probes 40C, 90A, 102G, 182C and 235.1A shared self dimer secondary structures with  $\Delta G$  values of more than - 6 kcal/mol. For all other probes self dimer  $\Delta G$  values were within the default limits (0 to - 6 kcal/mol). Since the dimer forming bases were in close proximity to the central SNP position, alternate probe sequences were not applicable. The concept of this array was defined to include all mutation positions, which were relevant for unambiguous identification of the different TEM variants, so that also probes with  $\Delta G$  values violating these limits were accepted and tested in hybridization experiments. For the probe performance in hybridization experiments see results below.

**Table 3.** TEM beta-lactamase polymorphism sites and corresponding mutants

Position <sup>c</sup>	Nucleotide		Amino acid <sup>a</sup>				TEM -X phenotype <sup>b</sup>			
	Codon in:		Ambler position	Position	Amino acid in:		ESBL	IRT	ESBL+ IRT	Not defined
<i>bla</i> <sub>TEM-1</sub>	<i>bla</i> <sub>TEM-X</sub>	TEM-1			TEM-X					
3-6	AGT	GAT	4	2	S	D			97, 98, 99, 102, 108	
7-9	ATT	CCT	5	3	I	P			97, 98, 99, 102, 108	
10	CAA	AAA	6	4	Q	K			87, 92	
55	CTT	TTT	21	19	L	F	4, 9, 25, 48, 49, 53, 63	73, 74	75, 85, 86, 94, 110	
55	CTT	ATT	21	19	L	I			67	
109	CAG	AAG	39	37	Q	K	3, 7, 8, 11, 16, 18, 21, 22, 24, 42, 46, 56, 60, 61, 66, 72	44, 59, 65	2, 67, 89, 101	
119	GCA	GTA	42	40	A	V	42			
146	CTC	CCT	51	49	L	P	60			
199	ATG	GTG	69	67	M	V		34, 36, 38, 78, 82	97	
199	ATG	CTG	69	67	M	L		33, 35, 39, 45, 50, 77, 80, 81		
199	ATG	TTG	69	67	M	L		45		
201	ATG	ATT	69	67	M	I		32, 37, 40, 83		
233	GTA	GAA	80	78	V	E			108	
244	GTT	ATT	84	82	V	I			116	
269	GGT	GAT	92	90	G	D	57, 66			
304	GAG	AAG	104	102	E	K	3, 4, 6, 8, 9, 13, 15, 16, 17, 18, 21, 22, 24, 26, 43, 46, 52, 56, 60, 63, 66	50	87, 88, 89, 92, 94, 106, 107, 111	
338	GAT	GGT	115	113	D	G			90	
365	AGT	AAT	124	122	S	N			105	
373	ATA	GTA	127	125	I	V		80, 81		
382	AGT	GGT	129	127	S	G		59, 76	89	
427	CCG	GCG	145	143	P	A			95	
452	CAC	CGC	153	151	H	R	21, 56			
482	GAT	GGT	163	161	D	G			96	
484	CGT	AGT	164	162	R	S	5, 7, 8, 9, 10, 12, 24, 26, 46, 53, 60, 63		85, 86, 102	
484	CGT	TGT	164	162	R	C			87, 91	
485	CGT	CAT	164	162	R	H	6, 11, 16, 27, 28, 29, 43, 61		107, 118	
487	TGG	CGG	165	163	W	R		39, 78		
489	TGG	TGT	165	163	W	C		83		
539	ATG	ACG	182	180	M	T	20, 43, 52, 63, 72	32	87, 88, 91, 92, 93, 94, 106, 107	
545	GCA	GTA	184	182	A	V			116	
580	GGC	AGC	196	194	G	D			88	
581	GGC	GAC	196	194	G	S			108	
605	CGG	CAG	204	202	R	Q			70	
647	GGA	GAA	218	216	G	E	55			
703	GCC	ACC	237	235	A	T	5, 24		86	
704	GCC	GGC	237	235	A	G	22			
706	GGT	AGT	238	236	G	S	3, 4, 8, 15, 19, 20, 21, 22, 25, 42, 47, 48, 49, 52, 66, 68, 72	50	71, 88, 89, 92, 93, 94, 101, 107	
707	GGT	GAT	238	236	G	D			111	
709	GAG	AAG	240	237	E	K	5, 10, 24, 27, 28, 42, 46, 47, 48, 49, 61, 72	68	71, 85, 86, 91, 93, 101	
721	CGC	AGC	244	241	R	S		30, 44, 74, 77	99	
721	CGC	TGC	244	241	R	C		31, 65, 73		
721	CGC	GGC	244	241	R	G		79		
722	CGC	CAC	244	241	R	H		51		
722	CGC	CTC	244	241	R	L	54			
772	GTT	ATT	262	258	V	I			58	
782	ACG	ATG	265	261	T	M	4, 9, 13, 25, 27, 42, 47, 48, 49	73, 74	68 85, 86, 94, 110, 111, 118	
790	AGT	GGT	268	264	S	G			49	
812	CGA	CTA	275	271	R	L		38	68	
812	CGA	CAA	275	271	R	Q		45, 82, 83		
814	AAT	GAT	276	272	N	D		35, 36, 37, 39, 78, 80	50 84	
827	GCT	GTC	280	276	A	V			101, 104	
854	CAT	CTT	289	285	H	L			97, 98, 99	

<sup>a</sup>Ambler position: position of the polymorphism in the amino acid sequence of TEM (<http://www.lahey.org/Studies/temtable.asp>) according to Ambler et al (3). Position: position of the polymorphism according to the amino acid sequence of TEM (GenBank accession number AAB59737). The amino acids at the position in the TEM-1 sequence and the mutated TEM (TEM-X) sequence are also indicated.

<sup>b</sup>The numbers in the table body are the TEM types with an amino acid substitution at the indicated position. The ESBL, IRT, ESBL-IRT phenotypes are as described by Bradford (16).

<sup>c</sup>Position refers to the position of the polymorphism site in the nucleotide sequence of the *bla*<sub>TEM</sub> gene (GenBank accession number J01749 region: complement (3293..4153)).

## Results

**Table 4.** Probe design results for the TEM-specific microarray<sup>a</sup>

Probe name	Probe sequence (5'-3')	Length	Tm	GC	Hairpin $\Delta G$	Hairpin bond	Dimer $\Delta G$	Dimer bond	Run/ repeat length
		(nt)	(°C)	(%)	(kcal/mol)	(nt)	(kcal/mol)	(nt)	(nt)
04C	ATGAGTATTCAACATTTTCGTG	22	49.4	31.8	0	0	0	0	4
04A	ATGAGTATTAACATTTTCGTG	22	47.2	27.3	-0.1	3	-0.7	4	4
19C	GCATTTTGCCTTCCTGTTTT	20	51.3	40	-1.9	3	-1.9	3	4
19T	GCATTTTGTCTTCCTGTTTT	20	49.5	35.0	-1.9	3	-1.9	3	4
37C	CTGAAGATCAGTTGGGTGC	19	51.4	52.6	0	0	-1.9	4	3
37A	CTGAAGATAAGTTGGGTGC	19	48.8	47.4	0	0	0	0	3
40C	ATCAGTTGGGTGCACGAGTGGGTGA	25	62.8	52	0	0	-6.7	6	3
40T	ATCAGTTGGGTGTACGAGTGGGTGA	25	60.1	48	0	0	-1.9	4	3
49T	ATCGAACTGGATCTCAACAGCGGTAAG	27	61.8	48.1	-1.1	3	-1.9	4	2
49C	ATCGAACTGGATCCTAACAGCGGTAAG	27	61.3	48.1	-1.1	3	-5.7	6	2
67.1A	CGTTTTCCAATGATGAGCACTTTTAA	26	56.3	34.6	0	0	0	0	4
67.1G	CGTTTTCCAATGGTGAGCACTTTTAA	26	58.1	38.5	0	0	-1.4	3	4
67.2G	TTTTCCAATGATGAGCACTTTTAA	24	52.3	29.2	0	0	-0.7	4	4
67.2T	TTTTCCAATGATTAGCACTTTTAA	24	50.2	25.0	0	0	-0.7	4	4
78T	ATGTGGTGCGGTATTATCCC	20	53.1	50	0	0	0	0	3
78A	ATGTGGTGCGGAATTATCCC	20	53.6	50	-1.3	3	-1.3	3	3
82G	TTATCCCGTGTGACGCCG	19	55.9	57.9	-1.9	3	-1.9	3	3
82A	TTATCCCGTATTGACGCCG	19	52.9	52.6	-1.9	3	-1.9	3	3
90G	GCAACTCGGTCGCCGCA	17	58.4	70.6	-2.3	3	-2.3	3	2
90A	GCAACTCGATCGCCGCA	17	55.8	64.7	0	0	-6.5	6	2
102G	GACTTGGTTGAGTACTCACC	20	51.1	50	-1.4	3	-10.3	10	2
102A	GACTTGGTTAAGTACTCACC	20	48.7	45	-1.4	3	-4.3	6	2
113A	ATCTTACGGATGGCATGAC	19	50.2	47.4	-0.3	3	-2.2	4	2
113G	ATCTTACGGGTGGCATGAC	19	52.6	52.6	0	0	-2.2	4	3
122G	AGAATTATGCAGTGCTGCCATA	22	54.3	40.9	-1.9	3	-3.4	4	2
122A	AGAATTATGCAATGCTGCCATA	22	52.6	36.4	-1.9	3	-3.3	4	2
125A	GTGCTGCCATAACCATGA	18	50.1	50.0	-0.5	3	-2.2	4	2
125G	GTGCTGCCGTAACCATGA	18	52.8	55.6	0	0	-2.2	4	2
127A	TGCCATAACCATGAGTGATAAACACTG	26	58.2	42.3	-2.5	4	-2.5	4	2
127G	TGCCATAACCATGGGTGATAAACACTG	26	60.1	46.2	-2.4	4	-6	6	3
143C	CGGAGGACCGAAGGAGC	17	53.9	70.6	-2.3	3	-2.3	3	2
143G	CGGAGGAGCGAAGGAGC	17	54.4	70.6	0	0	0	0	2
151A	CCGCTTTTTTGCACAACATGGGGG	24	62.4	54.2	0	0	-3.3	4	6
151G	CCGCTTTTTTGCGCAACATGGGGG	24	64.7	58.3	0	0	-10.2	8	6
161A	CTCGCCTTGATCGTTGGGA	19	55.2	57.9	0	0	-1.9	4	3
161G	CTCGCCTTGGTCGTTGGGA	19	57.6	63.2	0	0	0	0	3
162.1G	GCCTTGATCGTTGGGAA	17	49.0	52.9	0	0	-1.9	4	3
162.1A	GCCTTGATAGTTGGGAA	17	45.2	47.1	0	0	0	0	3
162.2G	GCCTTGATCGTTGGGAACC	19	54.2	57.9	-0.6	3	-1.9	4	3
162.2A	GCCTTGATCATTGGGAACC	19	51.6	52.6	0	0	-4.7	6	3
163.1T	TTGATCGTTGGGAACCG	17	49.2	52.9	-0.6	3	-1.9	4	3
163.1C	TTGATCGTCGGGAACCG	17	51.4	58.8	-2.3	3	-2.3	3	3
163.2G	TGATCGTTGGGAACCGGAG	19	54.8	57.9	-0.6	3	-4.2	4	3
163.2T	TGATCGTTGTGAACCGGAG	19	52.9	52.6	-0.6	3	-4.2	4	2
180T	CACCACGATGCCTGTAG	17	49.4	58.8	0	0	0	0	2
180C	CACCACGACGCCTGTAG	17	52.3	64.7	0	0	0	0	2
182C	CGATGCCTGCAGCAATGGC	19	58.2	63.2	-2.4	3	-6.3	6	2
182T	CGATGCCTGTAGCAATGGC	19	54.8	57.9	-2.4	3	-2.4	3	2
194.1G	AACTATTAAGTGGCGAACTACTT	23	52.0	34.8	0	0	-0.7	4	2
194.1A	AACTATTAAGTAGCGAACTACTT	23	49.4	30.4	-0	3	-1.5	4	2
194.2G	ACTATTAAGTGGCGAACTACTT	22	51.1	36.4	0	0	-0.7	4	2
194.2A	ACTATTAAGTACGAACTACTT	22	48.5	31.8	0	0	-0.7	4	2
202G	CTAGCTTCCCGGCAACAATTA	21	54.3	47.6	0	0	-4.2	4	3

Table 4. continued

202A	CTAGCTTCCCAGCAACAATTA	21	51.8	42.9	-1.7	3	-2.9	4	3
216G	AGTTGCAGGACCACTTCT	18	50.6	50	-0.8	3	-3.3	4	2
216A	AGTTGCAGAACCACTTCT	18	48.6	44.4	-1.7	4	-3.3	4	2
235.1G	AAATCTGGAGCCGGTGAGC	19	55.4	57.9	0	0	-4.2	4	3
235.1A	AAATCTGGAACCGGTGAGC	19	53.1	52.6	0	0	-7.0	6	3
235.2C	ATCTGGAGCCGGTGAGC	17	53.4	64.7	0	0	-4.2	4	2
235.2G	ATCTGGAGGCGGTGAGC	17	53.4	64.7	0	0	0	0	2
236.1G	CTGGAGCCGGTGAGCGT	17	56.6	70.6	0	0	-4.2	4	2
236.1A	CTGGAGCCAGTGAGCGT	17	53.7	64.7	-1.1	3	-2.9	4	2
236.2G	CTGGAGCCGGTGAGCGTG	18	58.3	72.2	0	0	-4.2	4	2
236.2A	CTGGAGCCGATGAGCGTG	18	55.8	66.7	0	0	0	0	2
237G	GAGCCGGTGAGCGTGGGT	18	59.8	72.2	0	0	-4.2	4	3
237A	GAGCCGTAAGCGTGGGT	18	57.1	66.7	0	0	-4.2	4	3
241.1C	GTGGGTCTCGCGGTATC	17	51.6	64.7	0	0	-5.1	4	3
241.1A	GTGGGTCTAGCGGTATC	17	48.0	58.8	0	0	-1.5	4	3
241.2G	GTGGGTCTCGCGGTATCAT	19	54.7	57.9	0	0	-5.1	4	3
241.2A	GTGGGTCTCACGGTATCAT	19	51.6	52.6	-1.2	3	-1.2	3	3
258G	CCGTATCGTAGTTATCTACACG	22	52.1	45.5	-1.7	4	-1.7	4	2
258A	CCGTATCGTAATTATCTACACG	22	50.5	40.9	-0.2	3	-2.4	6	2
261C	TTATCTACACGACGGGGA	18	49.3	50.0	0	0	0	0	4
261T	TTATCTACATGACGGGGA	18	46.4	44.4	0	0	-2.2	4	4
264A	CGACGGGGAGTCAGGCA	17	55.8	70.6	-1.1	3	-1.1	3	4
264G	CGACGGGGGGTCAGGCA	17	58.6	76.5	-1.1	3	-1.1	3	6
271G	ATGGATGAACGAAATAGACAG	21	49.4	38.1	0	0	0	0	3
271A	ATGGATGAACAAAATAGACAG	21	47.5	33.3	0	0	0	0	4
272A	GGATGAACGAAATAGACAGAT	21	49.1	38.1	0	0	0	0	3
272G	GGATGAACGAGATAGACAGAT	21	50.3	42.9	0	0	0	0	2
276C	TAGACAGATCGCTGAGATAGGTG	23	55.3	47.8	-1.1	3	-1.9	4	2
276T	TAGACAGATCGTCGAGATAGGTG	23	55	47.8	-1.1	3	-3	4	2

<sup>a</sup> For each polymorphism site one probe complementary to *bla*<sub>TEM-1</sub> (upper line) and one probe complementary to the mutated *bla*<sub>TEM-X</sub> (lower line) are displayed. The additional two mismatch probes of one complete probe set are not displayed. The probes are named for the position in the amino acid sequence of TEM and the nucleotide at the central base position (either A, G, C, or T). The probe length, the melting temperature (T<sub>m</sub>), GC content (GC), free energy of hairpin bonds (hairpin ΔG), the number of bases forming the hairpin bond (hairpin bond), free energy of dimers (dimer ΔG), the number of bases forming the dimer bond (dimer bond) were calculated by ArrayDesigner 2.0 software.

## Results

**Table 5.** Oligonucleotide probe sequences used in the TEM-specific microarray<sup>a</sup>

Tm (°C)	Length (nt)	Probe name	Probe sequence (5'-3') <sup>b</sup>
49.4	22	04	ATGAGTATT <u>NA</u> ACATTTCCGTG
51.3	20	19	GCATTTTGC <u>NT</u> ICCTGTTTT
51.4	19	37	CTGAAGAT <u>NAG</u> TTGGGTGC
62.8	25	40	ATCAGTTGGGT <u>GN</u> ACGAGTGGGTTA
61.8	27	49	ATCGAACTGGAT <u>CN</u> CAACAGCGTAAG
56.3	26	67	CGTTTTCCAAT <u>GNT</u> GAGCACTTTTAA
52.3	24	67.2	TTTTCCAAT <u>GATN</u> AGCACTTTTAA
53.1	20	78	ATGTGGTGCG <u>GN</u> ATTATCCC
55.9	19	82	TTATCCCGT <u>NTT</u> GACGCCG
58.4	17	90	GCAACT <u>C</u> GNTCGCCGCA
51.1	20	102	GACTTGGTT <u>NAG</u> TACTCACC
50.2	19	113	ATCTTAC <u>G</u> GNTGGCATGAC
54.3	22	122	AGAATTATGC <u>ANT</u> GCTGCCATA
50.1	18	125	GTGCTGCC <u>NTA</u> ACCATGA
58.2	26	127	TGCCATAACCAT <u>GNG</u> IGATAAAGCTG
53.9	17	143	CGGAGG <u>AN</u> CGAAGGAGC
62.4	24	151	CCGCTTTTTTGC <u>NCA</u> ACATGGGGG
55.2	19	161	CTCGCCT <u>GNT</u> CGTTGGGA
49.0	17	162	GCCTTGAT <u>N</u> GTGGGA
54.2	19	162.2	GCCTTGAT <u>CNT</u> TGGGAACC
49.2	17	163	TTGATCGT <u>N</u> GGGAACCG
54.8	19	163.2	TGATCGT <u>TGN</u> GAACCGGAG
49.4	17	180	CACCACG <u>AN</u> GCCTGTAG
58.2	19	182	CGATGCCT <u>GNA</u> GCAATGGC
52.0	23	194.2	AACTATTA <u>ACTN</u> CGGACTACTT
51.1	22	194	ACTATTA <u>ACTGN</u> CGACTACTT
54.3	21	202	CTAGCTTCC <u>C</u> NGCAACAATTA
50.6	18	216	AGTTGC <u>AGNA</u> CCACTTCT
55.4	19	235.2	AAATCTGG <u>ANCC</u> GGTGAGC
53.4	17	235	ATCTGG <u>AGNC</u> GGTGAGC
56.6	17	236	CTGGAGCC <u>NGT</u> GAGCGT
58.3	18	236.2	CTGGAGCC <u>GNT</u> GAGCGTG
59.8	18	237	GAGCCGGT <u>NAG</u> CGTGGGT
51.6	17	241	GTGGGTCT <u>NGC</u> GGTATC
54.7	19	241.2	GTGGGTCT <u>CNC</u> GGTATCAT
52.1	22	258	CCGTATCGT <u>ANT</u> IATCTACACG
49.3	18	261	TTATCTAC <u>ANG</u> ACGGGGA
55.8	17	264	CGACGGGG <u>NGT</u> CAGGCA
49.4	21	271	ATGGATGAAC <u>NAA</u> ATAGACAG
49.1	21	272	GGATGAACG <u>AN</u> ATAGACAGAT
55.3	23	276	TAGACAGAT <u>C</u> GNTGAGATAGGTG
52.3	18	process control	AGAAACGCTGGTGAAAGT
46.0	18	negative hybridization control	TCTAGACAGCCACTCATA
53.1	19	positive hybridization control	GATTGGACGAGTCAGGAGC
46.0	18	spot control	TCTAGACAGCCACTCATA-Cy3

<sup>a</sup> For the SNP specific probes, four probes for each SNP position were used. The probes are named for the position in the amino acid sequence of *bla*<sub>TEM</sub>. The four probes had either A, G, C, or T at the central base position (designated N in the probe sequence). The probe length and the melting temperatures (calculated for the probes matching the *bla*<sub>TEM-1</sub> sequence by Arraydesigner 2.0 software) are also provided.

<sup>b</sup>The triplet with the amino acid substitution is underlined.



### 3.1.2 Setting up the system on poly-L-lysine slides

The system was set up on low priced poly-L-lysine slides with a DMSO based spotting buffer. The probes were immobilized via non-directed covalent binding of a thymidine from within the probe sequence to the primary amino group of the lysine. The whole probe set was spotted in four replicates. Each replicate was spotted with a different pin. The array was hybridized with 260 ng of target DNA from a TEM-116 sample, derived from a pure culture of *Escherichia coli* (*E. coli*) K12 bearing a pUC19 plasmid. The target DNA had an incorporation ratio of fluorescence label, defined as the number of nucleotides/fluorophore (NT/F) = 90 and was hybridized for three hours in Corning hybridization chambers using standard cover glasses. The array layout and a corresponding fluorescence image of the hybridization are shown in figure 15. The aim of this experiment was to determine the performance and the reproducibility of the analysis under standard conditions and to assess if the identification of the correct perfect match positions was possible with the designed probe sets.

All perfect match positions could be identified by the highest signal intensity within a SNP probe set. The resulting overall signal intensity was low: the net signal intensity varied between 400 and 2500 arbitrary units for the perfect match probes. Most of the spots showed a donut shaped signal due to inhomogeneous drying of the spot. The not uniform signal distribution on the spots, low signal to noise ratios and the use of different pins for spotting of replicate spots resulted in standard deviations of the net perfect match signal intensities of in average 68 % between replicate spots (see figure 16).

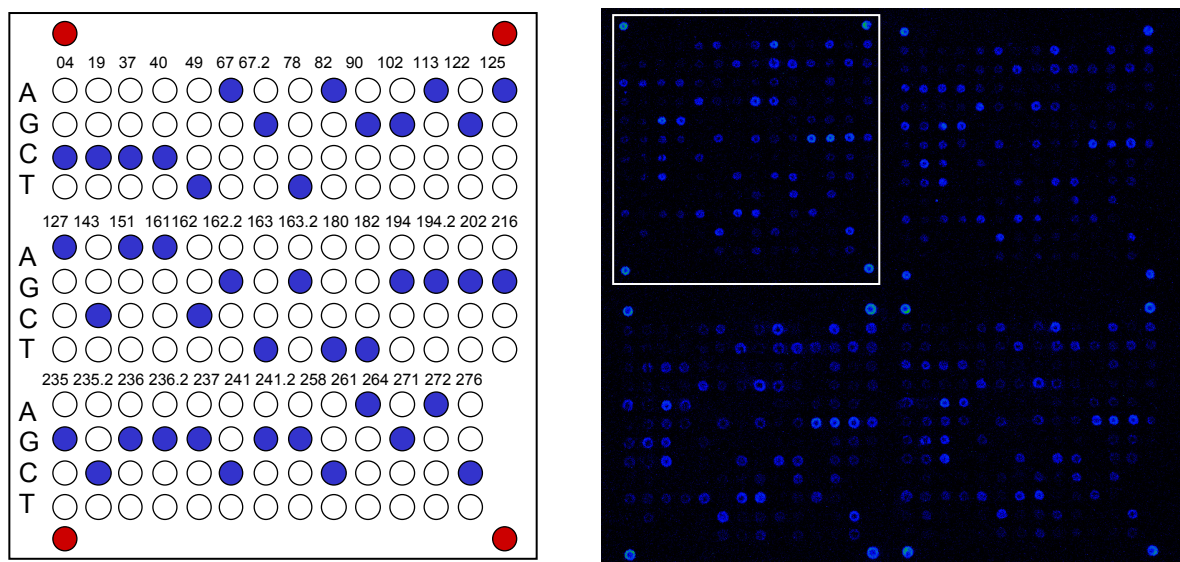


**Figure 15.** On the left the SNP capture probe layout of the TEM-microarray, on the right the fluorescence image of a hybridization experiment with 260 ng of *bla*<sub>TEM-116</sub> target DNA (NT/F = 90) for three hours is displayed. The TEM-array was spotted in 4 identical replicate layouts with four different pins. The upper left replicate is highlighted in the fluorescence image. In the layout the SNP position is indicated above each probe set. The central base in the probe sequence is indicated on the left side of the row as A, G, C, or T. Blue spots designate perfect match positions for *bla*<sub>TEM-116</sub> gene, white spots refer to mismatch positions. The spotting controls (indicated in red) frame each replicate layout spotted by a different pin. In the fluorescence image the signal intensity is shown in false color. Blue corresponds to the lowest signal intensity, red to white depict the highest signal intensities (as output by ImaGene 3.0).

## Results

Multiple experiments indicated that low signal intensities, unfavorable background signals and low reproducibility of experiments seemed to be a problem associated with the used spotting buffer and the low quality of the surface (data not shown). Due to the high standard deviations and the low signal to noise ratios a reliable and sensitive analysis was impossible with this method and new experimental strategies had to be developed. This led to the conclusion that not only for the spotting layout, but also for the surface and the spotting buffer alternatives had to be found.

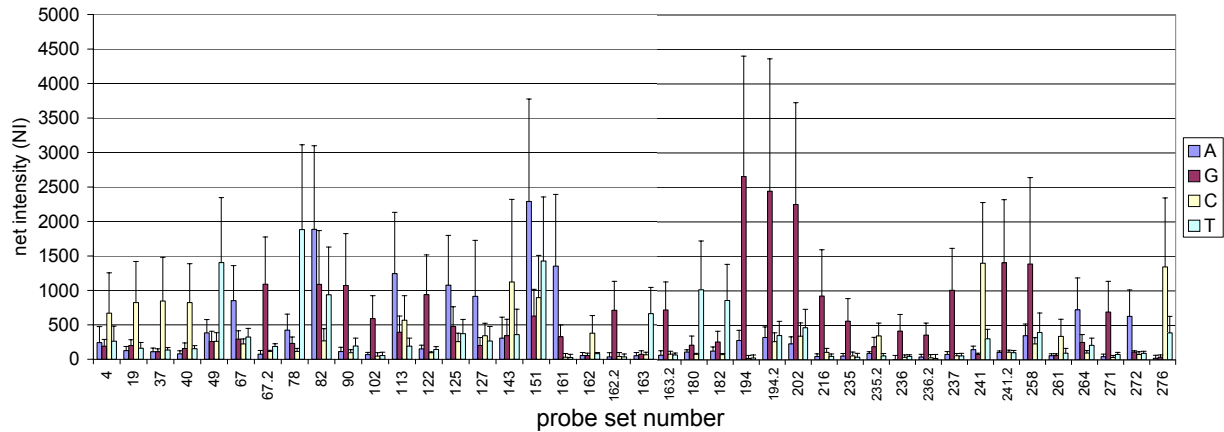


**Figure 16 .** Mean net signal intensities for each SNP position and corresponding probe (A, G, C or T refer to the central base position) from a hybridization experiment with 260 ng of *bla<sub>TEM-116</sub>* target DNA (NT/F = 90). The displayed standard deviation was calculated for the four replicate spots on one array.

### 3.1.3 Setting up the system on epoxy slides

Epoxy-coated slides were chosen as a new carrier and three different spotting buffers (DMSO-, betaine-, and phosphate-based spotting buffers) were tested for optimal probe immobilization and reproducible signal pattern by spotting a fluorescently labeled probe (a spotting control) and one conventional probe set (probes A, G, C and T). The slides were scanned directly after immobilization and blocking. The corresponding fluorescence image is shown in figure 17.

The DMSO-based buffer showed highest signal intensities, but the spot size and signal distribution was very inhomogeneous, which was unfavorable for data extraction. The spotting control spots with betaine based buffer showed homogeneous signal distribution and reproducible spot shapes, but on the probe spots A, G, C, T, where no signal should be observed, because no target DNA was hybridized, also fluorescence signals were detected. This was due to an incomplete immobilization of the spotting control in betaine buffer, which tended to attach to neighboring probe spots spotted with the same betaine-based buffer.

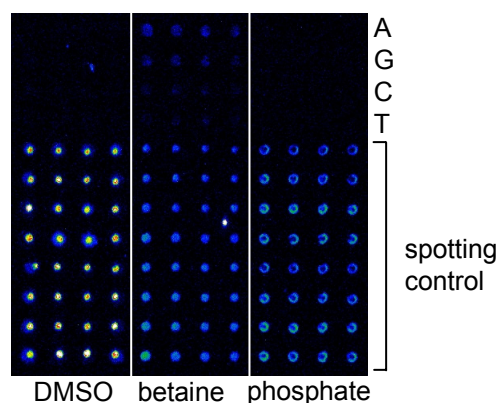


**Figure 17.** Fluorescence image of a spot test using a DMSO- betaine- or phosphate-based spotting buffer on epoxy slides. The spotting control was an oligonucleotide probe labeled with Cy5. A, G, C, T refers to an unlabeled control probe set, which was spotted in four replicates.

The phosphate based spotting buffer showed reproducible, but donut shaped spotting control spots. The first two buffers (DMSO and betaine) were excluded, because a reproducible and correct data analysis would not have been possible due to the observed problems regarding spot shape or incomplete immobilization. Therefore, the phosphate-based buffer was used for further experiments. The donut shaped spots with this buffer were not observed in following experiments (see proof of concept).

## Results

### 3.1.4 Proof of concept

To minimize the variability between replicate signals, in the new array layout a different spotting strategy was devised. Instead of spotting replicate spots with four different pins, replicate spots in the new layout were spotted directly one after the other by the same pin. To establish the TEM-array on the epoxy surface, and to show the feasibility of the method, the array was hybridized with 100 ng target DNA (*bla*<sub>TEM-116</sub>) in three repetitive experiments. The target DNA was hybridized for three hours in Corning hybridization chambers using standard cover glasses. It was the aim to analyze the performance of the designed probe sets regarding specificity of the perfect match identification and set a threshold indicating at which level all the perfect match positions for *bla*<sub>TEM-116</sub> could be considered as correctly identified. Furthermore the reproducibility of the system was determined under standard conditions. The array layout and a fluorescence image of the hybridized array is shown in figure 18.

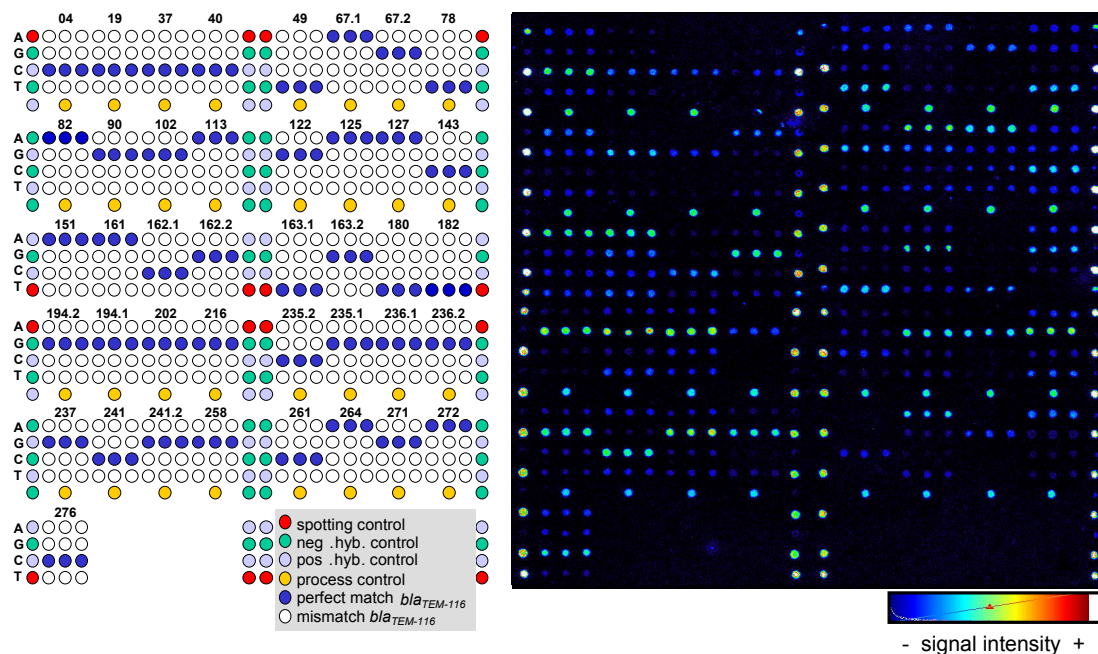


**Figure 18.** On the left, the SNP capture probe layout of the TEM microarray is shown. All SNP capture probes were spotted in triplicates. The SNP position is indicated above each triplicate. The central base in the probe sequence is indicated on the left side of each row as A, G, C, or T. Blue spots indicate perfect match positions for *bla*<sub>TEM-116</sub> gene, white spots indicate mismatch positions.

On the right, the fluorescence image of a hybridization experiment with 100 ng of *bla*<sub>TEM-116</sub> target DNA (incorporation ratio NT/F = 57) for three hours is displayed. The signal intensity is shown in false color. Blue corresponds to the lowest signal intensity, red to white depict the highest signal intensities (as output by ImaGene 3.0).

The mean signal intensity values and standard deviations of all SNP positions are shown in figure 19. The net signal intensity values ranged from 1,500 to 20,000 for the perfect match probes (figure 19a). 40 of 41 SNP positions were correctly identified. Since perfect match position 182T showed spotting errors in this slide batch, it was not taken into account. To investigate the discriminatory power of the system, the relative intensities were calculated (figure 19b). The relative intensity is

defined as the ratio of the net intensity of a given probe over the net intensity of the perfect match probe (the probe with the highest intensity within a SNP probe set). Thus, for a correctly identified perfect match the relative intensity ( $RI_{PM}$ ) should correspond to a value of 1, the relative intensity of a mismatch ( $RI_{MM}$ ) should be lower than 1. The lower the relative intensity of the mismatches is, the better the discrimination between a perfect match and a mismatch.

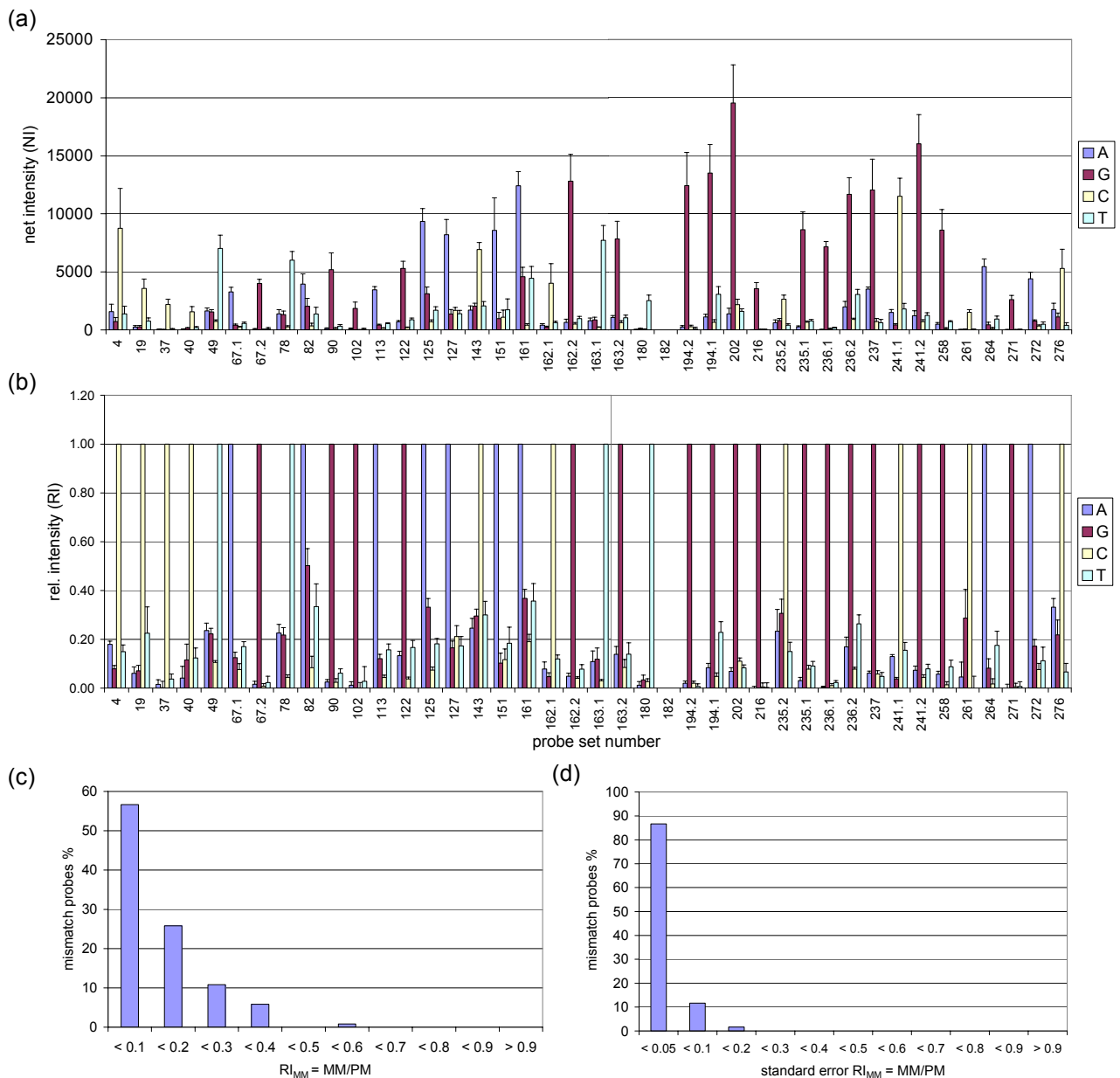


**Figure 19.** (a) Mean net signal intensities and (b) mean relative (rel.) signal intensities for each SNP position and corresponding probe (A, G, C or T refer to the central base position) from a hybridization experiment with 100 ng *bla<sub>TEM</sub>* from pUC19 (NT/F = 57). The displayed standard deviation was calculated for three replicate spots on each of three arrays (n = 9). (c) Percentage of mismatch probes depending on the MM/PM ratio (d) Percentage of mismatch probes depending on the standard error of the MM/PM ratio.



For a detailed analysis of the discrimination efficiency of all TEM-array probe sets the distribution all mismatch probes depending on their mismatch to perfect match ratio was plotted in figure 19c. Over 99 % of the relative intensity of mismatches remained below 0.4, only probe 82 showed higher  $RI_{MM}$  values up to 0.52. The standard deviations for the mean  $RI_{MM}$ s ranged between 0.01 and 0.12, over 98 % remained below 10 % of the perfect match intensity (figure 19d). A perfect match was further on considered as correctly identified ("ID limit"), if the relative intensity of any of the three mismatches of one probe set did not exceed 0.8.

In comparison to the array spotted on the poly-L-lysine substrate the net perfect match signal intensities on the epoxy coated slides were at least three times increased, although 1.6 times less fluorescently labeled nucleotides were applied within the hybridized target DNA. This was a sign of an improved immobilization efficiency or accessibility of the probes. The signal distribution on the spots was mostly uniform. The standard deviations of the perfect match net signal intensities were reduced from 68 % in between one array spotted on poly-L-lysine to an average of 18 % spotted on epoxy coated slides in between three arrays (compare figure 16 and figure 19a). The achievement of increased fluorescence signal intensities in combination with the more uniform signal distribution on the spot and the optimized spotting layout rendered the analysis more sensitive and reproducible, since discrimination of the specific signals from the background net intensity was facilitated and aberrations introduced through the spotting procedure were reduced.

### 3.1.5 Probe performance analysis

The perfect match to mismatch discrimination was feasible with all designed probes with varying efficiency. A linkage between optimal probe design parameters, such as no or only weak secondary structures (dimer  $\Delta G > -1.9$  kcal/mol) and optimal discrimination capabilities ( $RI_{MM} < 0.1$ ) could be observed for some probes (e.g. 37, 67.2, 180, 194.2, 271), but not for all. When comparing the determined probe parameters (table 4) and the hybridization results (figure 19), it can be noticed, that even though for example perfect match probe 102G formed the most stable secondary structure within the whole TEM-array probe set with a  $\Delta G$  value of - 10.3 kcal/mol (in contrast to mismatch probe 102A with a  $\Delta G$  value of only - 4.2), the discriminatory power of the probe set 102 was optimal with all  $RI_{MM}$  values below 0.03. Perfect match probe 40C, which also contained a stable self dimer structure of  $\Delta G = - 6.7$  kcal/mol, still remained accessible enough for target DNA hybridization to yield an efficient discrimination with all  $RI_{MM}$  values below 0.12. The probe with the weakest discrimination capability in this experiment, probe 82, showed a hairpin as well as a dimer structure with a  $\Delta G$  value of - 1.9 kcal/mol for both perfect match probe 82A and mismatch probe 82G, consequently both probes should be equally accessible for hybridization.

### 3.1.6 Reproducibility of the perfect match/mismatch discrimination

In this experiment it should be determined, if the ratio of perfect match to mismatch signal intensity after hybridization with target DNA from a set of different amplification/labeling and fragmentation reactions was reproducible. The array was therefore hybridized with five different *bla*<sub>TEM-1</sub> (400 ng target DNA) samples with varying incorporation ratios of fluorescence label (defined as the number of nucleotides per fluorophore: NT/F = 71 - 180) for three hours in the automated hybridization station HS4800 from Tecan. The net intensities of the same probes hybridized with different target DNA samples varied in some cases with a factor larger than three, due to the differences in the incorporation ratio or efficiency of fragmentation (data not shown). Since it should be determined, if the ratio of mismatch to perfect match signal intensity remained reproducible, the relative intensity was calculated. The mean and the standard deviation of the relative intensity values are given in figure 20.

All 41 perfect match positions for *bla*<sub>TEM-1</sub> could be identified correctly in every sample. The mean relative intensity of the mismatches (RI<sub>MM</sub>) varied, but 95 % remained below 0.4, only 4 % showed higher values of up to 0.6 (see figure 20b). Probe 161 showed the weakest discriminatory power with RI<sub>MM</sub> = 0.61. The standard deviations of the mean RI<sub>MM</sub> values varied from 0.01 to 0.21 (n = 15), but still remained for 79 % below 10 % of the perfect match intensity (see figure 20c). Thus, it was determined, that the identification of the perfect matches was reproducible, mainly independent from the diverse target DNA batches having varying incorporation ratios and which were prepared in different fragmentation reactions.

## Results

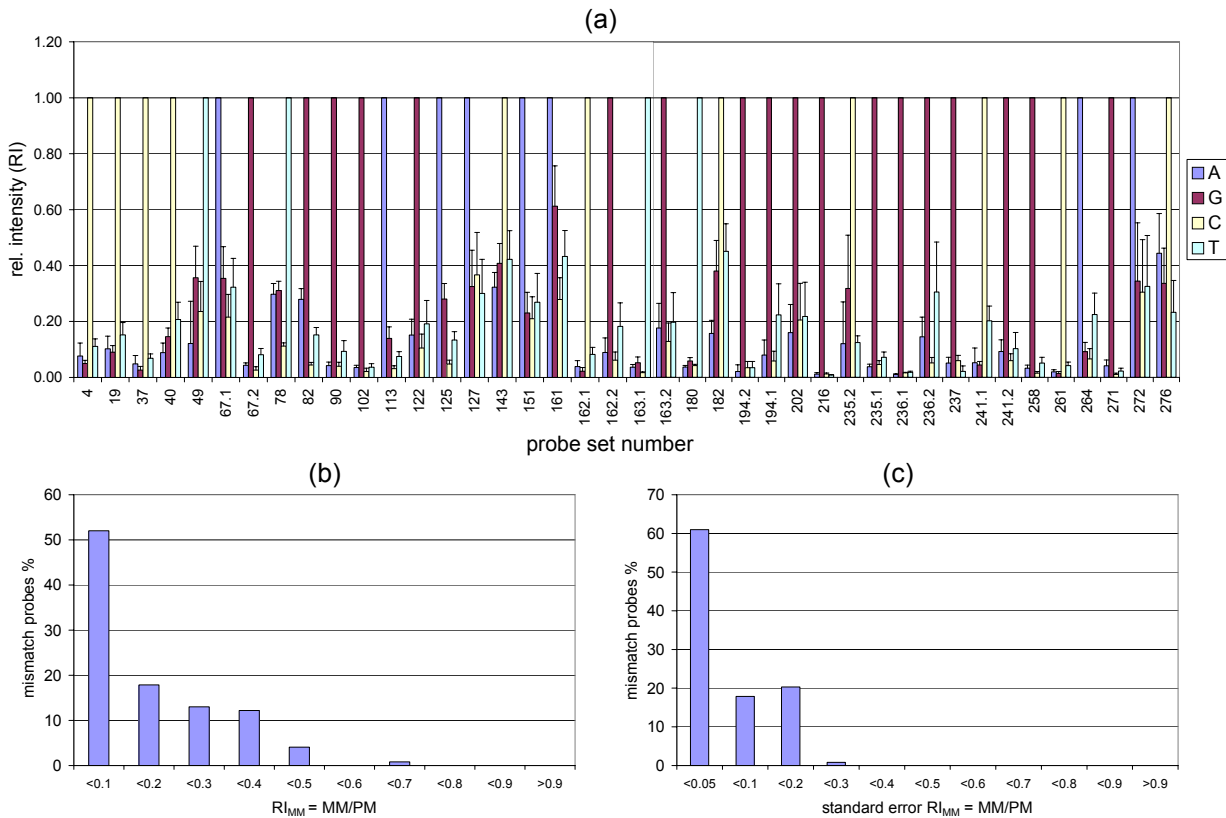


**Figure 20.** (a) Relative intensities of all TEM SNP positions averaged from five independent hybridizations with *bla<sub>TEM-1</sub>* target DNA (n = 15). The four probes per SNP are indicated by their central base (A, G, C, T) in the legend. The labeling efficiency (NT/F) of the hybridized sample DNA was 71-180; 400 ng of target DNA were applied. (c) Percentage of mismatch probes depending on the MM/PM ratio. (d) Percentage of mismatch probes depending on the standard error of the MM/PM ratio.



### 3.1.7 Testing of clinical isolates and reference strains

To test the performance of the array, a set of 17 clinical isolates, which were phenotypically characterized as ESBLs, were collected at the Robert Bosch Hospital (Stuttgart, Germany) during the daily routine over a period of 12/2000 to 05/2002. Additionally, four ESBL reference strains were provided by the Robert Koch Institute (Wernigerode, Germany). The isolated plasmid DNA was prescreened for the occurrence of TEM beta-lactamase genes by PCR (without fluorescence label) and subsequent agarose gel electrophoresis. For 14 clinical isolates and three reference strains a PCR product could be generated with a size corresponding to the *bla*<sub>TEM</sub>-amplicon (861 bp) (for agarose gel analysis of PCR products from clinical samples 1-19 see figure 21). The isolated plasmid DNA from the positively prescreened 14 clinical samples and the reference strains was amplified and fluorescently labeled during PCR with primers flanking the *bla*<sub>TEM</sub>-gene, yielding as expected a 861 bp fragment. The incorporation ratio NT/F varied between 50 to 150 NT/F depending on the quality of the template DNA.

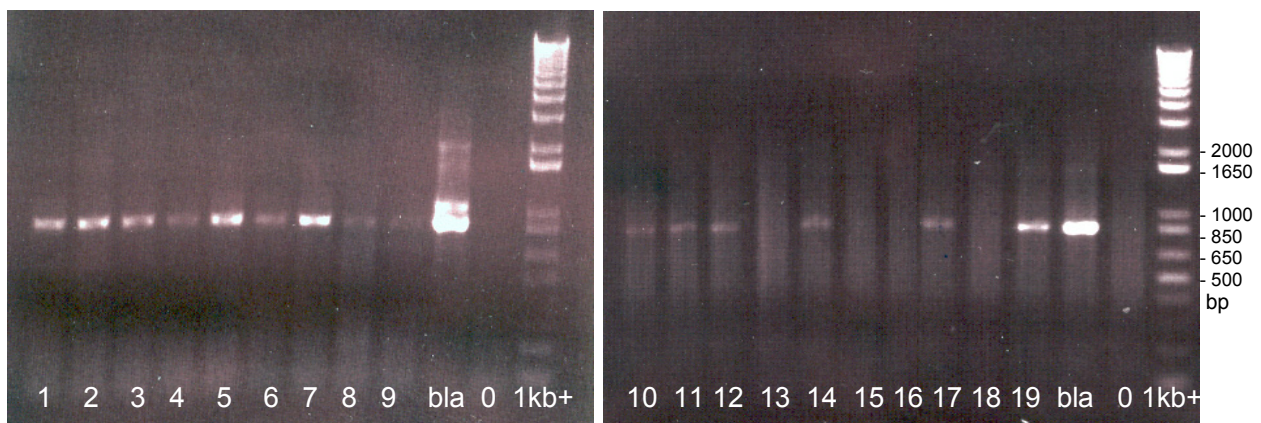


**Figure 21.** Agarose gel electrophoresis analysis of the PCR products of clinical isolates No. 1-19. The numbers designate the isolate number, which was applied on the corresponding lane. 0 and bla (for *bla* gene from pUC19) indicate the negative control and the positive control respectively. 1KB+ DNA ladder was used as a DNA size standard. The amplicon size of the target gene is 861 bp.

The PCR products were analyzed on the TEM microarray. In detail, the identified TEM-variants were: *bla*<sub>TEM-1</sub>, -3, -7, -8, and -116 as displayed in table 6. The fluorescence images of exemplary TEM-arrays hybridized with different *bla*<sub>TEM</sub> variants are displayed in figure 22. The *bla*<sub>TEM</sub> gene identified for reference strain EARSS UA1528 was *bla*<sub>TEM-8</sub>. For the other EARSS reference strain (EARSS UA1526) no amplicon could be obtained and no hybridization signals corresponding to a *bla*<sub>TEM</sub> variant were observed (data not shown), which is analog to the result of the PCR prescreening. For the reference strain designated as isolate number 21, the hybridization signals corresponded to a *bla*<sub>TEM-7</sub> gene, in contradiction to the label on the sample tube indicating TEM-5. The correct identification of *bla*<sub>TEM-7</sub> and all other variants by the TEM-array was confirmed by standard DNA sequencing.

## Results

**Table 6.** Results of testing of reference strains and clinical isolates from the RBK<sup>a</sup>

Isolate No.	Sample	Species	Phenotype	PCR <sup>b</sup>	Genotype <sup>c</sup> ( <i>bla</i> <sub>TEM-X</sub> )
1.	swab	<i>Enterobacter cloacae</i>	ESBL	+	(TEM-1)
2.	urine	<i>Enterobacter cloacae</i>	ESBL	+	TEM-1
3.	swab	<i>Enterobacter cloacae</i>	ESBL	+	TEM-1
4.	blood	<i>Enterobacter amnigenus</i>	ESBL	+	TEM-1
5.	swab	<i>Enterobacter cloacae</i>	ESBL	+	TEM-1
6.	urine	<i>Enterobacter</i> spp.	ESBL	+	TEM-1
7.	vaginal swab	<i>Enterobacter cloacae</i>	ESBL	+	TEM-1
8.	dialysate	<i>Enterobacter cloacae</i>	ESBL	+	TEM-1
9.	BAL	<i>Enterobacter cloacae</i>	ESBL	+	TEM-116
10.	urine	<i>Enterobacter cloacae</i>	ESBL	+	TEM-1
11.	urine	<i>Enterobacter cloacae</i>	ESBL	+	TEM-1
12.	tracheal swab	<i>Klebsiella</i> spp.	ESBL	+	TEM-1
13.	vaginal swab	<i>Escherichia coli</i>	ESBL	-	
14.	cervix swab	<i>Enterobacter cloacae</i>	ESBL	+	TEM-1
15.	urine	<i>Klebsiella pneumoniae</i>	ESBL	-	
16.	decubitus swab	<i>Klebsiella</i> spp.	ESBL	-	
17.	tracheal swab	<i>Enterobacter sakazakii</i>	ESBL	+	TEM-1
18.	ref. strain, EARSS, UA 1526	<i>Escherichia coli</i>	ESBL	-	
19.	ref. strain, EARSS, UA 1528	<i>Escherichia coli</i>	ESBL	+	TEM-8
20.	ref. strain, TEM-3	<i>Escherichia coli</i>	ESBL	+	TEM-3
21.	ref. strain, TEM-5	<i>Escherichia coli</i>	ESBL	+	TEM-7

<sup>a</sup> Sample collection, isolation of bacteria, species and phenotype determination was performed by standard procedures according to the NCCLS at the Robert Bosch Hospital (RBK) in Stuttgart.

<sup>b</sup> PCR: result of the PCR prescreening for determination of *bla*<sub>TEM</sub> gene presence (+ visible band at 861 bp in agarose gel electrophoresis, - no visible band at 861 bp in agarose gel electrophoresis).

<sup>c</sup> Result of TEM-array analysis, all *bla*<sub>TEM</sub> genes could be identified, except for isolate No. 1, which was identified by sequencing. All hybridizations were performed in duplicate (n = 6, n = number of analyzed spots), except for isolate No. 6 and 14 (n = 3) and isolate No. 19 (n = 9).

The results of the identification of *bla*<sub>TEM-1</sub> (isolate 3, n = 6), *bla*<sub>TEM-3</sub> (isolate 20, n = 6), *bla*<sub>TEM-7</sub> (isolate 21, n = 6), *bla*<sub>TEM-8</sub> (isolate 19, n = 9) and *bla*<sub>TEM-116</sub> (isolate 9, n = 6) are displayed in figure 23 as relative intensity values. Only the polymorphism positions, which varied in comparison to *bla*<sub>TEM-1</sub> are given. All of these positions were identified without ambiguity. Perfect match position 235 could not be identified for sample 10, *bla*<sub>TEM-3</sub>, *bla*<sub>TEM-7</sub> and *bla*<sub>TEM-8</sub> due to a spotting failure. 93 % of the analyzed mismatch positions remained below the relative intensity of the mismatches (RI<sub>MM</sub>) value of 0.4 (displayed in figure 24a). Only 7 % of the tested mismatch positions showed an RI<sub>MM</sub> of 0.4 - 0.7. The standard deviation of mean RI<sub>MM</sub> values varied from 0 to 0.36, but 95 % remained below 10% of the perfect match intensity (displayed in figure 24b). Two times the RI<sub>MM</sub> value of 0.7 was exceeded by probe 49A with an RI<sub>MM</sub> of 0.76 for isolate 14 and by probe 143T with an RI<sub>MM</sub> of 0.72 for isolate 10.

For both samples (isolate 10 and 14) and for isolate 1 (which could not be identified and therefore was omitted in the data evaluation) the overall discrimination was not optimal (data not shown), which was attributed to a suboptimal fragmentation of the target DNA due to handling problems and subsequent partial inactivation of DNaseI before starting the fragmentation. In summary, all detected *bla*<sub>TEM</sub> genes could be identified by the use of the TEM-array without ambiguity, except for the *bla*<sub>TEM</sub> gene of isolate 1. The results were confirmed by standard DNA sequencing of selected

samples of the tested TEM variants and the *bla<sub>TEM</sub>* gene of isolate 1 was thereby identified as *bla<sub>TEM-1</sub>* (data not shown).

Apart from the reference strains all positively prescreened clinical isolates except isolate 9 contained a *bla<sub>TEM-1</sub>* gene, which is a parental type and thus no ESBL. These isolates should contain other ESBL determinants, such as SHV, CTX-M or OXA causing the ESBL phenotype. These resistance genotypes were not determined for these isolates within the scope of this work. For the *bla<sub>TEM-116</sub>* gene variant, as identified in isolate 9, the conferred phenotype, whether ESBL or not ESBL, was up to date not conclusively determined (74).

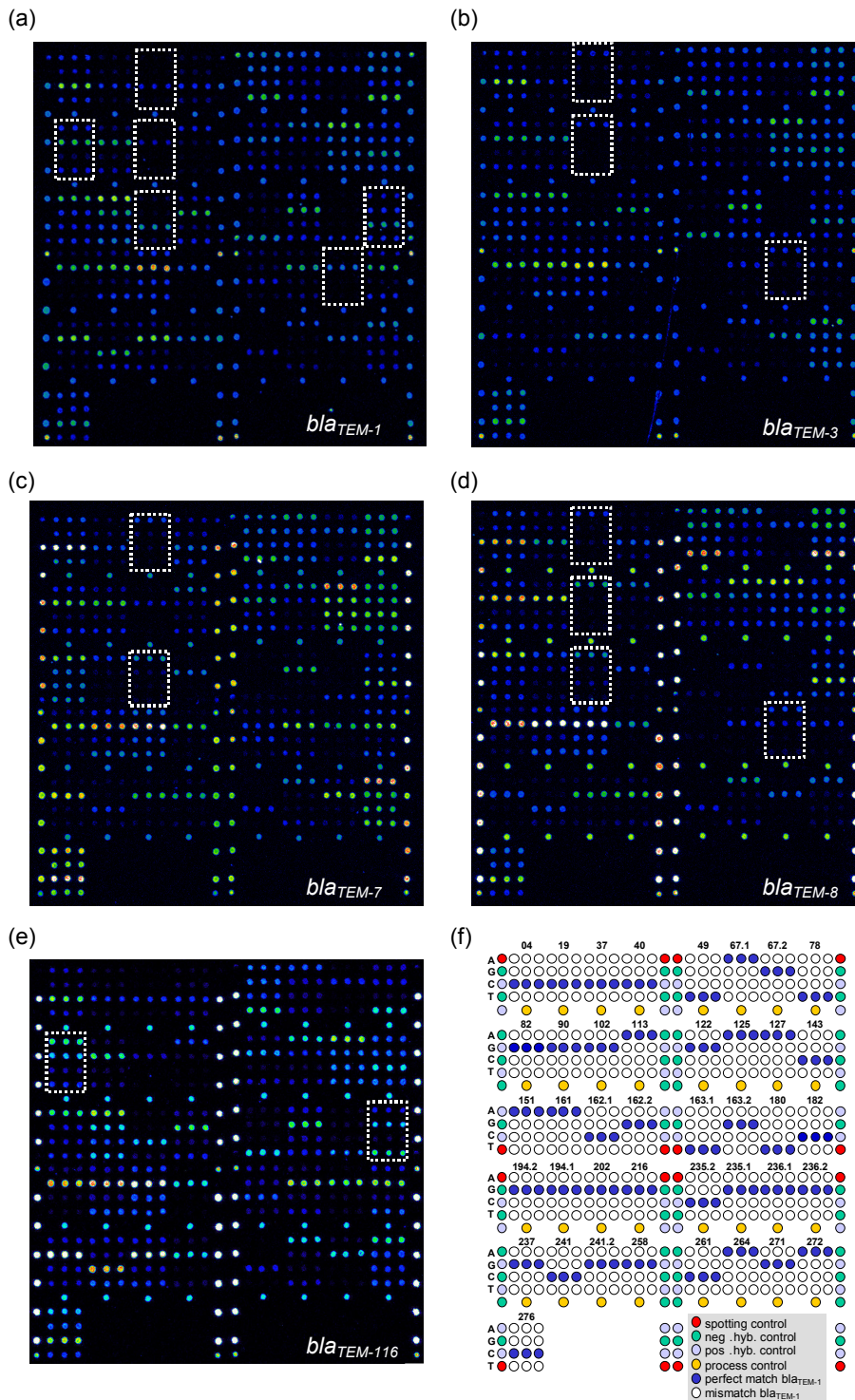
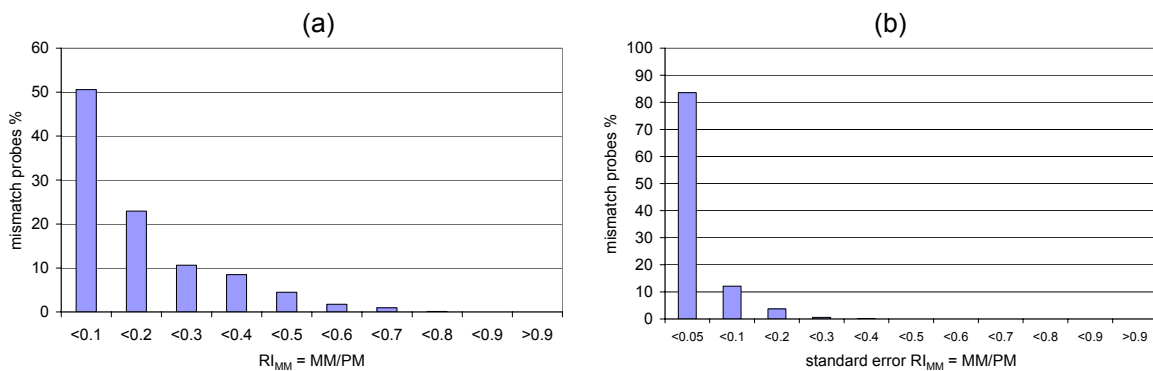
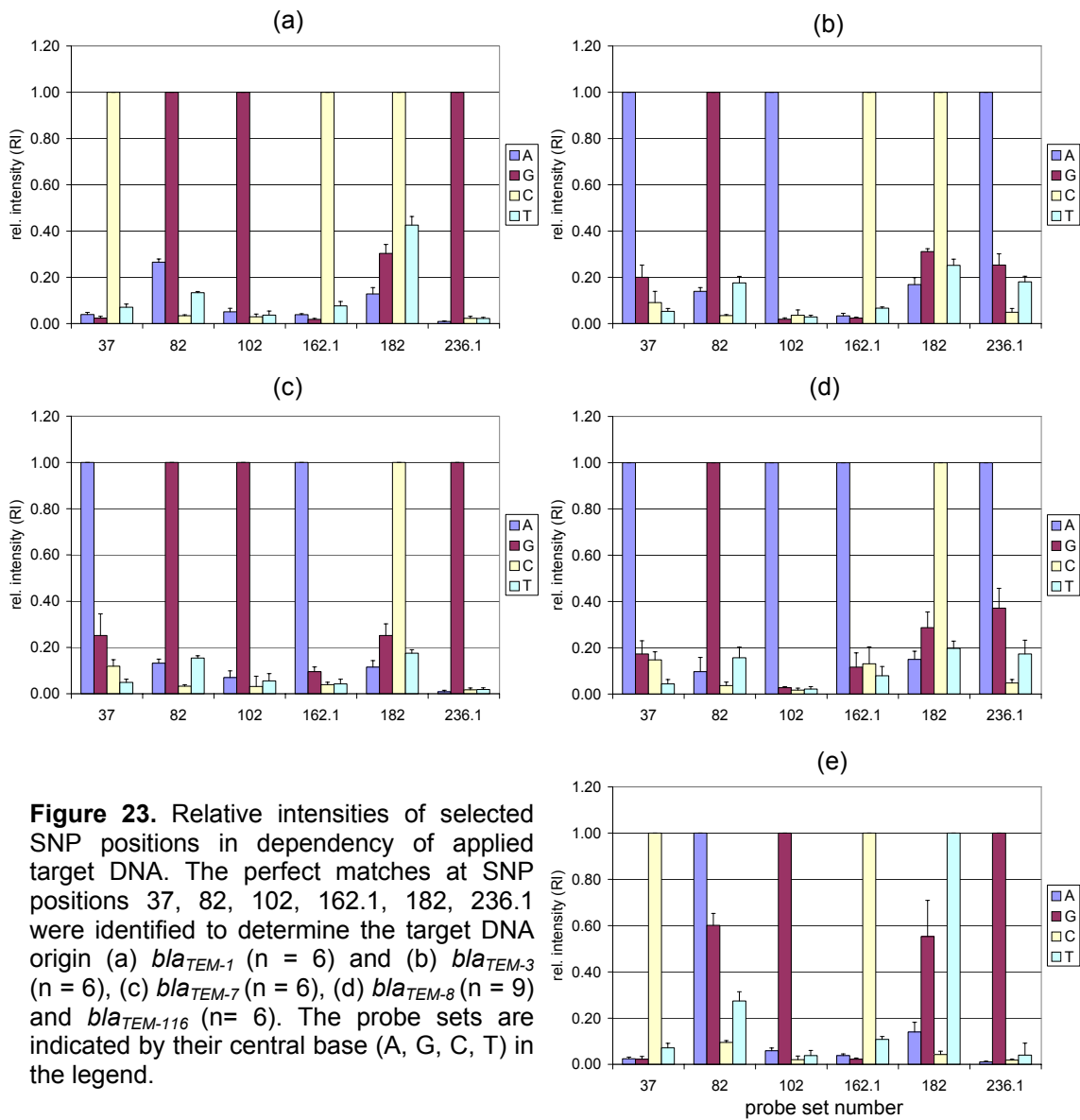


**Figure 22.** Fluorescence images of selected TEM-arrays hybridized with target DNA from different variants detected in clinical isolates collected at the RBK and reference strains. The varying SNP positions 37, 82, 102, 162.1, 182, 236.1 are highlighted. The identified variants were (a) *bla*<sub>TEM-1</sub>, (e.g. in isolate 3), (b) *bla*<sub>TEM-3</sub> (isolate 20), (c) *bla*<sub>TEM-7</sub> (isolate 21), (d) *bla*<sub>TEM-8</sub> (isolate 19) and (e) *bla*<sub>TEM-116</sub> (isolate 9). The signal intensity is shown in false color. Blue corresponds to the lowest signal intensity, red to white depict the highest signal intensities (as output by ImaGene 3.0). In (f) the SNP capture probe layout of the TEM microarray is displayed (for details see also figure 4).





## Results

### 3.1.8 Influence of target DNA properties

#### 3.1.8.1 Quantity of target DNA and incorporation ratio of the fluorescence label

This experiment was devised to determine the sensitivity of the detection concerning the amount of target DNA and the influence of the incorporation ratio of fluorescence label (number of nucleotides per fluorophore) under standard conditions. It was accomplished within the scope of a “Studienarbeit” from Christina Onaca at the ITB. For an optimal sensitivity of the array analysis every target DNA fragment should bear at least one fluorescence label, otherwise competition between labeled and unlabeled fragments can occur.

Two target DNA batches with differing incorporation ratios of the fluorescence label (number of nucleotides per fluorophore: NT/F = 87 and 166) were prepared. The target DNA was fragmented to fragment lengths between 50 and 150 bp. For an incorporation ratio of 87 NT/F 60 % to 100 % of the fragments should bear at least one fluorescence label, whereas for an incorporation ratio of 166 NT/F only 30 to 90 % of the fragments would bear a fluorescence label, so that an increased competition should occur. Increasing amounts of target DNA (25 - 200 ng) were hybridized in triplicate experiments.

The analysis of the net signal intensity averaged from all SNP specific probes yielded an unexpected result. The average net intensity increased as expected with a higher target DNA amount, but the corresponding average net signal intensities for an incorporation ratio of 87 NT/F were continuously lower (except for a target DNA amount of 200 ng) than those of the target DNA with an incorporation ratio of 166 NT/F (see figure 25).

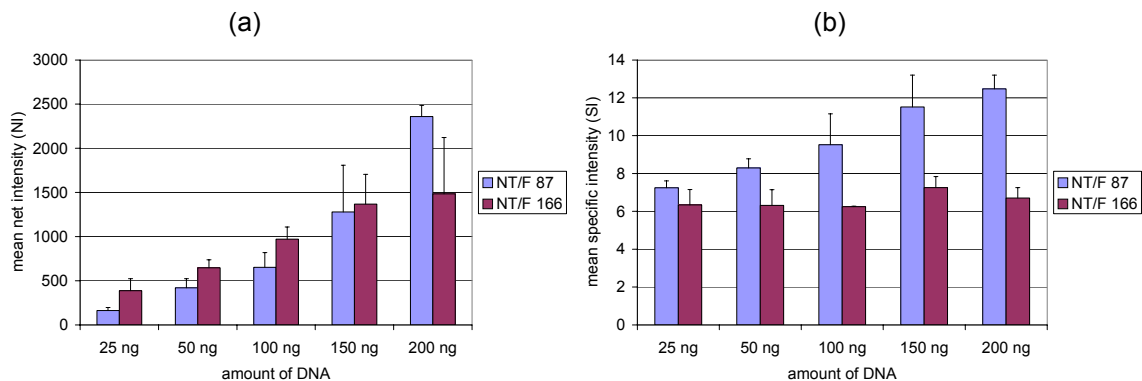


**Figure 25.** (a) Net intensity (NI) and (b) specific intensity (SI) averaged from all SNP positions for a hybridization experiment with 25 to 200 ng of *bla*<sub>TEM-116</sub> with an incorporation ratio of 87 or 166 nucleotides/fluorophore for 3 hours under standard cover slips (n = 9).

This result suggested either an underestimation of the DNA concentration in the target DNA with an incorporation ratio of 166 NT/F or an overestimation of the DNA concentration in the target DNA batch with a NT/F of 87.

However, the analysis of the specific intensities (defined as the ratio of the perfect match signal intensity over a mean of the three mismatch signal intensities) - averaged from all SNP specific probe sets - indicated that at least the tendency of the determined incorporation ratios was true. The average specific intensities for 87 NT/F were continuously higher (app. 14 – 42 %) in comparison to the corresponding signals for 166 NT/F. In case of the target DNA with an NT/F of 87 the signals increased for target DNA amounts from 25 ng towards 200 ng about 42 %. In contrast to that the average specific intensities for the DNA with an NT/F of 166 remained for all applied target DNA amounts at the same level.

A dependency of the mismatch to perfect match discrimination level of the applied target DNA amount could be observed for an incorporation ratio of 87 NT/F by analyzing the distribution of the relative intensities of the mismatches. The number of mismatches with an  $RI_{MM} < 0.1$  (optimal discrimination) increased steadily from 25 to 50 % for target DNA amounts from 25 to 200 ng as displayed in figure 26. For the hybridization of 25 ng DNA (NT/F = 87) all analyzed perfect match positions could be identified correctly, although the perfect match net intensities were very low with values between 83 and 1169, but the lowest mean perfect match net intensity was still five times above background level. Also for all other tested DNA amounts (50 - 200 ng) the perfect matches could be detected correctly.

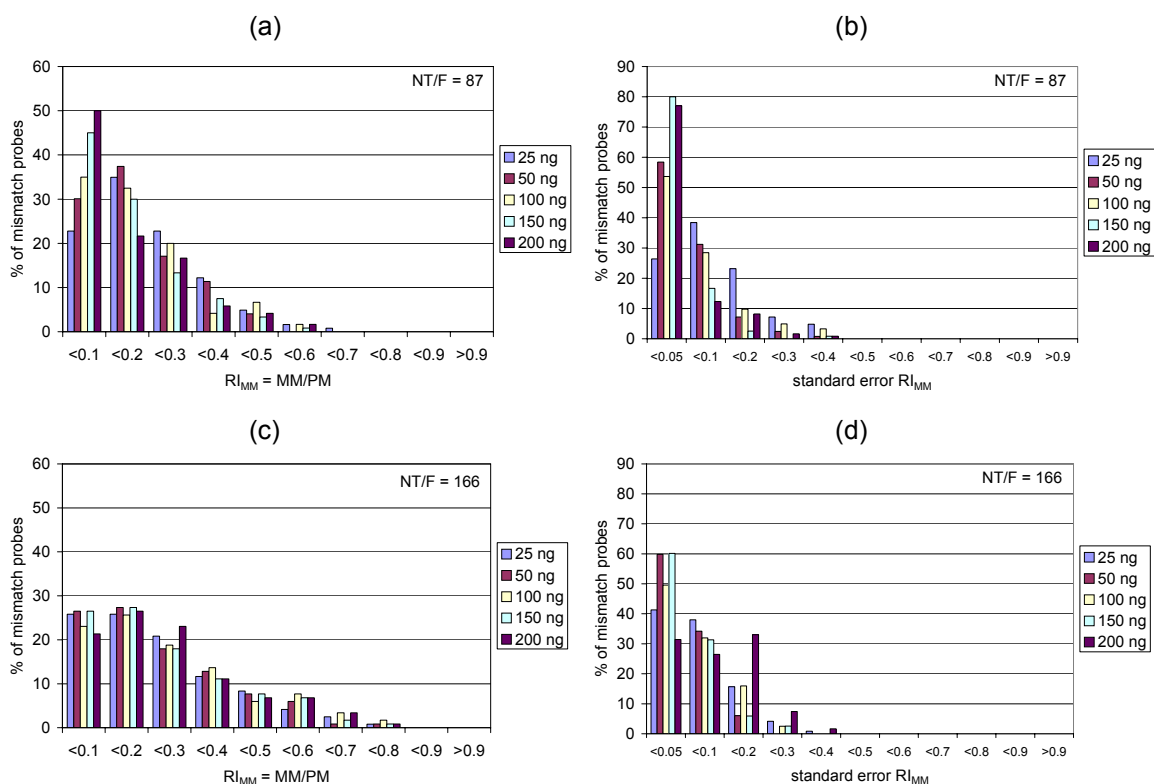


**Figure 26.** (a) Distribution of the relative intensities of the mismatch probes ( $RI_{MM}$ s) and (b) distribution of the standard errors of the relative intensities of the mismatch probes depending on the amount of the target DNA from a hybridization experiment with 25 to 200 ng of *bla*<sub>TEM-116</sub> with an NT/F of 87 (n = 9). (c) Distribution of the relative intensities of the mismatch probes ( $RI_{MM}$ s) and (d) distribution of the standard errors of the relative intensities of the mismatch probes depending on the amount of the target DNA from a hybridization experiment with 25 to 200 ng of *bla*<sub>TEM-116</sub> with an NT/F of 166 (n = 9).

## Results

---

The distribution of the  $RI_{MM}$  standard errors was shifted towards higher values for lower amounts of target DNA, consistently to a decreased signal to noise ratio (see figure 26), but remained in an acceptable range of 0 - 0.4. In contrast to that, the level of discrimination for an incorporation ratio of 166 was decreased compared to all tested amounts of target DNA with an incorporation ratio of 87. The distribution of the relative intensities of the mismatches for 166 NT/F was almost independent from the amount of target DNA. Nevertheless, all analyzed perfect match positions could be correctly identified for all tested DNA amounts, with perfect match net intensities between 276 and 2613 for 25 ng DNA, whereby the lowest analyzed perfect match intensity was still 17 times above background level. The  $RI_{MM}$  standard errors were between 0 and 0.32.

In conclusion, the specificity of the perfect match detection was enhanced for increasing amounts of target DNA with a majority of target DNA fragments bearing a label (87 NT/F). In contrast to that, the level of discrimination for target DNA with a decreased content of fluorescently labeled fragments (NT/F of 166) was lower and seemed to be independent from the applied amount of target DNA. The sensitivity limit of the array was not fully exploited with this experiment, since the lowest perfect match signals with 25 ng target DNA were still five times above background level. However, the negative influence on the discrimination and the reproducibility of a low signal to noise ratio were already obvious. Therefore, it was determined that for an optimal specificity and reproducibility the incorporation ratio should amount to at least 100 nucleotides per fluorophore, and at least 50 ng of target DNA should be applied.



### 3.1.8.2 Fragment length

The fragmentation of the target DNA was a crucial step during target DNA preparation and array analysis. To analyze the 41 polymorphisms in parallel, which were distributed over the whole length of 861 bp of the target gene, all target DNA regions had to be equally accessible for hybridization with oligonucleotide probes. Due to secondary structures a long target DNA fragment is partly inaccessible, since during the hybridization step the formation of secondary structures is favored. Furthermore, the hybridizing target DNA fragments had to bear at least one fluorescent label, otherwise competition between labeled and unlabeled fragments might occur. For target DNA with an incorporation ratio of usually 50-150 nucleotides per fluorophore, fragment sizes between 50 and 150 bp should be the optimal compromise between target DNA accessibility and sensitivity of the detection. To verify these assumptions, target DNA was fragmented with four different concentrations of DNaseI.

The fragment sizes were estimated using lab-on-a-chip electrophoresis (see figure 27). The signal peaks, which were detected at 43 s and 105 s, represented no signals specific for the analyzed sample, but were internal standard peaks. For the unfragmented target DNA (DNaseI, 0 U/ $\mu$ l) a sharp signal peak was detected at 100 s which corresponds to a fragment size - as determined by the DNA standard - of 850 to 1000 bp. The minor peak detected at 63 s corresponds most probably to an air bubble and thus was ignored. For the target DNA fragmented with 1.2 mU/ $\mu$ l DNaseI the major signal peak was starting at 88.5 s (500 bp), but the maximum fluorescence was detected at the time point corresponding to the unfragmented target DNA peak. The peak maximum was reduced by about 10 fluorescence units in comparison to the unfragmented target DNA (DNaseI, 0 U/ $\mu$ l). These observations indicated the target DNA was partly fragmented with 1.2 U/ml DNaseI to fragment sizes between 500 and 861 bp.

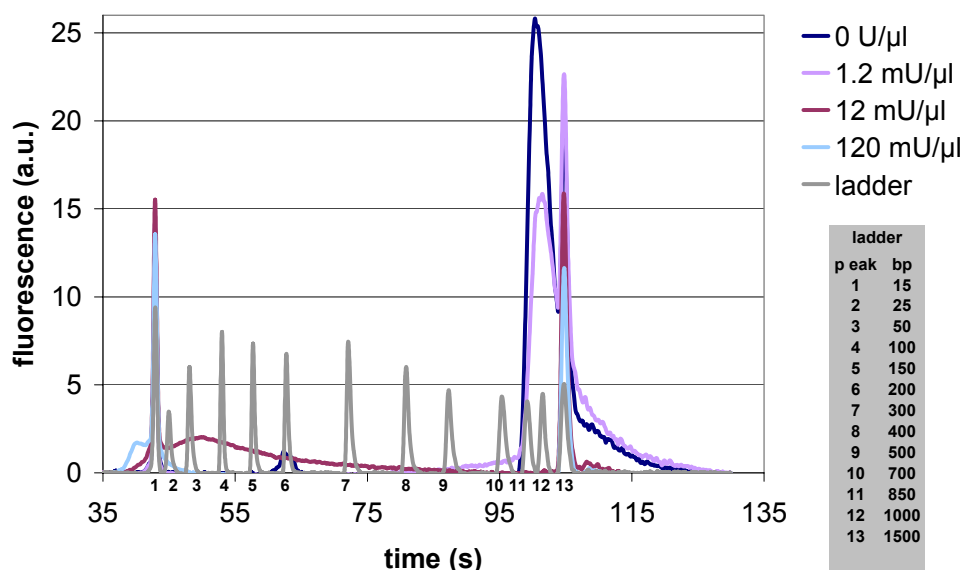


**Figure 27.** Analysis of target DNA fragment sizes from DNA fragmentation reactions with four different concentrations of DNaseI (0 – 120 mU/ $\mu$ l) by lab-on-a-chip electrophoresis. The fluorescence signal is given in arbitrary units (a.u.). The fluorescence signal peaks of the ladder correspond to fragment sizes between 15 - 1500 bp as indicated in the legend.

## Results

For a DNaseI concentration of 12 mU/ $\mu$ l an increased fluorescence signal was detected between 45 and 88 s corresponding to fragment sizes between 25-500 bp. The target DNA was completely fragmented, since no signal was detected at time points above 90 s. For the target DNA fragmented with 120 mU/ $\mu$ l a fluorescence signal was detected between 38 and 48 s corresponding to fragment sizes between less than 15 and up to 50 bp. Since the detected signals were partly outside of the size range covered by the DNA standard (43-105 s), a distinct analysis was not possible. Due to the limited resolution at the start and end point of the detection, this method could only yield an estimation of the fragment sizes.

To determine the effect of the different fragment lengths on the hybridization, the array was hybridized with 110 ng target DNA (NT/F = 76) from the different fragmentation reactions. The fluorescence images of the hybridized arrays are displayed in figure 28. Clearly visible is, that the distribution of the fluorescence signals is strongly dependent on the fragment size. In case of the target DNA fragmented with 0 or 1.2 mU/ $\mu$ l a major part of the fluorescence signals is below the detection limit. For the target DNA fragmented with 12 or 120 mU/ $\mu$ l the signals are distributed more evenly.

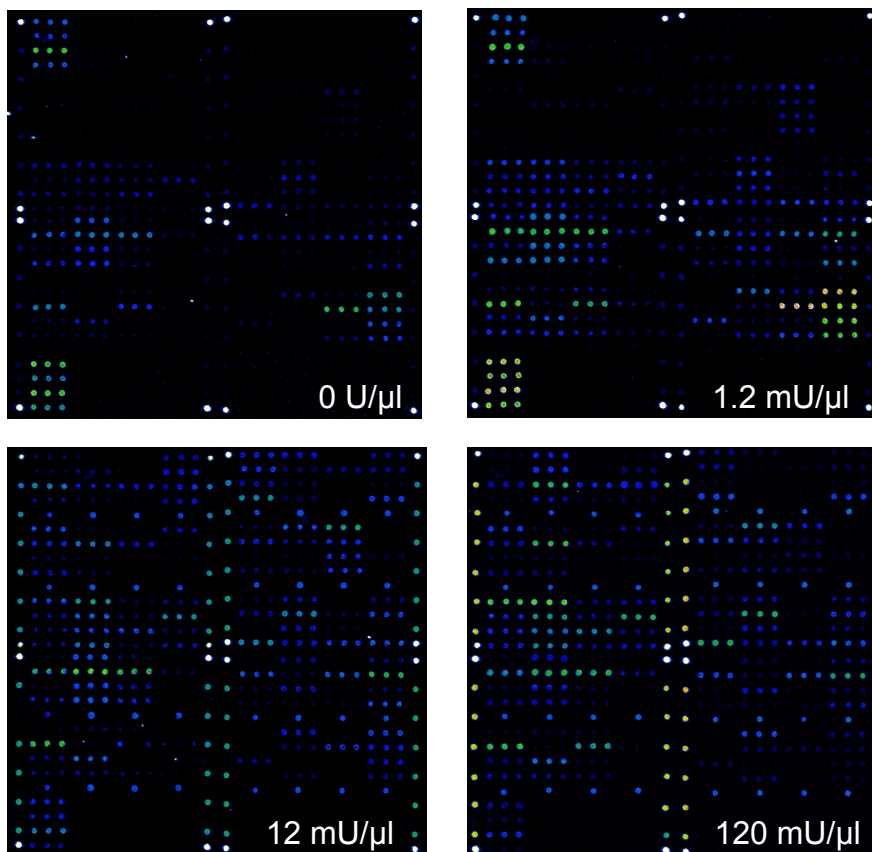


**Figure 28.** Fluorescence image of a hybridization experiment with 110 ng *b/a<sub>TEM</sub>* target DNA from pUC19 (NT/F = 76) fragmented with 0 U/ $\mu$ l, 1.2 mU/ $\mu$ l, 12 mU/ $\mu$ l and 120 mU/ $\mu$ l DNaseI as indicated in the lower right corner of the corresponding image. The signal intensity is shown in false color. Blue corresponds to the lowest signal intensity, red to white depict the highest signal intensities (as output by ImaGene 3.0).

The quantified data confirm these results (see figure 29). Especially the fluorescence signals on probe positions 19-182 for the target DNA fragmented with 0 or 1.2 mU/μl were so weak, that an accurate identification of the perfect matches was not possible. Apparently, no hybridization happened at these probe sets with mainly unfragmented target DNA. In contrast to that, the probe sets targeting the 5' end of the target strand showed higher perfect match signal intensities, when hybridized with less fragmented target DNA.

For the target DNA fragmented with 12 mU/μl all 41 perfect match positions for *bla<sub>TEM-116</sub>* could be identified correctly. 98 % of the mean relative intensities of the mismatches remained below 0.6. Probe 82G showed values up to 0.79 (data not shown). The relative intensity standard deviations ranged from 0 to 0.24.

For the target DNA fragmented with 120 mU/μl considerably lower net signal intensity for the majority of perfect match probes were detected (see figure 29) and only 40 of 41 perfect match positions for *bla<sub>TEM-116</sub>* could be identified by calculating the mean relative intensities. The perfect match of position 261 was misidentified. Although probes 67.1, 67.2, 258, 271, 272 had very low net perfect match signal intensities between 115 and 565 (which was still at least six times above net background signal intensity), 98 % of the mean relative intensities of the mismatches remained below 0.6. Probe 182G showed values up to 0.71 (data not shown). The relative intensity standard deviations ranged from 0 to 0.38.

In conclusion, the effect of long target DNA strands preventing target DNA accessibility could be observed for target DNA batches with mostly unfragmented target DNA. Hereby the 3' end of the captured target strand seemed to be less accessible for hybridization than the 5' end. The fragmentation with 12 mU/μl DNaseI produced fragments between 25-500 bp and performed best regarding sensitivity and specificity of the perfect match identification. As assumed, target DNA with smaller fragment sizes (15-50 bp), but with the same incorporation ratio, performed worse regarding sensitivity of the perfect match detection. In this case some of the net perfect match signal intensities approached the background level leading to increased standard deviations of the relative intensities and misidentification of one perfect match position.

## Results

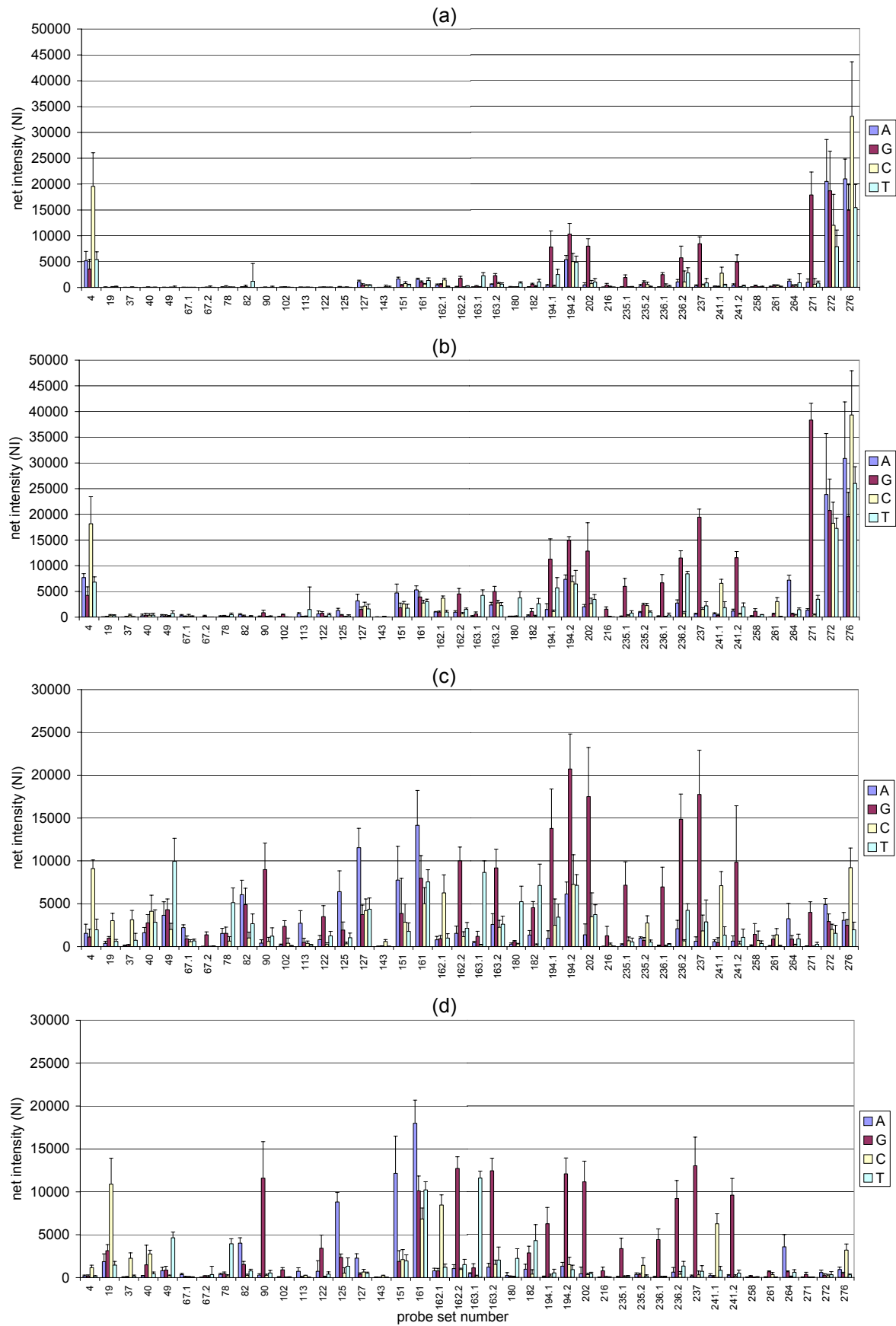


**Figure 29.** Mean net signal intensities for each SNP position and corresponding probe (A, G, C or T refer to the central base position) from a hybridization experiment with 110 ng *bla<sub>TEM</sub>* target DNA from pUC19 (NT/F = 76) fragmented with (a) 0 U/ $\mu$ l, (b) 1.2 mU/ $\mu$ l, (c) 12 mU/ $\mu$ l and (d) 120 mU/ $\mu$ l DNase (n = 9).

### *3.1.9 Reduction of assay time and test of hybridization devices*

The hybridization method used to set up the system was performed under a standard cover slip. These were incubated in Corning hybridization chambers during hybridization, followed by washing steps in agitated solution in glass jars and a manually performed drying step. Several features of this method offered a potential for optimization. The hybridization of DNA microarrays is diffusion limited and the net signal intensity is depending on the number of target molecules reaching the probe. This is a notoriously slow process for relatively big molecules such as DNA, so that with shorter incubation time a reduced sensitivity and specificity is usually associated. The overall time to perform the molecular diagnostics assay was initially six hours, including two hours for DNA amplification and labeling, 30 minutes for purification and fragmentation, three hours for hybridization and 30 minutes for washing. Since this array should be finally applied in the clinical setting, it was tested, if the rate limiting hybridization time could be significantly reduced by applying different hybridization devices, while keeping the sensitivity and specificity at a sufficient level. Furthermore, the reproducibility of experiments and quality of the generated data should be improved, as well as the most frequent sources of error compromising the array analysis should be reduced, so that the reliability necessary for a clinical application will be ensured.

The most frequent sources of error were the following: The hybridization under an unsealed cover glass could lead to evaporation and subsequent drying of the hybridization sample causing high background intensities. During washing the cover slip did not always dissociate right at the beginning, leading to an ineffective wash step, so that unspecific signals and high background intensities remained. The drying step had to be performed instantly (which was not always realizable when performing an experiment with several replicates) or remaining salt from the wash solution caused a high background intensity. Therefore, the application of different devices for improvement of hybridization conditions or partial automation of the hybridization process were evaluated.

Not all devices could be tested at the same time, therefore each analyzed device was compared to a standard cover slip hybridization in Corning hybridization chambers. Since for these experiments large target DNA batches were necessary, they had to be prepared in advance and had sometimes to be frozen and thawed before use. This storage parameters and differing incorporation ratios of fluorescence label could introduce a variable performance of the different target DNA batches, especially regarding the observed net signal intensities. However, through comparison to a standard cover slip hybridization, variations in the resulting data introduced by different target DNA batches could be estimated. The evaluation criteria included the increase of the overall net fluorescence signal intensity, the specificity of the perfect match identification in total and in detail, the reproducibility of the generated data, as well as low and uniform background signal intensities.

## Results

### 3.1.9.1 ArrayBooster

The first tested device was an ArrayBooster (Advantix, Brunnthal, Germany) hybridization station, using surface acoustic waves to agitate the sample solution during incubation of the target DNA. After hybridization, the slides had to be washed and dried manually. Hybridization times from three hours to 30 min were analyzed with 65 ng target DNA (57 NT/F) per array. For each condition only one array was tested. The increase of the fluorescence signals by using the surface acoustic waves for sample agitation during hybridization was distinct, as visible in the fluorescence images displayed in figure 30. This was confirmed by the analysis of the net signal intensities averaged from all SNP specific probes. The net signal intensities were increased in average about 1.7 times for three hours incubation to up to 8.5 times for one hour incubation time (see figure 31), while retaining equal background net intensities (approximately 20-30 arbitrary units).

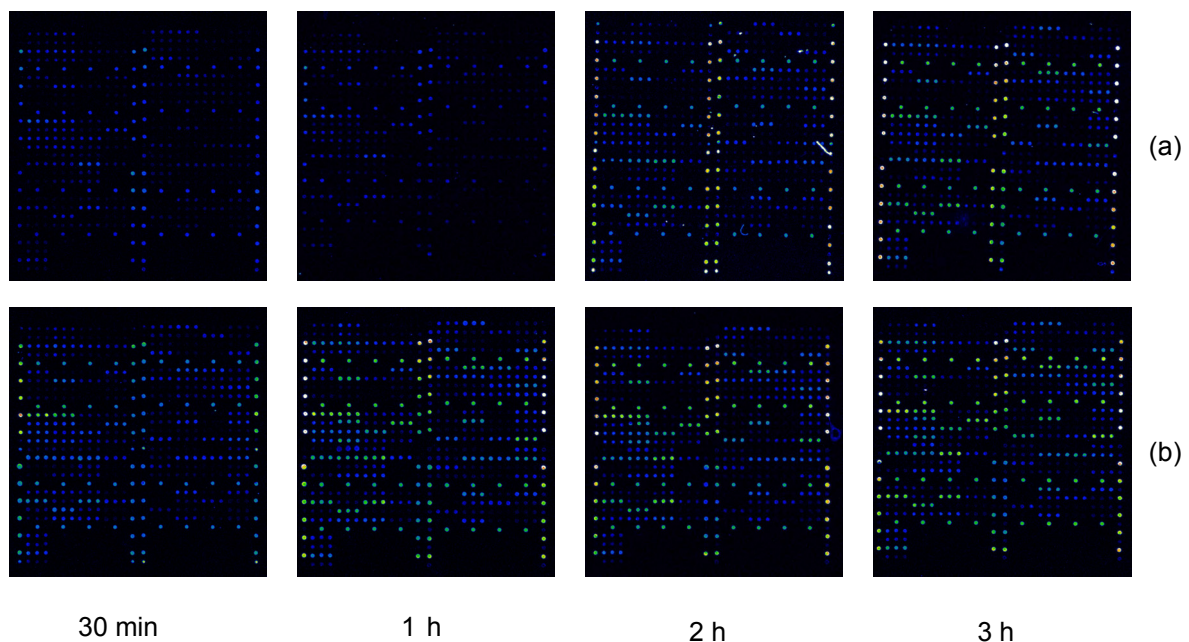


**Figure 30.** Fluorescence images of a hybridization experiment with 65 ng DNA (57 NT/F) used in a (a) diffusion dependent hybridization using standard cover slips in Corning hybridization chambers or (b) agitation dependent hybridization using surface acoustic waves produced by the ArrayBooster, for hybridization times of 30 min to 3 h.

An increase of the average net signal intensity was only advantageous in combination with an increase of the mismatch to perfect match discrimination, which was estimated in total by calculating the average specific intensities of all probe sets. The specific intensity was defined as the ratio of the net perfect match signal intensity over the mean of the three net mismatch signal intensities of each SNP probe set. The average specific intensity was clearly increased through agitation (see figure 31). The enhancement of the discrimination by the use of the ArrayBooster was the more pronounced the shorter the hybridization time.



All 41 perfect match positions could be identified at three hours, two hours and 30 minutes. Only in the cover slip hybridization of one hour one perfect match was misidentified (data not shown). This was attributed to aberrations in the spotting process.

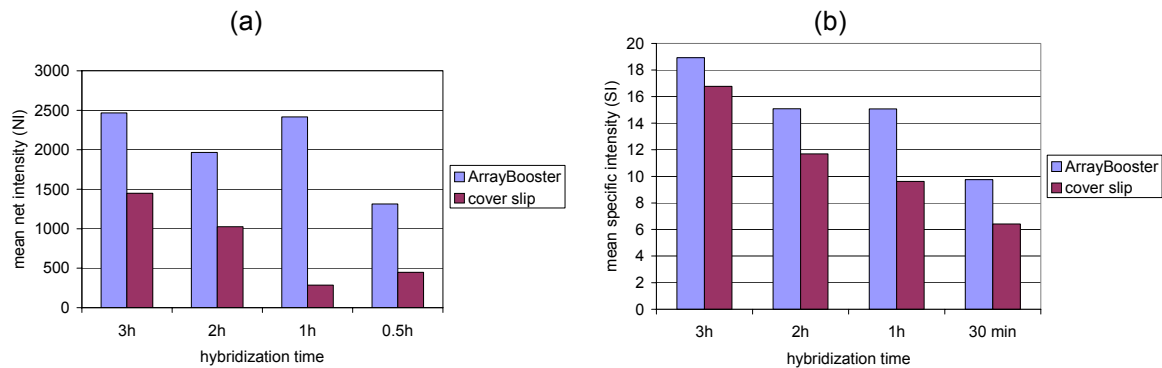


**Figure 31.** (a) Net intensities (NIs) averaged from all SNP specific probes and (b) specific intensities (SIs) averaged from all SNP probe sets depending on the hybridization time for a diffusion dependent (cover slip) and agitation dependent (ArrayBooster) hybridization ( $n = 3$ ).

The efficiency of the mismatch to perfect match discrimination was analyzed in detail by reviewing the distribution of all mismatches in dependency of the mismatch to perfect match ratio (defined as the relative intensity of the mismatch,  $RI_{MM} = MM/PM$ ) as displayed in figure 32. The discrimination is the more efficient the lower the mismatch to perfect match ratio. A perfect match is considered as not clearly identified if one or more of the three mismatches of one probe set have a relative intensity of  $> 0.8$ .

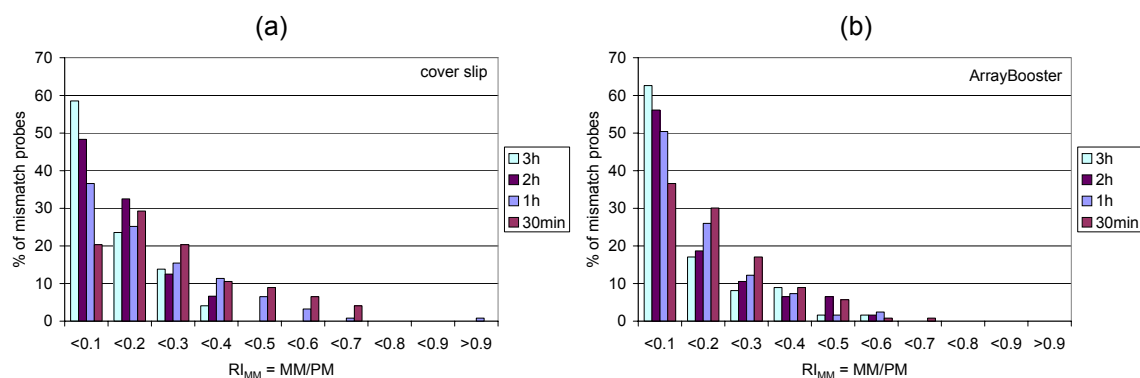


**Figure 32.** (a) Percentage of mismatch probes depending on the MM/PM ratio for a diffusion dependent (cover slip) hybridization and (b) percentage of mismatch probes depending on the MM/PM ratio for an agitation dependent (Arraybooster) hybridization for 3 h to 30 min ( $n = 3$ ).

The discrimination was clearly enhanced by agitation for hybridization times shorter than one hour. At one hour hybridization time, while using the ArrayBooster, over 50 % of the relative intensities of the mismatches were below 0.1, corresponding to an optimal perfect match to mismatch discrimination. In contrast to that only 37 % of the mismatches presented such a discrimination efficiency in case of the cover slip

## Results

hybridization. At 30 minutes hybridization time the divergent discrimination efficiency between the two methods was even more pronounced. By using the cover slip method, only 20 % of the  $RI_{MM}$ s showed optimal discrimination efficiency with values below 0.1, in contrast to 37 % under agitation of the hybridization sample. Generally, the better the discrimination, the further the  $RI_{MM}$  distribution was shifted towards lower  $RI_{MM}$ s with the majority of the mismatch relative intensities below 0.1. If the discrimination was less optimal, the maximum of the distribution of the relative intensities of the mismatches was shifted from a mismatch to perfect match ratio of 0.1 to higher values.

To analyze the variability of the system in total, the standard errors of the relative intensities were averaged from all mismatch probes. The average  $RI_{MM}$  standard errors are displayed in figure 33. The decrease of the net intensities and the resulting decreased signal to noise ratio caused an increase of the  $RI_{MM}$  standard errors as obvious for the cover slip hybridization of one hour and 30 minutes (see figure 33). It has to be taken into account, that the analysis of the different hybridization times was performed with only one array for each condition. In an additional experiment the reproducibility in between three arrays was tested for a hybridization time of three hours. Here the ArrayBooster did yield an average  $RI_{MM}$  standard error of 2.4 % in contrast to 1.2 % for the cover slip hybridization. So in terms of reproducibility no improvement was observed for this condition, but it can be assumed that for shorter hybridization times the effect would be more pronounced, mainly by increasing the signal to noise ratio as indicated by the results of the variation of the hybridization time.

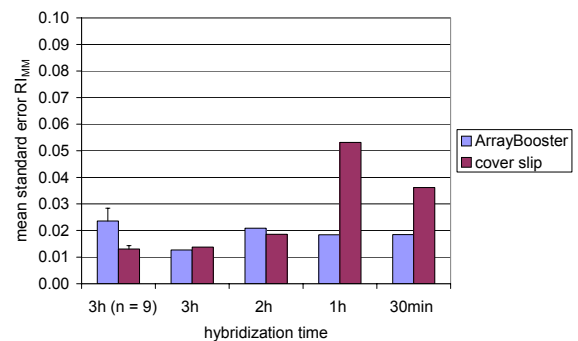


**Figure 33.** Standard errors of relative mismatch intensities ( $RI_{MM}$ ) averaged from all SNP positions depending on the hybridization time for a diffusion dependent (cover slip) and agitation dependent (ArrayBooster) hybridization. ( $n = 3$ , if not stated otherwise).

In summary, it was determined that by using both methods hybridization times of 30 minutes were sufficient for a correct identification of all perfect match positions. Although the ArrayBooster produced very convincing results considering the acceleration of the hybridization, more experiments were not performed, because several features of the tested device were disadvantageous. The application of the sample solution without air bubbles was problematic, because of the design of the fill nozzle of the hybridization chamber, so that several arrays had to be excluded from the analysis. Furthermore, removing of the hybridization chamber from the array after hybridization caused sometimes a smearing of the target DNA over the array surface, which could not be eliminated by subsequent washing. Even though these problems might be solved by a well trained user, it is a prerequisite to perform the assay user-



independently, and since these facts reduced the amount of analyzable data considerably, this device was not further investigated.

### 3.1.9.2 Lucidea Slide Pro

Besides the diffusion limitation of the hybridization process another source of experimental aberrations were the washing and drying steps. The second tested hybridization device (Lucidea Slide Pro, Amersham Pharmacia Biotech, Freiburg, Germany) included a flow chamber using a pumping mechanism to actively distribute the sample on the microarray surface during hybridization and allowed also to perform the washing steps automatically. A final drying step was a projected feature of this hybridization station, but was not ready for application so far according to the supplier, so that the drying step had to be performed manually. In the precedent experiment it was determined, that for hybridization times below one hour the effect of the sample agitation on the hybridization results was most pronounced and that the generated data was sufficient for a sensitive data analysis. Therefore, the influence of hybridization times from one hour to 15 minutes on the hybridization signals using the Lucidea Slide Pro in comparison to using cover slips in Corning hybridization chambers was investigated.

All experiments were performed in triplicate with 75 ng target DNA (75 NT/F) per array. The increase of the fluorescence signals after hybridization with the Lucidea Slide Pro in comparison to the cover slip hybridization was not as remarkable as for the ArrayBooster (see figure 34 for fluorescence images).

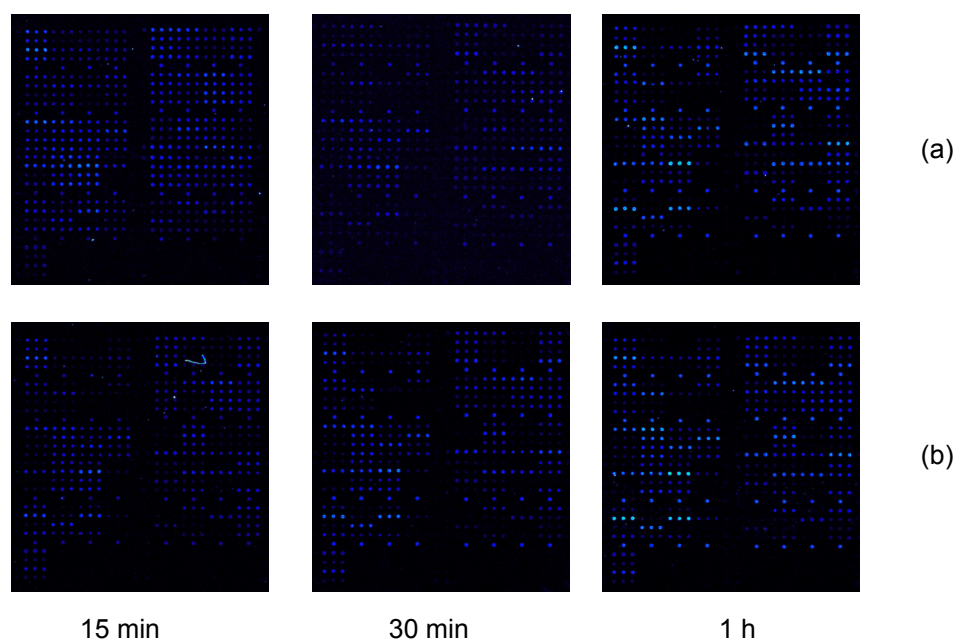


**Figure 34.** Fluorescence images of a hybridization experiment with 75 ng DNA (75 NT/F) used in a (a) diffusion dependent hybridization using standard cover slips in Corning hybridization chambers or (b) agitation dependent hybridization and wash in flow chambers of Lucidea Slide Pro, for hybridization times of 15 min to 1 h.

## Results

The resulting net signal intensities averaged from all SNP specific probes at one hour were comparable. At 30 minutes the hybridization station produced about two times higher net intensities. Using the hybridization station, the average net intensity observed at 30 min was surprisingly higher than the one determined with the same device at one hour hybridization time. This was attributed to problems associated with the sample injection. At 15 minutes the net intensities of one array of the cover slip hybridization were uncharacteristically high, resulting in a highly increased average net intensity. This might have been caused by inefficient washing due to a too late dissociation of the cover slip from the array during the wash steps. The effect of the differing hybridization times and devices was more comprehensible for the analyzed average specific intensities. Here the use of the Lucidea Slide Pro resulted in a clear increase of the average specific intensities, which was the better in comparison to the cover slip hybridization, the shorter the hybridization time (see figure 35).

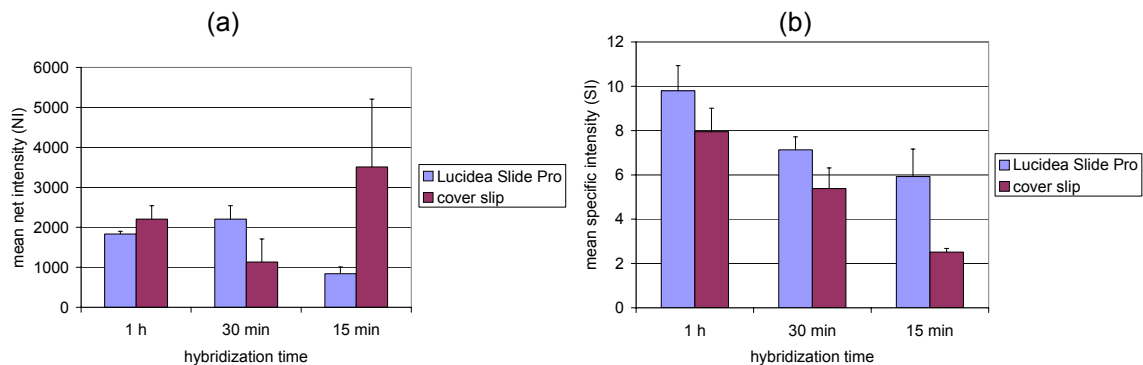


**Figure 35.** (a) Net intensities (NIs) averaged from all SNP specific probes depending on the hybridization time (b) Specific intensities (SI) averaged from all SNP probe sets depending on the hybridization time for a diffusion dependent (cover slip) and agitation dependent (Lucidea Slide Pro) hybridization ( $n = 9$ ).

At one hour and 30 minutes hybridization time all 41 perfect match positions could be identified by analyzing the relative intensities resulting from both hybridization methods, but at 30 minutes in the cover slip hybridization one mismatch position exceeded the predefined ID limit of 0.8 (as defined in section 3.1.4) with a value of 0.86. In the hybridization using the Lucidea Slide Pro at 15 minutes two perfect match positions were misidentified and for two others the predefined ID limit of 0.8 was exceeded with  $RI_{MM}$ s up to 0.86. At 15 min in the cover slip hybridization finally 12 % of the mismatch positions exceeded the ID limit. For six polymorphism positions the perfect matches were even misidentified.

Remarkably distinct for shorter hybridization times was the displacement of the maximum of the distribution of the relative intensity of the mismatches from 0.1 towards 0.5. Hereby the distribution pattern clearly approached a Gaussian distribution, which was especially pronounced for the cover slip  $RI_{MM}$  values at 15 min (see figure 36a).

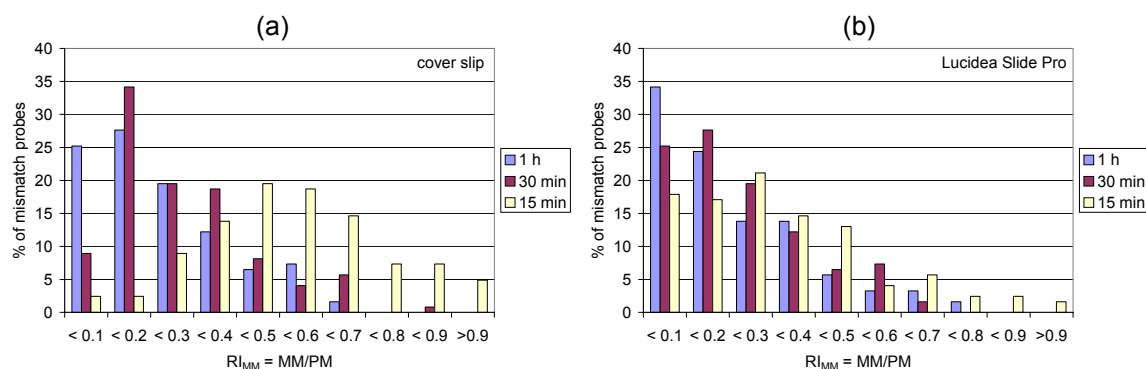


**Figure 36.** Percentage of mismatch probes depending on the MM/PM ratio from an hybridization experiment of 75 ng DNA (75 NT/F) (a) in Corning hybridization chambers and (b) in the Lucidea Slide Pro for 1 h, 30 min and 15 min ( $n = 9$ )

The analysis of the  $RI_{MM}$  standard errors did not yield conclusive results for favoring one of the tested methods (see figure 37). Generally, longer hybridization times led to a higher reproducibility, except for 30 min versus one hour hybridization in the Lucidea Slide Pro, which was attributed to a lower signal to noise ratio determined at one hour. This was most probably caused by incomplete probe injection and thus less applied target DNA in the hybridization taking one hour in comparison to the hybridization of 30 minutes.

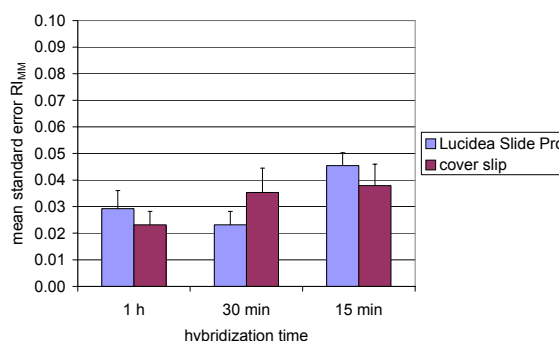


**Figure 37.** Standard errors of relative mismatch intensities ( $RI_{MM}$ ) averaged from all SNP positions depending on the hybridization time for a diffusion dependent (cover slip) and agitation dependent (Lucidea Slide Pro) hybridization ( $n = 9$ ).

In conclusion, all perfect match positions were correctly identified using both methods for hybridization times as short as 30 minutes. For the cover slip hybridization one mismatch position at 30 minutes exceeded the predefined ID limit of 0.8, however considering the correct perfect match identification and the reliable identification of all the other positions, this could be neglected. For a hybridization time of 15 minutes both hybridization systems failed to deliver a reliable perfect match identification. By using the Lucidea Slide Pro, an enhancement of the discrimination efficiency could be observed, but no general increase in the net signal intensities or reproducibility was detected. The major difficulty observed while using the Lucidea Slide Pro was the probe injection step. To avoid the injection of air bubbles, sometimes not the whole sample could be loaded, which led to the observed aberrations in the assay results.

## Results

---

### 3.1.9.3 Tecan HS400

The third tested hybridization device was the HS 400 from Tecan (Crailsheim Germany), which offered the possibility to automate the whole process starting from the hybridization up to the final drying step. The flow through chamber contained two membranes allowing an agitation of the sample by applying pressure alternately. The slides were dried automatically by N<sub>2</sub> flow. Hybridization times from one hour, 30 and 15 minutes were analyzed with 150 ng target DNA per array (136 NT/F). All experiments were performed in triplicate. An enhancement of the fluorescence signals by using the hybridization station could be observed as displayed in figure 38.

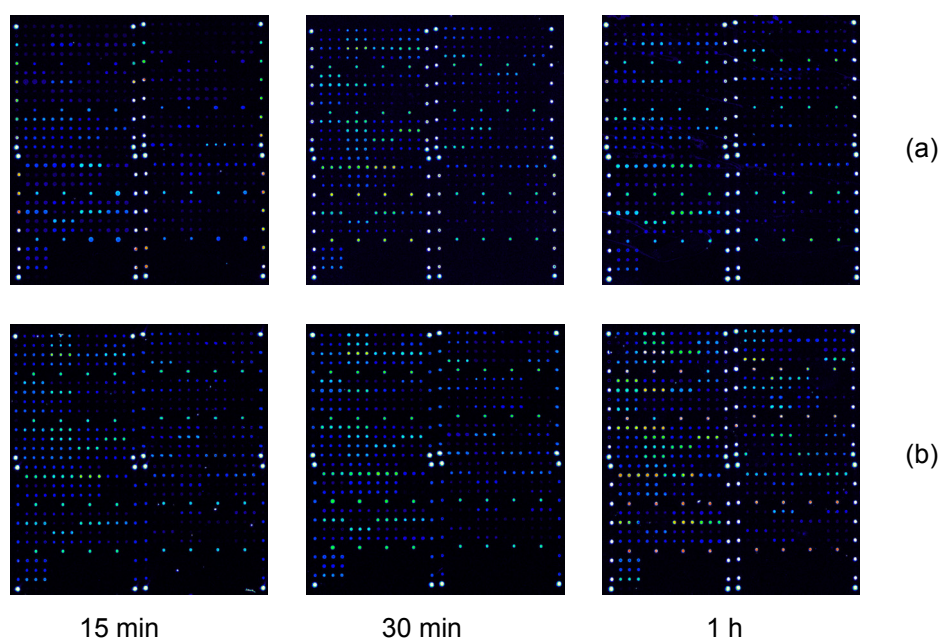


**Figure 38.** Fluorescence images of a hybridization experiment with 150 ng DNA (136 NT/F) used in a (a) diffusion dependent hybridization using standard cover slips in Corning hybridization chambers or (b) agitation dependent hybridization and wash in flow chambers of the HS400, for hybridization times of 15 min to 1 h.

The net signal intensities were increased by using the HS400 in average about 2.8 times at one hour up to 3.5 times at 15 minutes in comparison to the cover slip hybridization (see figure 39). The average specific intensity was enhanced by the use of the hybridization station within the same range (approximately with a factor of 1.2 -1.4 ) for all tested hybridization times.

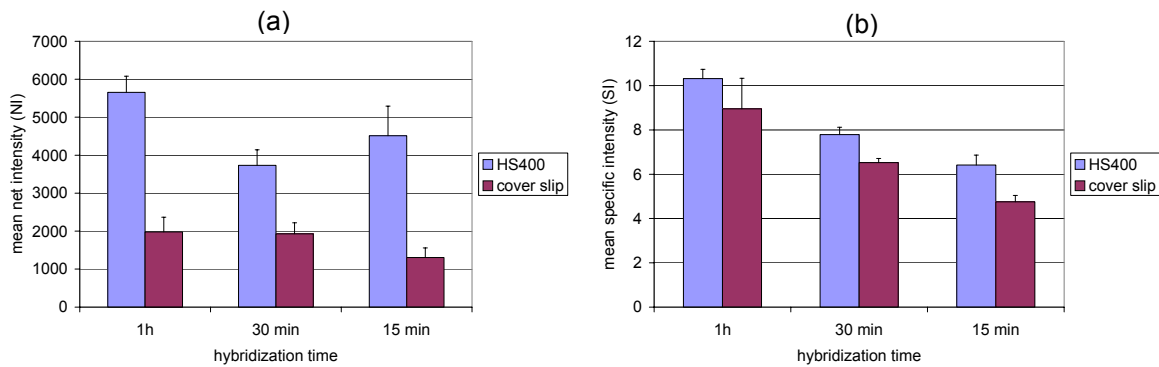


**Figure 39.** (a) Net intensities (NIs) averaged from all SNP specific probes and (b) specific intensities (SIs) averaged from all SNP probe sets depending on the hybridization time for a diffusion dependent (cover slip) and agitation dependent (HS400) hybridization (n = 9).

By using the HS400, all correct perfect match positions could be identified for the analyzed probe sets at one hour, 30 and even 15 minutes. (In the whole experiment position 182 had to be excluded from the data analysis, due to a spotting failure in the whole slide batch.) At one hour and 30 minutes in the cover slip hybridization also all perfect match positions could be identified, only at 30 minutes one probe exceeded the  $RI_{MM}$  limit of 0.8 with an  $RI_{MM}$  of 0.89. Two perfect matches were misidentified in the cover slip hybridization of 15 minutes.

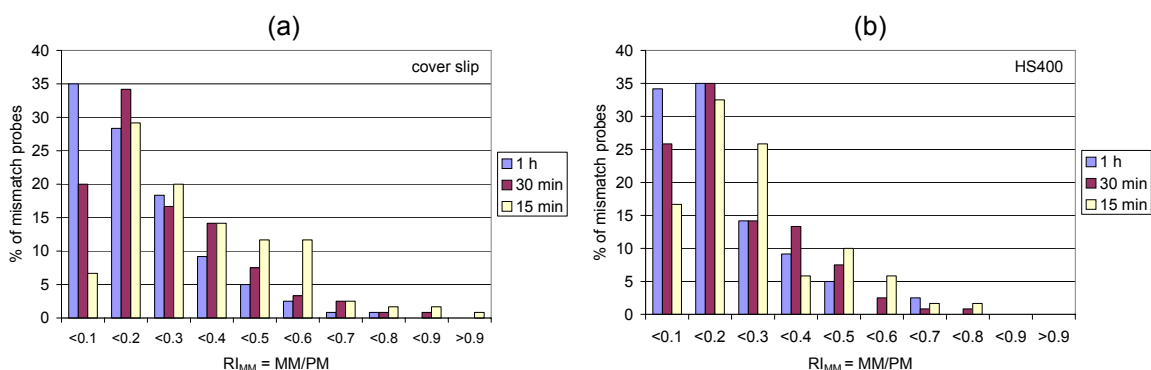


**Figure 40.** Percentage of mismatch probes depending on the MM/PM ratio from an hybridization experiment of 150 ng DNA (136 NT/F) (a) in Corning hybridization chambers and (b) in the HS400 for 1 h, 30 min and 15 min (n = 9)

## Results

The mismatch to perfect match discrimination was enhanced by using the hybridization station at hybridization times shorter than one hour as can be seen in detail in figure 40. At one hour hybridization time the discrimination efficiency was almost equal for both methods. At 30 minutes while using the HS400 26 % of the relative intensities of the mismatches were below 0.1, in contrast to only 20 % of the mismatches in case of the cover slip hybridization. At 15 minutes hybridization time the divergent discrimination efficiency between the two methods was even more pronounced. By using the cover slip method, only 7 % of the  $RI_{MM}$ s showed optimal discrimination efficiency with values below 0.1, in contrast to 17 % under agitation of the hybridization sample. In contrast to the coverslip method for the HS400 no  $RI_{MM}$  values greater than 0.8 were detected for all analyzed hybridization times.

The average  $RI_{MM}$  standard errors for the HS400 hybridization remained almost at the same level (about 2 %) for a reduced hybridization time, whereas the  $RI_{MM}$  standard errors for the cover slip hybridization showed a continuous increase (up to 4.5 % at 15 min) as displayed in figure 41.

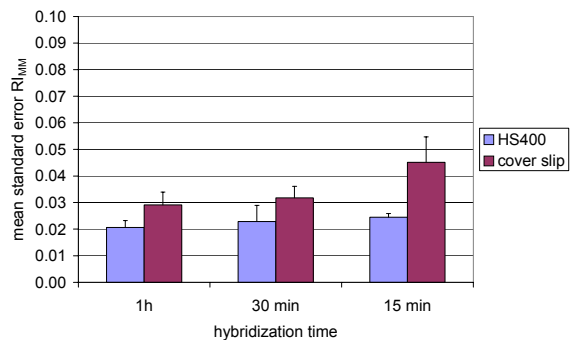


**Figure 41.** Standard errors of relative mismatch intensities ( $RI_{MM}$ ) averaged from all SNP positions depending on the hybridization time for a diffusion dependent (cover slip) and agitation dependent (HS400) hybridization (n = 9).

Overall, the HS400 enhanced the net and the specific signal intensities and increased the reproducibility of experiments. It allowed a reliable perfect match identification at all tested hybridization times, even at times as short as 15 minutes. In the cover slip hybridization at one hour and 30 minutes all perfect match positions could correctly be determined, although one position exceeded the predefined ID limit. However, at 15 minutes the cover slip method failed to deliver an accurate perfect match identification in contrast to the HS400.



#### 3.1.9.4 Thermomixer slide adapter

Additionally, two simple devices were tested for their effect on problems concerning the hybridization step. One was the application of sealing frames (Eppendorf, Hamburg, Germany) instead of cover slips, thereby forming an enclosed hybridization environment, so that the sample solution could not evaporate. Furthermore, it allowed to load a higher volume of the sample solution (65  $\mu\text{l}$  instead of 30  $\mu\text{l}$  for the cover slip hybridization). The second device was a slide adapter (Eppendorf, Hamburg, Germany), which allowed the heating and agitation of the array on a thermomixer, when a sealing frame was used for hybridization. The washing and the drying steps were performed manually. The applied target DNA (150 ng per array, 136 NT/F) stemmed from the target DNA batch used in the evaluation of the HS400, so that the data was directly comparable to the previous experiment. As before, hybridization times from one hour, 30 and 15 minutes were analyzed and all experiments were performed in triplicates.

An enhancement of the fluorescence signals by using the thermomixer was not obvious from the fluorescence images (displayed in figure 42), but a slight increase in the average net fluorescence intensities (about 1.3 times) could be determined for hybridization times of one hour and 15 minutes as displayed in figure 43.

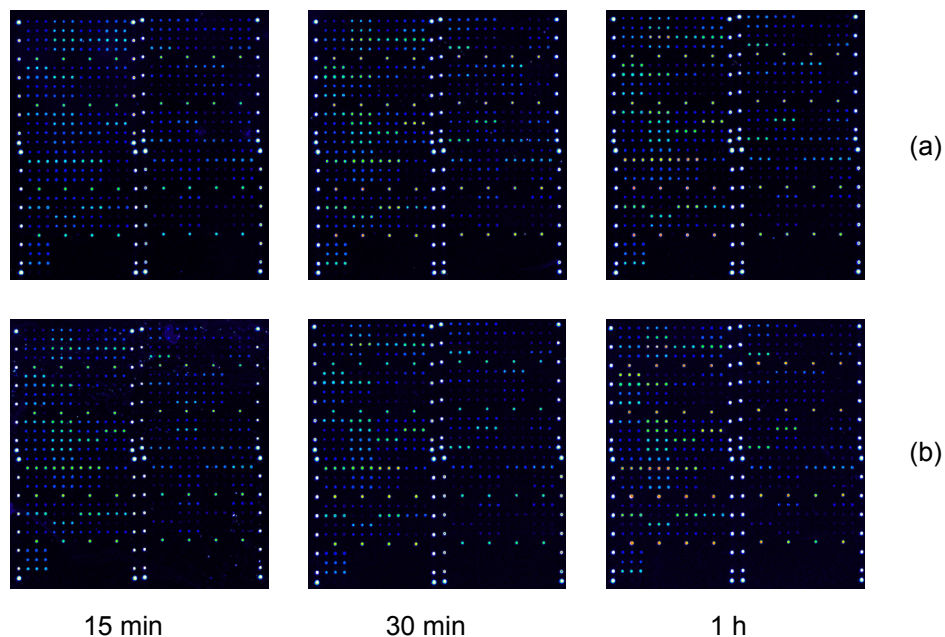


**Figure 42.** Fluorescence images of a hybridization experiment with 150 ng DNA (136 NT/F) used in a (a) diffusion dependent hybridization using sealing frames in Corning hybridization chambers or (b) agitation dependent hybridization in a thermomixer slide adapter, for hybridization times of 15 min to 1 h.

## Results

Although for the average net intensity calculated after 30 minutes hybridization time using the thermomixer a slight aberration could be observed, the average specific intensity was still increased compared to the sealing frame hybridization. The average specific intensity was enhanced by agitation from approximately 1.2 to 1.4 times.

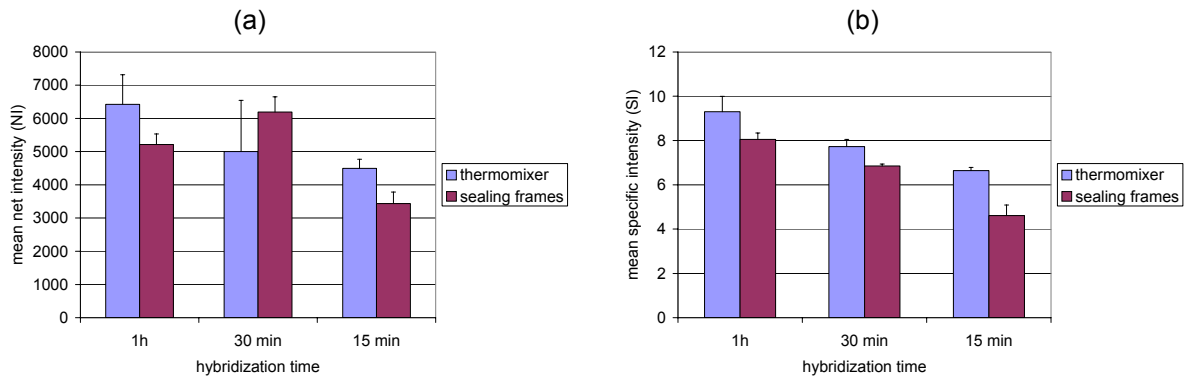


**Figure 43.** (a) Net intensities (NIs) averaged from all SNP specific probes and (b) specific intensities (SIs) averaged from all SNP probe sets depending on the hybridization time for a diffusion dependent (sealing frames) and agitation dependent (thermomixer) hybridization ( $n = 9$ ).

On all slides tested in the thermomixer the discrimination efficiency for position 161 was weak and at one hour hybridization time the perfect match of position 161 was even misidentified. Apart from that, under agitation all perfect matches could be identified correctly (except for position 182 due to the aforementioned spotting aberrations), but each time one mismatch exceeded the  $RI_{MM}$  limit of 0.8 at 15 and 30 minutes hybridization time. Without agitation, all analyzed perfect matches were detected correctly, but for the hybridizations lasting one hour and 30 minutes each time one mismatch exceeded the predefined  $RI_{MM}$  limit of 0.8.

Except for position 161 at one hour hybridization time, the mismatch to perfect match discrimination efficiency was enhanced for the agitation dependent hybridization as displayed figure 44. At 30 minutes, while using the thermomixer, 30 % of the relative intensities of the mismatches were below 0.1, in contrast to only 23 % of the mismatches in case of the hybridization without agitation. At 15 minutes hybridization time using the sealing frames only 8 % of the  $RI_{MM}$ s showed optimal discrimination efficiency with values below 0.1, in contrast to 23 % under agitation of the hybridization sample.



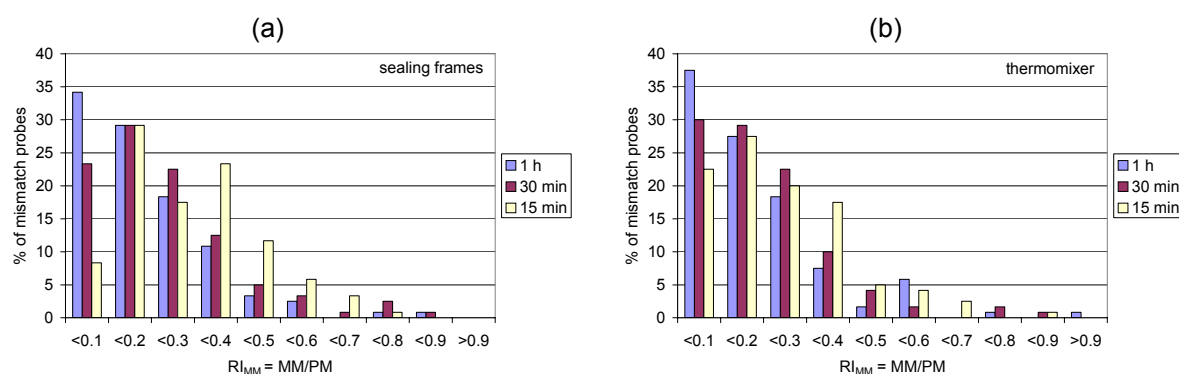


**Figure 44.** Percentage of mismatch probes depending on the MM/PM ratio from an hybridization experiment of 150 ng DNA (136 NT/F) (a) in a diffusion dependent (sealing frames) and (b) agitation dependent (thermomixer slide adapter) hybridization for 1 h, 30 min and 15 min ( $n = 9$ )

The average  $RI_{MM}$  standard remained almost at the same level for a hybridization time of one hour and 30 minutes, independent from hybridization with or without agitation, whereas the  $RI_{MM}$  standard errors for the hybridization without agitation showed a slight increase at 15 min as displayed in figure 45.

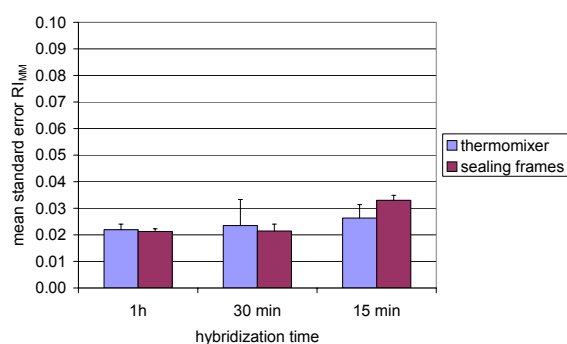


**Figure 45.** Standard errors of relative MM intensities ( $RI_{MM}$ ) averaged from all SNP positions depending on the hybridization time for a diffusion dependent (sealing frames) and agitation dependent (thermomixer slide adapter) hybridization ( $n = 9$ ).

In summary, the use of the sealing frame alone (without agitation) increased the average net signal intensities, but the overall perfect match to mismatch discrimination as determined by the average specific signal intensities were comparable to those achieved by the application of the cover slip. In other experiments it was determined, that the use of a higher hybridization volume could lead to enhanced net signal intensities. Therefore, it was assumed, that the increased volume was the cause of the detected enhanced fluorescence signals compared to the cover slip hybridization. The agitation by thermomixer increased the average net and specific signal intensities, but in detail the discrimination was worse than observed for the results achieved by using the HS400. The integration of these devices into the assay would require an adaptation of the washing protocol, so that more stringent washing steps are applied. However, the aforementioned problem of the probability of experimental aberrations introduced through the non-automated washing and drying steps were not addressed by these devices.

### 3.1.9.5 Conclusion of assay time and hybridization device testing

In conclusion, the evaluation of the different tested hybridization devices was as follows: The ArrayBooster performed best regarding the enhancement of the net and specific signal intensities and produced a good perfect match discrimination, but presented severe handling problems (e.g. probe injection, removing the hybridization chamber), which compromised the reproducibility of experiments. Furthermore, this device did not address the problem of the unreliability of the manual washing and drying steps.

The Lucidea Slide Pro did not deliver very conclusive results regarding enhancement of the net intensities and the reproducibility. This was also partly attributed to problems with the probe injection. The discrimination was considerably enhanced in comparison to the cover slip hybridization, which was attributed to a more effective washing through automation of the wash step, but the slides still had to be dried manually, which was not satisfying for a hybridization station claiming a high level of automation.

The Tecan HS 400 enhanced the net and specific signal intensities convincingly, as well as the perfect match discrimination and the reproducibility of the data. Furthermore, it offered the possibility to automate the whole process including hybridization and washing up to an effective final drying step. In combination with the easy handling, especially regarding the probe injection, this instrument was considered as the overall best performing hybridization device.

The tested sealing frame in combination with the thermomixer slide adapter offered a simple solution for several points of concern of the hybridization. The use of the thermomixer led to increased average net and specific signal intensities, but the additional requirement of an effective perfect match discrimination for this assay proved to be the major drawback, which would require the adaptation of the washing protocol.

In this experiment, it could be determined that by using the Tecan HS 400 the hybridization time could in principle be reduced to 15 minutes and the total assay time to less than 3.5 hours while keeping the discrimination power of the diagnostic array at a sufficient level. However, it was clearly determined that this reduction in hybridization time was only achieved at the expense of the specificity and the sensitivity of the analysis. To provide the possibility to achieve the most sensitive and specific results in an acceptable assay time, all following experiments were carried out using the Tecan HS400 with a hybridization time of one hour, which resulted in a reduction of the total assay time from initially 6 to 4 hours.

### 3.1.10 Mixed resistances

To determine if the detection of an ESBL TEM variant in presence of a narrow spectrum variant was possible, *bla*<sub>TEM-8</sub> and *bla*<sub>TEM-116</sub> target DNA with identical incorporation ratios (NT/F=76) were mixed in different ratios: 1:0; 1:1; 1:5, 1:10; 1:100, and 0:1.

All perfect match positions could be identified correctly for pure *bla*<sub>TEM-116</sub> with all relative intensities of the mismatches < 0.64 except for probe 258, which showed spotting errors and was thus not taken into account for the data analysis of all arrays. The standard deviations ranged from 0 - 0.23. For pure *bla*<sub>TEM-8</sub> all perfect match positions could be identified correctly with RI<sub>MMS</sub> < 0.46 (standard deviations 0 -0.19), except for probe sets 163.1 and 235.2, where the net fluorescence intensities for the perfect match positions were below the detection limit and no relative intensities could be calculated. This was due to the correctly detected mutations at positions 162.1 and 236.1, which represent an additional mismatch towards the target sequence for the probe sets with partially overlapping sequence. Thus the hybridization was for these positions disabled, but this did not affect the correct identification of *bla*<sub>TEM-8</sub>. For the whole test series the standard deviations of the relative intensities remained below 0.3.

In figure 46 a-e the probe sets with perfect matches differing between *bla*<sub>TEM-116</sub> and *bla*<sub>TEM-8</sub> are displayed. In figure 46 f and g the perfect match positions of the displayed probes were identical. The *bla*<sub>TEM-8</sub> perfect match signal pattern could be distinguished for positions 82 and 102 up to a ratio of 1:10, for 37, 162.1 and 236.1 up to a ratio of 1:5 from the relative intensity signal pattern of a pure narrow spectrum variant (*bla*<sub>TEM-116</sub>) with differences from 0.11-0.24. The mixed pattern for 37, 162.1, 236.1 at a ratio of 1:10 was still differing from the pure resistance pattern, but the difference of 0.06-0.07 was close to the inner variability of the system. The signal pattern of a ratio of 1:100 could not be distinguished from the pattern of pure *bla*<sub>TEM-116</sub> target DNA. As can be seen in figure 46 f and g the variation for the relative intensities of the mismatches of a probe set with the same perfect match was less than 0.07.

Due to the reproducibility of the relative intensities an identification of mixed resistances up to a ratio of 1:5 or even 1:10 should be possible, but for each probe set an individual RI<sub>MM</sub> threshold has to be defined. If this threshold is violated, a mixed resistance can be suspected. However, much more data has to be generated and more variants to be tested to ascribe an individual threshold to each probe set.

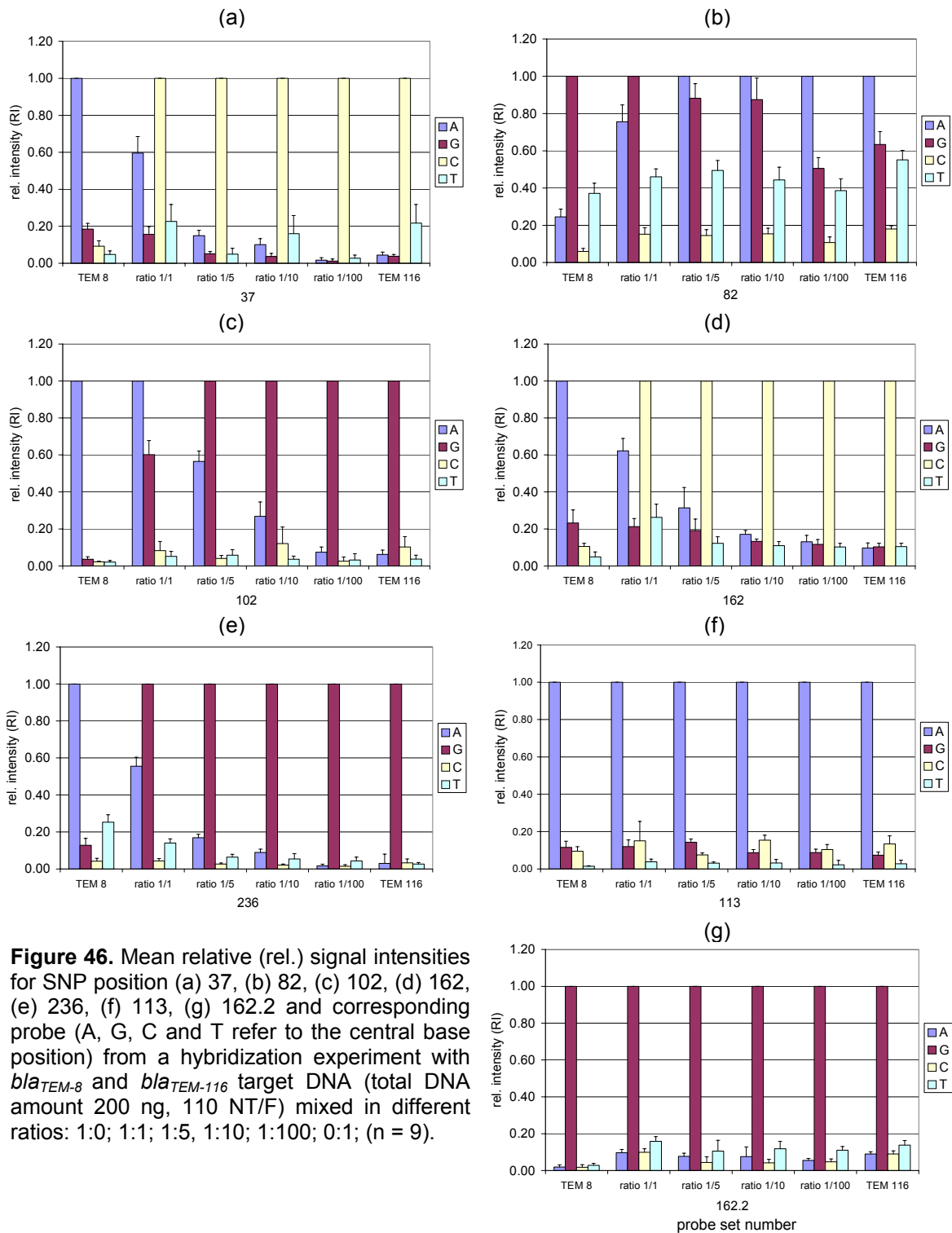


**Figure 46.** Mean relative (rel.) signal intensities for SNP position (a) 37, (b) 82, (c) 102, (d) 162, (e) 236, (f) 113, (g) 162.2 and corresponding probe (A, G, C and T refer to the central base position) from a hybridization experiment with *bla<sub>TEM-8</sub>* and *bla<sub>TEM-116</sub>* target DNA (total DNA amount 200 ng, 110 NT/F) mixed in different ratios: 1:0; 1:1; 1:5; 1:10; 1:100; 0:1; (n = 9).

### 3.1.11 Validation of the TEM-array with clinical samples from the NRCA

To validate the TEM-array, a set of 61 clinical isolates collected at four different Russian Hospitals (Moscow City Clinic No. 7, Central Russian Military Hospital, National Research Center for Pediatric Diseases, Tomsk City Hospital) was provided by the NRCA (National Research Center for Antibiotic Resistance, Moscow). Thirty of these isolates (displayed in table 7) contained a *bla*<sub>TEM</sub> gene, which was determined in a PCR prescreening with TEM-specific primers at the NRCA. The phenotypes and species identification were also carried out at the NRCA. By defining the MICs with broth microdilution tests, all isolates were classified as ESBL producers. An additional ESBL confirmatory disc diffusion test was performed at the Robert Bosch Hospital, Stuttgart. In this disk diffusion test a bigger than 5 mm increase in a zone diameter for ceftazidime, cefotaxime or cefpodoxime tested in combination with clavulanic acid versus its zone when tested alone confirmed an ESBL-producing organism. The ESBL phenotype could be confirmed for 22 of the 30 isolates. For five isolates no inhibition effect of clavulanic acid could be observed, which indicates the presence of a mobilized AmpC gene causing the resistance. The presence of an ESBL gene in addition to this could not be determined by this test, since the AmpC phenotype might mask the ESBL phenotype. In two cases the isolates were susceptible to all tested antibiotics, so that an ESBL phenotype was excluded. One sample was not purely isolated, so that a correct confirmatory test could not be performed. The discrepancy between the MIC and confirmatory test results prove the problem of an unambiguous phenotypic ESBL identification independent from the used method (broth microdilution or disc diffusion) or the institution where the tests are performed.

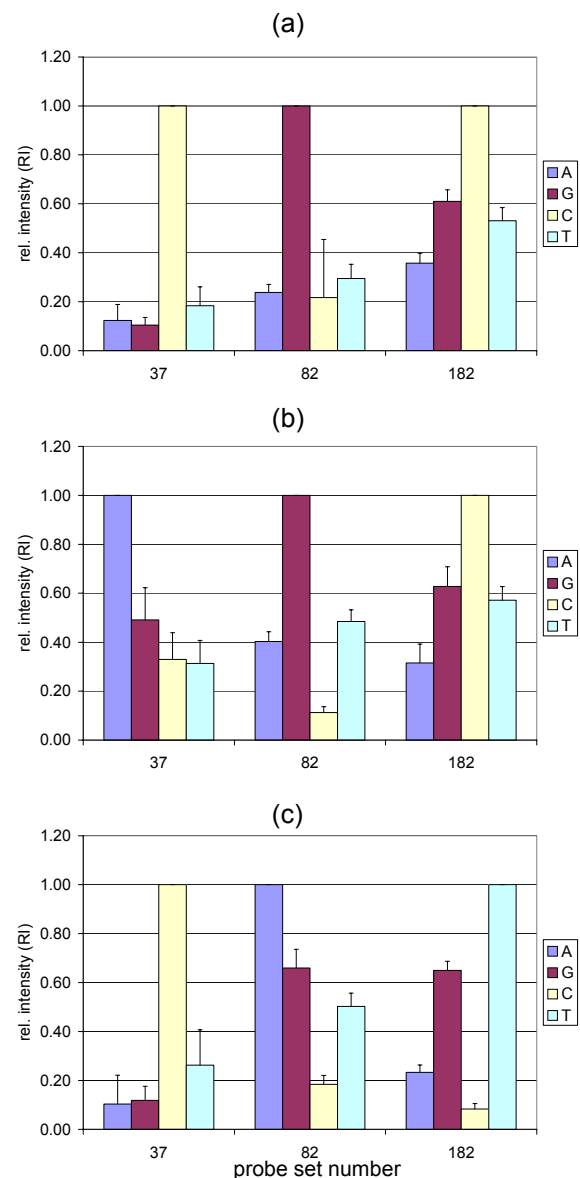


**Figure 47.** Relative intensities of selected SNP positions in dependency of applied target DNA. Only the SNP positions (37, 82 and 182) differing between *bla*<sub>TEM-1</sub> and the detected variants are displayed. The identified *bla*<sub>TEM</sub> gene variants were (a) *bla*<sub>TEM-1</sub> (n = 9) in 26 isolates (e.g. data displayed from isolate No 50) (b) *bla*<sub>TEM-2</sub> (n = 9) in isolate No 31 and (c) *bla*<sub>TEM-116</sub> (n = 9) in the control target DNA. The probe sets are indicated by their central base (A, G, C, T) in the legend.

## Results

The prescreening for and identification of CTX-M and SHV-type resistance was performed by coworkers at the NRCA. The DNA extracted from the isolates was prescreened by PCR for the occurrence of *bla*<sub>CTX-M</sub> and *bla*<sub>SHV</sub> genes in addition to the *bla*<sub>TEM</sub> genes. 24 of the isolates showed a PCR product with *bla*<sub>CTX-M</sub>-specific primers and 10 isolates showed a PCR product with *bla*<sub>SHV</sub>-specific primers. The *bla*<sub>CTX-M</sub> and *bla*<sub>SHV</sub> gene variants which could be subsequently identified by standard DNA sequencing are displayed in table 7. The detected variants comprised *bla*<sub>CTX-M</sub>-3, -14, -15 and *bla*<sub>SHV</sub>-2, -12, -38.

All *bla*<sub>TEM</sub> genes could be amplified and fluorescently labeled from the extracted isolate DNA. PCR products of isolate 94 and 100 were lost during purification due to silica columns with manufacturing errors and thus could not be tested on the TEM-array. With all other 28 PCR products an array analysis was performed. 26 tested genes of the clinical isolates were identified correctly by array analysis as *bla*<sub>TEM-1</sub>. Isolate 31 was identified to contain *bla*<sub>TEM-2</sub>. The positive control target DNA used in this experiment was an *bla*<sub>TEM-116</sub> gene, which could also be correctly identified. Isolate 39 could not be identified correctly, because of the low quality of the generated data and thus had to be excluded from the further data analysis.

The results of the identification of the different *bla*<sub>TEM</sub> gene variants (isolate 50 for *bla*<sub>TEM-1</sub>, isolate 31 for *bla*<sub>TEM-2</sub> and the positive control for *bla*<sub>TEM-116</sub>) are displayed in figure 47 as relative intensities. Only the SNP positions differing between *bla*<sub>TEM-1</sub>, *bla*<sub>TEM-2</sub> and *bla*<sub>TEM-116</sub> are displayed. All these perfect match positions could be identified without ambiguity. In total 40 of 41 perfect match positions could be correctly identified for all analyzed isolates: SNP position 143 had to be excluded from the analysis, because of a spotting failure for this position within the whole slide batch. 95 % of the analyzed mismatch positions remained below a relative intensity of the mismatch value of < 0.6 (displayed in figure 48). 5 % showed a relative intensity of the mismatch of 0.6 - 0.8. Two times the RI<sub>MM</sub> limit of 0.8 was violated by mismatch probes 122A (RI<sub>MM</sub> = 0.81) and 122T (RI<sub>MM</sub> = 0.87) of isolate No. 59: this could also be ascribed to sporadic aberrations in the spotting process. The standard deviations of the mean a relative intensities of the mismatches varied from 0 - 0.33, but 89 % remained below 10 % of the perfect match intensity (displayed in figure 48b). The results of the array analysis were confirmed by standard DNA sequencing. The *bla*<sub>TEM</sub> gene variants of isolate 39, 94 and 100 were thereby also identified as *bla*<sub>TEM-1</sub>.

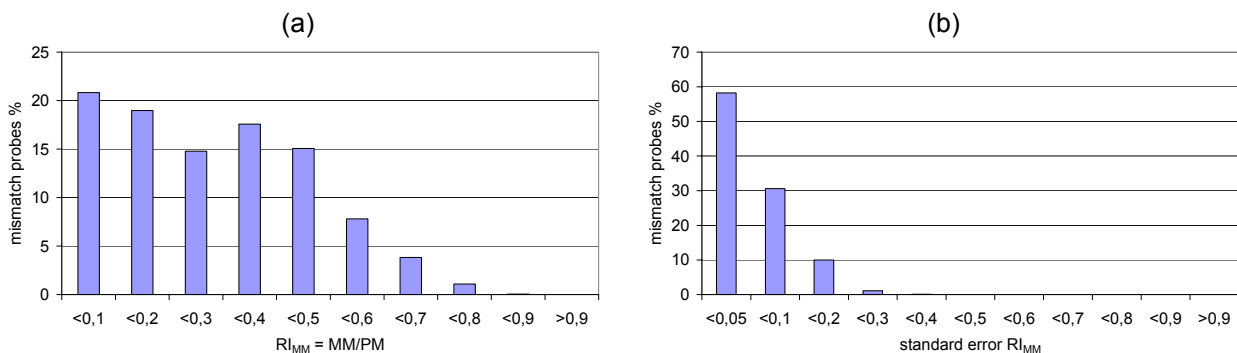


**Figure 48.** (a) Percentage of mismatch probes depending on the MM/PM ratio and (b) percentage of mismatch probes depending on the standard error of the MM/PM ratio of all identified SNP positions from 27 of in total 28 NRCA clinical isolate's target DNA tested on the TEM-array (isolate No 39 was excluded, because of poor data quality). All hybridizations were performed in triplicates (n = 9).

All *bla<sub>TEM</sub>* variants detected in the Russian clinical isolates belonged to the TEM parental types, which do not cause an ESBL phenotype. Therefore, the detected ESBL phenotype must have been caused by the SHV or CTX-M variants displayed in table 7, which were detected in all isolates by PCR and sequencing analysis performed at the NRCA in addition to the TEM gene, except for isolate 67, 96 or 100. For isolate 67 and 96 this was analog to the findings of the phenotypic tests from the RBK, which suggested an AmpC type resistance. For isolate 100 an ESBL was excluded consistently in the phenotypic test performed at the RBK and genotypic analysis. In case of isolate 41, which was phenotypically classified as no ESBL by the RBK, no conclusive analysis could be made, because the CTX-M variant detected in the first PCR screening was not identified so far.

**Table 7.** Results of testing of clinical isolates from the NRCA

Origin <sup>a</sup>	Isolate No	Species	Phenotype <sup>b</sup>	Genotype		
				<i>bla<sub>CTX-M</sub></i> <sup>c</sup>	<i>bla<sub>SHV</sub></i> <sup>d</sup>	<i>bla<sub>TEM</sub></i> <sup>e</sup>
M	25	<i>E. coli</i>	ESBL	+		TEM-1
M	26	<i>E. coli</i>	ESBL	+		TEM-1
M	31	<i>P. mirabilis</i>	ESBL/AmpC	+	+	TEM-2
M	37	<i>K. pneumoniae</i>	ESBL	+	+	TEM-1
M	39	Klebsiella spp.	ESBL		SHV-2	(TEM-1)
M	41	<i>E. coli</i>	no ESBL	+		TEM-1
M	43	<i>E. coli</i>	ESBL	CTX-M-14		TEM-1
C	50	<i>K. pneumoniae</i>	ESBL	+	SHV-12	TEM-1
C	52	<i>E. aerogenes</i>	ESBL	+	SHV-12	TEM-1
C	55	<i>E. coli</i>	ESBL	CTX-M-15	SHV-12	TEM-1
C	57	<i>E. coli</i>	ESBL	CTX-M-15	SHV-12	TEM-1
M	59	<i>K. pneumoniae</i>	ESBL	+		TEM-1
M	64	<i>K. pneumoniae</i>	ESBL	CTX-M-15		TEM-1
T	67	<i>C. freundii</i>	ESBL/AmpC			TEM-1
T	68	<i>M. morgani</i>	ESBL	+		TEM-1
N	75	<i>K. pneumoniae</i>	ESBL		SHV-38	TEM-1
M	77	<i>E. coli</i>	not pure	CTX-M-15	+	TEM-1
M	79	<i>E. coli</i>	ESBL	CTX-M-15		TEM-1
T	83	<i>E. coli</i>	ESBL	CTX-M-3		TEM-1
T	86	<i>C. freundii</i>	ESBL/AmpC		+	TEM-1
T	87	<i>E. coli</i>	ESBL	CTX-M-3		TEM-1
T	90	<i>P. vulgaris</i>	ESBL	CTX-M-3		TEM-1
N	92	<i>K. pneumoniae</i>	ESBL	CTX-M-3		TEM-1
T	93	<i>E. coli</i>	ESBL/AmpC	+		TEM-1
T	94	<i>E. coli</i>	ESBL	+		(TEM-1)
T	95	<i>K. pneumoniae</i>	ESBL	CTX-M-3		TEM-1
T	96	<i>C. freundii</i>	ESBL/AmpC			TEM-1
T	98	<i>C. freundii</i>	ESBL	+		TEM-1
T	99	<i>C. freundii</i>	ESBL	CTX-M-3		TEM-1
T	100	<i>E. coli</i>	no ESBL			(TEM-1)
	control target	<i>E. coli</i>				TEM-116

<sup>a</sup> Site of sample drawing: M-Moscow City Clinic # 7, C-Central Russian Military Hospital, N- National Research Center for Pediatric Diseases, T- Tomsk City Hospital. <sup>b</sup> The isolates were phenotypically tested at the NRCA and the RBK. Displayed here are the phenotypes detected by disk diffusion at the RBK. <sup>c,d</sup> *bla<sub>CTX-M</sub>* and *bla<sub>SHV</sub>* genotypes were identified by DNA sequencing, + indicates a detected product in a PCR prescreening with CTX-M and SHV specific primers, which has not been identified by sequencing up to date (analysis was performed by the NRCA). <sup>e</sup> *bla<sub>TEM</sub>* genotypes were determined by the TEM microarray for all isolates, except isolate 39, 94 and 100. For these isolates and all others the genotypes were determined and/or confirmed by standard DNA sequencing.

### 3.2 Results SHV-array

In order to establish a system, which was as reliable as and easily compatible with the already designed TEM microarray (53), an allele specific hybridization format was also chosen for the SHV microarray. In case of the SHV probe design, however, the traditional allele specific probe design proved to be not sufficient, so that an alternative strategy had to be devised.

#### 3.2.1 Probe design I

In contrast to the probes designed for the TEM-array, the SHV-array probes were equipped with an 5' aminomodified 13T spacer, which allowed a directed immobilization on the epoxy substrate and should improve the accessibility of the probes. Since these modified probes were considerably more expensive than the unmodified ones, a strategy was devised to minimize costs of the probe design process. After the theoretical probe design, the first tested probe set consisted only of the probe perfectly matching *bla*<sub>SHV-1</sub> and the probe perfectly matching the mutant *bla*<sub>SHV-x</sub>. If these probes performed satisfyingly in hybridization experiments the two mismatch probes completing the SNP probe set (with either A, G, C or T at the central base position) were ordered. Allele specific hybridization probe sets were designed covering 39 of the 40 SHV mutation positions displayed in table 8. The deletion at amino acid position 50 was omitted from the probe design, because of a highly unfavorable probe secondary structure as determined by *in silico* data analysis (data not shown). Furthermore, the SHV beta-lactamases (SHV-9, -10) carrying a mutation at the respective position could also be identified via position 136.

In table 9 the results of the probe design for the probes complementary for *bla*<sub>SHV-1</sub> and the mutant *bla*<sub>SHV-x</sub> are displayed. The probe length was between 15-25 bases and the T<sub>m</sub> values varied from 50.1 - 60.9 °C and the GC content was between 42.1 and 86.7 %. Probes with stable secondary structures should be excluded, because of non-optimal accessibility for the target DNA. The applied software default probe design parameters excluded probes with a hairpin  $\Delta G$  value of less than - 3 kcal/mol and self dimer  $\Delta G$  values of < - 6 kcal/mol. All probes met these criteria for the hairpin secondary structures with  $\Delta G$  values between 0 and - 2.8 kcal/mol, except probes 191C, 191A with a hairpin  $\Delta G$  value of - 3.4 kcal/mol.

For probes 115A, 136<sub>WILDTYPE</sub>, 136<sub>MUTANT</sub>, 201G, 201T, 202G, 222C, 234/5SEg, 238C the calculated dimer  $\Delta G$  results for the first probe versions, which were designed (see  $\Delta G$  values table 9) violated the predefined probe design parameter limits. The dimer forming bases were in all cases in close proximity to the mutation position and shifting of the mutation position within the probe sequence only led to even worse secondary structures *in silico* or/and resulted in loss of discriminatory power (data not shown). For example at position 262, the mutation was already shifted from the center to the 5' end of probe version 1, since with a central SNP a highly stable hairpin structure could be formed *in silico* in addition to the already existing dimer (data not shown). However, since this array should include the relevant mutation positions for unequivocal identification of all naturally occurring SHV variants, these probe sequences could not be excluded and were also tested in hybridization experiments.



**Table 8.** SHV beta-lactamase polymorphism sites and corresponding mutants

Nucleotide Position <sup>c</sup>	Codon in:		Amino acid <sup>a</sup>		SHV-X with the following phenotype <sup>b</sup>				
	bla <sub>SHV-1</sub>	bla <sub>SHV-X</sub>	Ambler position	Position	Amino acid in : SHV-1	SHV-X	ESBL	IRT	not defined
8	TAT	TTT	7	3	Y	F			28
10	ATT	TTT	8	4	I	F	7, 14, 18, 34		
10	ATT	GTT	8	4	I	V			36
40	ACC	GCC	18	14	T	A			25, 37
61	GCC	TCC	25	21	A	S			42
92	CTA	CAA	35	31	L	Q	2a, 12, 13, 15, 29		11, 25, 35, 36, 37, 40
115	CGC	AGC	43	39	R	S	7, 14, 18, 29, 34		
130	GAA	AAA	48	44	E	K	15		
148-150	GGC	-	54	50	G	Del	9	10	
180	GAA	GGA	64	60	E	G	34		
226	GTG	ATG	80	76	V	M	15		
253	GAA	AAA	89	85	E	K	15		35
325	CTT	TTT	113	109	L	F			43
343	GTC	ATC	119	115	V	I	48		
352	CTC	TTC	122	118	L	F	21		
365	GCC	GTC	126	122	A	V			32
373	ATG	GTG	129	125	M	V	25		37, 42
376	AGC	GGC	130	126	S	G		10	
406-408	GCC	CGG	140	136	A	R	9	10	
412	GTC	TTC	142	138	V	F			41
422	CCC	CTC	145	141	P	L			51
425	GCA	GTA	146	142	A	V			38
433	ACT	TCT	149	145	T	S			43
455	GGC	GAC	156	152	G	D			27, 32, 45
462	AAC	AAG	158	154	N	K	22		
474-475		TGA...AC insert	167-168	163-164		DRWET insert			16
505	CTT	TTT	173	169	L	F	19, 20, 21		
512	GGC	GCC	175	171	G	A			51
523	GAC	AAC	179	175	D	N	8		
524	GAC	GCC	179	175	D	A	6		
524	GAC	GGC	179	175	D	G	24		
547	GCC	ACC	187	183	A	T	26,		50
564	AAG	AAC	192	188	K	N	9,10		
565	CTG	GTG	193	189	L	V	9,10		
572	ACC	AAC	195	191	T	N	46		
572	ACC	ATC	195	191	T	I			53
602	CGG	CTG	205	201	R	L	3, 4,		44
606	CAG	CAT	206	202	Q	H			50
664	CCG	TCG	226	222	P	S			33
700-705	GGCGAG/A	AGCGAA/G	238/240	234/235	GEg	SE	2, 2a, 3, 20, 21, 30, 34, 39		
700-705	GGCGAG/A	AGCAAA/G	238/240	234/235	GEg	SK	4, 5, 7, 9, 12,10, 15, 22, 45, 46, 47, 48		
700-705	GGCGAG/A	GCCGAA/G	238/240	234/235	GEg	AE	29, 13		
700-705	GGCGAG/A	GCCAAA	238/240	234/235	GEg	AK	18		
713	GCG	GGG	243	238	A	G			35, 40
784	ACC/G	TCC	267	262	T	S	39		
816	CAA	CAT	278	272	Q	H			37

<sup>a</sup>Ambler position, position of the polymorphism in the amino acid sequence of SHV (<http://www.lahey.org/Studies/shvtable.asp>) according to Ambler et al. (3); position, position of the mutation according to SHV amino acid sequence (GenBank accession number CAA66727). The amino acids in the SHV-1 sequence and the mutated SHV (SHV-X) sequence are also indicated.

<sup>b</sup> The numbers in the table body are the SHV types with an amino acid substitution at the indicated position. The ESBL and IRT phenotypes are as described by Bradford (16). <sup>c</sup> Position refers to the position of the mutation in the nucleotide sequence of the bla<sub>SHV</sub> gene (GenBank accession number X98099, region: 74-934).

## Results

**Table 9.** Probe design I results for the SHV specific microarray

Probe name	Probe sequence (5'-3')	Length (nt)	Tm (°C)	GC (%)	Hairpin $\Delta G$ (kcal/mol)	Hairpin bond (nt)	Dimer $\Delta G$ (kcal/mol)	Dimer bond (nt)	Run/ repeat length (nt)
03A	ATGCGTTATATTCGCCTGT	19	50.2	42.1	-2.8	3	-2.8	3	2
03T	ATGCGTTTTATTCGCCTGT	19	51.3	42.1	-2.8	3	-2.8	3	4
04A	ATGCGTTATATTCGCCTGT	19	50.2	42.1	-2.8	3	-2.8	3	2
04T	ATGCGTTATTTTCGCCTGT	19	51.3	42.1	-2.8	3	-2.8	3	4
14A	CTGTTAGCCACCCTGCCG	18	55.5	66.7	0.0	0	0.0	0	3
14G	CTGTTAGCCGCCCTGCCG	18	58.6	72.2	0.0	0	0.0	0	3
21G	CGGTACACGCCAGCCC	16	54.6	75.0	0.0	0	-1.9	4	3
21T	CGGTACACTCCAGCCC	16	50.4	68.8	0.0	0	-1.9	4	3
31T	AGCAAATTAATAAGCGAAAGCC	24	55.4	37.5	0.0	0	-1.0	4	3
31A	AGCAAATTAACAAAGCGAAAGCC	24	56.4	37.5	0.0	0	-1.0	4	3
39C	TGTCGGGCCGCGTAGG	16	56.0	75.0	0.0	0	-5.1	4	3
39A	TGTCGGGCAGCGTAGG	16	53.0	68.8	0.0	0	0.0	0	3
44G	GTAGGCATGATAGAAATGGATCTGG	25	55.8	44.0	-0.6	3	-2.2	4	3
44A	GTAGGCATGATAAAATGGATCTGG	25	54.8	40.0	-0.5	3	-2.2	4	5
60A	CGCCGATGAACGCTTTCC	18	54.9	61.1	-0.5	3	-0.5	3	3
60G	CGCCGATGGACGCTTTCC	18	56.8	66.7	-1.3	3	-1.3	3	3
76G	CGGCGCAGTGCTGGC	15	55.9	80.0	0.0	0	-5.1	4	2
76A	CGGCGCAATGCTGGC	15	53.7	73.3	0.0	0	-5.1	4	2
85G	GCCGGTGACGAACAGCT	17	54.8	64.7	0.0	0	-4.2	4	2
85A	GCCGGTGACAAACAGCT	17	52.6	58.8	0.0	0	-4.2	4	3
109C	CGAAAAACATCTTGCCGACG	20	54.3	50.0	0.0	0	0.0	0	5
109T	CGAAAAACATTTTGCCGACG	20	53.1	45.0	-1.2	4	-1.2	4	5
115G	GCATGACGGTCGGCGAA	17	55.4	64.7	0.0	0	-2.2	4	2
115A	GCATGACGATCGGCGAA	17	52.8	58.8	0.0	0	-6.5	6	2
118C	GTCGGCGAACTCTGCG	16	52.7	68.8	0.0	0	-1.7	3	2
118T	GTCGGCGAATTCTGCG	16	50.7	62.5	0.0	0	-4.1	6	2
122C	CGCCGCCGCCATTACC	16	56.0	75.0	0	0	0	0	2
122T	CGCCGCCGTCATTACC	16	52.7	68.8	0	0	0	0	2
125A	GCCATTACCATGAGCGATAAC	21	53.2	47.6	-0.5	3	-2.2	4	2
125G	GCCATTACCGTGAGCGATAAC	21	55.5	52.4	0	0	0	0	2
126A	CCATTACCATGAGCGATAACAGC	23	56.2	47.8	-0.5	3	-2.2	4	2
126G	CCATTACCATGGGCGATAACAGC	23	58.2	52.2	-2.4	4	-6.0	6	3
136WT	CTGCTACTGGCCACCGTCGG	20	60.9	70	0	0	-7.1	6	2
136MT	CTGCTACTCCGGACCGTCGG	20	60.1	70	-2.3	3	-6.8	6	2
138G	GGCCACCGTCGGCGG	15	57.4	86.7	-2.4	3	-4.3	4	2
138T	GGCCACCTTCGGCGG	15	54.2	80	-2.4	3	-4.3	4	2
142C	GCGGCCCGCAGGAT	15	56.1	80	-2.8	3	-4.7	4	4
142T	GCGGCCTCGCAGGAT	15	53.0	73.3	-2.8	3	-4.3	4	2
143C	CGGCCCGCAGGATTG	16	55.0	75.0	0	0	-4.3	4	4
143T	CGGCCCGTAGGATTG	16	50.9	68.8	0	0	-4.3	4	4
145A	CAGGATTGACTGCCTTTTTGC	21	54.3	47.6	-1.2	3	-1.2	3	5
145T	CAGGATTGTCTGCCTTTTTGC	21	54.3	47.6	-1.2	3	-1.2	3	5
152G	CCAGATCGGCGACAACG	17	53.2	64.7	0	0	-1.9	4	2
152A	CCAGATCGACGACAACG	17	50.1	58.8	0	0	-3.0	4	2
154C	CGGCGACAACGTCACCC	17	56.1	70.6	-1.1	3	-3.3	4	3
154A	CGGCGACAAAGTCACCC	17	53.2	64.7	-1.1	3	-1.1	3	3
163WT	CTGGGAAACGGAAGTGAATG	20	52.4	50	0	0	0	0	3
163MT	CTGGGAAACTGACCGCTGGG	20	58.7	65	0	0	0	0	3
169C	ATGAGGCGCTTCCCGG	16	53.4	68.8	0	0	-5.1	4	3
169T	ATGAGGCGTTTCCCGG	16	50.7	62.5	0	0	-4.2	4	3
171G	GCTTCCCGGCGACGC	15	55.2	80.0	0	0	-4.2	4	3
171C	GCTTCCCGCCGACGC	15	55.2	80.0	0	0	0	0	3
175.1G	CGCCCGCGACACCAC	15	55.1	80	0	0	-5.1	4	3
175.1A	CGCCCGCAACACCAC	15	52.7	73.3	0	0	0	0	3

Table 9. continued

175.2A	GCCCGCGACACCACT	15	53.2	73.3	0	0	-5.1	4	3
175.2C	GCCCGCGCCACCACT	15	56.8	80	0	0	-5.1	4	3
183G	CCAGCATGGCCGCGAC	16	55.9	75.0	-1.4	3	-5.1	4	2
183A	CCAGCATGACCGCGAC	16	52.6	68.8	0	0	-5.1	4	2
188/9WT	GCGCAAGCTGCTGACCA	17	55.9	64.7	-1.9	3	-5.1	4	2
188/9MT	GCGCAACGTGCTGACCA	17	56.3	64.7	-1.9	3	-5.1	4	2
191C	GCTGCTGACCAGCCAGC	17	56.0	70.6	-3.4	4	-3.4	4	2
191A	GCTGCTGAACAGCCAGC	17	53.9	64.7	-3.4	4	-3.4	4	2
201G	GTTTCGCAACGGCAGCTG	17	54.8	64.7	-0.6	3	-6.3	6	2
201T	GTTTCGCAACTGCAGCTG	17	52	58.8	-0.6	3	-6.3	6	2
202G	GCAACGGCAGCTGCTG	16	54.0	68.8	-1.9	3	-11.0	8	2
202T	GCAACGGCATCTGCTG	16	50.7	62.5	-1.9	3	-1.9	3	2
222C	CGTGCTGCCGGCGGG	15	58.2	86.7	0	0	-8.9	6	3
222T	CGTGCTGTCCGGCGGG	15	54.8	80	0	0	0	0	3
234/5GEg	GGAGCTGGCGAGCGGG	16	57.2	81.2	-1.7	3	-2.9	4	3
234/5SEg	GGAGCTAGCGAGCGGG	16	53.7	75	-1.7	3	-6.2	6	3
238C	GGGTGCGCGCGGGAT	15	57.0	80	0	0	-9.8	6	3
238G	GGGTGGGCGCGGGAT	15	55.6	80	0	0	-5.1	4	3
262A	GGGATACCCCGCGGA	15	50.8	73.3	-1.9	3	-4.2	4	4
262T	GGGATTCCCCGCGGA	15	51.5	73.3	-1.9	3	-4.2	4	4
272A	AAATCAGCAAATCGCCGGG	19	54.6	52.6	0	0	-4.2	4	3
272T	AAATCAGCATATCGCCGGG	19	53.5	52.6	0	0	-4.2	4	3

<sup>a</sup> For each polymorphism site one probe complementary to *bla*<sub>SHV-1</sub> (upper line) and one probe complementary to the mutated *bla*<sub>SHV-X</sub> (lower line) are displayed. The probes are named for the position in the amino acid sequence of *bla*<sub>SHV</sub> and the nucleotide at the central base position (either A, G, C or T). The probe length, the melting temperature (T<sub>m</sub>), GC content (GC%), free energy of hairpin bonds (hairpin  $\Delta G$ ), the number of bases forming the hairpin bond (hairpin bond), free energy of dimers (dimer  $\Delta G$ ), the number of bases forming the dimer bond (dimer bond) were calculated by ArrayDesigner 2.0 software.

### 3.2.2 Probe performance analysis I

In a hybridization experiment with *bla*<sub>SHV-1</sub> and *bla*<sub>SHV-2</sub> target DNA the probe performance of a subset of the probes designed in the first step was tested. It should be determined, if a specific perfect match identification was possible and how the predetermined probe secondary structures affected the perfect match discrimination. In theory, secondary structures of perfect match probes lead to a decreased accessibility of the probe for hybridization of the target. If, in addition to this, the mismatch probe has no or a less stable secondary structure, the better accessibility of this probe could lead to a compensation of the duplex destabilising effect of the mismatched central base, so that high mismatch signals can occur and the discrimination of a perfect match towards a mismatch is impaired. The results for the hybridization of the SNP specific probes with *bla*<sub>SHV-1</sub> are displayed in figure 49.

All perfect match positions could be correctly identified, except for the perfect match positions 171G and 222C, which corresponded to an unfavorable perfect match to mismatch dimer  $\Delta G$  difference of - 4.2 or - 8.9 kcal/mol respectively. Apparently, the more stable secondary structure of the perfect match in comparison to the mismatch probe resulted in less binding of the target DNA. Although perfect match probes 191C, 201G and 202G also contained highly stable secondary structures, the correct perfect match positions were detected. For probes 191 and 201 this result can be explained by the fact that both probes contained in case of the probe perfectly matching *bla*<sub>SHV-1</sub> and the probe perfectly matching the mutant *bla*<sub>SHV-X</sub> the same

## Results

---

secondary structures, so both probes should be equally accessible. However, in case of probe 202G, which contained the most stable secondary structure of the whole SHV specific probe set with a  $\Delta G$  value of - 11.0 kcal/mol resulting in a difference between perfect match and mismatch self dimer  $\Delta G$  of - 9.1 kcal/mol, the correct perfect match could be identified and the discrimination was unexpectedly pronounced with an experimentally determined relative intensity of the mismatch of only 0.29.

Probes 39, 125, 145 and 238 showed a weak discrimination capability of the mismatch relative intensities with values greater than 0.5. A disadvantageous perfect match probe in contrast to the mismatch probe secondary structure could be assigned to probes 39 (difference between perfect match and mismatch self dimer  $\Delta G = - 5.1$  kcal/mol), 125 (- 2.2 kcal/mol) and 238 (- 4.7 kcal/mol). For probe 145 the weak discrimination was caused by the fact that the net signal intensity of the perfect match probe approached the saturation level of the detection system. For position 234/5 the identification of the correct *bla*<sub>SHV-1</sub> codons (GEg) was possible (relative intensity values see figure 50a), but for *bla*<sub>SHV-2</sub> the relative intensity of the GEg probe was almost as high as the correct SEg perfect match (figure 50b). This corresponds to a dimer  $\Delta G$  of - 6.2 kcal/mol for the SEg probe in contrast to a  $\Delta G$  of only - 2.9 kcal/mol for the GEg probe. The probes 115A and 126G, which also contained secondary structures violating the predefined  $\Delta G$  limits, could not be evaluated, since the SHV beta-lactamases bearing a perfect match at these positions (*bla*<sub>SHV-48</sub> and *bla*<sub>SHV--10</sub> respectively) were not available for testing.

In conclusion, probe 222 had to be redesigned to allow a correct identification of the perfect match. Probes 39, 125, 234/5, 238 and 145 should also be reviewed to enhance the discrimination efficiency. Probe 171 could be excluded, since SHV-51, the only SHV variant bearing a mutation at this position, could also be specifically identified via position 141.

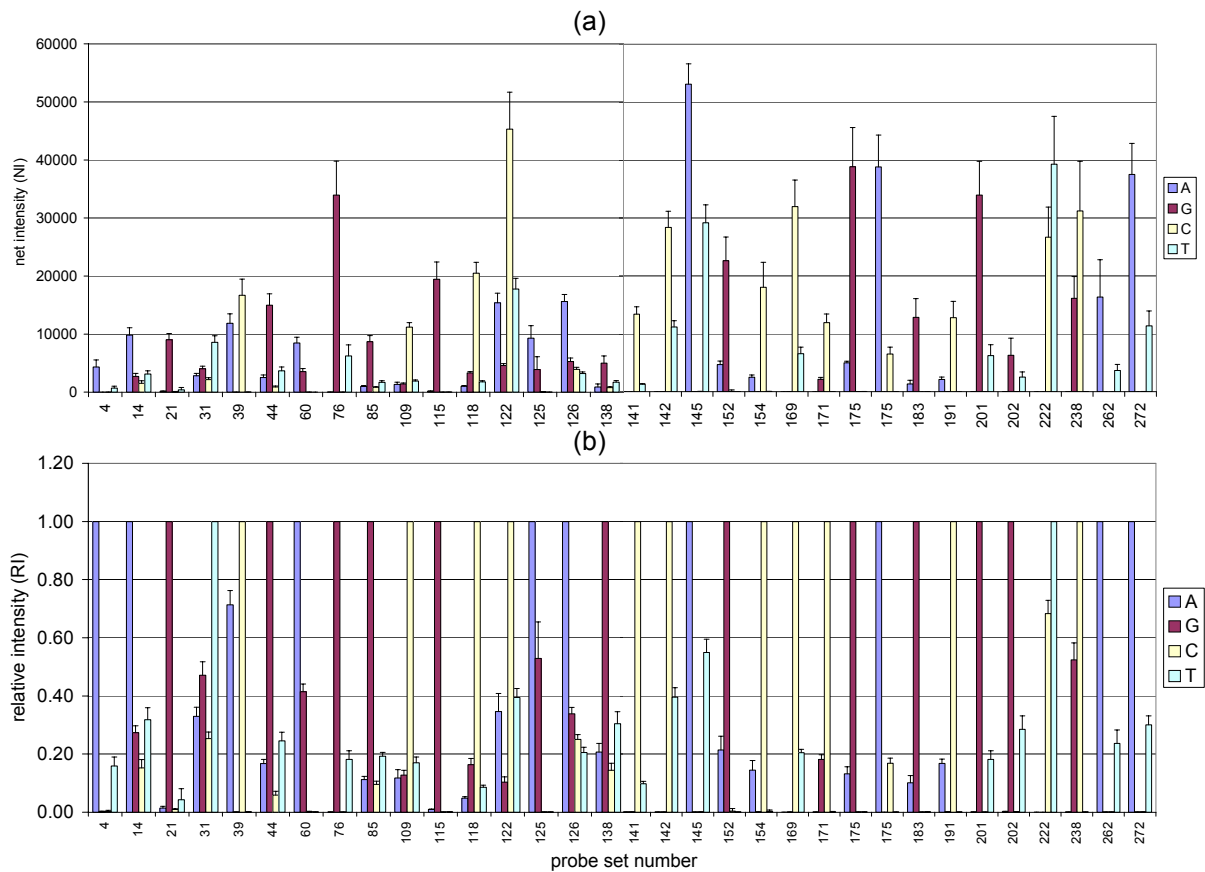


**Figure 49.** (a) Mean net signal intensities and (b) mean relative signal intensities for each SNP position and corresponding probe (A, G, C and T refer to the base at the central position) from a hybridization experiment with 200 ng *bla<sub>SHV-1</sub>* (NT/F = 48) (n = 9). Probe sets No. 14, 21, 31, 44, 85, 109, 118, 122, 126 and 138 consisted of 4 probes, all other probe sets consisted only of the probe perfectly matching *bla<sub>SHV-1</sub>* and the probe perfectly matching the mutant *bla<sub>SHV-x</sub>* in this experiment.

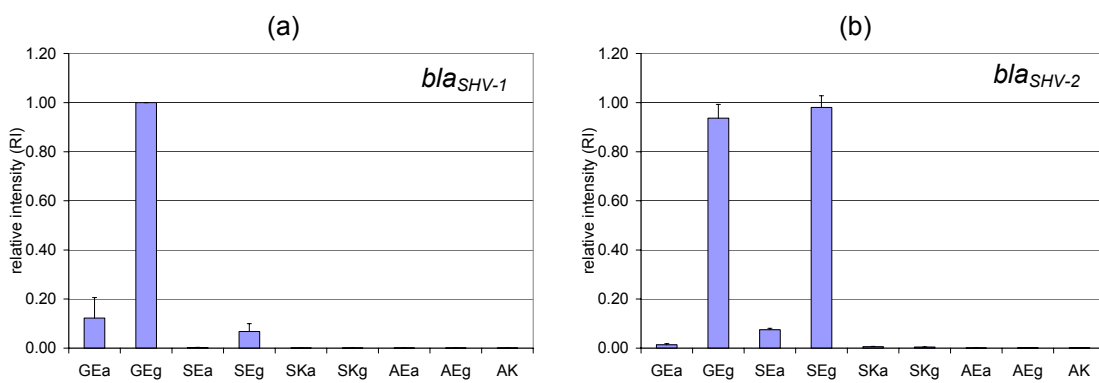


**Figure 50.** Mean relative (rel.) signal intensities of probe 234/5 hybridized with 200 ng (a) *bla<sub>SHV-1</sub>* (NT/F = 48), (n = 9) and (b) *bla<sub>SHV-2</sub>* (NT/F = 51), (n = 9).

3.2.3 Probe design II

In a first probe performance analysis it was determined that probes 39, 125, 222, 234/5, 238, and 145 should be redesigned to allow a correct or enhanced perfect match identification. The capture probe 262 also showed an insufficient mismatch to perfect match discrimination capability (see figure 52), when the complete probe set was tested (in the first experiment only oligos 262A and 262T were tested). The calculated hairpin and dimer  $\Delta G$  results for the first capture oligonucleotide versions of the complete probe sets are displayed in table 10. Since with the usual probe design options the disadvantageous secondary structures could not be avoided, a new probe design concept had to be developed. It was assumed, that through introduction of an additional mismatched base the secondary structure could be dissolved, while retaining enough hybridization capability to allow the mismatch to perfect match discrimination (see figure 51). In table 11 the redesigned probe sequences and parameters are displayed. The bases, which were exchanged from version I to version II are underlined in table 10 and 11. Furthermore, the positions and length were adjusted for optimal accessibility of the new oligonucleotides. In case of probes 234/5 and 262, through introduction of a mismatched base, the secondary structures could be considerably reduced or as in case of probe sets 222 and 238 even annihilated as shown in the corresponding  $\Delta G$  values displayed in table 11.

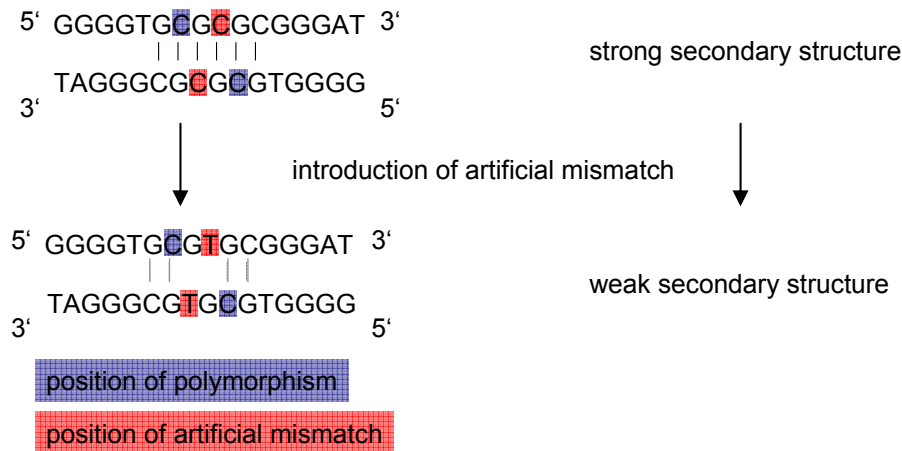


**Figure 51.** An application example for the new probe design concept is displayed. Through introduction of a mismatched base unfavorable probe secondary structures, such as dimers or hairpins are avoided, resulting in a better probe accessibility for target hybridization.

In case of probe 145 only the probe length was shortened to yield diminished fluorescence signal intensities. For probe 39 the probe design options were limited, because at least two bases flanking the polymorphism site formed *in silico* a very unfavorable dimer structure for the probe 39C. If one of the bases was replaced by a different nucleotide, one of the secondary structures was released, but an almost as stable secondary structure was formed involving the other base. However, it was highly improbable, that a probe with two additional mismatches retains enough hybridization capability to yield a satisfactory hybridization signal (this was experimentally confirmed, data not shown). Due to this the probe 39<sub>NEW</sub> with one mismatch and the least unfavorable  $\Delta G$  values was chosen. Probe 125 was first

redesigned retaining the probe sequence position and length of probe version I and introducing the mismatched base at the marked position. This led to a considerable reduction of the probe secondary structure of probe 125A, but the fluorescence signal determined in a hybridization experiment (data not shown) was not sufficiently above background level. Although an elongation of the probe sequence (see version II in table 11) led to more stable secondary structures in the whole probe set ( $\Delta G = -2.8$  kcal/mol), as displayed in table 11, this was the only option to gain enough fluorescence signal intensity for a sensitive data analysis (see probe performance analysis II).

## Results

**Table 10.** Probe version I<sup>a</sup>

Probe name	Probe sequence (5'-3')	Length	T <sub>m</sub>	GC	Hairpin $\Delta G$	Hairpin bond	Dimer $\Delta G$	Dimer bond	Run/ repeat length
		(nt)	(°C)	(%)	(kcal/mol)	(nt)	(kcal/mol)	(nt)	(nt)
39A	TGTCGG <u>G</u> CAGCGTAGG	16	53.0	68.8	0	0	0	0	3
39G	TGTCGG <u>G</u> GCGGCGTAGG	16	56	75	0	0	0	0	3
39C	TGTCGG <u>G</u> CCCGCGTAGG	16	56.0	75.0	0	0	-5.1	4	3
39T	TGTCGG <u>G</u> GCTGCGTAGG	16	53	68.8	0	0	0	0	3
125A	GCCATTACCAT <u>G</u> AGCGATAAC	21	53.2	47.6	-0.5	3	-2.2	4	2
125G	GCCATTACCGT <u>G</u> AGCGATAAC	21	55.5	52.4	0	0	0	0	2
125C	GCCATTACCCT <u>G</u> AGCGATAAC	21	54.8	52.4	0	0	0	0	3
125T	GCCATTACCTT <u>G</u> AGCGATAAC	21	53.1	47.6	0	0	0	0	2
145A	CAGGATTGACTGCCTTTTTGC	21	54.3	47.6	-1.2	3	-1.2	3	5
145G	CAGGATTGGCTGCCTTTTTGC	21	56.9	52.4	0	0	-2.4	3	5
145C	CAGGATTGCCTGCCTTTTTGC	21	56.9	52.4	0	0	0	0	5
145T	CAGGATTGTCTGCCTTTTTGC	21	54.3	47.6	-1.2	3	-1.2	3	5
222A	CGTGCTGAC <u>G</u> GCGGG	15	54.8	80	0	0	0	0	3
222G	CGTGCTGGC <u>G</u> GCGGG	15	58.2	86.7	0	0	0	0	3
222C	CGTGCTGCC <u>G</u> GCGGG	15	58.2	86.7	0	0	-8.9	6	3
222T	CGTGCTGTC <u>G</u> GCGGG	15	54.8	80	0	0	0	0	3
234/5GEa	GGAGCTGG <u>C</u> GAACGGG	16	54.6	75	0	0	-2.9	4	3
234/5GEg	GGAGCTGG <u>C</u> GAGCGGG	16	57.2	81.2	-1.7	3	-2.9	4	3
234/5SEa	GGAGCTAG <u>C</u> GAACGGG	16	51.1	68.8	0	0	-6.2	6	3
234/5SEg	GGAGCTAG <u>C</u> GAGCGGG	16	53.7	75	-1.7	3	-6.2	6	3
234/5SKa	GGAGCTAG <u>C</u> AAACGGG	16	48.7	62.5	0	0	-6.2	6	3
234/5SKg	GGAGCTAG <u>C</u> AAGCGGG	16	51.3	68.8	-1.7	3	-6.2	6	3
234/5AEa	GGAGCTG <u>C</u> GAACGGG	16	54.6	75	0	0	-2.9	4	3
234/5AEg	GGAGCTG <u>C</u> GAGCGGG	16	57.2	81.2	-1.7	3	-2.9	4	3
234/5AK	GGAGCTG <u>C</u> AAACGGG	16	52.3	68.8	0	0	-2.9	4	3
238A	GGGGTGAG <u>C</u> GCGGGAT	16	56	75	0	0	-5.1	4	4
238G	GGGGTGGG <u>C</u> GCGGGAT	16	58.9	81.2	0	0	-5.1	4	4
238T	GGGGTGTG <u>C</u> GCGGGAT	16	56.7	75	0	0	-5.1	4	4
238C	GGGGTGCG <u>C</u> GCGGGAT	16	60.1	81.2	0	0	-9.8	6	4
262A	GGGATACCCCGGCGA	15	50.8	73.3	-1.9	3	-4.2	4	4
262G	GGGATGCCCGGCGA	15	55.2	80	-1.9	3	-4.2	4	4
262C	GGGATCCCCGGGCGA	15	53.9	80	-1.9	3	-9.5	8	5
262T	GGGATCCCCGGGCGA	15	51.5	73.3	-1.9	3	-4.2	4	4

<sup>a</sup> Probe secondary structure  $\Delta G$  values, length, and sequences of oligonucleotide probes version I of probe 39, 125, 145, 222, 234/5, 238 and 262. The probe length, the melting temperature (T<sub>m</sub>), GC content (GC), free energy of hairpin bonds (hairpin  $\Delta G$ ), the number of bases forming the hairpin bond (hairpin bond), free energy of dimers (dimer  $\Delta G$ ), the number of bases forming the dimer bond (dimer bond) were calculated by ArrayDesigner 2 software.

<sup>b</sup> The exchanged nucleotide from probe version I to II (see table 11) is underlined. In probe 145 no nucleotide was exchanged, only the probe length was adjusted.



Table 11. Probe version II<sup>a</sup>

Probe name	Probe sequence (5'-3')	Length	T <sub>m</sub>	GC	Hairpin $\Delta G$	Hairpin bond	Dimer $\Delta G$	Dimer bond	Run/ repeat length
		(nt)	(°C)	(%)	(kcal/mol)	(nt)	(kcal/mol)	(nt)	(nt)
39A <sub>NEW</sub>	TGTCGGGGCAGC <u>I</u> TAGG	16	49.9	62.5	0	0	-2.9	4	3
39G <sub>NEW</sub>	TGTCGGGGCGGC <u>I</u> TAGG	16	53	68.8	0	0	0	0	3
39C <sub>NEW</sub>	TGTCGGGGCCGC <u>I</u> TAGG	16	53	68.8	0	0	-4.3	4	3
39T <sub>NEW</sub>	TGTCGGGGCTGC <u>I</u> TAGG	16	49.9	62.5	0	0	0	0	3
125A <sub>NEW</sub>	CCGCCATTACCATTAGCGATAACAG	25	58.8	48	-2.8	3	-2.8	3	2
125G <sub>NEW</sub>	CCGCCATTACCGT <u>I</u> AGCGATAACAG	25	60.7	52	-2.8	3	-2.8	3	2
125C <sub>NEW</sub>	CCGCCATTACCCT <u>I</u> AGCGATAACAG	25	60.2	52	-2.8	3	-2.8	3	3
125T <sub>NEW</sub>	CCGCCATTACCTT <u>I</u> AGCGATAACAG	25	58.8	48	-2.8	3	-2.8	3	3
145A <sub>NEW</sub>	AGGATTGACTGCCTTT	16	43.1	43.8	0	0	0	0	3
145G <sub>NEW</sub>	AGGATTGGCTGCCTTT	16	46.6	50	0	0	-2.4	3	3
145C <sub>NEW</sub>	AGGATTGCCTGCCTTT	16	46.6	50	0	0	0	0	3
145T <sub>NEW</sub>	AGGATTGTCTGCCTTT	16	43.1	43.8	0	0	0	0	3
222A <sub>NEW</sub>	CCGTGCTGACT <u>I</u> GCG	14	47.9	71.4	0	0	0	0	2
222C <sub>NEW</sub>	CCGTGCTGGC <u>I</u> GCG	14	51.5	78.6	0	0	0	0	2
222C <sub>NEW</sub>	CCGTGCTGCC <u>I</u> GCG	14	51.5	78.6	0	0	0	0	2
222T <sub>NEW</sub>	CCGTGCTGTC <u>I</u> GCG	14	47.9	71.4	0	0	0	0	2
234/5GEa <sub>NEW</sub>	GGAGCTGGTGAACGG	15	47.4	66.7	0	0	-2.9	4	2
234/5GEg <sub>NEW</sub>	GGAGCTGG <u>I</u> GAGCGG	15	50.2	73.3	-1.7	3	-2.9	4	2
234/5SEa <sub>NEW</sub>	GGAGCTAGTGAACGG	15	43.6	60	0	0	-2.9	4	2
234/5SEg <sub>NEW</sub>	GGAGCTAG <u>I</u> GAGCGG	15	46.4	66.7	-1.7	3	-2.9	4	2
234/5SKa <sub>NEW</sub>	GGAGCTAGTAAACGG	15	40.4	53.3	0	0	-2.9	4	3
234/5SKg <sub>NEW</sub>	GGAGCTAGTAAACGG	15	43.3	60	-1.7	3	-2.9	4	2
234/5AEa <sub>NEW</sub>	GGAGCTGCTGAACGG	15	48	66.7	0	0	-2.9	4	2
234/5AEG <sub>NEW</sub>	GGAGCTGC <u>I</u> GAGCGG	15	50.8	73.3	-1.7	3	-2.9	4	2
234/5AK <sub>NEW</sub>	GGAGCTGC <u>I</u> AAACGG	15	44.8	60	0	0	-2.9	4	3
238A <sub>NEW</sub>	CGGGGTGAG <u>I</u> GCGGG	15	53.3	80	0	0	0	0	4
238G <sub>NEW</sub>	CGGGGTGGG <u>I</u> GCGGG	15	56.4	86.7	0	0	0	0	4
238C <sub>NEW</sub>	CGGGGTGCC <u>I</u> GCGGG	15	57.7	86.7	0	0	0	0	4
238T <sub>NEW</sub>	CGGGGTGTG <u>I</u> GCGGG	15	54.1	80	0	0	0	0	4
262A <sub>NEW</sub>	CTGCGTIGATACCCCG	15	47.3	66.7	0	0	0	0	4
262G <sub>NEW</sub>	CTGCG <u>I</u> GATGCCCG	15	51.6	73.3	0	0	0	0	4
262C <sub>NEW</sub>	CTGCGTIGATCCCCCG	15	50.4	73.3	0	0	-1.9	4	5
262T <sub>NEW</sub>	CTGCG <u>I</u> GATTCCCG	15	48.1	66.7	0	0	0	0	4

<sup>a</sup> Probe secondary structure  $\Delta G$  values, length, and sequences of oligonucleotide probes version II of probe 39, 125, 145, 222, 234/5, 238 and 262. The probe length, the melting temperature (T<sub>m</sub>), GC content (GC), free energy of hairpin bonds (hairpin  $\Delta G$ ), the number of bases forming the hairpin bond (hairpin bond), free energy of dimers (dimer  $\Delta G$ ), the number of bases forming the dimer bond (dimer bond) were calculated by ArrayDesigner 2.0 software.

<sup>b</sup> The exchanged nucleotide from probe version I to II (see table 10) is underlined. In probe 145<sub>NEW</sub> no nucleotide was exchanged, only the probe length was adjusted.

### 3.2.4 Probe performance analysis II

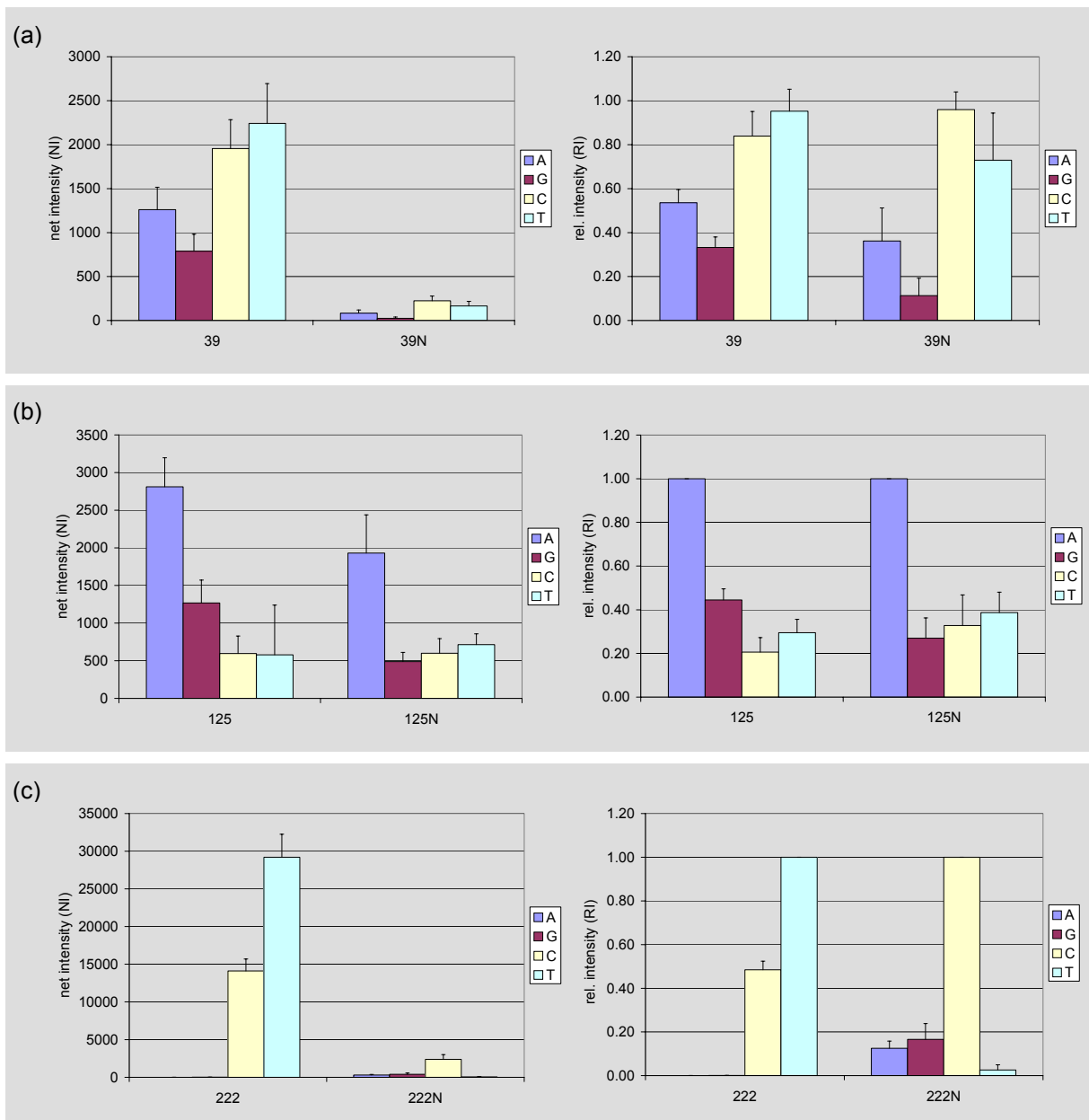
The newly designed probe sets were compared with the former probe version in a hybridization experiment with 200 ng target DNA representing *bla*<sub>SHV-1</sub>, *bla*<sub>SHV-2</sub> or *bla*<sub>SHV-4</sub> genotypes. The net and relative intensities of probe versions I (e.g. probe 39) and version II (e.g. probe 39<sub>NEW</sub>) are displayed in figure 52 as relative and net intensities. In case of probe sets 222 and 262 only probe version II (222<sub>NEW</sub> and 262<sub>NEW</sub>) allowed the identification of the correct perfect match positions (see figure 52c and e). For probe set 238<sub>NEW</sub>, the discrimination of the perfect match from a mismatch was visibly enhanced with a reduction of the relative intensities of the mismatches from app. 0.7 in probe version I to values < 0.1 in probe version II. The net signal intensities of the probe version II were as expected for the majority of these probe sets considerably reduced (up to six times) compared to probe version I, but remained at a sufficient level (> 1000 arbitrary units) for a sensitive data analysis. These probes were included in the SHV-array instead of the former probe versions and were furtheron designated as probes 222, 238 and 262.

The perfect match net probe signal intensity of probe 39<sub>NEW</sub> (figure 52a) was considerably reduced and approached the background level. The resulting relative intensities of probe 39<sub>NEW</sub> showed a low reproducibility and were not reliable for perfect match identification, so it could not be used for the SHV-specific microarray (figure 52b). The relative intensities of probe version I of probe 39 produced a higher mismatch fluorescence signal for probe 39T in comparison to the correct *bla*<sub>SHV-1</sub> perfect match position 39C. However the 39C perfect match of *bla*<sub>SHV-1</sub> can be identified correctly, when compared to the relative intensity of probe 39A, which is the perfect match for the mutant *bla*<sub>SHV-x</sub>. Since all other probe design attempts produced no promising alternative, as explained above, a different data analysis strategy was devised. For a more comprehensive perfect match identification, in this case the four probe concept per single nucleotide polymorphism was skipped and only probe 39C (alias 39<sub>WILDTYPE</sub>) in comparison to 39A (alias 39<sub>MUTANT</sub>) was furtheron considered (see proof of concept). Thus a specific identification of the mutant *bla*<sub>SHV-x</sub> or *bla*<sub>SHV-1</sub> was possible (see section 3.2.6).

The relative intensities of the mismatches of probe 125G in contrast to probe 125G<sub>NEW</sub> was reduced about 0.2, but the redesign resulted also in an about 30 % reduced net signal intensity (see figure 52). The discrimination was also in probe set version I more specific than determined in the first experiment (relative intensity of the mismatch =0.53) with a value of 0.42. This was attributed to the fact that in this experiment the complete probe sets 125 and 125<sub>NEW</sub> were spotted in contrast to the first one where only probes 125A and G were spotted, so that more probes were competing within one reaction for the same target DNA region.

The perfect match net signal intensity of probe 145<sub>NEW</sub> was reduced to 30 % of the perfect match net signal intensity of probe 145 (see figure 52). The perfect match discrimination of probe 145A towards probe 145T could be advanced, but as in case of probe 125 the discrimination of probe set version I was more specific in this experiment with a maximum relative intensity of the mismatches of 0.32 compared to 0.55 as determined in the first experiment. In this case this could be attributed to the decreased amplitude of the perfect match net signal intensity (which was here not in the range of the saturation level) and the aforementioned increased competition for the target DNA. Probes 125<sub>NEW</sub> and 145<sub>NEW</sub> were included because of their increased discrimination potential in the SHV-specific microarray and furtheron designated as probes 125 and 145.

The results of the probe performance analysis of probe 234/5 are displayed in figure 53a for hybridization with *bla<sub>SHV-1</sub>* target DNA, in figure 53b for hybridization with *bla<sub>SHV-2</sub>* target DNA and in figure 53c for hybridization with *bla<sub>SHV-4</sub>* target DNA. With probe version I the identification of the correct *bla<sub>SHV-1</sub>* codons (GEg) was possible, but for *bla<sub>SHV-2</sub>* (SEg) and *bla<sub>SHV-4</sub>* (SKg) the relative intensity of the GEg probe was as high or even higher as the correct perfect match. This corresponded to a more stable dimer structure with a  $\Delta G$  of - 6.2 kcal/mol for the SEg or SKg probe in contrast to a less stable dimer structure with a  $\Delta G$  of only - 2.9 kcal/mol of the GEg probe. In contrast, probe version II of probe set 234/5 allowed a highly specific identification of each correct perfect match due to minimized secondary structures. The perfect match net signal intensities were diminished due to the additional mismatched base, but remained at a sufficient level of at least ten times above background net signal intensity. Therefore, probes 234/5<sub>NEW</sub> were included in the SHV microarray and were furtheron designated as probe set 234/5. The complete probe set of the SHV specific microarray resulting from the probe design and probe performance analysis is displayed in table 12 and was applied in all following SHV-array analyses.



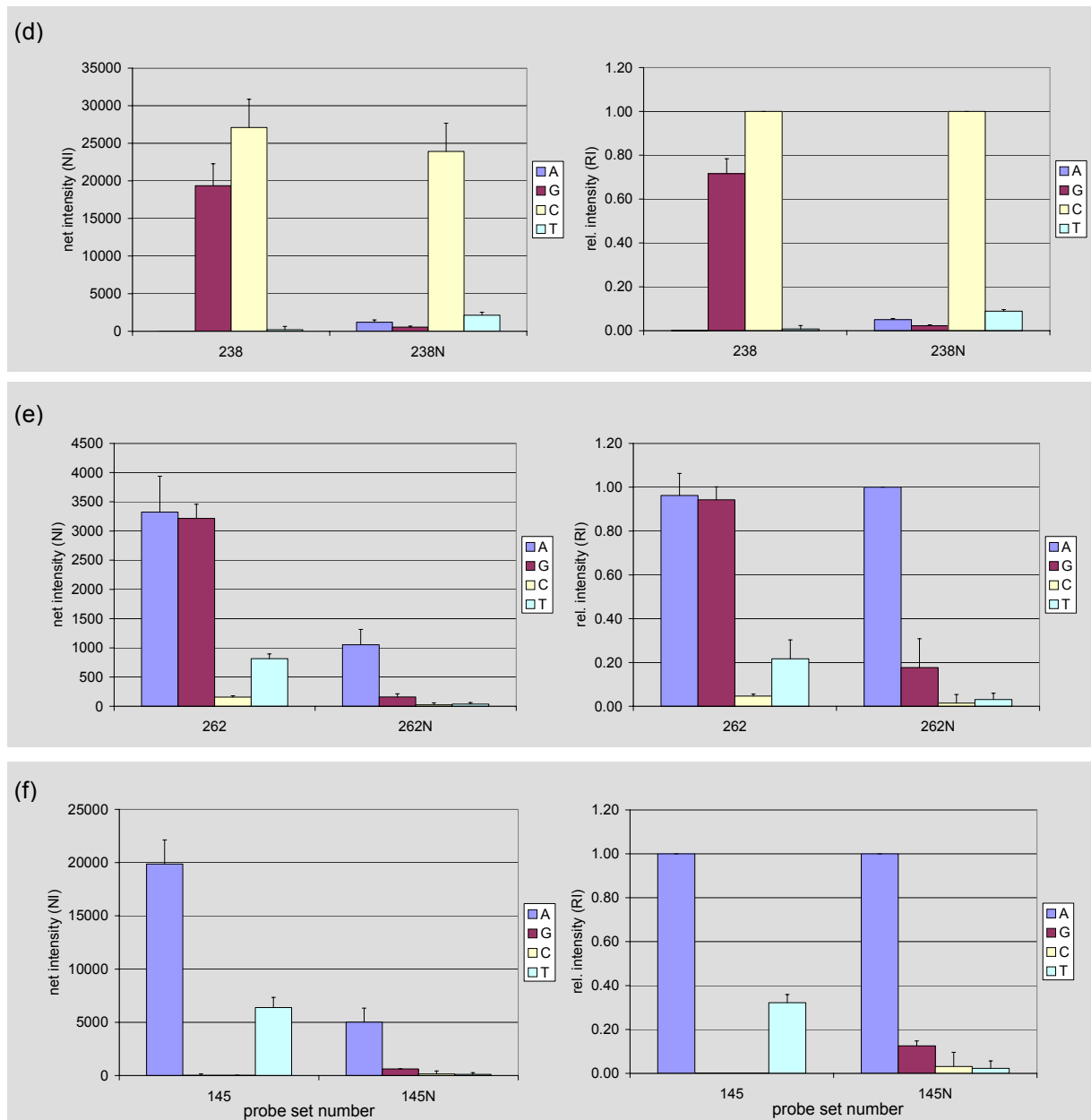


**Figure 52.** Mean net intensities (right chart) and mean relative intensities (left chart) of probe version I (e.g. 39) and version II (e.g. 39N for 39<sub>NEW</sub>) are displayed. Results of a hybridization with 200 ng *bla<sub>SHV-1</sub>* (NT/F = 48) with (a) probe set 39, (b) 125, (c) 222, (d) 238, (e) 262, (f) 145 are shown (n = 9).

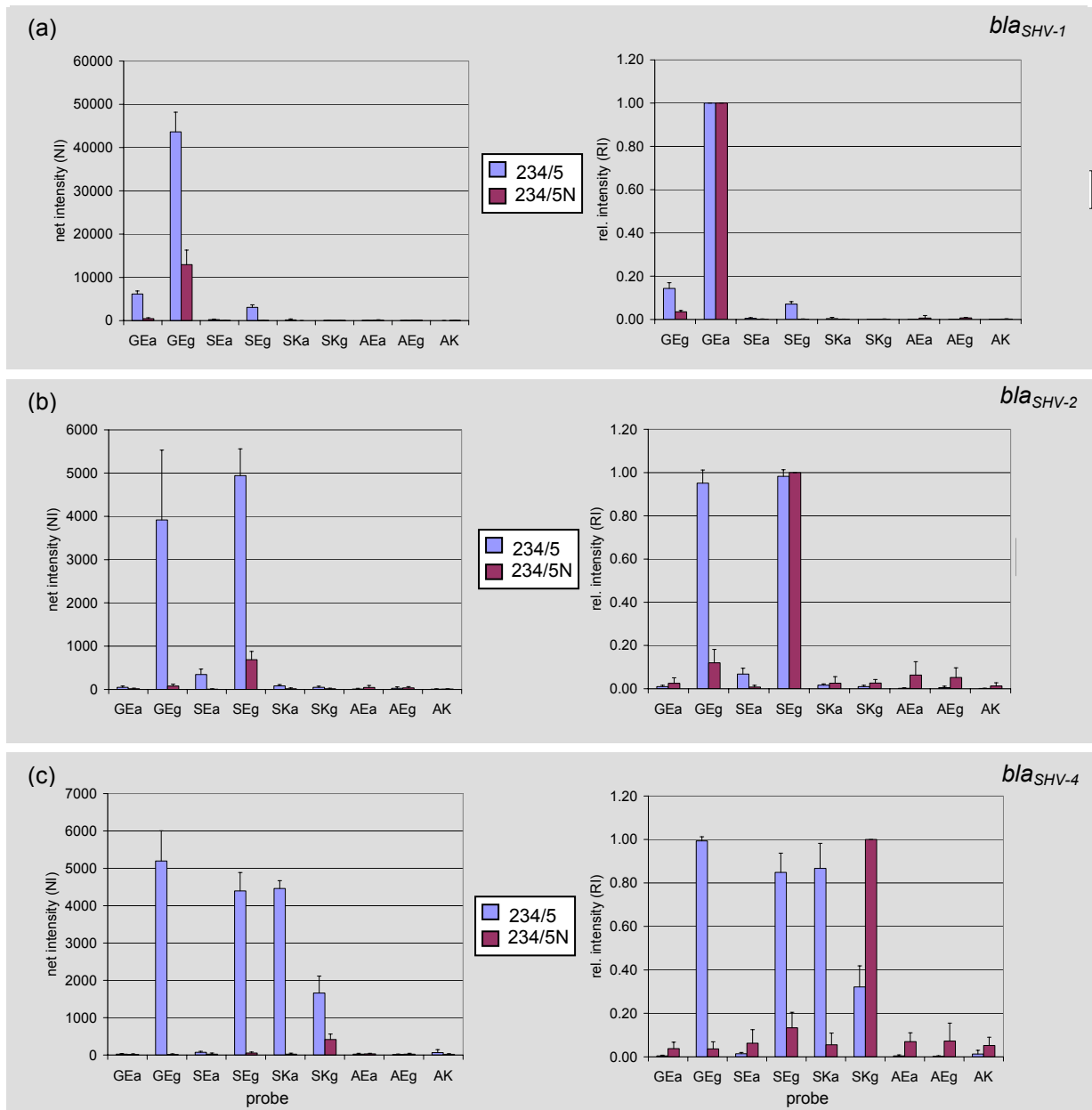


**Figure 53.** Mean net (left chart) and mean relative (right chart) signal intensities of probe versions I (234/5) and version II (234/5N for 234/5<sub>NEW</sub>) hybridized with (a) *bla<sub>SHV-1</sub>* (NT/F = 48), (b) *bla<sub>SHV-2</sub>* (NT/F = 51) and (c) *bla<sub>SHV-4</sub>* (NT/F = 85) are displayed (n = 9).

**Table 12.** Oligonucleotide probe sequences used in the SHV-specific microarray<sup>a</sup>

Melting temp (°C)	Length (bases)	Name	Probe sequence (5'-3') <sup>b</sup>
50.2	19	3	ATGCGT <u>T</u> NIATTTCGCCTGT
50.2	19	4	ATGCGT <u>T</u> ATNITTCGCCTGT
55.5	18	14	CTGTTAGCC <u>N</u> CCCTGCCG
54.6	16	21	CGGTACAC <u>N</u> CCAGCCC
55.4	24	31	AGCAAATTA <u>A</u> ACNAAGCGAAAGCC
56.0	16	39	TGTCGGGC <u>N</u> CGTAGG
55.8	25	44	GTAGGCATGATANA <u>A</u> ATGGATCTGG
54.9	18	60	CGCCGAT <u>G</u> NA <u>C</u> GCCTTTCC
55.9	15	76	CGGCGC <u>A</u> NT <u>G</u> CTGGC
54.8	17	85	GCCGGTGAC <u>N</u> A <u>C</u> AGCT
54.3	21	109	TCGAAAAACAC <u>N</u> ITGCCGACG
55.4	17	115	GCATGACG <u>N</u> TCCGGCGAA
52.7	16	118	GTCGGCGA <u>A</u> NTCTGCG
56.0	16	122	CGCCGCC <u>G</u> NCATTACC
58.8	25	125	CCGCCATTACC <u>N</u> ITGCGATAACAG
56.2	23	126	CCATTACCATG <u>N</u> GCGATAACAGC
60.9	20	136 <sub>WILDTYPE</sub>	CTGCTACTGGCC <u>A</u> CCGTCGG
60.1	20	136 <sub>MUTANT</sub>	CTGCTACTCC <u>G</u> GACCCTCGG
57.4	15	138	GGCCACC <u>N</u> TCCGGCGG
56.1	15	141	GCGGC <u>C</u> NCGCAGGAT
55.0	16	142	CGGCC <u>C</u> C <u>G</u> NA <u>G</u> GGATTG
43.1	16	145	AGGATTG <u>N</u> CTGCCTTT
53.2	17	152	CCAGATC <u>G</u> NCGACAACG
56.1	17	154	CGGCGA <u>C</u> A <u>A</u> NGTCACCC
52.4	20	163 <sub>WILDTYPE</sub>	CTGGGAAACGGA <u>A</u> CTGAATG
58.7	20	163 <sub>MUTANT</sub>	CTGGGAAACTGACC <u>G</u> CTGGG
53.4	16	169	ATGAGGCG <u>N</u> ITCCCGG
55.1	15	175.1	CGCCCGC <u>N</u> ACACCAC
53.2	15	175.2	GCCCGC <u>G</u> NCACCCT
55.9	16	183	CCAGCATG <u>N</u> CCGCGAC
55.9	17	188/9 <sub>WILDTYPE</sub>	GCGC <u>A</u> AGCTGCTGACCA
56.3	17	188/9 <sub>MUTANT</sub>	GCGC <u>A</u> ACGTGCTGACCA
56.0	16	191	GCTGCTG <u>A</u> NCAGCCAGC
54.8	17	201	GTTGCAAC <u>N</u> GCAGCTG
54.0	16	202	GCAACGGC <u>A</u> NTGCTG
51.5	14	222	CCGTGCTG <u>N</u> CTGCG
50.2	15	234/5 GEG	GGAGCTG <u>G</u> TGAGCGG
47.4	15	234/5 GEa	GGAGCTG <u>G</u> TG <u>A</u> ACGG
43.6	15	234/5 SEa	GGAGCTA <u>G</u> TG <u>A</u> ACGG
46.4	15	234/5 SEg	GGAGCTA <u>G</u> TGAGCGG
40.4	15	234/5 SKa	GGAGCTA <u>G</u> TAAACGG
43.3	15	234/5 SKg	GGAGCTA <u>G</u> TAAACGG
48.0	15	234/5 AEa	GGAGCTG <u>C</u> TG <u>A</u> ACGG
50.8	15	234/5 AEG	GGAGCTG <u>C</u> TGAGCGG
44.8	15	234/5 AK	GGAGCTG <u>C</u> TAAACGG
57.7	15	238	CGGGGTG <u>N</u> GTCGGG
47.3	15	262	CTGCGTGAT <u>N</u> CCCCG
54.6	19	272	AAATCAGC <u>A</u> NATCGCCGGG
54.9	21	process control	TTTAAAGTAGTGCTCTGCGGC
46.0	18	negative hybridization control	TCTAGACAGCCACTCATA
53.1	19	positive hybridization control	GATTGGACGAGTCAGGAGC
46.0	18	spot control	TCTAGACAGCCACTCATA-Cy3

<sup>a</sup> For the SNP specific probes, four probes for each SNP position were used. The probes are named for the position in the amino acid sequence of *bla<sub>SHV</sub>*. The four probes had either A, G, C or T at the central base position (designated N in the probe sequence). The probe length and the melting temperatures calculated for the probes matching the *bla<sub>SHV-1</sub>* sequence by ArrayDesigner 2.0 software are also provided. The probes 234/5 are designated by the targeted amino acids at position 234/5 (GE, SE, SK, AE, AK) and the nucleotide at the third codon position for amino acid 235 (e.g. GEa or GEG). For probes where more than one neighboring nucleotide differs in the mutant sequence from the wildtype sequence, one probe (136<sub>WILDTYPE</sub>, 188/9<sub>WILDTYPE</sub>, 163<sub>WILDTYPE</sub>) matching the wildtype sequence (*bla<sub>SHV-1</sub>*) and one probe (136<sub>MUTANT</sub>, 188/9<sub>MUTANT</sub>, 163<sub>MUTANT</sub>) matching the mutant sequence *bla<sub>SHV-x</sub>* were designed.

<sup>b</sup>The triplet with the amino acid substitution is underlined. All probes carried a 13T spacer and a C<sub>6</sub>-aminomodification at the 3'end.

### 3.2.5 Proof of concept

As a proof of concept it was shown, that all perfect match positions could be identified for a hybridization with 200 ng *bla<sub>SHV-1</sub>* target DNA, which was derived from a laboratory culture of *E. coli* DH5 $\alpha$  bearing a pCCR9 plasmid. The target DNA with a incorporation ratio (NT/F) of 55 was hybridized for one hour under medium agitation in a hybridization station (see figure 54). It was the aim to assess the specificity and the reproducibility of the perfect match detection of the SHV-array under standard conditions. All perfect match positions for *bla<sub>SHV-1</sub>* were correctly identified. The absolute net signal intensities ranged from 2400 to 46000 for the probes with perfect matches (displayed in figure 55 a,c,e). The relative intensities were calculated to investigate the discriminatory power of the system. The mean relative intensities and standard deviations for all mutation positions are shown in figure 55 b,d,f. Up to 97 % of the relative intensities of the mismatches remained < 0.5, more than 92 % of the mismatch signal intensities remained even below 10 % of the perfect match signal intensities (see figure 56). The highest relative intensity of a mismatch was detected for probe 39<sub>MUTANT</sub> with 0.67. The standard deviations for the mean relative intensities of the mismatches ranged from 0 to 0.17.

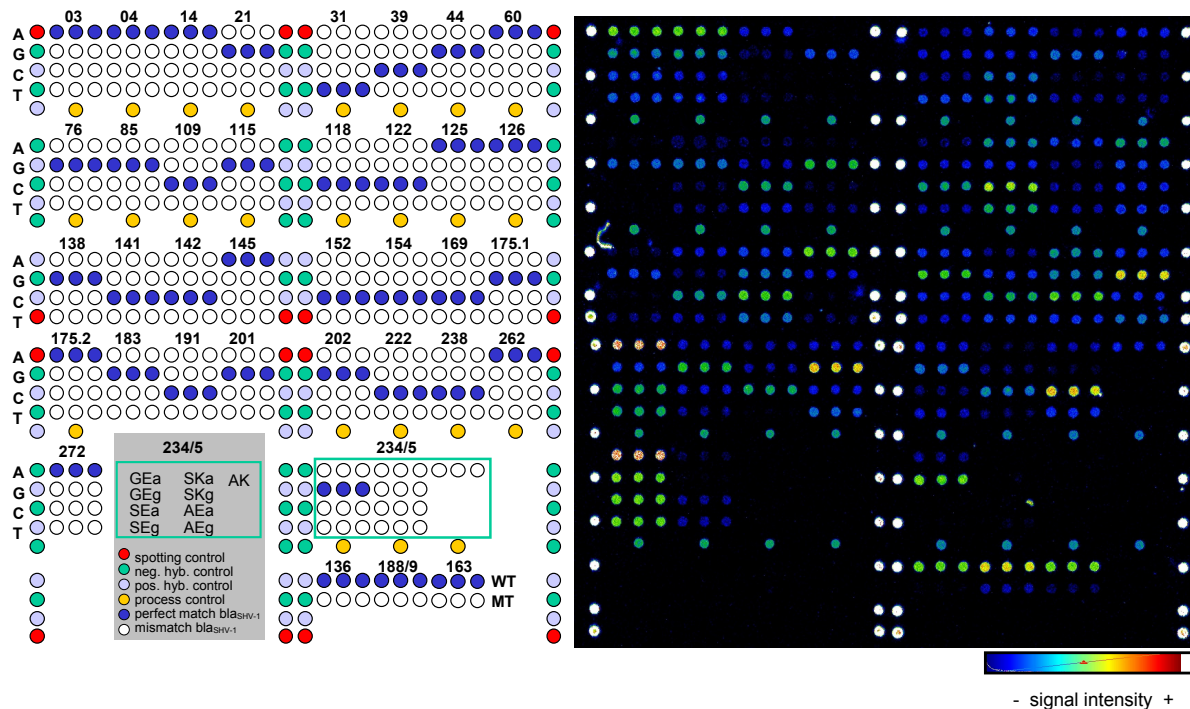


**Figure 54.** On the left, the layout of the mutation capture probes of the SHV microarray is displayed. All mutation specific capture probes were spotted in triplicates. The mutation position is indicated above each triplicate. For the SNP specific probes the nucleotide at the central base is indicated on the left side of each row as A, G, C or T. For probe No 234/5 the probes are designated by the targeted amino acids at position 234/5 (GE, SE, SK, AE, AK) and the nucleotide at the third codon position for amino acid 235 (GEa or GEg) as indicated in the legend. For position 136, 188/9, 163 one probe triplet (WT) matching the wild type sequence (*bla<sub>SHV-1</sub>*) and one probe triplet (MT) matching the mutant sequence (*bla<sub>SHV-x</sub>*) are spotted. Negative and positive hybridization controls are indicated as neg. hyb. and pos. hyb. controls respectively. On the right the fluorescence image of a hybridization experiment with 200 ng target DNA *bla<sub>SHV-1</sub>* (NT/F = 55) for 1 h in an HS 400 hybridization station is shown. The signal intensity is shown in false color. Blue corresponds to the lowest signal intensity and red to white depict the highest signal intensities.

## Results

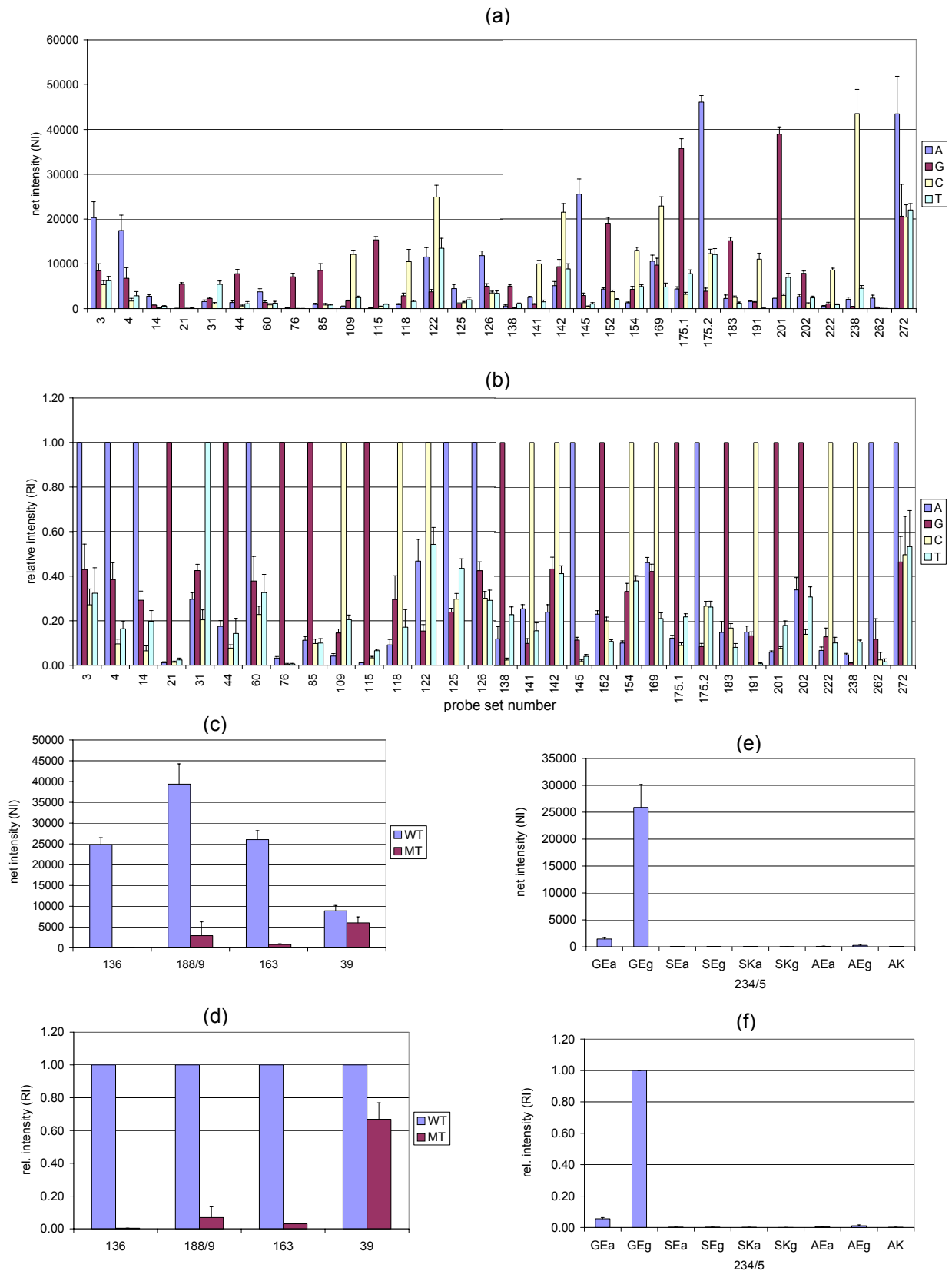


**Figure 55.** Mean net signal intensities (a) and mean relative signal intensities (b) for each SNP position and corresponding probe (A, G, C and T refer to the base at the central position) from a hybridization experiment with 200 ng *bla<sub>SHV-1</sub>* (NT/F = 55) ( $n = 9$ ). Mean net signal intensities (c) and mean relative signal intensities (d) for mutation position and corresponding probe No. 39, 136, 188/9, 163 WT matching the wildtype sequence (*bla<sub>SHV-1</sub>*) and MT matching the mutant sequence (*bla<sub>SHV-x</sub>*). Mean net signal intensities (e) and mean relative signal intensities (f) for mutation position and corresponding probe 234/5 designated by the targeted amino acids at position 234/5 (GE, SE, SK, AE, AK) and the nucleotide at the third codon position for amino acid 235 (GEa or GEg).



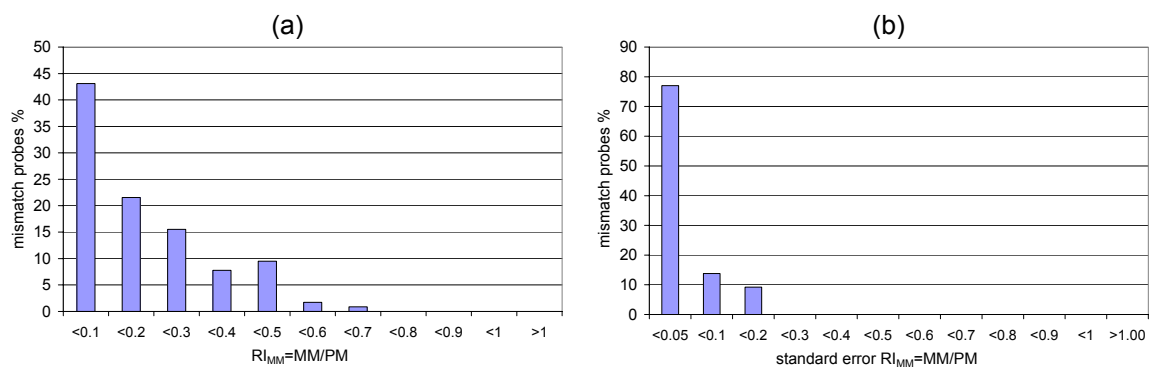


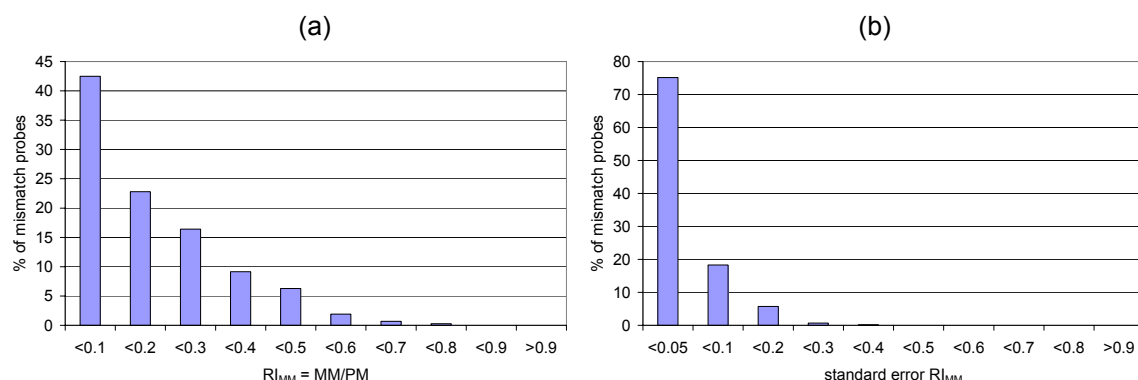
**Figure 56.** (a) Percentage of mismatch probes depending on the MM/PM ratio (b) Percentage of mismatch probes depending on the standard error of the MM/PM ratio from a hybridization experiment with 200 ng *bla*<sub>SHV-1</sub> (NT/F = 55), (n = 9).

## Results

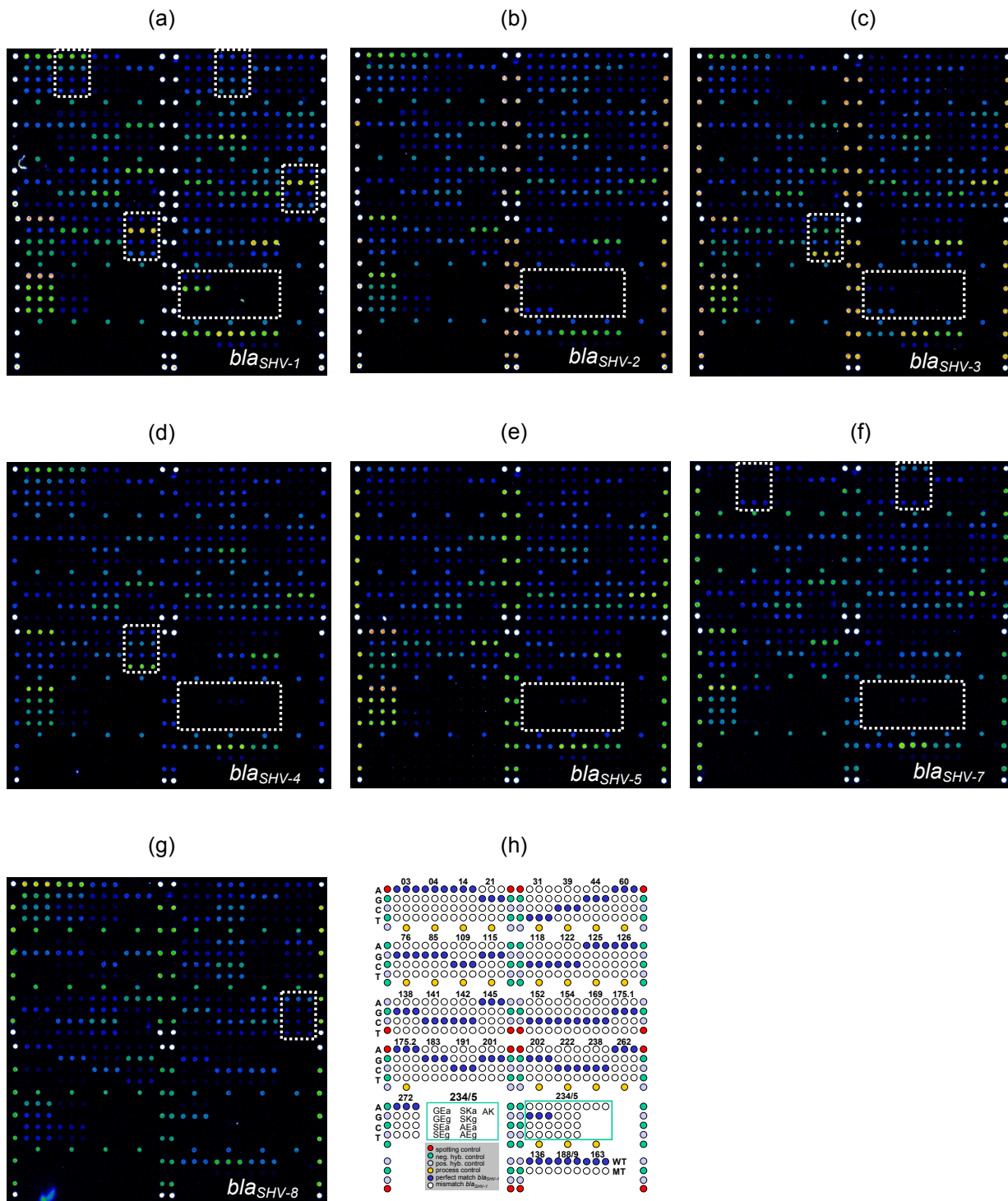
### 3.2.6 Identification of SHV variants

The performance of the array was tested with a set of genetically and phenotypically well characterized SHV gene variants (131). More precisely the investigated SHV variants were SHV-1, -2, -3, -4, -5, -7 and -8. The results of the hybridization of *bla*<sub>SHV-1</sub>, *bla*<sub>SHV-2</sub>, *bla*<sub>SHV-3</sub>, *bla*<sub>SHV-4</sub>, *bla*<sub>SHV-5</sub>, *bla*<sub>SHV-7</sub> and *bla*<sub>SHV-8</sub> are given as fluorescence images in figure 58. The resulting relative intensity values are displayed in figure 59. Only the mutation positions, which varied in comparison to *bla*<sub>SHV-1</sub> are shown. All correct perfect matches were identified without ambiguity. The relative intensity of the mismatches remained for 97 % of the mismatch positions below a limit of 0.5. Only 3 % of the relative intensities of the mismatches ranged from 0.4 to 0.7 (see figure 57). Two times the value of 0.7 was exceeded by probe 39<sub>MUTANT</sub> with values up to 0.79 for the identification of *bla*<sub>SHV-2</sub> and *bla*<sub>SHV-4</sub>. This was due to the aforementioned unfavorable secondary structure of the 39<sub>WILDTYPE</sub> probe. However, a reliable differentiation between a mutated and wildtype variant at this position was still possible, since as shown for the identification of *bla*<sub>SHV-7</sub>, the detection of a mutated position 39 in the target was highly specific with a relative intensity of the 39<sub>WILDTYPE</sub> probe of only 0.02 (see figure 59f). The standard deviations of the mean relative intensities of the mismatches varied from 0 to 0.33, but 93 % of the values remained below 10 % of perfect match intensity (see figure 57).

Probe sets with probe net signal intensities below background level were excluded from the data analysis. This was the case for probe set 262: probe 262A was perfectly complementary to the *bla*<sub>SHV-1</sub> codon (ACC) and probe 262T was perfectly complementary to the codon of *bla*<sub>SHV-39</sub> (TCC). A probe perfectly complementary to a silent mutation ACG present for example in *bla*<sub>SHV-2</sub>, -3, -4, -5, -7, -8 was so far not included in this probe set. Therefore, the perfect match position of probe 262 could only be identified for *bla*<sub>SHV-1</sub> (data not shown), since the probe net signal intensities for the other not perfectly complementary variants were not above background level. Variants *bla*<sub>SHV-3</sub> and *bla*<sub>SHV-4</sub> carry a mutation at position 201. The neighboring probe 202 does therefore not perfectly match those variants and thus, the net signal intensities were not above background level and were also excluded from the calculation of the relative intensities. However, all the directly targeted positions were detected and allowed an unequivocal identification of each tested SHV variant.

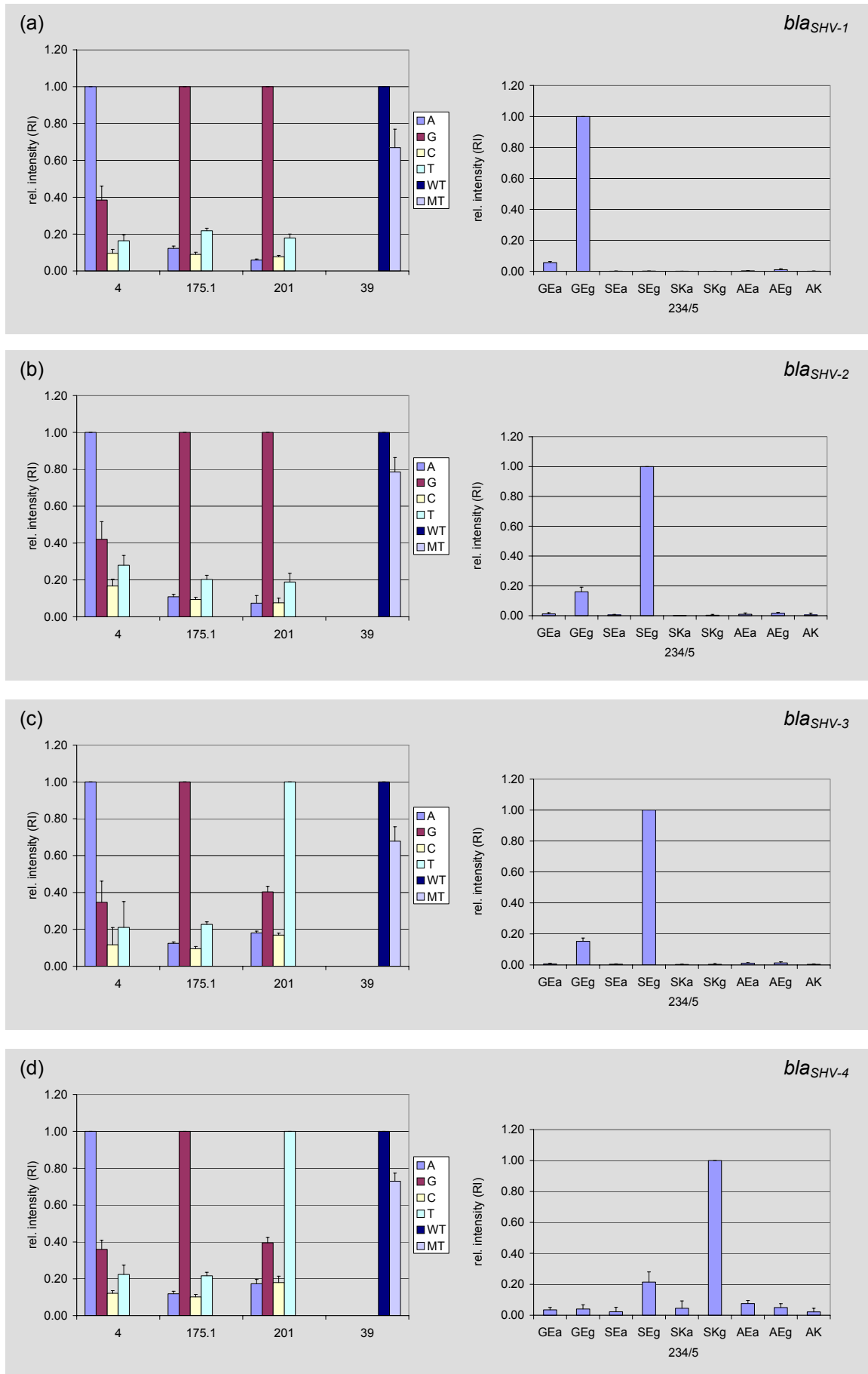


**Figure 57.** (a) Percentage of mismatch probes depending on the MM/PM ratio, (b) percentage of mismatch probes depending on the standard error of the MM/PM ratio from a hybridization experiment with 200 ng of each *bla*<sub>SHV-1</sub>, *bla*<sub>SHV-2</sub>, *bla*<sub>SHV-3</sub>, *bla*<sub>SHV-4</sub>, *bla*<sub>SHV-5</sub>, *bla*<sub>SHV-7</sub> and *bla*<sub>SHV-8</sub> (n = 9).



**Figure 58.** Fluorescence images of selected SHV arrays hybridized with target DNA originating from different variants from diverse reference strains. The SNP positions varying towards *bla<sub>SHV-1</sub>* (4, 39, 175.1, 201, 234/5) are highlighted. The identified variants were (a) *bla<sub>SHV-1</sub>*, (b) *bla<sub>SHV-2</sub>*, (c) *bla<sub>SHV-3</sub>*, (d) *bla<sub>SHV-4</sub>*, (e) *bla<sub>SHV-5</sub>*, (f) *bla<sub>SHV-7</sub>* and (g) *bla<sub>SHV-8</sub>* as indicated in the right corner of the fluorescence images. The signal intensity is shown in false color. Blue to white depict the lowest signal intensities, red to yellow depict the highest signal intensities (as output by ImaGene 3.0). In (h) the SNP capture probe layout of the SHV microarray is displayed (for details see also figure 49).

# Results



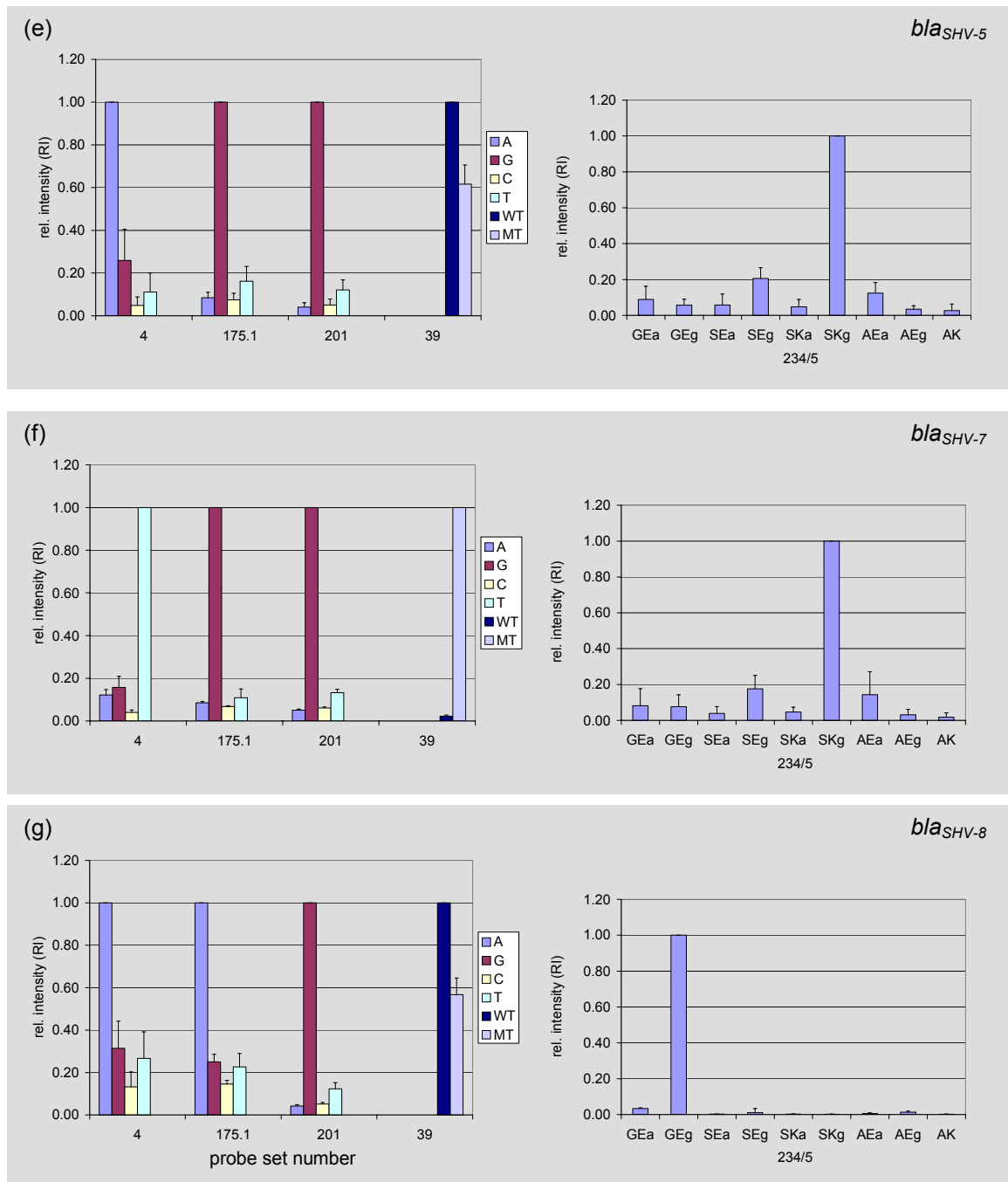


**Figure 59.** Relative (rel.) intensities of the signals for selected mutation positions according to the target DNA applied. Only the mutation positions (4, 39, 175.1, 201, and 234/5) differing between the tested variants: (a) *bla<sub>SHV-1</sub>*, (b) *bla<sub>SHV-2</sub>*, (c) *bla<sub>SHV-3</sub>*, (d) *bla<sub>SHV-4</sub>*, (e) *bla<sub>SHV-5</sub>*, (f) *bla<sub>SHV-7</sub>* and (g) *bla<sub>SHV-8</sub>* are displayed ( $n = 9$ ). For the SNP specific probes, the probe sets are indicated in the legend by their central base (A, G, C or T), for mutation position 39<sub>WILDTYPE</sub> (39WT) is indicated in the legend for the probe matching the wildtype sequence (*bla<sub>SHV-1</sub>*) and 39<sub>MUTANT</sub> (39MT) for the probe matching the mutant sequence (*bla<sub>SHV-X</sub>*). For probe 234/5 the probe set is designated by the targeted amino acids at position 234/5 (GE, SE, SK, AE, AK) and the nucleotide at the third codon position for amino acid 235 (GEa or GEg).

### 3.3 Validation of the SHV- and TEM-array with clinical isolates collected in Croatia

To validate the TEM and SHV-array a set of 35 isolates, as displayed in table 13, collected during 02/2001-10/2003 at the Zadar Hospital in Zadar, Croatia was provided by Dr. Susa (Department of Clinical Microbiology, Robert-Bosch Hospital, Stuttgart). These isolates were classified as possible ESBL producers through a standard phenotypic screening carried out at the Zadar Hospital. An additional phenotypic ESBL screening and species identification was performed at the Robert Bosch hospital using the MicroScan system (an automated microdilution test). The identified isolates species included 22 *K. pneumoniae*, 10 *E. coli*, one *K. ornithinolytica*, one *K. terrigena* and one *K. oxytoca*. By analyzing the antibiogram, 28 of the isolates were classified as ESBL producers. A reference antibiogram for identification of ESBL, AmpC, K1 (only for *K. oxytoca*) and CTX-M according to Livermore et al. (97) is given at the bottom of table 13. For isolates 13, 21 and 32 the results did not indicate an ESBL phenotype and an ESBL confirmatory test did support these results. For isolate 36 no phenotype clearly matching the aforementioned ones was detected, since it was tested as being resistant to ceftazidime, excluding an ESBL phenotype as ESBLs are susceptible to cephamycins. It also appeared to be susceptible to several cephalosporins, thereby contradicting an AmpC resistance type, so that no clear classification was possible. The antibiogram of isolate 20 matched an AmpC resistance type, since it was resistant to the tested cephalosporins and ceftazidime, however this does not exclude an ESBL, since this phenotype might be masked by the dominant AmpC phenotype. The *K. ornithinolytica* isolate 2 matched a CTX-M resistant phenotype according to Livermore, because of the susceptibility to ceftazidime (at a concentration of 8 µg/ml), while being resistant to all other cephalosporins except ceftazidime. The antibiogram and the identified species (*K. oxytoca*) of isolate 26 matched the guidelines for identification of a K1 type resistance.

#### 3.3.1 TEM-array

The plasmidic DNA extracted from the isolates was used in PCR labeling reactions as a template. For all samples a PCR product with TEM specific primers could be obtained corresponding to the correct *bla<sub>TEM</sub>* amplicon size of 861 bp. With all generated PCR products an array analysis was performed. The hybridizations were carried out in triplicates for the TEM-array analysis. The identified *bla<sub>TEM</sub>* - genes are displayed in table 14. Eight isolates contained a *bla<sub>TEM-1</sub>* gene, in all others *bla<sub>TEM-116</sub>* genes were detected. The differing

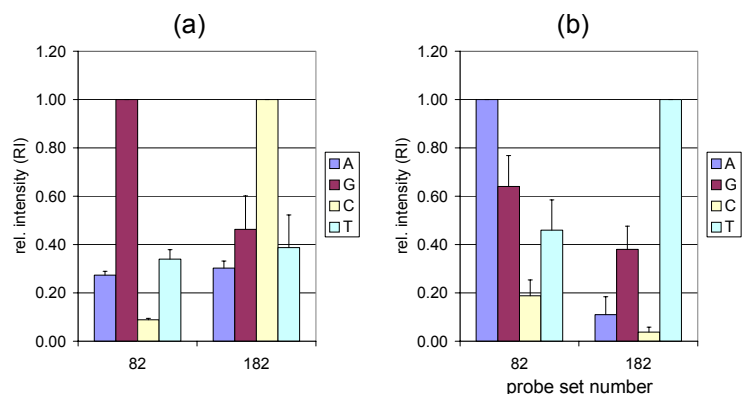


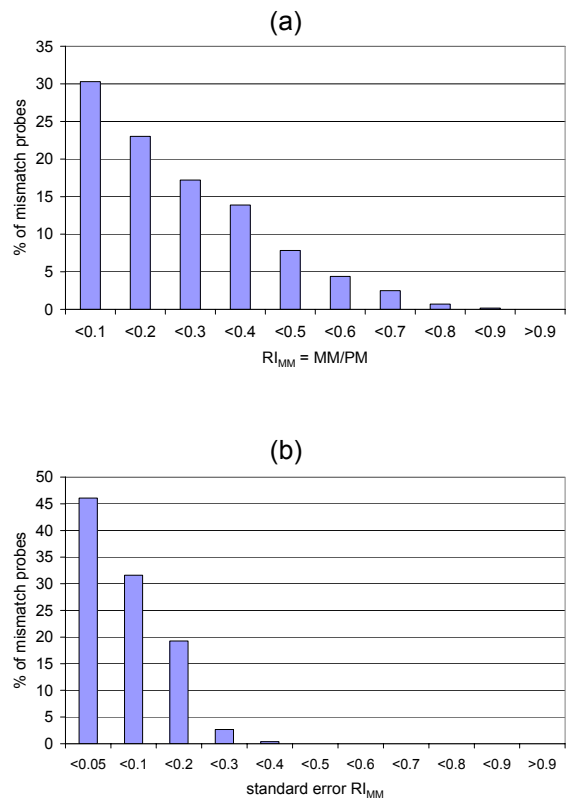
**Figure 60.** Representative identification of (a) *bla<sub>TEM-1</sub>* in isolate No. 3 and (b) *bla<sub>TEM-116</sub>* in isolate No. 5 from clinical isolates collected in Croatia. Only the relative intensities (RIs) of SNP positions (82, 182) differing between *bla<sub>TEM-1</sub>* and *bla<sub>TEM-116</sub>* are displayed. The probe sets are indicated by their central base (A, G, C, T) in the legend (n = 9).



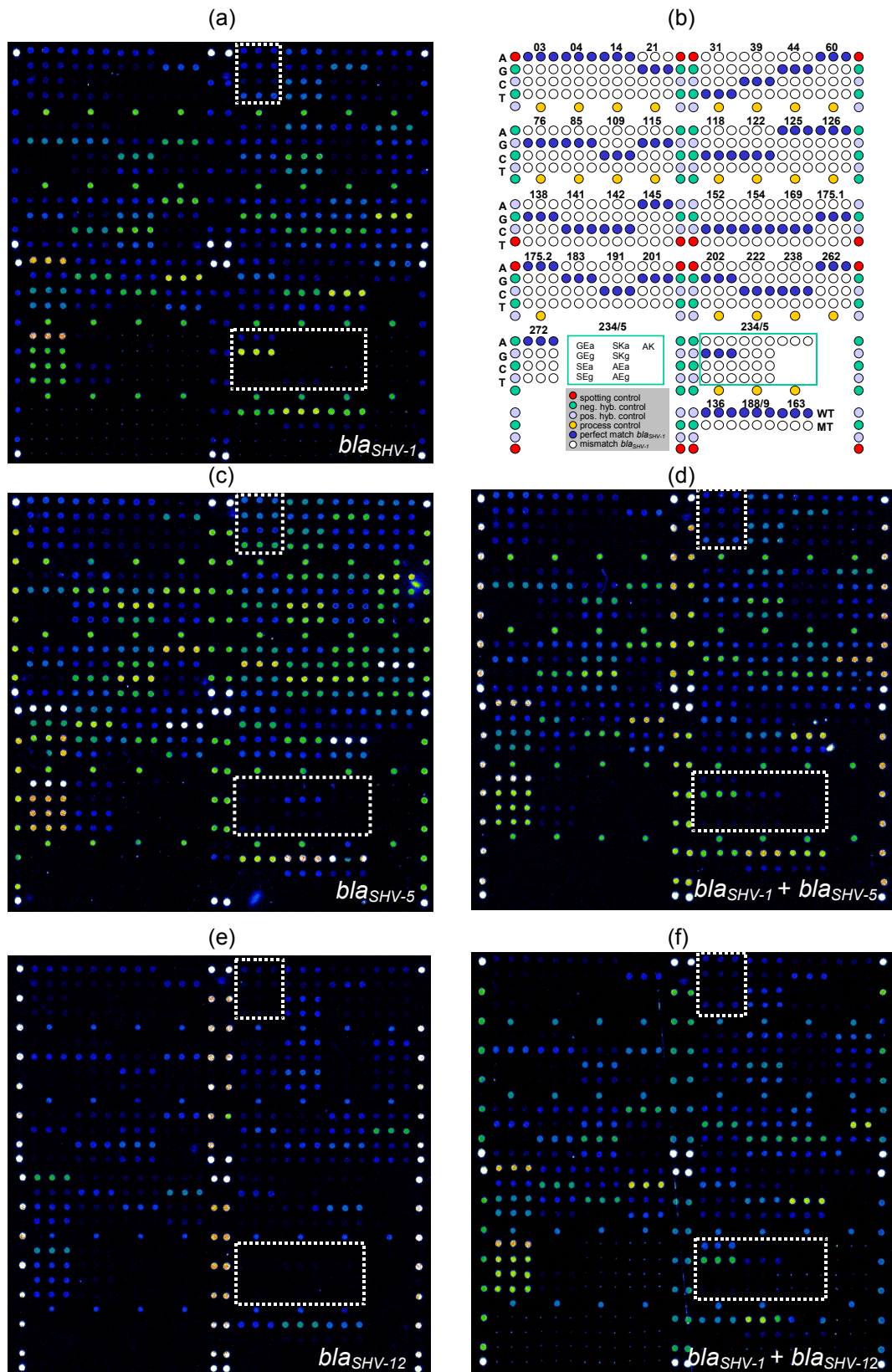
polymorphism positions are displayed for isolates 3 (TEM-1) and 5 (TEM-116) as relative intensity values in figure 60. All correct TEM perfect match positions could be identified for 34 of the 35 isolates. Only in isolate 21 the probe set 235.2 had to be excluded from the analysis due to a spotting failure. Over 99 % of the analyzed perfect match positions could be unambiguously identified, since their relative intensities of the mismatches remained below a limit of 0.8 (see figure 61a). Only for 0.16 % of the analyzed values this limit was violated with relative intensities of the mismatches up to 0.88, which was attributed to sporadic aberrations during the spotting process. The standard deviations of the mean relative intensities of the mismatches varied from 0 to 0.38, whereby 78 % remained below 10 % of the perfect match intensity (see figure 61b). Usually about 90 % of the standard deviations of the mean relative intensities of the mismatches remained below this limit, but in this case two slide batches with differing production parameters were used (new spotting pins and a new microtiterplate as probe source had to be applied). Since the standard deviations still remained within a range of 0 - 0.4, the results were considered reliable enough for a significant analysis.

### 3.3.2 SHV-array

Except for isolates 2, 21, 26, 27 and 36 a SHV amplicon with an expected amplicon size of 932 bp could be obtained for each isolate. All hybridizations were carried out in duplicates for the SHV-array analysis. The SHV-variants could be identified successfully by the SHV microarray analysis for 29 of the 30 SHV-amplicons. For two isolates a *bla<sub>SHV-1</sub>* gene, for six isolates a *bla<sub>SHV-5</sub>* gene, for one isolates a *bla<sub>SHV-12</sub>* gene was detected. In the other isolates the coexistence of two *bla<sub>SHV</sub>* variants was detected, four times *bla<sub>SHV-1</sub>* and *bla<sub>SHV-12</sub>*, 16 times *bla<sub>SHV-1</sub>* and *bla<sub>SHV-5</sub>* (see table 14). Exemplary hybridization results of detected SHV-variants are displayed in figure 62 as fluorescence images. The differing polymorphism positions are displayed for each detected genotype: *bla<sub>SHV-1</sub>* (e.g. isolate 32), *bla<sub>SHV-5</sub>* (e.g. isolate 23), *bla<sub>SHV-12</sub>* (e.g. isolate 3), *bla<sub>SHV-1</sub>* and *bla<sub>SHV-5</sub>* (e.g. isolate 1) and *bla<sub>SHV-1</sub>* and *bla<sub>SHV-12</sub>* (e.g. isolate 11 or 20) as relative intensity (for position 31) and net intensity (for position 234/5) values in figure 63.

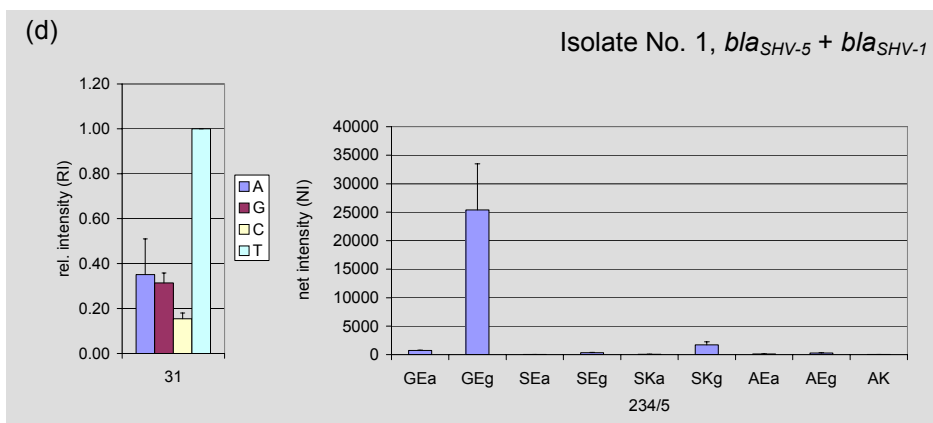
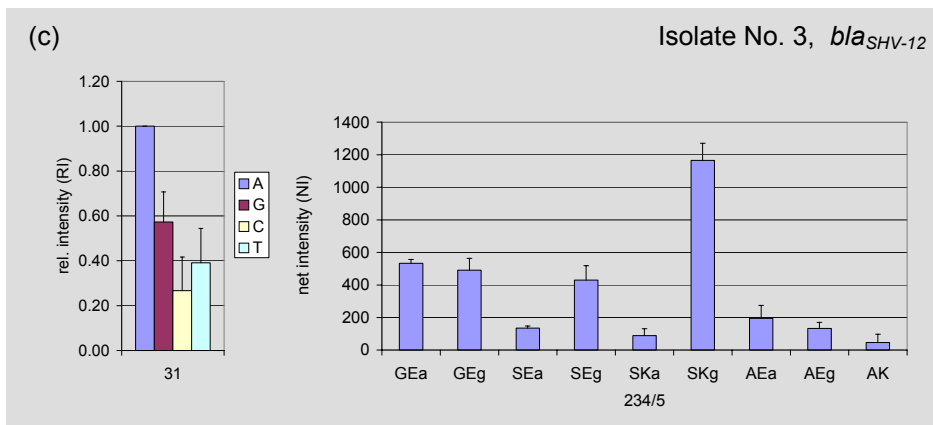
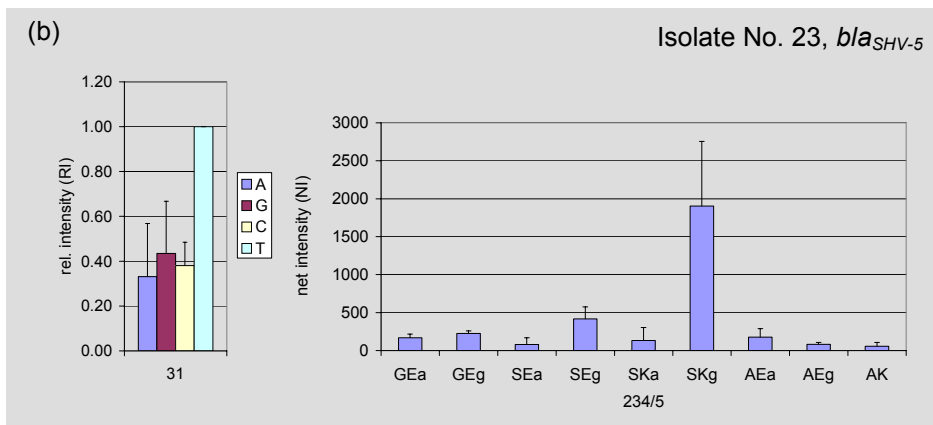
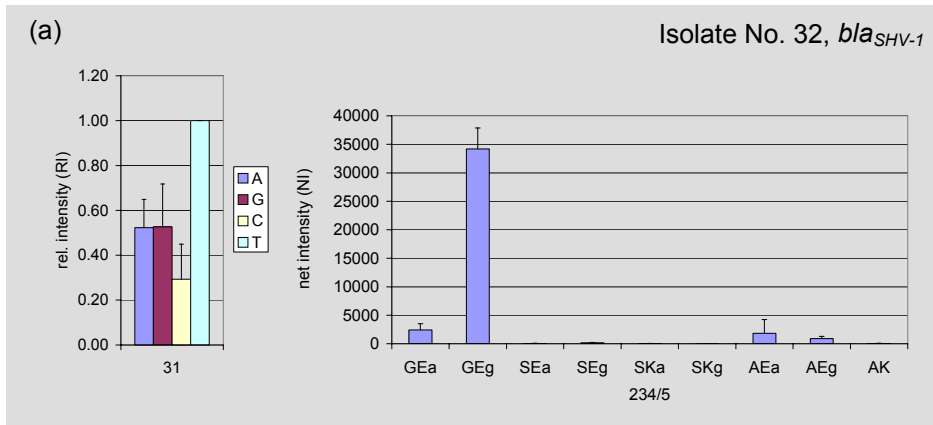


**Figure 61.** (a) Percentage of mismatch probes depending on the MM/PM ratio (b) Percentage of mismatch probes depending on the standard error of the MM/PM ratio from the TEM-array analysis of 35 clinical samples collected in Croatia.



**Figure 62.** Fluorescence images of selected SHV-arrays hybridized with target DNA presenting different genotypes originating from clinical isolates collected in Croatia. The varying SNP positions 31, 234/5 are highlighted with white boxes. The identified variants were (a) *bla<sub>SHV-1</sub>* in isolate No. 32, (c) *bla<sub>SHV-5</sub>* in isolate No. 23, (d) *bla<sub>SHV-5</sub> + bla<sub>SHV-1</sub>* in isolate No. 1 (e) *bla<sub>SHV-12</sub>* in isolate No. 3, (f) *bla<sub>SHV-12</sub> + bla<sub>SHV-1</sub>* in isolate No. 11. The signal intensity is shown in false color. Blue corresponds to the lowest signal intensity, red to white depict the highest signal intensities (as output by ImaGene 3.0). In (b) the capture probe layout of the SHV-microarray is displayed (for details see also figure 52).





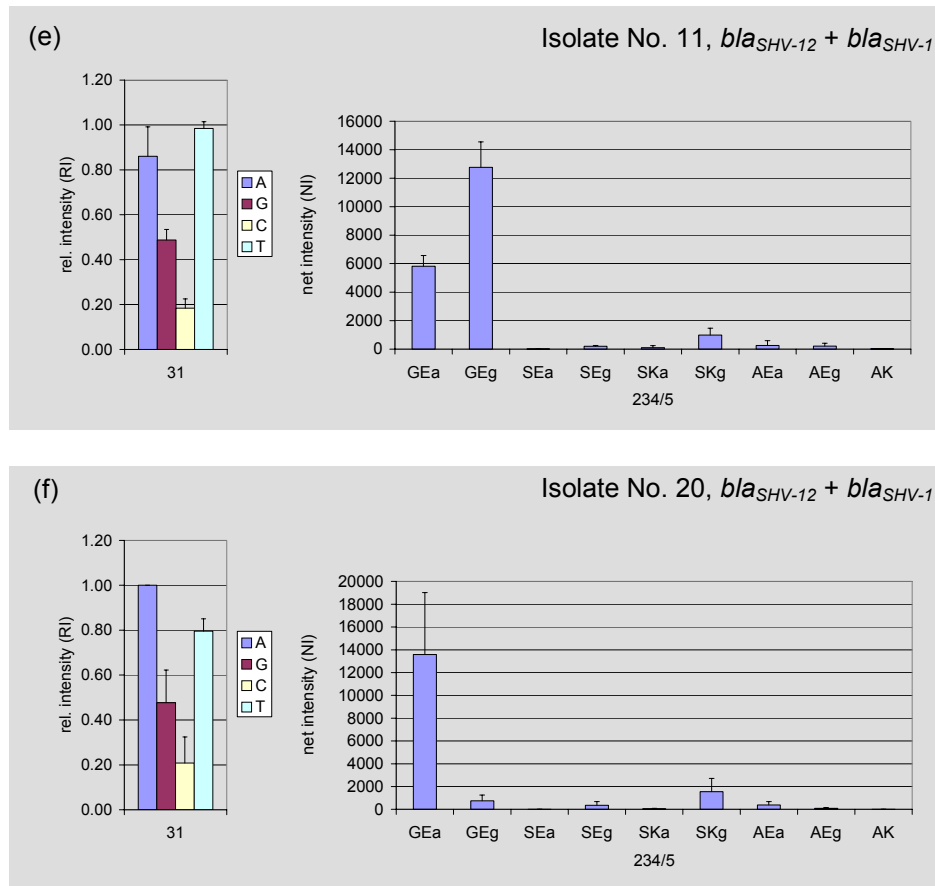


**Figure 63.** Representative identification of (a)  $bla_{SHV-1}$  in isolate No. 32, (b)  $bla_{SHV-5}$  in isolate No. 23, (c)  $bla_{SHV-12}$  in isolate No. 3, (d)  $bla_{SHV-5} + bla_{SHV-1}$  in isolate No. 1, (e)  $bla_{SHV-12} + bla_{SHV-1}$  in isolate No. 11, (f)  $bla_{SHV-12} + bla_{SHV-1}$  in isolate No. 20 from clinical isolates collected in Croatia (n = 6 for all isolates). Only the mutation positions differing between  $bla_{SHV-1}$  and the other SHV variants are displayed as relative intensities (RIs) for SNP position 31 and as net intensities (NIs) for mutation position 234/5. Probe set 31 is indicated by the central base (A, G, C, T) in the legend. Probe set 234/5 is designated by the targeted amino acids at position 234/5 (GE, SE, SK, AE, AK) and the nucleotide at the third codon position for amino acid 235 (GEa or GEg).

For the detection of more than one  $bla_{SHV}$  variant, the net intensities of position 234/5 had to be considered. SHV-1 has at this position the amino acids GE, in contrast to the ESBL variants SHV-5 and SHV-12 carrying the amino acids SK. In case of the detection of a  $bla_{SHV-5}$  or  $bla_{SHV-12}$  alone, net signal intensities between approximately 700 and 2300 arbitrary units (a.u.) for the perfect match probe SKg could be detected, in contrast to net signal intensities between approximately 28,000 and 34,000 a.u. for the perfect match probe GEg in pure  $bla_{SHV-1}$ . This corresponded to a diminished melting temperature of the SKg probe (43.3 °C) in comparison to the GEg probe (50.2 °C) due to a lower GC content (see table 11). For the detection of a SK- in presence of a GE-carrying variant this difference in signal intensities has to be taken into account. Therefore, the net signal intensities of 234/5 had to be closely analyzed. In figure 63 a-f the differing net signal intensities of probes SKg in contrast to probe Geg or GEa can be noticed easily.

To clarify the specific detection of a mixed in contrast to a pure SHV-genotype, the net signal intensities of probe 234/5SKg of all different genotypes for all analyzed isolates are given in figure 64a. In case of the detection of pure  $bla_{SHV-1}$  (detected in isolate 13, 32 and the positive control target DNA) SKg net signal intensities of maximal 50 a.u. could be detected, which was not above net intensity background level. In all other tested SHV amplicons the presence of an ESBL variant could be detected by SKg net intensity values between 561 and 2236 a.u., which were at least six times above background net intensity. For the detection of  $bla_{SHV-12}$  in presence of another  $bla_{SHV}$ -variant, the relative intensities of position 31 had to be considered. In contrast to a wild type T, a mutated position 31 carried an A at the concerned position. The presence of a pure  $bla_{SHV-12}$  or a  $bla_{SHV-12}$  in presence of  $bla_{SHV-1}$  could be confirmed by 31A relative intensities of > 0.83. The non- $bla_{SHV-12}$  genotype 31A relative intensities remained all below 0.6 (see figure 64b). The unusually high variation in between 31A relative intensities within the non- $bla_{SHV-12}$  genotypes was attributed to the aforementioned changes in the spotting routine.

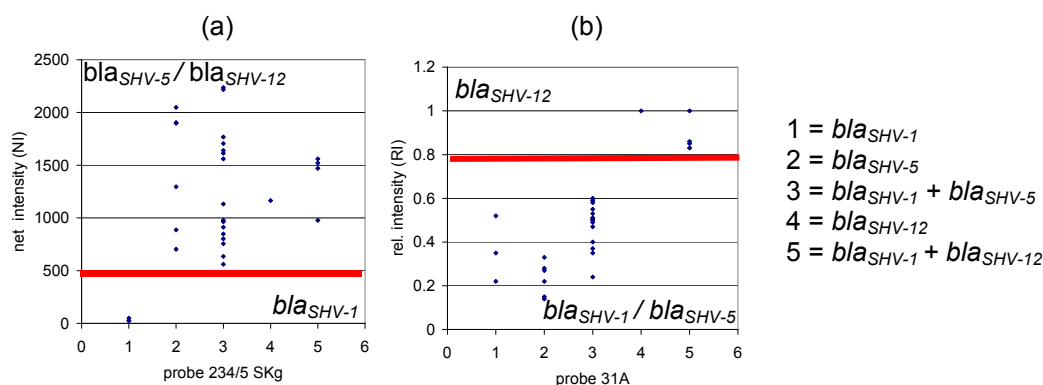


**Figure 64.** (a) Net intensities of probe 234/5 SKg and (b) relative intensities of probe 31A depending on the detected genotype ( $bla_{SHV-1}$  (N = 3),  $bla_{SHV-5}$  (N = 6),  $bla_{SHV-5} + bla_{SHV-1}$  (N = 16),  $bla_{SHV-12}$  (N = 1),  $bla_{SHV-12} + bla_{SHV-1}$  (N = 4) from the SHV array analysis of 29 of 30 SHV containing clinical samples collected in Croatia and the positive control target DNA ( $bla_{SHV-1}$ ), (N= Number of samples). The RI or NI limit value discriminating between the differing genotypes is displayed as a red line.

## Results

All *bla<sub>SHV</sub>* perfect match positions could be identified correctly for the analyzed SHV samples, except for position 202, which could not be analyzed for six of the tested samples due to incorrect spotting of this position in one batch of the slides. For isolate 34 the generated data was not sufficient for an unambiguous identification, therefore it was omitted from the further data analysis. Over 99% of the analyzed perfect match positions of the remaining 29 SHV containing isolates could be identified correctly, since their relative intensities of the mismatches remained below a limit of 0.8 (see figure 65a). Only for 0.23 % of the analyzed values this limit was violated with relative intensities up to 0.93, which was in six of eight cases caused by the mismatch position 39<sub>MUTANT</sub>. The unfavorable mismatch to perfect match ratio of this probe has already been described before (see section 3.2.5 and 3.2.6) and can be attributed to the unfavorable secondary structure of the perfect match probe 39<sub>WILDTYPE</sub>. The other two cases of an relative intensities of the mismatches > 0.8 were attributed to sporadic aberrations during the spotting process. The standard deviations of the mean relative intensities of the mismatches varied from 0 to 0.42, whereby 83 % remained below 10 % of the perfect match intensity (see figure 65b). Hereby the problematic of two slide batches with differing production parameters has to be reconsidered, since usually about 90 % of the standard deviations of the mean relative intensity of the mismatch values remained below 10 %.

When comparing the phenotypic and the genotypic data, it has to be noted that in all *K. pneumoniae* and in one *K. terrigena* isolates a *bla<sub>SHV-1</sub>* gene was found either alone or in combination with a *bla<sub>SHV</sub>*-ESBL gene variant. In contrast to that no *E. coli* isolate contained a *bla<sub>SHV-1</sub>* type gene.

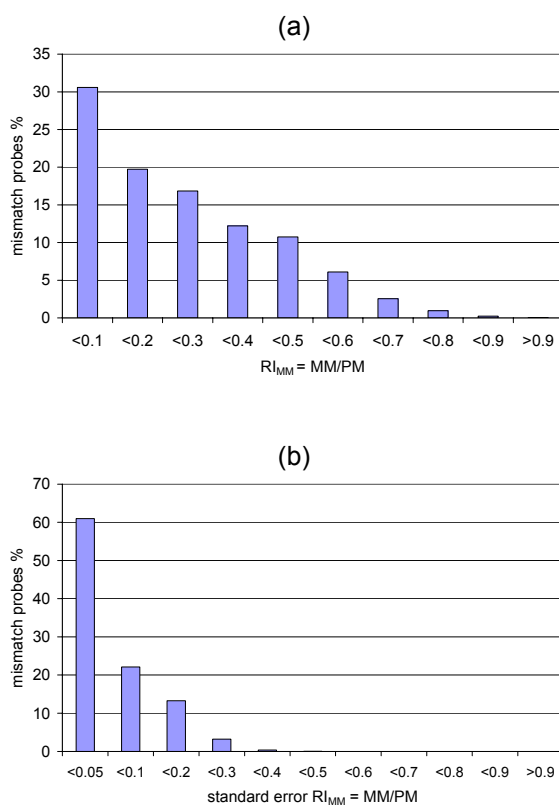


**Figure 65.** (a) Percentage of mismatch probes depending on the MM/PM ratio (b) Percentage of mismatch probes depending on the standard error of the MM/PM ratio from the SHV array analysis of 29 of 30 SHV containing clinical samples collected in Croatia.

For all isolates (except isolate 27), which were resistant or showed intermediate resistance against all cephalosporins except cefoxitin, an SHV-type ESBL variant (either *bla*<sub>SHV-5</sub> or *bla*<sub>SHV-12</sub>) was detected alone for *E. coli*, or in combination with *bla*<sub>SHV-1</sub> for *K. pneumoniae*. It is remarkable, that all other isolates, which were susceptible to one or more of the cephalosporins displayed in table 13, did not contain such a gene variant. In case of isolates 13 and 32 only *bla*<sub>TEM-116</sub> in combination with *bla*<sub>SHV-1</sub> and in case of isolate 21 only *bla*<sub>TEM-116</sub> was detected. These isolates were confirmed to be no ESBL producers by a phenotypic confirmatory test. The *K. oxytoca* isolate No. 26, which could be phenotypically classified as a likely K1 producer, also contained only a *bla*<sub>TEM-116</sub> gene variant. As has already been mentioned before, it is not clear, whether TEM-116 can confer an ESBL phenotype or not (see also section 3.1.7). According to these results, it appears not to be an ESBL conferring gene variant. Isolate 2 and 36 contained only a *bla*<sub>TEM-1</sub> gene and no *bla*<sub>SHV</sub> variant. The phenotype of isolate 2 suggested a CTX-M-type resistance, for which was not genotypically screened in this study. As aforementioned, isolate 36 could phenotypically not be classified as an ESBL producer.

## Results

**Table 13.** Properties and phenotypic data of samples collected in Croatia

Origin <sup>a</sup>	# <sup>b</sup>	Sample <sup>c</sup>	Species <sup>d</sup>	Antibiogram <sup>e</sup>									Enzyme <sup>f</sup>
				AZT	CAX	CAZ	CFT	CRM	CFX	CPD	CAZ <sup>1</sup>	IMP	
P	1	urine	<i>K. pneumoniae</i>	R	R	R	R	R	S	R	R	S	ESBL
P	4	urine	<i>K. pneumoniae</i>	R	R	R	R	R	S	R	R	S	ESBL
P	5	urine	<i>K. pneumoniae</i>	R	R	R	R	R	S	R	R	S	ESBL
P	6	urine	<i>K. pneumoniae</i>	R	R	R	I	R	S	R	R	S	ESBL
P	7	urine	<i>K. pneumoniae</i>	R	R	R	R	R	S	R	R	S	ESBL
n.s.	8	n.s.	<i>K. pneumoniae</i>	R	R	R	R	R	S	R	R	S	ESBL
n.s.	11	n.s.	<i>K. pneumoniae</i>	R	R	R	R	R	I	R	R	S	ESBL
S	12	w. swab	<i>K. pneumoniae</i>	R	R	R	R	R	S	R	R	S	ESBL
n.s.	13	n.s.	<i>K. pneumoniae</i>	S	S	S	S	R	S	S	R	S	no ESBL
P	14	blood	<i>K. pneumoniae</i>	R	R	R	R	R	S	R	R	S	ESBL
P	16	urine	<i>K. pneumoniae</i>	R	R	R	R	R	S	R	R	S	ESBL
P	19	urine	<i>K. pneumoniae</i>	R	R	R	R	R	S	R	R	S	ESBL
P	20	urine	<i>K. pneumoniae</i>	R	R	R	R	R	R	R	R	S	AmpC/ESBL
P	25	urine	<i>K. pneumoniae</i>	R	R	R	R	R	S	R	R	S	ESBL
P	28	urine	<i>K. pneumoniae</i>	R	R	R	R	R	S	R	R	S	ESBL
P	29	urine	<i>K. pneumoniae</i>	R	R	R	R	R	S	R	R	S	ESBL
n.s.	30	n.s.	<i>K. pneumoniae</i>	R	R	R	R	R	S	R	R	S	ESBL
N	31	urine	<i>K. pneumoniae</i>	R	R	R	R	R	S	R	R	S	ESBL
P	32	urine	<i>K. pneumoniae</i>	S	S	S	S	S	S	S	R	S	no ESBL
P	33	urine	<i>K. pneumoniae</i>	R	R	R	R	R	S	R	R	S	ESBL
n.s.	34	n.s.	<i>K. pneumoniae</i>	R	R	R	R	R	S	R	R	S	ESBL
n.s.	35	n.s.	<i>K. pneumoniae</i>	R	R	R	R	R	S	R	R	S	ESBL
S	2	w. swab	<i>K. ornithinolytica</i>	R	R	S	R	R	S	R	R	S	CTX-M
P	9	urine	<i>K. terrigena</i>	R	R	R	R	R	S	R	R	S	ESBL
Ga	26	urine	<i>K. oxytoca</i>	R	R	S	I	R	S	R	S	S	K1
n.s.	3	n.s.	<i>E. coli</i>	R	R	R	R	R	S	R	R	S	ESBL
P	10	urine	<i>E. coli</i>	R	I	R	I	I	S	R	R	S	ESBL
P	15	urine	<i>E. coli</i>	R	R	R	I	R	S	R	R	S	ESBL
Gy	18	urine	<i>E. coli</i>	R	R	R	R	R	S	R	R	S	ESBL
P	21	urine	<i>E. coli</i>	S	S	S	S	R	S	R	R	S	no ESBL
P	22	blood	<i>E. coli</i>	R	R	R	I	R	S	R	R	S	ESBL
Gy	23	v. swab	<i>E. coli</i>	R	R	R	R	R	S	R	R	S	ESBL
n.s.	24	n.s.	<i>E. coli</i>	R	R	R	R	R	S	R	R	S	ESBL
n.s.	27	n.s.	<i>E. coli</i>	R	R	R	R	R	S	R	R	S	ESBL
n.s.	36	n.s.	<i>E. coli</i>	S	S	R	S	R	R	R	R	S	not clear
				V	V	R	V	V	S	R	R	S	ESBL
			<sup>g</sup> <i>E. coli</i> and Klebsiellae	R	R	R	R	R	R	R	R	S	AmpC
				R	V/R	S	V	R	S	R	S	S	K1, ( <i>K. oxytoca</i> )
				V	R	V	R	R	S	R	R	S	CTX-M

<sup>a</sup> Site of sample drawing: P-Department of Pediatrics, S-Department of Surgery, Gy-Department of Gynecology, Ga-Department of Gastrology, N-Department of Nephrology at Zadar Hospital, Zadar Croatia; n.s. = no specification.

<sup>b</sup> Isolate No.

<sup>c</sup> Sample type: w. swab - wound swab, v. swab - vaginal swab, n.s. = no specification

<sup>d, e</sup> Species identification and ESBL screening were performed at the RBK using an automated microdilution test system (WalkAway 5105, MicroScan, Neg Breakpoint Combo Panel Type 30). AZT-Aztreonam (R > 16 µg/ml, S <= 8 µg/ml, I = 16 µg/ml), CAX-Ceftriaxone (R > 32 µg/ml, S <= 8 µg/ml, I = 32 µg/ml), CAZ-Ceftazidime (R > 16 µg/ml, S <= 8 µg/ml, I = 16 µg/ml), CFT-Cefotaxime (R > 16 µg/ml, S <= 4 µg/ml, I = 16 µg/ml), CFX-Cefoxitin (R > 16 µg/ml, S <= 8 µg/ml, I = 16 µg/ml), CRM-Cefuroxime (R > 32 µg/ml, S <= 16 µg/ml, I = 32 µg/ml), CPD-Cefpodoxime (R > 4 µg/ml, S < 4 µg/ml) CAZ<sup>1</sup>-Ceftazidime (R > 1 µg/ml, S < 1 µg/ml), IMP-Imipenem (R > 8 µg/ml, S <= 4 µg/ml, I = 8 µg/ml)

<sup>f</sup> Enzyme type defined by antibiogram according to Livermore et al. (see g)

<sup>g</sup> Antibiogramm of Klebsiellae and *E. coli* with potent beta-lactamases, R-resistant, S-Susceptible, V-variable with type and amount of enzyme, see Livermore et al. (97)

**Table 14.** Phenotype-genotype correlation of samples collected in Croatia

Isolate No.	Species	Phenotype <sup>a</sup>	Genotype( <i>bla</i> <sub>TEM</sub> or <i>bla</i> <sub>SHV</sub> ) <sup>b</sup>		
		Enzyme	TEM-array	SHV-array	
1	<i>K. pneumoniae</i>	ESBL	TEM-116	SHV-1	SHV-5
4	<i>K. pneumoniae</i>	ESBL	TEM-116	SHV-1	SHV-5
5	<i>K. pneumoniae</i>	ESBL	TEM-116	SHV-1	SHV-5
6	<i>K. pneumoniae</i>	ESBL	TEM-116	SHV-1	SHV-5
7	<i>K. pneumoniae</i>	ESBL	TEM-116	SHV-1	SHV-12
8	<i>K. pneumoniae</i>	ESBL	TEM-116	SHV-1	SHV-5
11	<i>K. pneumoniae</i>	ESBL	TEM-1	SHV-1	SHV-12
12	<i>K. pneumoniae</i>	ESBL	TEM-1	SHV-1	SHV-12
13	<i>K. pneumoniae</i>	no ESBL	TEM-116	SHV-1	
14	<i>K. pneumoniae</i>	ESBL	TEM-116	SHV-1	SHV-5
16	<i>K. pneumoniae</i>	ESBL	TEM-116	SHV-1	SHV-5
19	<i>K. pneumoniae</i>	ESBL	TEM-116	SHV-1	SHV-5
20	<i>K. pneumoniae</i>	ESBL/AmpC	TEM-1	SHV-1	SHV-12
25	<i>K. pneumoniae</i>	ESBL	TEM-116	SHV-1	SHV-5
28	<i>K. pneumoniae</i>	ESBL	TEM-116	SHV-1	SHV-5
29	<i>K. pneumoniae</i>	ESBL	TEM-1	SHV-1	SHV-12
30	<i>K. pneumoniae</i>	ESBL	TEM-116	SHV-1	SHV-5
31	<i>K. pneumoniae</i>	ESBL	TEM-116	SHV-1	SHV-5
32	<i>K. pneumoniae</i>	no ESBL	TEM-116	SHV-1	
33	<i>K. pneumoniae</i>	ESBL	TEM-116	SHV-1	SHV-5
34	<i>K. pneumoniae</i>	ESBL	TEM-116	(SHV-1	SHV-5)
35	<i>K. pneumoniae</i>	ESBL	TEM-116	SHV-1	SHV-5
2	<i>K. ornithinolytica</i>	CTX-M	TEM-1		
9	<i>K. terrigena</i>	ESBL	TEM-116	SHV-1	SHV-5
26	<i>K. oxytoca</i>	K1	TEM-116		
3	<i>E. coli</i>	ESBL	TEM-1		SHV-12
10	<i>E. coli</i>	ESBL	TEM-116		SHV-5
15	<i>E. coli</i>	ESBL	TEM-116		SHV-5
18	<i>E. coli</i>	ESBL	TEM-116		SHV-5
21	<i>E. coli</i>	no ESBL	TEM-116		
22	<i>E. coli</i>	ESBL	TEM-116		SHV-5
23	<i>E. coli</i>	ESBL	TEM-116		SHV-5
24	<i>E. coli</i>	ESBL	TEM-116		SHV-5
27	<i>E. coli</i>	ESBL	TEM-1		
36	<i>E. coli</i>	not clear	TEM-1		

<sup>a</sup> Phenotype: Phenotypic resistance detection was performed at the RBK using an automated microdilution test system. Enzyme type definition by antibiogram according to Livermore et al. (97) (see also table 13). <sup>b</sup> Genotype was determined by TEM- (n = 9) and SHV-array (n = 6) analysis (except for SHV genotype of isolate No. 34) and was confirmed by standard DNA sequencing.

### 3.4 Ongoing developments

#### 3.4.1 Transfer of the TEM-array to a marketable array format

Through the cooperation partner Eppendorf Array Technology (EAT, Namur, Belgium) an alternative not disclosed immobilization method and labeling technique was available, which would allow the development of a marketable ESBL chip. As a proof of concept for the feasibility of the transfer of the developed TEM- or SHV-array to the EAT proprietary format a small subset of probes used for the TEM-array was immobilized on the EAT array format and hybridized with different amounts (25-150 ng) of biotinylated *bla*<sub>TEM-116</sub> target DNA. The hybridized targets were detected using fluorescence and silver based (1) post-labeling techniques.

In figure 66 some of the resulting fluorescence and silver images are displayed. Perfect match positions of all probe sets could be identified correctly with both systems. The resulting net fluorescence signal intensities are also displayed in figure 66 a and b. The detected signal intensities and the discrimination efficiency on the new format after fluorescence labeling were decreased compared to the currently used system. The silver labeling resulted in visibly enhanced signals compared to the fluorescence labeling, although six times less target DNA was used. It has to be noted that the quantified data resulting from the fluorescence and silver labeling process were not directly comparable, since different detection systems (for detection of transmitted light or emitted fluorescence) had to be used. The overall discrimination of the perfect matches towards the mismatches was in case of the silver staining drastically reduced and high background signals were observed. However, in principle SNP detection was possible with both formats, but further optimization is needed.



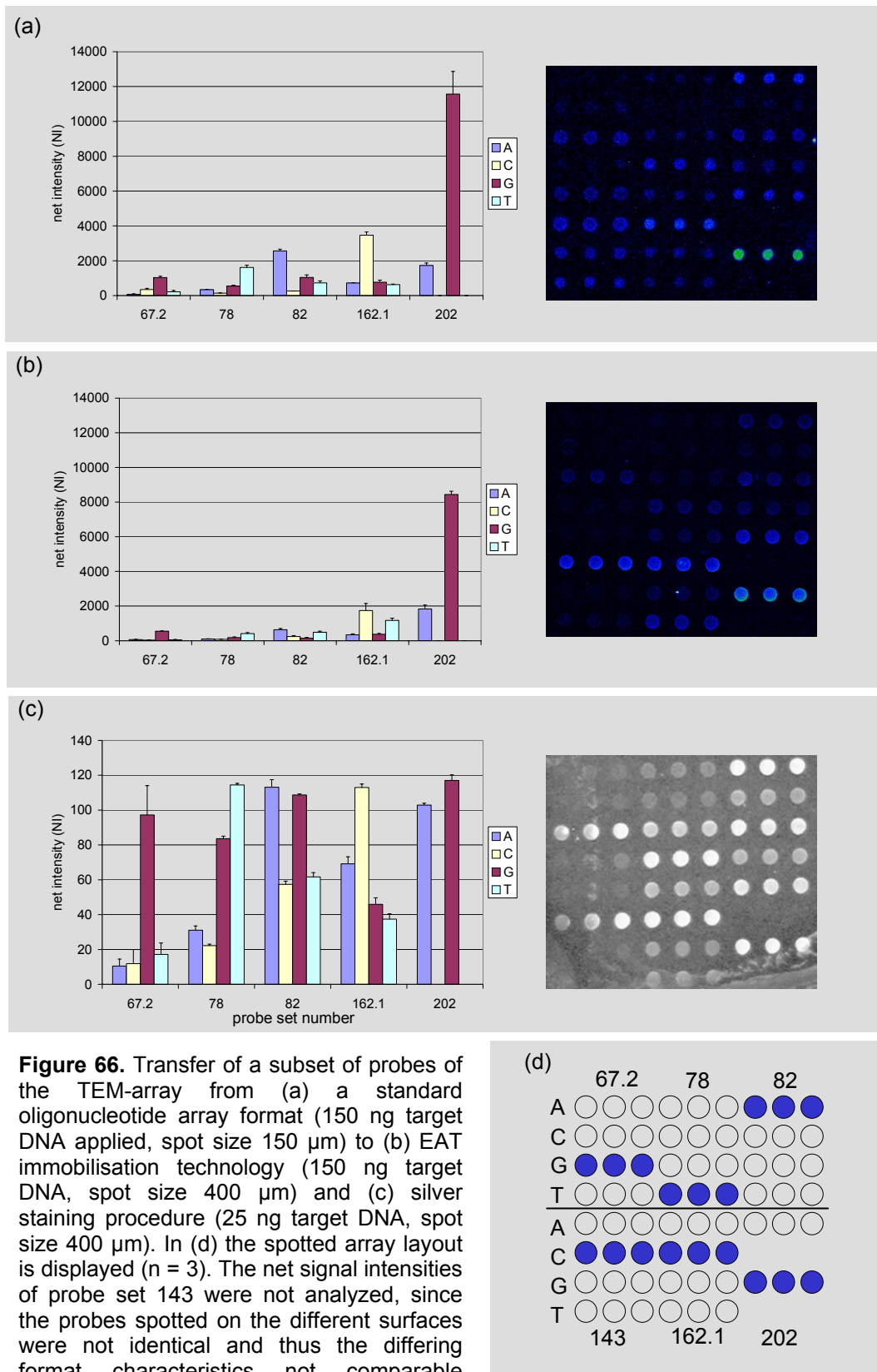


**Figure 66.** Transfer of a subset of probes of the TEM-array from (a) a standard oligonucleotide array format (150 ng target DNA applied, spot size 150  $\mu$ m) to (b) EAT immobilisation technology (150 ng target DNA, spot size 400  $\mu$ m) and (c) silver staining procedure (25 ng target DNA, spot size 400  $\mu$ m). In (d) the spotted array layout is displayed ( $n = 3$ ). The net signal intensities of probe set 143 were not analyzed, since the probes spotted on the different surfaces were not identical and thus the differing format characteristics not comparable regarding this probe.

## Results

### 3.4.2 Link of the resistance to the pathogenic bacteria

The assignment of the resistance to the pathogenic bacteria is a crucial step during resistance analysis, because otherwise the occurrence of resistance traits of a non pathogenic organism could result in errors in treatment. In a proof of principle experiment *Escherichia coli* were enriched from a urine sample by hybridization to species specific polynucleotide probes, which were subsequently immobilized in microtiterplate wells. Afterwards a PCR reaction with TEM-specific primers was carried out. These steps were performed by Kathrin Fichtl (Department of Microbiology, Technical University of Munich). At our institute the generated amplicon was used as a template in a labeling PCR and the resulting product was analyzed on the TEM-array. The identification of a TEM-1 resistance gene by array analysis was successful. The corresponding fluorescence image is displayed in figure 67. All analyzed perfect match positions were correctly identified (except probe set 122, which was not correctly spotted) within the predefined limits by calculation of the relative intensities as displayed in figure 68. Thus, a resistance detection by TEM microarray analysis after a species specific enrichment by polynucleotide probes was shown in this experiment. This experiment delivers the proof of principle, that the culture dependent and therefore time consuming preisolation step can be replaced by a molecular enrichment method.

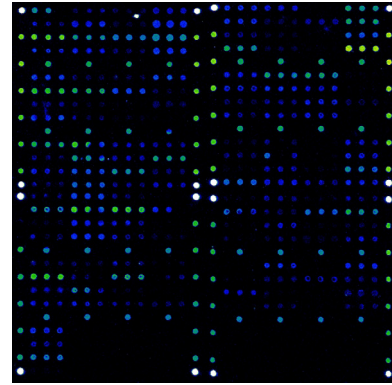


**Figure 67.** Fluorescence image of an identification of  $bla_{TEM-1}$  originating from a specific enrichment of *E. coli* from a urine sample.

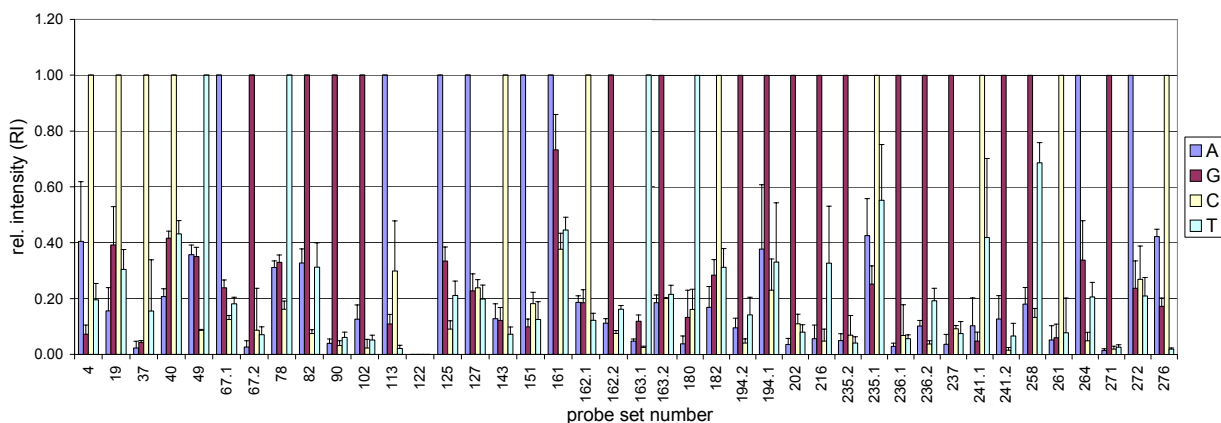


**Figure 68.** (a) Relative intensities of  $bla_{TEM-1}$  target DNA originating from a specific enrichment of *E. coli* from a urine sample ( $n = 6$ ). The four probe sets are indicated by their central base (A, G, C, T) in the legend. The labeling efficiency of the hybridized sample DNA was 178 NT/F; 200 ng of target DNA was applied. Probe set 122 was not analyzed, since it was not correctly spotted.

## 4 Discussion

The increased occurrence of microorganisms, which are resistant to commonly used antibiotics, enhances the need for a faster diagnostic and a strict monitoring of the spread of resistances throughout the hospital and the community. In average the phenotypic standard methods of resistance detection take two to three days, before a resistance profile is provided. This situation is unacceptable regarding the current resistance situation. The resulting empiric antibiotic treatment is one of the major causes of the further development and spread of resistances. Therefore, new strategies allowing a predictive diagnostic in contrast to a retrospective one for an early and accurate resistance detection and monitoring have to be developed. The molecular antibiotic resistance tests devised in this study target a group of the clinically most relevant and problematic resistances: the extended spectrum beta-lactamases. These enzymes are especially difficult to detect with phenotypic standard methods. The emphasis of this work was to develop a method allowing the sensitive and specific detection, identification and monitoring of the majority of the numerous resistance traits causing the ESBL and IRT phenotype. Furthermore, this test system should be fast, reliable and manageable in a clinical diagnostic laboratory.

### **4.1 Phenotypic resistance tests**

Phenotypic tests are still the standard method of resistance detection, since they are cost-effective, applicable for the detection of a wide range of antibiotic resistances caused by different mechanisms and test the microorganisms directly regarding their *in vitro* activity against the antibiotics most commonly used to treat those infections. On the one hand the spectrum of detectable resistances in phenotypic screening tests is broad, on the other hand the lack of a specific identification of the responsible resistance trait makes a closed monitoring of emerging or spreading resistances and the underlying mechanisms impossible. The results obtained by the commonly applied agar diffusion tests used in clinical routine diagnostic rely on subjective interpretation of growth inhibition zones, requiring experienced personnel. Misinterpretation can still occur and result in treatment failures (95,97). Furthermore, some resistances might remain undetected for example for uncultivable organisms or if an inappropriate selection of antibiotics or a too low inoculum is used to perform the test. Low-level-expression of the resistance gene or the expression of resistance genes, which mask effects of another resistance are also disadvantageous for detection. A major drawback is also the need for preisolation and cultivation of the bacteria, which prolongs the analysis time. Automated broth microdilution methods such as the MicroScan (Dade MicroScan, West Sacramento, US), Vitek (bioMérieux, Nürtingen, Germany) or BD Phoenix (Becton Dickinson, Heidelberg, Germany) for speeding up the cultivation and resistance testing have been developed, but these analyses still need a preisolation and up to 9 to 11 h of analysis time (39,93,137,138). Since serious infections have to be treated as early as possible, the antibiotic treatment often has to start before the resistance is unequivocally identified. Due to this fact the current phenotypic antibiotic resistance diagnostic is more retrospective than predictive. To avoid treatment failures more extended spectrum antibiotics are prescribed than necessary, which enhances the development of new resistances.

## Discussion

---

In case of the detection of enterobacteriaceae producing ESBLs the standard phenotypic tests have several pitfalls, which have to be considered. An ESBL does not always increase the MICs to levels high enough to be called resistant by NCCLS interpretive guidelines. A variety of cephalosporins has to be tested, otherwise about one third of the organisms might be reported to be susceptible in broth microdilution and disc diffusion tests, although carrying an ESBL-type beta-lactamase (42,70). Furthermore, the MICs of most cephalosporins increase dramatically, when the inoculum is raised in susceptibility tests (108). These effects can lead to susceptible test results *in vitro*, whereas *in vivo* the infection is not stopped, if treated with the false negatively tested antibiotic.

Several studies evaluated the reliability of the current phenotypic ESBL detection methods. The test methods included disc diffusion methods as well as automated broth microdilution testing. Errors were encountered with both automated and disc diffusion methods. In a survey of 38 laboratories in Connecticut in 1999 only 18 % of the tested institutions categorized at least one of the four tested isolates (one AmpC and three ESBL) as potential ESBL producers (163). In 2000 a proficiency test assessing the ability of hospital laboratories participating in the project ICARE (Intensive Care Antimicrobial Resistance Epidemiology) to detect specific types of antimicrobial resistances, it was reported, that up to 58 % of the laboratories failed to detect and report ESBL isolates correctly (158). In a study conducted by the WHO in 2001, 130 laboratories were tested with a TEM-3 producing *Klebsiella pneumoniae* challenge strain. 5.4 % of the tested laboratories using disc diffusion tests reported this strain to be susceptible to all cephalosporins. Only two of 130 laboratories specifically reported the isolate as an "ESBL producing strain" (164).

Apart from the need for a reliable prescreening method, also the ESBL confirmatory methods pose an important issue. In an evaluation of the NCCLS ESBL confirmation methods for *E. coli* in 2003 with isolates collected during the project ICARE it was determined, that after a prescreening according to NCCLS criteria, it is indispensable to perform additional confirmatory methods for ESBL detection, since otherwise a large percentage of false resistance results was reported. In this study only 16 % of 131 *E. coli* isolates identified as potential ESBL producers by the NCCLS screening criteria were confirmed as ESBL producers. Changing the interpretation of extended-spectrum cephalosporins and aztreonam results from the susceptible to the resistant category after prescreening, without confirming the presence of an ESBL phenotype, would lead to a large percentage of false resistance results and is not recommended. However, 45 % of the false-positive results were due to a cefpodoxime MIC screening breakpoint of 2 µg/ml, by increasing the breakpoint to 8 µg/ml, these false-positive results could be eliminated. NCCLS has incorporated this change in the cefpodoxime screening breakpoint in its recent documents (165).

These reports confirm the dilemma of phenotypic ESBL detection. Infections with ESBL producing organisms in *E. coli* and *K. pneumoniae* are associated with significantly longer hospital stays and increased hospital costs (85). These facts in combination with the increased prevalence of ESBLs worldwide has prompted the search for more accurate tests to detect the presence of ESBLs in clinical isolates.

#### **4.2 Genotypic resistance tests**

Genotypic analysis of resistant microorganisms has the potential to offer a more rapid and reliable solution, providing an increased information depth for antimicrobial resistance testing than the conventional susceptibility methods. The advantages of a genotypic resistance analysis are the following. (i) The test can in principle be performed directly starting with DNA isolation from clinical samples without the need for preisolation or cultivation of the bacteria. (ii) Genotyping is faster, especially regarding tests of slow growing organisms. (iii) Even uncultivable organisms can be assessed. (iv) The risk of propagation of the pathogenic organisms due to prolonged exposition of laboratory personal to bacterial cultures is minimized. (v) Resistances are detectable genotypically even if their phenotypic pattern is not conclusive due to a not induced state, low-level expression, masking phenotypes, inoculum effect, etc.. (vi) Genotypic test results can be more objective through *in silico* data analysis than comparable phenotypic methods relying on visual determination of growth inhibition zones.

However, genotypic analysis also has several potential drawbacks compared to conventional phenotypic analysis (30). (i) They might lack sensitivity if only few organisms are present in a higher volume of clinical sample. This problem can be solved by appropriate concentration methods. (ii) Due to low multiplexing capability of some genotypic methods, a separate test has to be developed for each tested resistance trait. (iii) Resistance can be caused by different mechanisms and a wide variety of genes or single nucleotide polymorphisms. Therefore, the development of a genetic test targeting a specific resistance problematic might turn out to be very complex. (iv) The detection is usually limited to specifically targeted and thus known resistances, so emerging resistances might remain undetected. This problem might also occur in case of the phenotypic analysis, if resistances emerge with a substrate spectrum widely differing from the conventionally tested ones. (v) The molecular background of some antibiotic resistance mechanisms might still be unknown. (vi) Genotypic testing might not differentiate between low-level and high-level expression and therefore between clinical relevance or irrelevance of the resistance. (vi) False positive results might occur due to the presence of nonpathogenic organisms which might carry a resistance gene or due to contamination of the sample prior the nucleic acid amplification step. (vii) No standards exist so far for performing molecular methods for resistance detection. (viii) Clinical trials to assess the accuracy, reproducibility and utility of these methods were only conducted for few of these tests. (ix) Genotypic tests are usually more expensive compared to standard dilution or disc diffusion tests.

#### **4.3 Methods for molecular ESBL detection**

One of the first methods for molecular detection of different ESBL variants was the determination of the isoelectric point of the enzymes. This procedure is labour intensive and not specific enough, since at the present time multiple variants with similar isoelectric points are observed. The use of oligonucleotide probes for the detection of different TEM variants was first described in 1988 for discrimination between TEM-1 and TEM-2 (120), in 1990 for TEM-1, TEM-3 and TEM-6 (166) and in 1991 for discrimination of TEM-1 to TEM-7 (101). These probes were labeled with radioisotopes or biotin and were used in southern blotting or in colony hybridization experiments. The combination of different hybridization patterns from the 12 radiolabeled primers developed by Mabilat and Courvalin allowed the identification of

## Discussion

---

previously unknown enzyme variants with a novel combination of known polymorphisms (101). However, southern blotting and colony hybridization experiments are time-consuming and restricted to the analysis of a limited number of features, since multiple separate hybridization reactions have to be performed. Radioactively labeled intragenic fragment probes were also used in colony hybridization experiments to differentiate between different beta-lactamase families such as TEM or SHV, but these probes were not specific for the identification of polymorphisms leading to an extended substrate range (5).

Another approach for the detection of different ESBL variants is the analysis of restriction fragment length polymorphisms in combination with PCR (PCR-RFLP). After amplification by PCR the generated amplicons are digested by restriction enzymes, producing different fragment lengths due to the presence or absence of a restriction site caused by a mutation. The fragment sizes are then analyzed by agarose gel electrophoresis. Thereby a limited number of different TEM or SHV ESBL variants could be detected (4,119). The major limitation of the RFLP method is the requirement of polymorphisms in specific restriction sites. It is impossible to find an analyzable feature for each relevant mutation position, thus numerous TEM or SHV variants can not be detected by this method (26). Additionally the resolution of different fragment lengths by agarose gel electrophoresis is limited. Furthermore, restriction length polymorphism can also be caused by a silent mutation and therefore false interpretation of the results can occur.

The analysis of single strand conformational polymorphisms (PCR-SSCP) was also applied for characterization of ESBL variants. After amplification of the target region and restriction with a restriction enzyme the fragments are denatured and analyzed on a polyacrylamide gel. This method allowed the detection of 12 different inhibitor resistant TEM variants (155) and six different SHV variants (100,114). The simultaneous detection of different SHV-types within one strain also was possible. However, some mutations leading to different variants are difficult to differentiate, hence the resolution of this method and the specificity of the discrimination is limited.

To increase the spectrum of detectable SHV variants a combination of PCR-SSCP and PCR-RFLP was described by Chanawong et al. (25). It theoretically allowed the discrimination of up to 17 SHV variants. After digestion with two different restriction enzymes the genes could be differentiated by the aforementioned methods. Although the combination of these methods was applicable to the identification of a wider range of variants, the problem of a limited detectable and differentiable variant spectrum of the assay persists. The same group developed a restriction site insertion PCR to extend the identification of SHV beta-lactamases by the aforementioned methods (26). Hereby the amplification primers were designed to create a restriction site specific to *bla*<sub>SHV-1</sub> at five different restriction sites. If a mutation was present, the amplified fragments could not be digested by the endonucleases and displayed a restriction pattern differing from *bla*<sub>SHV-1</sub> in the agarose gel electrophoresis. However, the resolution of the differing fragment sizes in the displayed results was not very high, so that correct interpretation of the results might be difficult. Furthermore, the primer design was not applicable for all mutation positions and a combination of the different methods as suggested by the authors is not really appropriate for the application in clinical microbiology laboratories.

The use of the ligase chain reaction (LCR) has also been described for SHV detection. Niederhauser et al. described the detection of the glycine to serine mutation at Ambler position 238 by the use of two adjacent oligonucleotides, which contained template independent tails (117). After the ligation reaction a PCR reaction was performed with two primers that match the tails of the oligonucleotides. The products were detected by agarose gel electrophoresis. It was shown that this method was very sensitive, since it allowed the detection of a point mutation in a background of 100,000 wild-type bacteria. Kim et al. described a LCR method for the detection of four different mutation positions (79). The LCR product was detected by an enzymatic reaction using NADPH-alkaline phosphatase in a microtiterplate format.

Real time PCR and melting curve analysis was applied by Randegger et al. for the detection of three SHV polymorphism positions relevant for the ESBL phenotype (129). This assay applies fluorescently labeled oligonucleotide hybridization probes. Mutations are differentiated by the detection of diverging melting profiles. This assay allowed a rapid and sensitive discrimination between SHV ESBL and non-ESBL type beta-lactamases and the categorization of SHV ESBL producers in three phenotypically relevant groups.

A minisequencing-based assay for the discrimination of SHV ESBL or non-ESBL type beta-lactamases was reported by Howard et al (64). The method interrogates two polymorphic ESBL relevant sites through primer annealing immediately upstream of the polymorphic site followed by a primer extension reaction and determination of the identity of the incorporated base.

Nucleotide sequencing remains so far the standard for determination of the specific beta-lactamase gene present in the isolate. However, results can still vary depending on the method used (15) and the presence of more than one gene variant is also difficult to detect by this method. Furthermore, this method is still time-consuming and technically demanding for high throughput screening purposes.

A major drawback of most of the aforementioned methods remains the application of agarose gel electrophoresis for detection of the different gene variants. They are therefore difficult to adapt to automation and high throughput analysis. The detection in a microtiterplate format increases the throughput, but for all reported methods so far the number of simultaneously analyzable polymorphisms was limited. Thus, not all polymorphisms relevant for identification of the numerous variants were detected and only a minor number of TEM or SHV variants could be discriminated. A genotyping assay detecting the majority of the relevant mutation positions for TEM or SHV-type beta-lactamases for rapid high throughput analysis has - to our knowledge - not been described up to date. DNA microarray technology offers in contrast to most other genotypic methods the possibility to analyze a high number of features simultaneously. All resistance and variant specific mutations can be identified, so that a conclusion about the substrate spectrum and the responsible genotype can be drawn. Only this makes a closed monitoring of spreading resistances possible.

#### **4.4 DNA microarrays for molecular resistance detection**

Due to the urgent need for faster and more precise test methods for species identification and antimicrobial resistance detection for clinical microbiology diverse DNA microarrays were already described. Troesch reported in 1999 the development of an allele specific high density DNA probe array for the identification of Mycobacterium species and mutations in *rpoB*, which are responsible for rifampicin

resistance (171). Mikhailovich also reported an assay for the identification of mutant variants of the *rpoB* gene in *Mycobacterium tuberculosis* strains (110). Here allele specific hybridization, PCR and ligase detection reaction on oligonucleotide chips were applied. A microelectronic chip array for the detection of diverse resistances in *E. coli*, Salmonella, Campylobacter, Staphylococcus and Chlamydia was described by Westin et al. (179). DNA microarrays for detection of quinolone resistant *Neisseria gonorrhoeae* (14) or *E. coli* (183) have also been described. Volokhov et al. reported a microarray for the analysis of erythromycin resistance in Staphylococcus and Streptococcus species (175).

DNA microarrays allowing the detection of beta-lactamase resistance genes were only reported twice so far. Call et al. developed an oligonucleotide DNA microarray for the detection of tetracycline resistance genes in *E. coli* (22). This array also contained one probe specific for *bla*<sub>TEM-1</sub>. Lee et al used spotted PCR products for detection of various beta-lactamase genes (PSE, OXA, FOX, MEN, CMY, TEM, SHV, OXY, AmpC) (88). ESBL or non-ESBL variants could not be identified and discriminated with these arrays, since the detection of the single nucleotide polymorphisms relevant for the discrimination of the different phenotypes and variants was not possible. The genotyping arrays developed in this work fills this gap for the identification and discrimination for 96% of the TEM and 100% of the SHV variants known up to date.

### 4.5 Implementation of the system

To produce oligonucleotide microarrays for a reproducible, specific and sensitive analysis, the surface for immobilization, the spotting technique and buffer, as well as the method of probe immobilization have to be carefully chosen (12). However, also the budget for the numerous experiments necessary for implementation of the system has to be considered. Therefore, in the beginning the most cost-effective alternatives were tested.

It was reported that unmodified oligonucleotides can be efficiently immobilized without compromising hybridisation efficiency (23). Hence, the system was first implemented on low-priced poly-L-lysine slides, which allow to immobilize oligonucleotide probes without an amino-modification or spacer. This undirected immobilization of the oligonucleotide probes is done via the formation of a covalent bond between a base from within the probe sequence to the surface (see section 1.3.4.3). A DMSO-based spotting buffer was chosen, since it was reported that this buffer provides uniform spot shapes and allows long spotting rounds, because of low evaporation rates (12).

However, after hybridization of the target on the poly-L-lysine slides the observed signal intensities were low and the spot shapes irregular. Furthermore, multiple failures of experiments due to high background signal intensities occurred. The low signal intensities and irregular spot shapes resulted in high standard deviations of up to 68 % in between signal intensities of replicate spots. The regularity of the spot shapes depends on the spotting equipment and process, the surface, the spotting buffer and the spotting parameters, such as surrounding humidity (27). Since the surrounding humidity could be monitored during spotting and remained constantly at 54 %, it was assumed that the spotting buffer and the chosen surface were mainly responsible for the varying spot shapes. Another possible source of variation was the



use of different pins to spot the replicate spots. To avoid variation inherent in the spotting process with multiple pins replicate spots should be spotted with the same pin (12).

The most probable reasons for the overall low signal intensity were either a low immobilization or hybridization efficiency of the probes. The surface density of the probes obtained in the immobilization procedure is an important parameter of the system. A low surface coverage can result in low hybridization signals. Conversely, high surface densities might result in steric interference, impeding access to the target DNA strand (55,125). The hybridization efficiency of the target DNA to the immobilized oligonucleotide probes is influenced by several parameters. The binding capacity of the surface bound probes, secondary structure of the target DNA (151), the position of the short capture probe on the target nucleic acid (127), as well as steric interactions are important. Steric hindrance is influenced by the probe density, spacer length, as well as hydrophobicity and charge of the solid support (28). The steric hindrance is enhanced, the closer the target sequence has to hybridize to the surface (126). Since in an undirected immobilization of the capture probes the surface is very close, an increased steric hindrance could occur resulting in low hybridization yields.

Consequently, due to the observed low reproducibility and sensitivity of the microarray analysis on the poly-L-lysine support, the immobilisation chemistry and the spotting process had to be reviewed. Therefore, a new surface in combination with various spotting buffers and a new spotting strategy was tested to determine whether (i) the used unmodified oligonucleotide probes were the major cause of low hybridization efficiency or (ii) if the surface characteristics of the poly-L-lysine support were responsible for an inefficient immobilization and uneven background intensities, and (iii) if the variability could be reduced by changing the spotting strategy and buffers. Slides coated with epoxy groups were therefore tested with three different spotting buffers and replicate spots were spotted with the same pin. These parameters had a major effect on sensitivity and reproducibility. No unfavorable background effects were observed as with the previous system, which was attributed to a higher quality of the surface. By using a phosphate based spotting buffer the reproducibility of spot shapes and the regularity of the signal distribution within the spot was generally improved. The net signal intensities after hybridization were increased about more than three times, although target DNA with less fluorescence label was applied. This was an indication of most probably an enhanced immobilization efficiency and/or better accessibility of the probes on the epoxy surface. The combination of a new spotting strategy, surface and buffer led to a reduction of the mean variability in between replicate spots from 68 % on one array to 18 % in between three arrays.

## **4.6 Probe design and performance**

### **4.6.1 Sequence analysis**

The occurrence of extended spectrum beta-lactamases was reported since 1985 (171) and since then the number of registered amino acid exchanges with a potential influence on the substrate spectrum grew rapidly. To standardize the nomenclature of the new beta-lactamase variants Bush and Jacoby created a data base registering all naturally occurring ESBL conferring and related enzymes and their amino acid exchanges versus TEM-1 or SHV-1 (<http://www.lahey.org/Studies/>). Usually the

corresponding nucleotide sequences are available in GenBank, but sometimes only the amino acid exchanges are published. First steps of this work were to align all available nucleotide sequences of the classified TEM or SHV variants, to identify and confirm the mutation positions and to combine amino acid and nucleotide exchange information.

Many of the substitutions affect enzyme structure and activity and lead to the widely differing substrate spectra of the numerous variants. However, there are also substitutions for which no functional change is currently evident, but most enzymes will have been sequenced because of a change in properties, and these substitutions might still affect the interaction with a future substrate or inhibitor (51). Furthermore, the concept of this array was to provide a tool for the identification and detection of all the known TEM or SHV variants and not merely the classification in ESBL, non-ESBL or IRT categories. Therefore, even substitutions which do not alter the substrate spectrum are considered as useful epidemiological markers and were included in the design of the probe set. Thus, the developed arrays should allow a monitoring of the occurrence of TEM or SHV gene variants and the consideration of a predetermined substrate spectrum of previously characterized enzymes for treatment options.

DNA arrays allow the simultaneous detection of a high number of features. However, the analysis is still limited to amplifiable sequences. In the case of this work, the regions which sequences matched the primer sequences could not be included in the genotyping test, resulting in the exclusion of the ability to detect TEM-97, -98, -99, -102. TEM-108, which also shows point mutations in the primer specific regions, could theoretically be identified by the SNPs at position 194.2 and 78. The four other TEM variants are seldom described and may be considered as exceptional or endemic variants (S. Fanning and coworkers have directly submitted the TEM-97, -98, -99, and -108 to GenBank, which can be found under accession numbers AF397066, AF397067, AF397068, and AF506748, respectively). For TEM-87 and -92 the mutation at amino acid exchange position 4 is not detectable, since the probe set 4 included on the array is overlapping the sequence of the currently used primer set. However, these variants also carry other mutation positions, which can be detected with the presented array (see also table 3). The design of a different primer set outside the open reading frame (ORF) to circumvent the problematic of the detection of end-standing SNPs was presently not advisable, since for a considerable part of the published TEM variants no ORF flanking sequences are available. Methods to circumvent the problem arising from the consensus primer regions still have to be investigated and create the need for alternative amplification strategies.

### 4.6.2 Performance analysis

An important premise for the probe sets developed for a SNP detection microarray is an equal hybridization efficiency of all capture probes under the applied hybridization conditions (55). Therefore, the probes should have similar melting temperatures, similar lengths and as little secondary structures as possible (12). To design a probe set for all relevant SNP positions, sometimes a compromise between these parameters had to be found to achieve similar hybridization efficiencies. For example, to avoid unfavorable secondary structures, some probes were designed shorter resulting in lower melting temperatures, or some probes had to be designed longer to gain sensitivity. However, although algorithms for calculating probe parameters, such as melting temperatures and secondary structures facilitate probe design *in silico*, the probes have to be optimized empirically after the theoretical

probe design, since certain target DNA effects have already been identified (127), but remain difficult to predict for probe design.

Although the probes for the TEM-array were not immobilized in a directed way, all polymorphisms could be identified correctly with a good mismatch to perfect match discrimination efficiency. Even though some perfect match probes had an unfavorable secondary structure in comparison to the mismatch probes, the perfect match probes were accessible enough for the hybridization of the target sequence to yield a specific perfect match detection signal. Generally, no distinct linkage between optimal probe design parameters and optimal discrimination and performance could be determined for the TEM-array probe sets. This might be due to the fact that the undirected immobilization and the proximity of the surface (since no spacer was used) further influenced the accessibility of the probes, so that secondary structures might not have the impact as determined by  $\Delta G$  values, which were calculated for hybridization in solution. Solid-phase hybridization is a more complex process than solution hybridization (90). The aforementioned assumptions are also supported by a study from Peterson and coworkers (126). In this study it was determined that hybridization for surface immobilized DNA is quite different from the well-studied solution-phase reaction. Surface hybridization strongly depended on the target sequence and probe density. Steric crowding at high probe density had a negative influence on the hybridization efficiency. Furthermore, it was shown that hybridization kinetics were slower, the closer the hybridization of the target sequence to the probe sequence occurred to the surface. This was explained by the fact that the target must penetrate into the probe DNA film before hybridization can take place. These steric effects also have to be considered in case of the indirectly immobilized probes used on the TEM-array.

In case of the SHV probe sets amino-modifications were applied for a directed immobilization and spacers were used to achieve a higher hybridization efficiency through increased accessibility (55,144,151). The extension of the distance between the surface and the probe sequence led to an approximation of the hybridization conditions to a hybridization in solution. Generally, the predetermined parameters of the probe design of the SHV-array probe set were more concordant with the detected hybridization results of the designed probes than observed for the TEM probe set. The results of an incorrect perfect match identification or a weak perfect match to mismatch discrimination efficiency could usually be ascribed to a more stable secondary structure of the perfect match probe in comparison to the mismatch probe - as determined during probe design. It is well known, that secondary structures can lead to a diminished accessibility of the capture probe to the target DNA (111,112). The resulting decreased hybridization efficiency of the perfect match probe is unfavorable for a clear perfect match/mismatch discrimination. However, there were also exceptions from the observation that secondary structure had an unfavorable effect on hybridization efficiency. The greatest difference in  $\Delta G$  values in the whole SHV probe set between the perfect match and the mismatch probes secondary structure was observed for probe 202 with a difference of the  $\Delta G$  values of - 9.1 kcal/mol. Nevertheless, the discrimination of the perfect match was distinct. It could not be determined why less stable probe secondary structures were in some cases more unfavorable towards discrimination efficiency than in case of probe 202. As mentioned before, the sequence context of the target DNA might play also a role (127).

### 4.6.3 *New probe design strategy*

For five SHV probe sets perfect match secondary structures led to high mismatch probe hybridization signals. Here a redesign of the probe sets was necessary. Since the bases forming the secondary structures were close to the central mismatch, a shifting or shortening of the probe sequence to avoid the secondary structure was not possible. Therefore, a new probe design concept had to be developed. In order to enhance specificity of polymorphism detection, enzymatic reactions (ligase detection reaction, primer extension) (170), structured DNA probes (13) (molecular beacons) or gold nanoparticle probes (161), have been developed. Unfortunately, all these approaches require new materials or complex processes and are not easily adaptable to the chosen allele specific hybridization format.

A simpler approach described by Guo et al. involves the introduction of artificial mismatches in the short oligonucleotide probes to enhance the discrimination of SNPs (56). They reported that the effect of the artificial mismatches on hybridization stability depends strongly on the relative position of the mismatches, with the greatest destabilization occurring with a centralized mismatch and a three to four base distance between the true and artificial mismatches. However, they introduced artificial nucleotides. Such probes are usually more expensive and not generally available from conventional suppliers. Lee et al. provided guidelines for designing non-perfectly matched probes by the introduction of mismatches using conventional nucleotides in order to increase the specificity of the target hybridization (86). Their data indicated that the position of the artificial mismatch is less significant than the identity of the nucleotides involved in the exchange, excluding the three positions at either end of a oligo probe with a length of 19 nucleotides. The mutation of a not centered G produced a significantly greater effect on hybridization efficiency than more centered mutations from A or T to G. However, their study was limited to properties in solution and in microarray analysis the distance from the mismatch to the solid support might also effect hybridization efficiency (126).

Both approaches were designed to generally improve probe specificity to inhibit cross hybridization. In this work additional mismatches had to be introduced to avoid the formation of unfavorable probe secondary structures in order to allow SNP identification at specific target DNA sites. Therefore, the choice of the nucleotide to be exchanged was very limited and the results of the aforementioned publications were not generally applicable for this purpose. An approach to release secondary structure by introduction of additional mismatches in oligonucleotide probes used for SNP detection has - to our knowledge - not been reported so far.

In case of four of five probes this design strategy proved to be successful. Although, as expected, the resulting net intensities were considerably diminished due to the steric hindrance of the additional mismatch, the resulting discrimination efficiency was generally increased, slightly in case of probe 125 and distinctively for probe 238. In case of probe 222 and 262 only the new probe version allowed the identification of the correct perfect match position. The decrease of the perfect match net signal intensities could be avoided by designing longer oligonucleotide probes, but as shown in case of probe 125, this also implies a higher probability of other secondary structure formation. Therefore, in this study the probes were, if possible, designed with a length identical to the first version.

For probe 39 the new probe design strategy could not generate an improvement, since here two highly stable dimer structures could be formed flanking the central polymorphism position in the probe sequence at either side. If one was resolved by introduction of a mismatched base, the other one persisted. Probes designed with one or two additional mismatches to resolve one or both of the dimer structures did not produce enough hybridization signal to discriminate the perfect match correctly. However, a specific differentiation between mutant and wild type SHV sequences was possible in spite of the unfavorable wild type probe secondary structure, since the mutant probe was well accessible and the observed hybridization patterns for the detection of a mutated versus a wildtype sequence were clearly distinguishable (see section 3.2.6).

In conclusion, the new probe design concept of releasing secondary structures by introduction of additional mismatched bases proved to be successful in the majority of the newly designed probe sets by increasing the specificity of the discrimination, but can not be applied to every problematic sequence, as shown in case of probe 39. Careful analysis of the different secondary structures and the loss of sensitivity through mismatch introduction have to be considered.

## **4.7 Array performance**

### **4.7.1 Discrimination efficiency**

The overall discrimination efficiency of allele specific hybridization array for SNP detection is depending on an almost equal hybridization efficiency of all used probes under the applied experimental conditions (55). Therefore, not only the probe design parameters, such as secondary structure (112) or melting temperature are important, but also the sequence context (151) and fragment length (78) of the target DNA, the immobilization strategy, hybridization and washing conditions as well as the hybridization time (55). To achieve similar hybridization efficiencies for a set of different probes interrogating specific SNP positions in an allele specific hybridization format is thus very complex and needs experimental optimization. Alternatively multiplex allele specific oligonucleotide hybridization reactions are performed using arrays carrying a highly redundant set of probes (31). However, these analyses are complex, laborious and expensive and are not applicable for clinical routine diagnostics. Furthermore, not all genotypes can be identified correctly, in spite of the complex analysis (29,178).

The diverse probe sets displayed different hybridization efficiencies, which could be observed by analysing the absolute signal intensities of the perfect matches in the proof of concept. The absolute signal intensities of the perfect matches exhibited a wide range from 1500 to 20000 for the TEM-array and 2400 to 46000 arbitrary units for the SHV-array. This was to be expected, since it is well known that probes with differing sequences display different hybridization behavior (151,154). However, all targeted polymorphism positions could be distinctively identified. The highest mismatch signal intensities reached only 52 % (TEM-array) or 67 % (SHV-array) of the perfect match signal intensity in these experiments. The identification of all tested *bla*<sub>TEM</sub> - or *bla*<sub>SHV</sub> - variants originating from reference strains was also shown. In all cases the differing nucleotides present at the polymorphism positions could be identified distinctively, because all intensities of the mismatches remained below a value of maximal 80 % of the perfect match signal intensity. Although the hybridization efficiency of each probe can be influenced by changing the

hybridization conditions, such as temperature or salt concentration, it was not possible to do this for each probe individually in the currently chosen microarray format, since here all hybridizations were carried out simultaneously in one hybridization compartment. A promising alternative would be to set the hybridization condition for each probe individually, which has already been shown in microarray systems using electric field control (41,150).

The measured hybridization signal in microarray experiments is time dependent (55). This due to the fact that the target DNA has to diffuse towards the probes. Mixing of the hybridization solution can therefore enhance the rate of hybridization (151). These parameters should hence also affect the discrimination level. A dependency of the discrimination level from the hybridization time and agitation level was clearly observed during the testing of the different hybridization devices and times. The efficiency of the mismatch to perfect match discrimination was analyzed by reviewing the distribution of all mismatches in dependency of the mismatch to perfect match ratio (the relative intensity of the mismatches,  $RI_{MM}$ ). The discrimination was the more efficient the lower the mismatch to perfect match ratio was. The better the discrimination level, the more the distribution of the relative intensity of the mismatches was shifted towards lower relative intensity values. Lower  $RI_{MM}$  values were observed for hybridizations under agitation or for longer incubation times. In comparison to that - at shorter hybridization times and without agitation - the maximum of the  $RI_{MM}$  distribution was shifted towards higher  $RI_{MM}$  values and the distribution approached a Gaussian standard distribution (see section 3.1.9.2). This observation proved that the discrimination level was depending on the number of meeting events between probe and target molecules. By increasing the number of meeting events by agitation or longer incubation times, the discrimination level was as expected enhanced.

Furthermore, a dependency of the discrimination level to the incorporation ratio of fluorescence label, the amount of target DNA and fragment sizes could be shown (for a detailed discussion see below).

### 4.7.2 Reproducibility

The reproducibility of the microarray analysis is an important premise for the development of a microarray as a diagnostic tool. Sources of variation are numerous in microarray experiments, starting from manufacturing of the array, to PCR amplification and labeling of the targets, to differences in hybridisation efficiencies of probes (12). The current state of the art provides 5 - 10 % variation in signal intensities among replicate array elements, and 10 - 30 % variation among corresponding array elements on different (self manufactured, cDNA) microarrays for expression analysis (157,185). Unfortunately a comparable evaluation study, evaluating variations in self manufactured oligonucleotide microarrays for genotyping purposes could not be found.

In this study the inter-array variation was determined in the proof of concept by calculation of the standard error of the relative mismatch intensities between three repetitive hybridizations of a *bla<sub>TEM</sub>* or *bla<sub>SHV</sub>* reference sample. The detected standard errors were between 0 - 12 % or 0 - 17 % respectively. However, 98 % (for TEM) or 92 % (for SHV) of the standard errors remained below 10 % variation among replicate relative intensities. To determine the inter-sample variation five *bla<sub>TEM-1</sub>* samples were analyzed, originating from different isolates, amplification

and fragmentation reactions. Although the overall net signal intensities after hybridization varied due to different incorporation ratios of fluorescent label from the different target DNA batches, the detected mismatch to perfect match ratios remained fairly reproducible with standard errors up to 21 %. Thus, it was determined that the observed inter-array and inter-sample variations were in the range of reported values for the current state of the technology. Therefore, the identification of the same genotype originating from differing samples was reproducible and a reliable detection of different genotypes was rendered possible with the presented microarray system.

Unexceptionally high variations in between replicate signal intensities, which were detected from time to time, were mostly attributed to problems of the spotting process. A problem occurring repeatedly during the microarray analysis was the misidentification of a perfect match caused by aberrations in the spotting process. These aberrations were identified by hybridization of one or more arrays of a produced slide batch to a known reference target. These positions were then excluded from the further data analysis. A complete exclusion of the concerned slides was generally not possible due to cost reasons. Multiple features of the contact printing process can be the cause of these spotting failures (27,102). Among the most frequent sources of error were the clogging of the split pin by dust particles or crystallized salt, the obstruction of the pin movement by contamination of the pin holder, the incomplete loading of the probe solution due to inhomogeneous well content, insufficient filling level or solution attached to the walls of the wells. Furthermore, aberrations on the slide surface can also inhibit probe deposition or attachment. Although extensive optimization regarding spotting protocols and preparation of the probe source plate were made, the sporadic occurrence of these spotting failures could not be excluded. An on-line monitoring of the probe deposition process and automatic exclusion or correction of erroneous arrays would be a necessary feature for the commercial production of microarrays for the use in clinical diagnostics.

### 4.7.3 Sensitivity

The sensitivity of the hybridization on the DNA microarray was determined regarding the necessary quantity of target DNA, which is needed for analyzing all perfect matches correctly. The amount of target DNA needed depends on multiple parameters: characteristics of the surface, such as background intensity and immobilization efficiency, nature, quantity and accessibility of the probe DNA, as well as target DNA characteristics, such as content of fluorescence label and fragment length, as well as the hybridization parameters and the signal detection method (27). Therefore, it is quite challenging to compare the results to other systems.

The sensitivity was determined testing the minimum amount of target DNA for two different incorporation ratios (87 or 166 NT/F), which is needed for a correct detection of all polymorphism positions of the TEM-array. The detection limit of the array was not fully exploited with the applied target DNA amounts, since even with the smallest amount tested (25 ng equivalent to app. 0.04 pmol) for both incorporation ratios all perfect matches could be discriminated from the mismatches. It has to be noted, that these results were obtained in a conventional cover slip hybridization for three hours. In comparable microarray experiments sensitivity limits of 0.125 pmol (10 minutes with agitation of the hybridization solution) (184), or 1 pmol in 30 min (182) were obtained. In terms of quantity of detectable DNA amount our developed system can

be considered therefore as very sensitive. As has been shown in the results part the hybridization time can still be reduced to at least one hour by using an automated hybridization station without a significant loss of sensitivity for the analysis (see section 3.1.9.1). Although all perfect matches were detected with the lowest amount of target DNA tested, the negative effects on the discrimination and the reproducibility of a low signal to noise ratio were already obvious. Therefore, it was determined that for an optimal specificity and reproducibility the incorporation ratio should amount to at least 100 nucleotides per fluorophore and at least 50 ng (app. 0.09 pmol) of target DNA should be applied.

A dependency of the discrimination efficiency from the amount of applied target DNA was clearly determined in case of the target DNA with a higher content of fluorescence label (87 nucleotides/fluorophore). By increasing the amount of target DNA molecules with an incorporation ratio of 87 the discrimination level was enhanced. In contrast to that the discrimination efficiency for an incorporation ratio of 166 nucleotides/fluorophore was almost independent from the amount of applied target DNA and the level of discrimination was decreased compared to all tested amounts of target DNA for an incorporation ratio of 87. A probable explanation for this observation is an increased competition between unlabeled and labeled fragments in case of the target DNA containing less fluorescence label. To reach an optimal discrimination between a perfect match and a mismatch, a sufficient number of target molecules has to reach the probe. This is depending on the time and the amount and size of the available target molecules. In case of the higher content of fluorescence label, more labeled target fragments are available, when the amount of target DNA is increased, so that the number of probe/target meeting events is increased and thus the discrimination level enhanced. In case of the lower content of fluorescence label more unlabeled fragments than labeled fragments are available. The duplexes with unlabeled fragments are more stable due to steric reasons, since the Cy molecule has a relatively big size in comparison to the bases of the DNA (see figure 9) and presents a steric hindrance for duplex formation. The stability of the heteroduplex products also determines dissociation rates (112). Therefore, the hybridization of unlabeled target DNA molecules in case of the target DNA with the lower content of fluorescence label is favored in comparison to the labeled ones and probably counteracts the enhancement of the discrimination level by increasing probe/target meeting events.

In this study the arrays were validated with DNA extracted from clinical isolates, and due to an effective DNA extraction step performed at the Robert Bosch Hospital sufficient template DNA was present to achieve satisfactory amounts of target DNA for all tested isolates (unpublished results). The sensitivity of the system was so far not determined regarding the quantity of template DNA needed for the amplification of sufficient target DNA for the detection on the microarray. Hereby it has to be noted that the PCR, used for target DNA production in this study, was more optimized towards cost effectiveness (with low concentrations of dNTPs, fluorescence labels and a relatively low priced Taq polymerase) than towards optimal sensitivity. Furthermore, a direct labeling approach was used, which was very effective for implementation of the system, since it was time-saving and allowed to monitor the incorporation ratio of fluorescence label easily, but also lead to a less effective target DNA production, since the relatively large size of the fluorescent dye was disadvantageous for the polymerase reaction (184). These parameters would have to be optimized for increased sensitivity of the target DNA production.



An optimization of the PCR protocol is only reasonable in combination with the species specific molecular enrichment step and the development of a multiplex PCR approach or an alternative DNA amplification strategy for the simultaneous amplification of all ESBL or IRT relevant target genes. This was beyond the scope of this study, but will be the subject of subsequent research for implementation of a complete ESBL chip.

#### **4.8 Parameters influencing the hybridization**

##### **4.8.1 Fragmentation**

The fragmentation of the target DNA for analysis with an oligonucleotide microarray is usually performed to minimize secondary structure and to allow the hybridization of different sequence parts independently from each other on the microarray (78). Although single stranded targets promise a better accessibility for duplex formation (55), in our approach double stranded, directly labeled and fragmented target DNA was used for hybridization without prior denaturation. DNA hybridization is a reaction process, where ssDNA and dsDNA are present in an equilibrium. The shorter the fragments are and the closer their  $T_m$  is to the surrounding temperature the more strand exchanges can occur, thus probe/target duplex formation also takes place, if short dsDNA fragments are used. In this study the denaturation prior hybridization to produce single stranded target DNA could be omitted, because, as proven by the results of the hybridization, strand exchange could occur within the applied hybridization condition. This target DNA preparation method yielded in our approach fast, sensitive and specific hybridization results.

The fact that long target DNA strands prevented the accessibility of the target DNA could be observed for target DNA batches containing mostly unfragmented target DNA. Hereby the capture probes targeting the 3' end of the targeted DNA strand delivered close to background signals when hybridized with unfragmented target DNA in contrast to probes targeting the 5' end. A higher amount of secondary structures at the 3' end of the target molecule compared to the 5' end could be an explanation for this observation.

Another reason could be interactions between the two strands of the target molecule during hybridization to the probe sequence. The group of Bergeron, reported that 5' immobilized capture probes gave stronger hybridization signals when the 5' overhanging tail of the bound target strand was short and showed near background signals when the 5' tail reached a length over 600 nucleotides (127). The increase of the 3' end had no major effect on the hybridization signals. This was a counterintuitive result, since one would expect a weaker hybridization signal when a 5' end immobilized probe binds a target molecule close to its 5' end, because of steric hindrances caused by a longer 3' overhanging tail directed towards the surface. This observation was explained by the fact that when a probe recognize an area close to the 3' end of the captured target strand most of the overhanging 5' end of nonhybridized DNA is exposed to the liquid phase above. The protruding tail of the target molecule can thus interact with the complementary strand, which destabilizes the probe target complex. The capture probe sets used in this study presented the same kind of behavior as the probe sets used in the study from the group of Bergeron, although undirectly immobilized probes were used. This result is surprising, since the theories of the group of Bergeron are not applicable, when the

probes are immobilized in an undirected way. Most probably other target molecule effects have to be considered. One possible explanation could be, that in case of the TEM target strand the 5' end is more accessible for reassociation of the complementary target strand than the 3' end. However, if this hypothesis is valid, could not be discerned within the scope of this study.

As expected, best results regarding identification of the perfect match positions were achieved for conditions, where - according to the determined incorporation ratio of fluorescence label - a majority of the fragments should still bear a fluorescence label. Although shorter fragments might still perform better regarding accessibility of the target sequence, it could be observed that target DNA with smaller fragment sizes (15-50 bp) performed less well regarding sensitivity of the perfect match detection. This was most probably due to the presence of an increased number of unlabeled target DNA fragments.

The method chosen for fragmentation was the digestion by DNaseI enzyme. This enzyme cleaves internal phosphodiesterbonds independently from the DNA sequence (173). The major advantage of this procedure was the rapidness of the reaction (15 min) and the fact that no purification prior hybridization was necessary. The reaction conditions for obtaining a specific size range of fragments has to be determined empirically and can be quite diverse, depending on the enzyme batch, enzyme activity and the initial target DNA size. Crucial was, as observed during the tests of the clinical isolates, the exact timing of the reaction, which was sometimes problematic, when multiple fragmentation reactions were performed simultaneously. Furthermore, exposure of the enzyme to room temperature could quickly lead to inactivation of the enzyme. This could cause incomplete fragmentation, which led to a poor discrimination efficiency. To avoid the variations introduced through the use of different enzyme batches or decreasing enzyme activity during the multiple utilization of one enzyme batch, other enzyme-independent methods for DNA fragmentation are also available. The fragmentation can also be performed chemically (78,128) or mechanically (68). Among the disadvantages of a chemical fragmentation is the fact that harsh reaction conditions (such as alkali or acid treatment) can make the target DNA unsuitable for direct hybridization, so that prior purification or neutralization is necessary. It also might interfere with the fluorescence label, so that only indirect labeling can be used. Most chemical treatment protocols make a more elaborate purification necessary and require more time. The mechanical fragmentation of target DNA is difficult to control for the used low sample volumina and DNA concentrations.

### ***4.8.2 Assay time and hybridization devices***

For a clinical application the assay time is of crucial importance. The major limitations hereby are the amplification and hybridization steps with two and initially three hours. Also the manual washing steps with 30 minutes additional assay time offer a potential for improvement. A shortening of the amplification time can cause a loss of sensitivity of the detection. As mentioned before, the optimization of the amplification regarding sensitivity and also assay time involves the combination with the specific enrichment method and was beyond the scope of this work. The focus in the here presented approach was on optimization of the hybridization process, regarding reaction time, sensitivity and reproducibility. Therefore, different devices for the improvement of specific features of the hybridization step or for automation of the whole process were applied. The different parameters influencing the hybridization results were described in detail in the results part. Hereby, it was shown that an

automation of the hybridization, washing and drying steps had an advantageous effect on the sensitivity and the specificity of the analysis. The tested devices performed variably and required different levels of skillfulness from the user. Since one prerequisite was to perform the assay as user-independently as possible, the most user-friendly equipment with the most convincing assay results was chosen (HS400 from Tecan). In an application note from Tecan it was shown, that the hybridization station improved the reproducibility and homogeneity of the hybridization results in comparison to a manual hybridization method (162). This was confirmed by the results obtained in this study. With this device a shortening of the hybridization time to only 15 minutes was successfully shown. Furthermore, the washing steps were also reduced to two times two minutes and one time 1.5 minutes, but the automated exchange of solutions, pumping and complete drying process did still add up to 30 minutes in total. However, a decreased hybridization time did also result in a reduced discrimination efficiency and sensitivity of the analysis. To achieve a compromise between optimal results of the analysis and decreased time requirements, the hybridization time was shortened to one hour and the HS400 was used for all following experiments.

Alternative methods for speeding up hybridization is the use of electronic forces for annealing or dissociation of the target. The duplex formation and dissociation can then be done in seconds. This method requires special carriers with individually addressable electrodes for each probe site. First prototypes of electronic microarrays have already been developed (45), but up to date a limitation regarding the number of individual probe sites is still observed. However, the principle is quite promising and presuming a more complex layout with a high number of electrodes in combination with a flow cell and on-line monitoring could allow the sequential hybridization, detection and removal of multiple samples within a short period of time.

#### **4.9 Detection of mixed resistances**

The coexistence of different beta-lactamase variants from the same family in a single strain has already been reported for TEM- (17) and SHV-type beta-lactamases (43). There is not much known so far about the frequency of occurrence of these resistance gene patterns especially in case of TEM beta-lactamase. However, it is known that TEM-1 (95) and SHV-1 (8) are widespread enzymes and in case of SHV the coexistence of SHV-1 and an ESBL variant of this enzyme has been observed (64). The possibility for a molecular detection assay to detect and identify an ESBL variant in presence of a non-ESBL variant in an isolate therefore is of crucial importance. Due to the high level of reproducibility of the mismatch to perfect match signal intensity ratios as shown in section 3.1.6, it was assumed that hybridization patterns diverging from the usually observed ones can be interpreted regarding mixed resistance patterns. The results of a model experiment for the TEM array showed, that the level of discrimination between a mixed genotype and a non-mixed genotype was differing, depending on the analyzed polymorphism position. A detection of mixed resistance patterns was possible for some probe sets up to a ratio of 1:5 of target DNA from differing variants, in some cases up to a ratio of 1:10. There is not much known about the relative copy number of the different genes in one isolate, so that no definite conclusion can be made, whether this range of detection is relevant or not. Howard et al. reported a relatively equal copy number of different SHV variants in two of three cases, but they did not mention actual ratios (64). The detection of the coexistence of different SHV beta-lactamase variants in real clinical

isolates with the presented system was possible as shown for the isolates collected in Croatia.

However, if this assay system should be used without prior isolation of the resistant bacteria, the observed discrimination level is insufficient, because the presence of a resistant bacteria in a high excess of non-resistant bacteria in a crude sample is definitely possible. Higher discrimination levels (up to one ESBL producing bacterium in a background of 100,000 wild-type bacteria) can be achieved by LDR (ligase detection reaction) based methods as described by Niederhauser et al. (117). In this study only a single polymorphism position was detected and the presented system showed only limited multiplexing capacity. LDR-based methods on the microarray have already been described (35,38), but these procedures require more complex assay features than the allele specific hybridization method and the adaptation of this concept to an analysis of a higher number of features is challenging. Generally, methods with increased discrimination level (e.g. primer extension, LDR) also require more complex protocols, which is a clear disadvantage for clinical application. In the future on-line monitored and electronically directed dissociation and association profiles could also be used to advance the discrimination level while applying traditional allele specific hybridization probes.

### 4.10 Test of clinical isolates

In total 113 clinical isolates were provided by the cooperation partners for validation of the TEM- or SHV-array. Seventy-two *bla*<sub>TEM</sub>-gene containing isolates were analyzed on the TEM-array. Seventy of these variants could be identified by the TEM-microarray analysis. Two variants exhibited insufficient discrimination pattern, which were attributed to incomplete fragmentation. Thirty of the 35 clinical isolates collected in Croatia contained *bla*<sub>SHV</sub> variants and 29 of these could be identified by the microarray analysis. One variant was not identified due to the aforementioned problem of insufficient fragmentation. The observed problem during the fragmentation step was caused by the simultaneous manual preparation of multiple samples, leading to a premature inactivation of DNaseI for these samples. In a clinical application this step should be automated or a restricted number of samples should be prepared simultaneously to avoid such aberrations. All genotypes detected by microarray analysis were confirmed by standard DNA sequencing.

The correlation to the phenotypic data could only be made in a limited scale, since not all ESBL or IRT relevant genes were detected. In case of the analysis of all *bla*<sub>TEM</sub>-genes, only *bla*<sub>TEM-1</sub>, *bla*<sub>TEM-2</sub> and *bla*<sub>TEM-116</sub> were found. *Bla*<sub>TEM-1</sub> and *bla*<sub>TEM-2</sub> are parental types, which do not confer an ESBL phenotype. For *bla*<sub>TEM-116</sub> the phenotypic characteristics are not clearly defined. Although Jeong et al. (74) stated, that a transconjugant bearing this gene exhibited an ESBL phenotype, it was not definitely proven, that this was the only resistance gene present. Furthermore, *bla*<sub>TEM-116</sub> bears only two mutations towards TEM-1 at position 82 and 182, which have not been found in any other TEM ESBL gene variant so far. It still has to be determined whether there is a functional advantage in such changes, so currently no conclusion can be drawn if the ESBL phenotype might be caused by this variant. The results from the analysis of the samples collected in Croatia suggest a non-ESBL phenotypic substrate pattern for variants carrying this genotype. Thus, in the isolates tested in this study the ESBL phenotype was probably not caused by TEM variants.

In case of the analysis of the SHV genotypes from the isolates collected in Croatia *bla*<sub>SHV-1</sub> and *bla*<sub>SHV-5</sub>, *bla*<sub>SHV-12</sub> alone or in presence of *bla*<sub>SHV-1</sub> were detected. Hereby it was shown that the differentiation of mixed and pure resistance patterns is possible and that an ESBL variant can be identified in presence of a non-ESBL variant by SHV-array analysis. The fact that in all *K. pneumoniae* and the *K. terrigena* isolates a *bla*<sub>SHV-1</sub> gene was found either alone or in combination with a *bla*<sub>SHV</sub>-ESBL gene variant (in contrast to the *E. coli* isolates, which did not contain a *bla*<sub>SHV-1</sub> type gene), could be explained by the frequent occurrence of a chromosomally encoded *bla*<sub>SHV-1</sub> in *K. pneumoniae* (8). Although the template DNA consisted of extracted plasmid DNA, the presence of a background of chromosomal DNA could not be excluded (64) and was the most probable cause of the *bla*<sub>SHV-1</sub> genotype detection in the *K. pneumoniae* isolates.

The correlation of the genotypic analysis to the phenotypic data was for the isolates from Croatia consistent for 34 of the 35 isolates. The isolates phenotypically classified as ESBL producers contained an SHV-type ESBL variant, except for isolate 27, which must contain a non-SHV- or TEM-type ESBL variant, which was not genotypically identified. Isolates clearly classified as non-ESBL producers (isolates 13, 21, 32) or showing substrate patterns corresponding to K1 (isolate 26) or CTX-M (isolate 2) type resistance contained only parental variants (SHV-1, TEM-1) or TEM-116 and no SHV-ESBL variant. A final conclusion could not be drawn for isolates 2 or 26, since it was not genotypically screened for CTX-M or K1 type resistances within this study. Isolate 36 showed an unusual resistance pattern (see section 3.3) and could not be classified phenotypically as an ESBL, AmpC or other usual beta-lactamase producer and contained according to the genotypic analysis no *bla*<sub>TEM</sub> or *bla*<sub>SHV</sub>-ESBL variant. Thus, the reliability of the array analysis for ESBL detection and identification could be validated, but the need for an extension of the detectable spectrum of ESBL variants to other families than TEM or SHV also was observed, since otherwise no definite correlation to the phenotypic data can be made.

#### **4.11 Ongoing developments**

##### **4.11.1 Transfer to a marketable format**

The identification of the perfect match positions was possible with the EAT proprietary system, but further optimization to achieve comparable discrimination and sensitivity levels, as for the well-characterized currently used system, still has to follow for a full implementation of the new format. The use of the silver label (1) showed very promising enhancements of the sensitivity of the detection, but the necessity to improve the wash protocol for reduced background signals and improved discrimination efficiency was observed. Since the transfer of the system to the EAT format was in principle successful, the development of a marketable product for clinical microbiology is considered as possible.

##### **4.11.2 Link of the resistance to the pathogenic bacteria**

In this proof concept experiment a *bla*<sub>TEM-1</sub> gene could be amplified after a species-specific enrichment by polynucleotide probes of *E. coli* from a urine sample in microtiter wells. This amplificate could be used as a template in a labeling PCR and was used for a successful identification of *bla*<sub>TEM-1</sub> with the TEM-microarray. In the future the labeling PCR should be carried out directly after enrichment. So far this

direct amplification and labeling was not successful (data not shown), but an optimization of the PCR protocol should solve this problem. However, the proof that the combination of both systems can establish a link between a genotypic species detection and resistance identification was rendered by this experiment. A culture independent preisolation of the pathogenic organism could be a considerable time advantage for the clinical application.

### ***4.11.3 Extension of the detection spectrum of the ESBL chip***

The developed TEM- and SHV-arrays yield a clear identification of the known TEM and SHV resistance determinants, enabling a monitoring of the occurrence of different variants in the clinical setting. Furthermore, the ESBL relevant polymorphisms are identified, so that the choice of antibiotics for treatment can be facilitated by considering existing resistance profiles of previously characterized variants. However, a major advantage of the phenotypic diagnostic remains that a wider variety of resistance determinants can be detected. To enable the ESBL chip to compete with phenotypic standard methods, the majority of the ESBL resistance determinants have to be covered. The third major ESBL causing genotype is attributed to genes from the CTX-M gene family (13). These resistances are of increasing importance especially in eastern Europe and belong to the most rapidly growing groups. Therefore, a CTX-M array is currently developed as a complementary feature to the TEM- and SHV-arrays in cooperation with coworkers from the National Research Center of Antibiotics in Moskow (NRCA). In contrast to SHV and TEM the different CTX-M variants present a high level of polymorphism with only up to 70% of sequence identity within the gene family. A prototype array has already been developed, conferring a hierarchic identification, where family, group and subtype specific probes are combined in an allele specific hybridization format. So far 11 of the 37 classified CTX-M variants can be specifically identified by these probes. Seven group specific probes allow the correct classification of the tested CTX-M variants according to their different subgroups. The development of family specific and the missing subtype specific probe sets is still in progress. To design microarrays for the detection of AmpC and OXA-type beta-lactamases is projected.

#### **4.12 Conclusion**

The ultimate goal in this project was the development of an ESBL-Chip for the rapid, sensitive and reliable detection and identification of the clinically relevant ESBL and IRT producing beta-lactamases for application in clinical microbiology diagnostics as well as epidemiologic studies. This was achieved for the majority of the most relevant ESBLs, the TEM and SHV beta-lactamases. The developed assay systems allow the detection of 96 % of the currently known TEM-variants and 100 % of the known SHV-variants. The assay enabled the detection and identification of 99 % of the relevant polymorphisms for TEM beta-lactamases and 100 % of the mutations of SHV beta-lactamases. Consensus primers were developed and used for target amplification covering the majority of the known variant sequences. The sensitivity, reproducibility and identification capability of the developed arrays was validated with numerous reference samples and clinical isolates. The simultaneous detection of an extended spectrum-variant in presence of a narrow spectrum-variant was shown in a model system for TEM up to a ratio of 1:10, as well as in clinical isolates for SHV. Starting from the isolated DNA, the assay could be performed in less than 3.5 hours. The discrimination level, the sensitivity and the reproducibility were enhanced by automation of the hybridization procedure. The extension of the developed system towards the detection of other beta-lactamase families is possible and is already in progress.

The rapid detection of resistant bacteria by genotypic resistance testing at a competitive price should reduce the emergence of drug resistances. The prescription of antibiotics could be more targeted and thus more effective, since expected substrate profiles could be deducted from the genotypic profile and considered before treatment. The use of broad spectrum antibiotics could be limited to severe infections and a spread of resistances could be averted by an early isolation of infected patients. The developed genotypic resistance tests could therefore have a major impact on the clinical management of infectious diseases and health care costs.

### 5 References

#### Reference List

1. **Alexandre, I., S. Hamels, S. Dufour, J. Collet, N. Zammateo, F. De Longueville, J. L. Gala, and J. Remacle.** 2001. Colorimetric silver detection of DNA microarrays. *Analytical Biochemistry* **295**:1-8.
2. **Ambler, R. P.** 1980. The Structure of Beta-Lactamases. *Philosophical Transactions of the Royal Society of London Series B - Biological Sciences* **289**:321-331.
3. **Ambler, R. P., A. F. Coulson, J. M. Frere, J. M. Ghuysen, B. Joris, M. Forsman, R. C. Levesque, G. Tiraby, and S. G. Waley.** 1991. A standard numbering scheme for the class A beta-lactamases. *Biochemical Journal* **276**:269-270.
4. **Arlet, G., G. Brami, D. Decre, A. Flipppo, O. Gaillot, P. H. Lagrange, and A. Philippon.** 1995. Molecular Characterization by Pcr-Restriction Fragment Length Polymorphism of Tem Beta-Lactamases. *Fems Microbiology Letters* **134**:203-208.
5. **Arlet, G. and A. Philippon.** 1991. Construction by Polymerase Chain-Reaction and Intragenic Dna Probes for 3 Main Types of Transferable Beta-Lactamases (Tem, Shv, Carb). *Fems Microbiology Letters* **82**:19-25.
6. **Arthur, M. and P. Courvalin.** 1993. Genetics and Mechanisms of Glycopeptide Resistance in Enterococci. *Antimicrobial Agents and Chemotherapy* **37**:1563-1571.
7. **Babini, G. S. and D. M. Livermore.** 2000. Antimicrobial resistance amongst *Klebsiella* spp. collected from intensive care units in Southern and Western Europe in 1997-1998. *Journal of Antimicrobial Chemotherapy* **45**:183-189.
8. **Babini, G. S. and D. M. Livermore.** 2000. Are SHV beta-lactamases universal in *Klebsiella pneumoniae*? *Antimicrobial Agents and Chemotherapy* **44**:2230.
9. **Baner, J., A. Isaksson, E. Waldenstrom, J. Jarvius, U. Landegren, and M. Nilsson.** 2003. Parallel gene analysis with allele-specific padlock probes and tag microarrays. *Nucleic Acids Research* **31**.
10. **Baron, S.** 1996. Section 1. Bacteriology: Inhibition of Bacterial Cell Wall Synthesis, *In Medical Microbiology*. The University of Texas Medical Branch at Galveston.
11. **Blanchard, A. P., R. J. Kaiser, and L. E. Hood.** 1996. High-density oligonucleotide arrays. *Biosensors & Bioelectronics* **11**:687-690.



12. **Bodrossy, L.** 2003. Diagnostic oligonucleotide microarrays for microbiology, p. 43-92. *In* E. Blalock (ed.), *A Beginner's Guide to Microarrays*. Kluwer Academic Publishers, New York.
13. **Bonnet, R.** 2004. Growing group of extended-spectrum beta-lactamases: The CTX-M enzymes. *Antimicrobial Agents and Chemotherapy* **48**:1-14.
14. **Booth, S. A., M. A. Drebot, I. E. Martin, and L. K. Ng.** 2003. Design of oligonucleotide arrays to detect point mutations: molecular typing of antibiotic resistant strains of *Neisseria gonorrhoeae* and hantavirus infected deer mice. *Molecular and Cellular Probes* **17**:77-84.
15. **Bradford, P. A.** 1999. Automated thermal cycling is superior to traditional methods for nucleotide sequencing of *bla*(SHV) genes. *Antimicrobial Agents and Chemotherapy* **43**:2960-2963.
16. **Bradford, P. A.** 2001. Extended-spectrum beta-lactamases in the 21st century: characterization, epidemiology, and detection of this important resistance threat. *Clinical Microbiology Reviews* **14**:933-51, table.
17. **Bradford, P. A., C. E. Cherubin, V. Idemyor, B. A. Rasmussen, and K. Bush.** 1994. Multiply Resistant *Klebsiella-Pneumoniae* Strains from 2 Chicago Hospitals - Identification of the Extended-Spectrum Tem-12 and Tem-10 Ceftazidime-Hydrolyzing Beta-Lactamases in A Single Isolate. *Antimicrobial Agents and Chemotherapy* **38**:761-766.
18. **Broude, N. E., K. Woodward, R. Cavallo, C. R. Cantor, and D. Englert.** 2001. DNA microarrays with stem-loop DNA probes: preparation and applications. *Nucleic Acids Research* **29**:E92.
19. **Brown, P. O. and D. Botstein.** 1999. Exploring the new world of the genome with DNA microarrays. *Nature Genetics* **21**:33-37.
20. **Bush, K.** 2001. New beta-lactamases in gram-negative bacteria: Diversity and impact on the selection of antimicrobial therapy. *Clinical Infectious Diseases* **32**:1085-1089.
21. **Bush, K., G. A. Jacoby, and A. A. Medeiros.** 1995. A functional classification scheme for beta-lactamases and its correlation with molecular structure. *Antimicrobial Agents and Chemotherapy* **39**:1211-1233.
22. **Call, D. R., M. K. Bakko, M. J. Krug, and M. C. Roberts.** 2003. Identifying antimicrobial resistance genes with DNA microarrays. *Antimicrobial Agents and Chemotherapy* **47**:3290-3295.
23. **Call, D. R., D. P. Chandler, and F. Brockman.** 2001. Fabrication of DNA microarrays using unmodified oligonucleotide probes. *Biotechniques* **30**:368-372.
24. **Chakravarti, A.** 1999. Population genetics--making sense out of sequence. *Nature Genetics* **21**:56-60.

## References

---

25. **Chanawong, A., F. H. M'Zali, J. Heritage, A. Lulitanond, and P. M. Hawkey.** 2000. Characterisation of extended-spectrum beta-lactamases of the SHV family using a combination of PCR-single strand conformational polymorphism (PCR-SSCP) and PCR-restriction fragment length polymorphism (PCR-RFLP). *Fems Microbiology Letters* **184**:85-89.
26. **Chanawong, C., F. H. M'Zali, J. Heritage, A. Lulitanond, and P. M. Hawkey.** 2001. Discrimination of SHV beta-lactamase genes by restriction site insertion-PCR. *Antimicrobial Agents and Chemotherapy* **45**:2110-2114.
27. **Cheung, V. G., M. Morley, F. Aguilar, A. Massimi, R. Kucherlapati, and G. Childs.** 1999. Making and reading microarrays. *Nature Genetics* **21**:15-9.
28. **Chizhikov, V., A. Rasooly, K. Chumakov, and D. D. Levy.** 2001. Microarray analysis of microbial virulence factors. *Applied and Environmental Microbiology* **67**:3258-3263.
29. **Cho, R. J., M. Mindrinos, D. R. Richards, R. J. Sapolsky, M. Anderson, E. Drenkard, L. Dewdney, T. L. Reuber, M. Stammers, N. Federspiel, A. Theologis, W. H. Yang, E. Hubbell, M. Au, E. Y. Chung, D. Lashkari, B. Lemieux, C. Dean, R. J. Lipshutz, F. M. Ausubel, R. W. Davis, and P. J. Oefner.** 1999. Genome-wide mapping with biallelic markers in *Arabidopsis thaliana*. *Nature Genetics* **23**:203-207.
30. **Cockerill, F. R., III.** 1999. Genetic methods for assessing antimicrobial resistance. *Antimicrobial Agents and Chemotherapy* **43**:199-212.
31. **Cronin, M. T., R. V. Fucini, S. M. Kim, R. S. Masino, R. M. Wespi, and C. G. Miyada.** 1996. Cystic fibrosis mutation detection by hybridization to light-generated DNA probe arrays. *Human Mutation* **7**:244-255.
32. **Dahl, F., J. Baner, M. Gullberg, M. Mendel-Hartvig, U. Landegren, and M. Nilsson.** 2004. Circle-to-circle amplification for precise and sensitive DNA analysis. *Proceedings of the National Academy of Sciences of the United States of America* **101**:4548-4553.
33. **Datta, N., and P. Kontomic.** 1965. Penicillinase Synthesis Controlled by Infectious R Factors in Enterobacteriaceae. *Nature* **208**:239.
34. **Davies, J.** 1994. Inactivation of Antibiotics and the Dissemination of Resistance Genes. *Science* **264**:375-382.
35. **De Bellis, G., B. Castiglioni, R. Bordoni, A. Mezzelani, E. Rizzi, A. Frosini, E. Busti, C. Consolandi, L. R. Bernardi, and C. Battaglia.** 2002. Ligase detection reaction (LDR) and universal array (Zip Code): application to DNA genotyping. *Minerva Biotechnologica* **14**:247-252.
36. **de Leon, J., M. T. Susce, R. M. Pan, M. Fairchild, W. H. Koch, and P. J. Wedlund.** 2005. The CYP2D6 poor metabolizer phenotype may be associated with risperidone adverse drug reactions and discontinuation. *Journal of Clinical Psychiatry* **66**:15-27.

37. **Delrio-Lafreniere, S. A., M. K. Browning, and R. C. McGlennen.** 2004. Low-density addressable array for the detection and typing of the human papillomavirus. *Diagnostic Microbiology and Infectious Disease* **48**:23-31.
38. **Deng, J. Y., X. E. Zhang, Y. Mang, Z. P. Zhang, Y. F. Zhou, Q. Liu, H. B. Lu, and Z. J. Fu.** 2004. Oligonucleotide ligation assay-based DNA chip for multiplex detection of single nucleotide polymorphism. *Biosensors & Bioelectronics* **19**:1277-1283.
39. **Donay, J. L., D. Mathieu, P. Fernandes, C. Pregermain, P. Bruel, A. Wargnier, I. Casin, F. X. Weill, P. H. Lagrange, and J. L. Herrmann.** 2004. Evaluation of the automated phoenix system for potential routine use in the clinical microbiology laboratory. *Journal of Clinical Microbiology* **42**:1542-1546.
40. **Duggan, D. J., M. Bittner, Y. Chen, P. Meltzer, and J. M. Trent.** 1999. Expression profiling using cDNA microarrays. *Nature Genetics* **21**:10-4.
41. **Edman, C. F., D. E. Raymond, D. J. Wu, E. Tu, R. G. Sosnowski, W. F. Butler, M. Nerenberg, and M. J. Heller.** 1997. Electric field directed nucleic acid hybridization on microchips. *Nucleic Acids Research* **25**:4907-14.
42. **Emery, C. L. and L. A. Weymouth.** 1997. Detection and clinical significance of extended-spectrum beta-lactamases in a tertiary-care medical center. *Journal of Clinical Microbiology* **35**:2061-2067.
43. **Essack, S. Y., L. M. C. Hall, and D. M. Livermore.** 2004. Klebsiella pneumoniae isolate from South Africa with multiple TEM, SHV and AmpC beta-lactamases. *International Journal of Antimicrobial Agents* **23**:398-400.
44. **Fan, J. B., X. Chen, M. K. Halushka, A. Berno, X. Huang, T. Ryder, R. J. Lipshutz, D. J. Lockhart, and A. Chakravarti.** 2000. Parallel genotyping of human SNPs using generic high-density oligonucleotide tag arrays. *Genome Research* **10**:853-60.
45. **Feng, L. and M. Nereberg.** 1999. Electronic microarray for DNA analysis. *Gene Therapy and Molecular Biology* **4**:183-191.
46. **Fichtl, K. M.** 2005. Polynucleotide Probe Based Enrichment of Bacterial Cells: Development of Probes for Species of Clinical Relevance München, Technische Universität, Dissertation.
47. **Fisher, J. F., S. O. Meroueh, and S. Mobashery.** 2005. Bacterial resistance to beta-lactam antibiotics: Compelling opportunism, compelling opportunity. *Chemical Reviews* **105**:395-424.
48. **Fluit, A. C., M. R. Visser, and F. J. Schmitz.** 2001. Molecular detection of antimicrobial resistance. *Clinical Microbiology Reviews* **14**:836-71, table.
49. **Foglieni, B., L. Cremonesi, M. Travi, A. Ravani, A. Giambona, M. C. Rosatelli, C. Perra, P. Fortina, and M. Ferrari.** 2004. beta-thalassemia microelectronic chip: A fast and accurate method for mutation detection. *Clinical Chemistry* **50**:73-79.

## References

---

50. **Gerry, N. P., N. E. Witowski, J. Day, R. P. Hammer, G. Barany, and F. Barany.** 1999. Universal DNA microarray method for multiplex detection of low abundance point mutations. *Journal of Molecular Biology* **292**:251-262.
51. **Gniadkowski, M.** 2001. Evolution and epidemiology of extended-spectrum beta-lactamases (ESBLs) and ESBL-producing microorganisms. *Clinical Microbiology and Infection* **7**:597-608.
52. **Gniadkowski, M., A. Palucha, P. Grzesiowski, and W. Hryniewicz.** 1998. Outbreak of ceftazidime-resistant *Klebsiella pneumoniae* in a pediatric hospital in Warsaw, Poland: Clonal spread of the TEM-47 extended-spectrum beta-lactamase (ESBL)-producing strain and transfer of a plasmid carrying the SHV5-like ESBL-encoding gene. *Antimicrobial Agents and Chemotherapy* **42**:3079-3085.
53. **Grimm, V., S. Ezaki, M. Susa, C. Knabbe, R. D. Schmid, and T. T. Bachmann.** 2004. Use of DNA microarrays for rapid genotyping of TEM beta-lactamases that confer resistance. *Journal of Clinical Microbiology* **42**:3766-3774.
54. **Gunderson, K. L., X. C. Huang, M. S. Morris, R. J. Lipshutz, D. J. Lockhart, and M. S. Chee.** 1998. Mutation detection by ligation to complete n-mer DNA arrays. *Genome Research* **8**:1142-53.
55. **Guo, Z., R. A. Guilfoyle, A. J. Thiel, R. F. Wang, and L. M. Smith.** 1994. Direct Fluorescence Analysis of Genetic Polymorphisms by Hybridization with Oligonucleotide Arrays on Glass Supports. *Nucleic Acids Research* **22**:5456-5465.
56. **Guo, Z., Q. H. Liu, and L. M. Smith.** 1997. Enhanced discrimination of single nucleotide polymorphisms by artificial mismatch hybridization. *Nature Biotechnology* **15**:331-335.
57. **Guschin, D. Y., B. K. Mobarry, D. Proudnikov, D. A. Stahl, B. E. Rittmann, and A. D. Mirzabekov.** 1997. Oligonucleotide microchips as genosensors for determinative and environmental studies in microbiology. *Applied and Environmental Microbiology* **63**:2397-2402.
58. **Hacia, J. G.** 1999. Resequencing and mutational analysis using oligonucleotide microarrays. *Nature Genetics* **21**:42-47.
59. **Haff, L. A. and I. P. Smirnov.** 1997. Single-nucleotide polymorphism identification assays using a thermostable DNA polymerase and delayed extraction MALDI-TOF mass spectrometry. *Genome Research* **7**:378-388.
60. **Hawkey, P. M.** 1998. The origins and molecular basis of antibiotic resistance. *BMJ* **317**:657-660.
61. **Heller, M.** 2002. DNA microarray technology: devices, systems, and applications. *Annual Review of Biomedical Engineering* **4**:129-153.

62. **Heritage, J., F. H. M'Zali, D. Gascoyne-Binzi, and P. M. Hawkey.** 1999. Evolution and spread of SHV extended-spectrum beta-lactamases in Gram-negative bacteria. *Journal of Antimicrobial Chemotherapy* **44**:309-318.
63. **Hirschhorn, J. N., P. Sklar, K. Lindblad-Toh, Y. M. Lim, M. Ruiz-Gutierrez, S. Bolk, B. Langhorst, S. Schaffner, E. Winchester, and E. S. Lander.** 2000. SBE-TAGS: An array-based method for efficient single-nucleotide polymorphism genotyping. *Proceedings of the National Academy of Sciences of the United States of America* **97**:12164-12169.
64. **Howard, C., A. van Daal, G. Kelly, J. Schooneveldt, G. Nimmo, and P. M. Giffard.** 2002. Identification and minisequencing-based discrimination of SHV beta-lactamases in nosocomial infection-associated *Klebsiella pneumoniae* in Brisbane, Australia. *Antimicrobial Agents and Chemotherapy* **46**:659-664.
65. **Hsu, T. M., S. M. Law, S. H. Duan, B. P. Neri, and P. Y. Kwok.** 2001. Genotyping single-nucleotide polymorphisms by the invader assay with dual-color fluorescence polarization detection. *Clinical Chemistry* **47**:1373-1377.
66. **Huang, Y., J. Shirajian, A. Schroder, Z. Yao, T. Summers, D. Hodko, and R. Sosnowski.** 2004. Multiple sample amplification and genotyping integrated on a single electronic microarray. *Electrophoresis* **25**:3106-3116.
67. **Huovinen, P., S. Huovinen, and G. A. Jacoby.** 1988. Sequence of Pse-2 Beta-Lactamase. *Antimicrobial Agents and Chemotherapy* **32**:134-136.
68. **Hussey, M.** 1985. *Basic Physics and Technology of Medical Diagnostic Ultrasound.* Elsevier Science, New York.
69. **Jacoby, G. A. and I. Carreras.** 1990. Activities of Beta-Lactam Antibiotics Against *Escherichia-Coli* Strains Producing Extended-Spectrum Beta-Lactamases. *Antimicrobial Agents and Chemotherapy* **34**:858-862.
70. **Jacoby, G. A. and P. Han.** 1996. Detection of extended-spectrum beta-lactamases in clinical isolates of *Klebsiella pneumoniae* and *Escherichia coli*. *Journal of Clinical Microbiology* **34**:908-911.
71. **Jacoby, G. A. and A. A. Medeiros.** 1991. More Extended-Spectrum Beta-Lactamases. *Antimicrobial Agents and Chemotherapy* **35**:1697-1704.
72. **Jacoby, G. A. and L. Sutton.** 1985. Beta-Lactamases and Beta-Lactam Resistance in *Escherichia-Coli*. *Antimicrobial Agents and Chemotherapy* **28**:703-705.
73. **Jaurin, B. and T. Grundstrom.** 1981. Ampc Cephalosporinase of *Escherichia-Coli* K-12 Has A Different Evolutionary Origin from That of Beta-Lactamases of the Penicillinase Type. *Proceedings of the National Academy of Sciences of the United States of America-Biological Sciences* **78**:4897-4901.
74. **Jeong, S. H., I. K. Bae, J. H. Lee, S. G. Sohn, G. H. Kang, G. J. Jeon, Y. H. Kim, B. C. Jeong, and S. H. Lee.** 2004. Molecular characterization of extended-spectrum beta-lactamases produced by clinical isolates of *Klebsiella*

## References

---

- pneumoniae and *Escherichia coli* from a Korean nationwide survey. *Journal of Clinical Microbiology* **42**:2902-2906.
75. **Ji, J. and M. Manak.** 2002. Genotyping of single nucleotide polymorphisms for epidemiological studies: A review of current methods. *Journal of Clinical Ligand Assay* **25**:199-210.
76. **Kafatos, F. C., C. W. Jones, and A. Efstratiadis.** 1979. Determination of Nucleic-Acid Sequence Homologies and Relative Concentrations by A Dot Hybridization Procedure. *Nucleic Acids Research* **7**:1541-1552.
77. **Kalinina, O., I. Lebedeva, J. Brown, and J. Silver.** 1997. Nanoliter scale PCR with TaqMan detection. *Nucleic Acids Research* **25**:1999-2004.
78. **Kelly, J. J., B. K. Chernov, I. Tovstanovsky, A. D. Mirzabekov, and S. G. Bavykin.** 2002. Radical-generating coordination complexes as tools for rapid and effective fragmentation and fluorescent labeling of nucleic acids for microchip hybridization. *Analytical Biochemistry* **311**:103-118.
79. **Kim, J. and H. J. Lee.** 2000. Rapid discriminatory detection of genes coding for SHV beta-lactamases by ligase chain reaction. *Antimicrobial Agents and Chemotherapy* **44**:1860-1864.
80. **Kliebe, C., B. A. Nies, J. F. Meyer, R. M. Tolxdorffneutzling, and B. Wiedemann.** 1985. Evolution of Plasmid-Coded Resistance to Broad-Spectrum Cephalosporins. *Antimicrobial Agents and Chemotherapy* **28**:302-307.
81. **Knothe H, Shah P, Krcmery V, Antal M, and Mitsunashi S.** 1983. Transferable resistance to cefotaxime, cefoxitin, cefamandole and cefuroxime in clinical isolates of *Klebsiella pneumoniae* and *Serratia marcescens*. *Infection* **11**:315-317.
82. **Knox, J. R.** 1995. Extended-Spectrum and Inhibitor-Resistant Tem-Type Beta-Lactamases - Mutations, Specificity, and 3-Dimensional Structure. *Antimicrobial Agents and Chemotherapy* **39**:2593-2601.
83. **Kurg, A., N. Tonisson, I. Georgiou, J. Shumaker, J. Tollett, and A. Metspalu.** 2000. Arrayed primer extension: Solid-phase four-color DNA resequencing and mutation detection technology. *Genetic Testing* **4**:1-7.
84. **Landegren, U., M. Nilsson, and P. Y. Kwok.** 1998. Reading bits of genetic information: Methods for single-nucleotide polymorphism analysis. *Genome Research* **8**:769-776.
85. **Lautenbach, E., J. B. Patel, W. B. Bilker, P. H. Edelstein, and N. O. Fishman.** 2001. Extended-spectrum beta-lactamase-producing *Escherichia coli* and *Klebsiella pneumoniae*: Risk factors for infection and impact of resistance on outcomes. *Clinical Infectious Diseases* **32**:1162-1171.
86. **Lee, I., A. A. Dombkowski, and B. D. Athey.** 2004. Guidelines for incorporating non-perfectly matched oligonucleotides into target-specific

- hybridization probes for a DNA microarray. *Nucleic Acids Research* **32**:681-690.
87. **Lee, S. H., D. R. Walker, P. B. Cregan, and H. R. Boerma.** 2004. Comparison of four flow cytometric SNP detection assays and their use in plant improvement. *Theoretical and Applied Genetics* **110**:167-174.
  88. **Lee, Y., C. S. Lee, Y. J. Kim, S. Chun, S. Park, Y. S. Kim, and B. D. Han.** 2002. Development of DNA chip for the simultaneous detection of various beta-lactam antibiotic-resistant genes. *Molecules and Cells* **14**:192-197.
  89. **Leverstein-van Hall, M. A., A. C. Fluit, A. Paauw, A. T. A. Box, S. Brisse, and J. Verhoef.** 2002. Evaluation of the Etest ESBL and the BD Phoenix, VITEK 1, and VITEK 2 automated instruments for detection of extended-spectrum beta-lactamases in multiresistant *Escherichia coli* and *Klebsiella* spp. *Journal of Clinical Microbiology* **40**:3703-3711.
  90. **Levicky, R. and A. Horgan.** 2005. Physicochemical perspectives on DNA microarray and biosensor technologies. *Trends in Biotechnology* **23**:143-149.
  91. **Levy, S. B.** 1998. The challenge of antibiotic resistance. *Scientific American* **278**:46-53.
  92. **Lindroos, K., S. Sigurdsson, K. Johansson, L. Ronnblom, and A. C. Syvanen.** 2002. Multiplex SNP genotyping in pooled DNA samples by a four-colour microarray system. *Nucleic Acids Research* **30**:e70.
  93. **Linscott, A. J. and W. J. Brown.** 2005. Evaluation of four commercially available extended-spectrum beta-lactamase phenotypic confirmation tests. *Journal of Clinical Microbiology* **43**:1081-1085.
  94. **Lipshutz, R. J., S. P. Fodor, T. R. Gingeras, and D. J. Lockhart.** 1999. High density synthetic oligonucleotide arrays. *Nature Genetics* **21**:20-24.
  95. **Livermore, D. M.** 1995. beta-Lactamases in laboratory and clinical resistance. *Clinical Microbiology Reviews* **8**:557-584.
  96. **Livermore, D. M.** 1998. Beta-lactamase-mediated resistance and opportunities for its control. *Journal of Antimicrobial Chemotherapy* **41 Suppl D**:25-41.
  97. **Livermore, D. M. and D. F. Brown.** 2001. Detection of beta-lactamase-mediated resistance. *Journal of Antimicrobial Chemotherapy* **48 Suppl 1**:59-64.
  98. **M'Zali, F. H., A. Chanawong, K. G. Kerr, D. Birkenhead, and P. M. Hawkey.** 2000. Detection of extended-spectrum beta-lactamases in members of the family Enterobacteriaceae: comparison of the MAST DD test, the double disc and the Etest ESBL. *Journal of Antimicrobial Chemotherapy* **45**:881-885.
  99. **M'Zali, F. H., A. Chanawong, K. G. Kerr, D. Birkenhead, and P. M. Hawkey.** 2000. Detection of extended-spectrum beta-lactamases in members of the

## References

---

- family Enterobacteriaceae: comparison of the MAST DD test, the double disc and the Etest ESBL. *Journal of Antimicrobial Chemotherapy* **45**:881-885.
100. **M'Zali, F. H., J. Heritage, D. M. Gascoyne-Binzi, A. M. Snelling, and P. M. Hawkey.** 1998. PCR single strand conformational polymorphism can be used to detect the gene encoding SHV-7 extended-spectrum beta-lactamase and to identify different SHV genes within the same strain. *Journal of Antimicrobial Chemotherapy* **41**:123-125.
  101. **Mabilat, C. and P. Courvalin.** 1990. Development of Oligotyping for Characterization and Molecular Epidemiology of Tem Beta-Lactamases in Members of the Family Enterobacteriaceae. *Antimicrobial Agents and Chemotherapy* **34**:2210-2216.
  102. **Martinsky, T.** 2003. Printing technologies and microarray manufacturing techniques: making the perfect microarray, p. 93-122. *In* E. Blalock (ed.), *A Beginner's Guide to Microarrays*. Kluwer Academic Publishers, New York.
  103. **Maskos, U. and E. M. Southern.** 1993. A novel method for the analysis of multiple sequence variants by hybridisation to oligonucleotides. *Nucleic Acids Research* **21**:2267-8.
  104. **Maskos, U. and E. M. Southern.** 1993. A novel method for the parallel analysis of multiple mutations in multiple samples. *Nucleic Acids Research* **21**:2269-70.
  105. **Maskos, U. and E. M. Southern.** 1993. A study of oligonucleotide reassociation using large arrays of oligonucleotides synthesised on a glass support. *Nucleic Acids Research* **21**:4663-9.
  106. **Matthew, M.** 1979. Plasmid-Mediated Beta-Lactamases of Gram-Negative Bacteria - Properties and Distribution. *Journal of Antimicrobial Chemotherapy* **5**:349-358.
  107. **Matthew, M., R. W. Hedges, and J. T. Smith.** 1979. Types of Beta-Lactamase Determined by Plasmids in Gram-Negative Bacteria. *Journal of Bacteriology* **138**:657-662.
  108. **Medeiros, A. A. and J. Crellin.** 1997. Comparative susceptibility of clinical isolates producing extended spectrum beta-lactamases to ceftibuten: Effect of large inocula. *Pediatric Infectious Disease Journal* **16**:S49-S55.
  109. **Meyer, K. S., C. Urban, J. A. Eagan, B. J. Berger, and J. J. Rahal.** 1993. Nosocomial Outbreak of Klebsiella Infection Resistant to Late-Generation Cephalosporins. *Annals of Internal Medicine* **119**:353-358.
  110. **Mikhailovich, V., S. Lapa, D. Gryadunov, A. Sobolev, B. Strizhkov, N. Chernyh, O. Skotnikova, O. Irtuganova, A. Moroz, V. Litvinov, M. Vladimirkii, M. Perelman, L. Chernousova, V. Erokhin, A. Zasedatelev, and A. Mirzabekov.** 2001. Identification of rifampin-resistant Mycobacterium tuberculosis strains by hybridization, PCR, and ligase detection reaction on oligonucleotide microchips. *Journal of Clinical Microbiology* **39**:2531-2540.



111. **Milner, N., K. U. Mir, and E. M. Southern.** 1997. Selecting effective antisense reagents on combinatorial oligonucleotide arrays. *Nature Biotechnology* **15**:537-541.
112. **Mir, K. U. and E. M. Southern.** 1999. Determining the influence of structure on hybridization using oligonucleotide arrays. *Nature Biotechnology* **17**:788-792.
113. **Moutereau, S., R. Narwa, C. Matheron, N. Vongmany, E. Simon, and M. Goossens.** 2004. An improved electronic microarray-based diagnostic assay for identification of MEFV mutations. *Human Mutation* **23**:621-628.
114. **Mzali, F. H., D. M. GascoyneBinzi, J. Heritage, and P. M. Hawkey.** 1996. Detection of mutations conferring extended-spectrum activity on SHV beta-lactamases using polymerase chain reaction single strand conformational polymorphism (PCR-SSCP). *Journal of Antimicrobial Chemotherapy* **37**:797-802.
115. **NCCLS.** 1999. Performance standards for antimicrobial susceptibility testing. National Committee for Clinical Laboratory Standards, Wayne, PA. M100-S9.
116. **Newton, C. R., A. Graham, L. E. Heptinstall, S. J. Powell, C. Summers, N. Kalsheker, J. C. Smith, and A. F. Markham.** 1989. Analysis of Any Point Mutation in Dna - the Amplification Refractory Mutation System (Arms). *Nucleic Acids Research* **17**:2503-2516.
117. **Niederhauser, C., L. Kaempf, and I. Heinzer.** 2000. Use of the ligase detection reaction-polymerase chain reaction to identify point mutations in extended-spectrum beta-lactamases. *European Journal of Clinical Microbiology & Infectious Diseases* **19**:477-480.
118. **Nikiforov, T. T., R. B. Rendle, P. Goelet, Y. H. Rogers, M. L. Kotewicz, S. Anderson, G. L. Trainor, and M. R. Knapp.** 1994. Genetic Bit Analysis - A Solid-Phase Method for Typing Single Nucleotide Polymorphisms. *Nucleic Acids Research* **22**:4167-4175.
119. **NueschInderbinen, M. T., H. Hächler, and F. H. Kayser.** 1996. Detection of genes coding for extended-spectrum SHV beta-lactamases in clinical isolates by a molecular genetic method, and comparison with the E test. *European Journal of Clinical Microbiology & Infectious Diseases* **15**:398-402.
120. **Ouellette, M., G. C. Paul, A. M. Philippon, and P. H. Roy.** 1988. Oligonucleotide Probes (Tem-1, Oxa-1) Versus Isoelectric-Focusing in Beta-Lactamase Characterization of 114 Resistant Strains. *Antimicrobial Agents and Chemotherapy* **32**:397-399.
121. **Pastinen, T., A. Kurg, A. Metspalu, L. Peltonen, and A. C. Syvanen.** 1997. Minisequencing: a specific tool for DNA analysis and diagnostics on oligonucleotide arrays. *Genome Research* **7**:606-14.
122. **Pastinen, T., M. Raitio, K. Lindroos, P. Tainola, L. Peltonen, and A. C. Syvanen.** 2000. A system for specific, high-throughput genotyping by allele-specific primer extension on microarrays. *Genome Research* **10**:1031-1042.

## References

---

123. **Paterson, D. L., K. M. Hujer, A. M. Hujer, B. Yeiser, M. D. Bonomo, L. B. Rice, and R. A. Bonomo.** 2003. Extended-spectrum beta-lactamases in *Klebsiella pneumoniae* bloodstream isolates from seven countries: dominance and widespread prevalence of SHV- and CTX-M-type beta-lactamases. *Antimicrobial Agents and Chemotherapy* **47**:3554-3560.
124. **Paterson, D. L., W. C. Ko, A. Von Gottberg, J. M. Casellas, L. Mulazimoglu, K. P. Klugman, R. A. Bonomo, L. B. Rice, J. G. McCormack, and V. L. Yu.** 2001. Outcome of cephalosporin treatment for serious infections due to apparently susceptible organisms producing extended-spectrum beta-lactamases: implications for the clinical microbiology laboratory. *Journal of Clinical Microbiology* **39**:2206-2212.
125. **Peterson, A. W., R. J. Heaton, and R. M. Georgiadis.** 2001. The effect of surface probe density on DNA hybridization. *Nucleic Acids Research* **29**:5163-5168.
126. **Peterson, A. W., L. K. Wolf, and R. M. Georgiadis.** 2002. Hybridization of mismatched or partially matched DNA at surfaces. *Journal of the American Chemical Society* **124**:14601-14607.
127. **Peytavi, R., L. Y. Tang, F. R. Raymond, K. Boissinot, L. Bissonnette, M. Boissinot, F. J. Picard, A. Huletsky, M. Ouellette, and M. G. Bergeron.** 2005. Correlation between microarray DNA hybridization efficiency and the position of short capture probe on the target nucleic acid. *Biotechniques* **39**:89-96.
128. **Proudnikov, D. and A. Mirzabekov.** 1996. Chemical methods of DNA and RNA fluorescent labeling. *Nucleic Acids Research* **24**:4535-4542.
129. **Randegger, C. C. and H. Hächler.** 2001. Real-time PCR and melting curve analysis for reliable and rapid detection of SHV extended-spectrum beta-lactamases. *Antimicrobial Agents and Chemotherapy* **45**:1730-1736.
130. **Randegger, C. C., A. Keller, M. Irla, A. Wada, and H. Hachler.** 2000. Contribution of natural amino acid substitutions in SHV extended-spectrum beta-lactamases to resistance against various beta-lactams. *Antimicrobial Agents and Chemotherapy* **44**:2759-2763.
131. **Randegger, C. C., A. Keller, M. Irla, A. Wada, and H. Hächler.** 2000. Contribution of natural amino acid substitutions in SHV extended-spectrum beta-lactamases to resistance against various beta-lactams. *Antimicrobial Agents and Chemotherapy* **44**:2759-2763.
132. **Rice, L. B., J. D. C. Yao, K. Klimm, G. M. Eliopoulos, and R. C. Moellering.** 1991. Efficacy of Different Beta-Lactams Against An Extended-Spectrum Beta-Lactamase-Producing *Klebsiella-Pneumoniae* Strain in the Rat Intraabdominal Abscess Model. *Antimicrobial Agents and Chemotherapy* **35**:1243-1244.
133. **Ronaghi, M., M. Uhlen, and P. Nyren.** 1998. A sequencing method based on real-time pyrophosphate. *Science* **281**:363-365.

134. **Roy, C., A. Foz, C. Segura, M. Tirado, C. Fuster, and R. Reig.** 1983. Plasmid-Determined Beta-Lactamases Identified in A Group of 204 Ampicillin-Resistant Enterobacteriaceae. *Journal of Antimicrobial Chemotherapy* **12**:507-510.
135. **Saiki, R. K., P. S. Walsh, C. H. Levenson, and H. A. Erlich.** 1989. Genetic-Analysis of Amplified Dna with Immobilized Sequence-Specific Oligonucleotide Probes. *Proceedings of the National Academy of Sciences of the United States of America* **86**:6230-6234.
136. **Samiotaki, M., M. Kwiatkowski, J. Parik, and U. Landegren.** 1994. Dual-Color Detection of Dna-Sequence Variants by Ligase-Mediated Analysis. *Genomics* **20**:238-242.
137. **Sanders, C. C., M. Peyret, E. S. Moland, S. J. Cavalieri, C. Shubert, K. S. Thomson, J. M. Boeufgras, and W. E. Sanders.** 2001. Potential impact of the VITEK 2 system and the advanced expert system on the clinical laboratory of a university-based hospital. *Journal of Clinical Microbiology* **39**:2379-2385.
138. **Sanders, C. C., M. Peyret, E. S. Moland, C. Shubert, K. S. Thomson, J. M. Boeufgras, and W. E. Sanders.** 2000. Ability of the VITEK 2 advanced expert system to identify beta-lactam phenotypes in isolates of Enterobacteriaceae and *Pseudomonas aeruginosa*. *Journal of Clinical Microbiology* **38**:570-574.
139. **SantaLucia, J.** 1998. A unified view of polymer, dumbbell, and oligonucleotide DNA nearest-neighbor thermodynamics. *Proceedings of the National Academy of Sciences of the United States of America* **95**:1460-1465.
140. **Schena, M., D. Shalon, R. W. Davis, and P. O. Brown.** 1995. Quantitative monitoring of gene expression patterns with a complementary DNA microarray. *Science* **270**:467-470.
141. **Schentag, J. J., J. M. Hyatt, J. R. Carr, J. A. Paladino, M. C. Birmingham, G. S. Zimmer, and T. J. Cumbo.** 1998. Genesis of methicillin-resistant *Staphylococcus aureus* (MRSA), how treatment of MRSA infections was selected for vancomycin-resistant *Enterococcus faecium*, and the importance of antibiotic management and infection control. *Clinical Infectious Diseases* **26**:1204-1214.
142. **Schiappa, D. A., M. K. Hayden, M. G. Matushek, F. N. Hashemi, J. Sullivan, K. Y. Smith, D. Miyashiro, J. P. Quinn, R. A. Weinstein, and G. M. Trenholme.** 1996. Ceftazidime-resistant *Klebsiella pneumoniae* and *Escherichia coli* bloodstream infection: A case-control and molecular epidemiologic investigation. *Journal of Infectious Diseases* **174**:529-536.
143. **Schwaber, M. J., P. M. Raney, J. K. Rasheed, J. W. Biddle, P. Williams, J. E. McGowan, and F. C. Tenover.** 2004. Utility of NCCLS guidelines for identifying extended-spectrum beta-lactamases in non-*Escherichia coli* and non-*Klebsiella* spp. of Enterobacteriaceae. *Journal of Clinical Microbiology* **42**:294-298.

## References

---

144. **Shchepinov, M. S., S. C. Case-Green, and E. M. Southern.** 1997. Steric factors influencing hybridisation of nucleic acids to oligonucleotide arrays. *Nucleic Acids Research* **25**:1155-61.
145. **Shchepinov, M. S., I. A. Udalova, A. J. Bridgman, and E. M. Southern.** 1997. Oligonucleotide dendrimers: synthesis and use as polylabelled DNA probes. *Nucleic Acids Research* **25**:4447-4454.
146. **Simpson, I. N., P. B. Harper, and C. H. Ocallaghan.** 1980. Principal Beta-Lactamases Responsible for Resistance to Beta-Lactam Antibiotics in Urinary-Tract Infections. *Antimicrobial Agents and Chemotherapy* **17**:929-936.
147. **Singh-Gasson, S., R. D. Green, Y. J. Yue, C. Nelson, F. Blattner, M. R. Sussman, and F. Cerrina.** 1999. Maskless fabrication of light-directed oligonucleotide microarrays using a digital micromirror array. *Nature Biotechnology* **17**:974-978.
148. **Sirot, D., J. Sirot, R. Labia, A. Morand, P. Courvalin, A. Darfeuillemichaud, R. Perroux, and R. Cluzel.** 1987. Transferable Resistance to 3Rd-Generation Cephalosporins in Clinical Isolates of *Klebsiella-Pneumoniae* - Identification of Ctx-1, A Novel Beta-Lactamase. *Journal of Antimicrobial Chemotherapy* **20**:323-334.
149. **Siu, L. K., P. L. Lu, P. R. Hsueh, F. M. Lin, S. C. Chang, K. T. Luh, M. Ho, and C. Y. Lee.** 1999. Bacteremia due to extended-spectrum beta-lactamase-producing *Escherichia coli* and *Klebsiella pneumoniae* in a pediatric oncology ward: Clinical features and identification of different plasmids carrying both SHV-5 and TEM-1 genes. *Journal of Clinical Microbiology* **37**:4020-4027.
150. **Sosnowski, R. G., E. Tu, W. F. Butler, J. P. O'Connell, and M. J. Heller.** 1997. Rapid determination of single base mismatch mutations in DNA hybrids by direct electric field control. *Proceedings of the National Academy of Sciences of the United States of America* **94**:1119-23.
151. **Southern, E., K. Mir, and M. Shchepinov.** 1999. Molecular interactions on microarrays. *Nature Genetics* **21**:5-9.
152. **Southern, E. M.** 1975. Detection of Specific Sequences Among Dna Fragments Separated by Gel-Electrophoresis. *Journal of Molecular Biology* **98**:503-&.
153. **Southern, E. M.** 2001. DNA Microarrays: History and Overview, *In* J. B. Rampal (ed.), *DNA Arrays: Methods and Protocols*. Humana Press Inc., Totowa, NJ.
154. **Southern, E. M., U. Maskos, and J. K. Elder.** 1992. Analyzing and comparing nucleic acid sequences by hybridization to arrays of oligonucleotides: evaluation using experimental models. *Genomics* **13**:1008-17.
155. **Speldooren, V., B. Heym, R. Labia, and M. H. Nicolas-Chanoine.** 1998. Discriminatory detection of inhibitor-resistant beta-lactamases in *Escherichia*

- coli by single-strand conformation Polymorphism-PCR. *Antimicrobial Agents and Chemotherapy* **42**:879-884.
156. **Spratt, B. G.** 1994. Resistance to antibiotics mediated by target alterations. *Science* **264**:388-393.
157. **Stears, R. L., T. Martinsky, and M. Schena.** 2003. Trends in microarray analysis. *Nature Medicine* **9**:140-145.
158. **Steward, C. D., D. Wallace, S. K. Hubert, R. Lawton, S. K. Fridkin, R. P. Gaynes, J. E. McGowan, and F. C. Tenover.** 2000. Ability of laboratories to detect emerging antimicrobial resistance in nosocomial pathogens: a survey of Project ICARE laboratories. *Diagnostic Microbiology and Infectious Disease* **38**:59-67.
159. **Syvanen, A. C.** 1999. From gels to chips: "Minisequencing" primer extension for analysis of point mutations and single nucleotide polymorphisms. *Human Mutation* **13**:1-10.
160. **Szabo, D., Z. Filetoth, J. Szentandrassy, M. Nemedi, E. Toth, C. Jeney, G. Kispal, and F. Rozgonyi.** 1999. Molecular epidemiology of a cluster of cases due to *Klebsiella pneumoniae* producing SHV-5 extended-spectrum beta-lactamase in the premature intensive care unit of a Hungarian hospital. *Journal of Clinical Microbiology* **37**:4167-4169.
161. **Taton, T., C. Mirkin, and R. Letsinger.** 2000. Scanometric DNA array detection with nanoparticle probes. *Science* **289**:1757-1760.
162. **Tecan.** 2005. Application Note: HS 4800 Microarray Hybridization - A comparison of manual and automated methods with a focus on homogeneity and reproducibility. <http://www.tecan.com/>.
163. **Tenover, F. C., M. J. Mohammed, T. S. Gorton, and Z. F. Dembek.** 1999. Detection and reporting of organisms producing extended-spectrum beta-lactamases: Survey of laboratories in Connecticut. *Journal of Clinical Microbiology* **37**:4065-4070.
164. **Tenover, F. C., M. J. Mohammed, J. Stelling, T. O'Brien, and R. Williams.** 2001. Ability of laboratories to detect emerging antimicrobial resistance: Proficiency testing and quality control results from the World Health Organization's External Quality Assurance System for Antimicrobial Susceptibility Testing. *Journal of Clinical Microbiology* **39**:241-250.
165. **Tenover, F. C., P. M. Raney, P. P. Williams, J. K. Rasheed, J. W. Biddle, A. Oliver, S. K. Fridkin, L. Jevitt, and J. E. McGowan.** 2003. Evaluation of the NCCLS extended-spectrum beta-lactamase confirmation methods for *Escherichia coli* with isolates collected during project ICARE. *Journal of Clinical Microbiology* **41**:3142-3146.
166. **Tham, T. N., C. Mabilat, P. Courvalin, and J. L. Guesdon.** 1990. Biotinylated Oligonucleotide Probes for the Detection and the Characterization of Tem-Type Extended Broad-Spectrum Beta-Lactamases in Enterobacteriaceae. *Fems Microbiology Letters* **69**:109-115.

## References

---

167. **Tham, T. N., C. Mabilat, P. Courvalin, and J. L. Guesdon.** 1990. Biotinylated Oligonucleotide Probes for the Detection and the Characterization of Tem-Type Extended Broad-Spectrum Beta-Lactamases in Enterobacteriaceae. *Fems Microbiology Letters* **69**:109-115.
168. **ThauvinEliopoulos, C., M. F. Tripodi, R. C. Moellering, and G. M. Eliopoulos.** 1997. Efficacies of piperacillin-tazobactam and cefepime in rats with experimental intra-abdominal abscesses due to an extended-spectrum beta-lactamase-producing strain of *Klebsiella pneumoniae*. *Antimicrobial Agents and Chemotherapy* **41**:1053-1057.
169. **Thomson, K. S.** 2001. Controversies about extended-spectrum and AmpC beta-lactamases. *Emerging Infectious Diseases* **7**:333-336.
170. **Tillib, S. V. and A. D. Mirzabekov.** 2001. Advances in the analysis of DNA sequence variations using oligonucleotide microchip technology. *Current Opinion in Biotechnology* **12**:53-8.
171. **Troesch, A., H. Nguyen, C. G. Miyada, S. Desvarenne, T. R. Gingeras, P. M. Kaplan, P. Cros, and C. Mabilat.** 1999. Mycobacterium species identification and rifampin resistance testing with high-density DNA probe arrays. *Journal of Clinical Microbiology* **37**:49-55.
172. **Uehara, H., G. Nardone, I. Nazarenko, and R. J. Hohman.** 1999. Detection of telomerase activity utilizing energy transfer primers: Comparison with gel- and ELISA-Based detection. *Biotechniques* **26**:552-558.
173. **Vanecko, S. and M. Laskowski.** 1961. Studies of the specificity of deoxyribonuclease I. III. Hydrolysis of chains carrying a monoesterified phosphate on carbon 5'. *Journal of Biological Chemistry* **236**:3312-3316.
174. **Vatopoulos, A. C., A. Philippon, L. S. Tzouveleakis, Z. Komninou, and N. J. Legakis.** 1990. Prevalence of A Transferable Shv-5 Type Beta-Lactamase in Clinical Isolates of *Klebsiella-Pneumoniae* and *Escherichia-Coli* in Greece. *Journal of Antimicrobial Chemotherapy* **26**:635-648.
175. **Volokhov, D., V. Chizhikov, K. Chumakov, and A. Rasooly.** 2003. Microarray analysis of erythromycin resistance determinants. *Journal of Applied Microbiology* **95**:787-798.
176. **Waley, S. G.** 1992. Beta-lactamases: mechanism of action, p. 198-222. *In* M.I.Page (ed.), *The chemistry of beta lactams*. A. and P. Blackie, London.
177. **Walsh, C.** 2000. Molecular mechanisms that confer antibacterial drug resistance. *Nature* **406**:775-781.
178. **Wang, D. G., J. B. Fan, C. J. Siao, A. Berno, P. Young, R. Sapolsky, G. Ghandour, N. Perkins, E. Winchester, J. Spencer, L. Kruglyak, L. Stein, L. Hsie, T. Topaloglou, E. Hubbell, E. Robinson, M. Mittmann, M. S. Morris, N. P. Shen, D. Kilburn, J. Rioux, C. Nusbaum, S. Rozen, T. J. Hudson, R. Lipshutz, M. Chee, and E. S. Lander.** 1998. Large-scale identification, mapping, and genotyping of single-nucleotide polymorphisms in the human genome. *Science* **280**:1077-1082.

179. **Westin, L., C. Miller, D. Vollmer, D. Canter, R. Radtkey, M. Nerenberg, and J. P. O'Connell.** 2001. Antimicrobial resistance and bacterial identification utilizing a microelectronic chip array. *Journal of Clinical Microbiology* **39**:1097-104.
180. **Winokur, P. L., R. Canton, J. M. Casellas, and N. Legakis.** 2001. Variations in the prevalence of strains expressing an extended-spectrum beta-lactamase phenotype and characterization of isolates from Europe, the Americas, and the Western Pacific region. *Clinical Infectious Diseases* **32 Suppl 2**:S94-103.
181. **Witte and Mielke.** 2003. Beta-Laktamasen mit breitem Wirkungsspektrum. *Bundesgesundheitsblatt - Gesundheitsforschung-Gesundheitsschutz* 881-890.
182. **Yershov, G., V. Barsky, A. Belgovskiy, E. Kirillov, E. Kreindlin, I. Ivanov, S. Parinov, D. Guschin, A. Drobishev, S. Dubiley, and A. Mirzabekov.** 1996. DNA analysis and diagnostics on oligonucleotide microchips. *Proceedings of the National Academy of Sciences of the United States of America* **93**:4913-4918.
183. **Yu, X., M. Susa, C. Knabbe, R. D. Schmid, and T. T. Bachmann.** 2004. Development and Validation of a Diagnostic DNA Microarray To Detect Quinolone-Resistant *Escherichia coli* among Clinical Isolates. *Journal of Clinical Microbiology* **42**:4083-4091.
184. **Yu, X.** 2004. Entwicklung eines diagnostischen DNS-Mikroarrays zur Genotypisierung der Chinolon-Resistenz von *Escherichia coli* Stuttgart, Universität Stuttgart, Dissertation, <http://elib.uni-stuttgart.de/opus/volltexte/2004/1963/>.
185. **Yue, H., P. Eastman, B. Wang, J. Minor, M. Doctolero, R. Nuttall, R. Stack, J. Becker, J. Montgomery, M. Vainer, and R. Johnston.** 2001. An evaluation of the performance of cDNA microarrays for detecting changes in global mRNA expression. *Nucleic Acids Research* **29**:E41-1.

## 6 Appendix

### 6.1 List of abbreviations

A, G, C, T	Adenine, Guanine, Cytosine, Thymine
AmpC	name of beta lactamase
APEX	arrayed primer extension
APS	ammonium persulfate
ASPE	allele specific primer extension
a. u.	arbitrary unit
BAL	bronchoalveolar lavage
BLAST	basic local alignment tool
BES	name of beta-lactamase
bp	base pair
CCD	charge-coupled device
CFU	colony forming unit
CME	name of beta-lactamase
CMY	name of beta-lactamase
CTX-M	cefotaxime resistant (beta-lactamase)
Cy	cyanin dye
ddH <sub>2</sub> O	double distilled water
ddNTP	dideoxynucleotidetriphosphate
DMSO	dimethylsulfoxide
DNA	desoxyribonucleic acid
dNTP	desoxynucleotidetriphosphate
dsDNA	double stranded DNA
EARSS	European Antibiotic Resistance Surveillance System
EAT	Eppendorf Array Technology
<i>E. amnigenus</i>	<i>Enterobacter amnigenus</i>
<i>E. cloacae</i>	<i>Enterobacter cloacae</i>
<i>E. coli</i>	<i>Escherichia coli</i>
EDTA	ethylenediaminetetraacetate
EGTA	ethylene glycol bis(2-aminoethyl ether)-N,N,N',N'-tetraacetic acid
ESBL	extended spectrum beta-lactamase
FEC	name of beta-lactamase
FDA	US Food and Drug Administration
FOX	name of beta-lactamase
ΔG	free energy
GES	name of beta-lactamase
h	hour
HPLC	high performance liquid chromatography
ID limit	identification limit
ICU	intensive care unit
IRT	inhibitor resistant TEM (beta-lactamase)
K1	name of beta lactamase
kb	kilobase
<i>K. oxytoca</i>	<i>Klebsiella oxytoca</i>
<i>K. ornithinolytica</i>	<i>Klebsiella ornithinolytica</i>
<i>K. pneumoniae</i>	<i>Klebsiella pneumoniae</i>
<i>K. terrigena</i>	<i>Klebsiella terrigena</i>
MALDI-TOF	matrix assisted laser desorption/ionization-time of flight detector
MEN	name of beta-lactamase
MIC	minimum inhibitory concentration
min	minute
MM	mismatch
MT	mutant
NCCLS	National Committee for Clinical Laboratory Standards
NI	net intensity
NRCA	National Research Center for Antibiotic Resistance, Moscow



---

n. s.	no specification
NT/F	number of nucleotides per fluorophore
ORF	open reading frame
OXA	oxacillin resistant (beta-lactamase)
OXY	name of beta-lactamase
PBP	penicillin binding protein
PCR	polymerase chain reaction
PER	name of beta-lactamase
PSE	name of beta-lactamase
PLL	poly-L-lysine
PM	perfect match
<i>P. mirabilis</i>	<i>Proteus mirabilis</i>
PMT	photomultiplier
PNA	peptide nucleic acid
RFLP	restriction fragment length polymorphism
RI	relative intensity
RI <sub>MM</sub>	relative intensity of the mismatch
RI <sub>PM</sub>	relative intensity of the perfect match
RNA	ribonucleic acid
rRNA	ribosomal RNA
SDA	strand displacement amplification
SDS	sodium dodecyl sulfate
SFO	name of beta-lactamase
SHV	sulphydryl variable (beta-lactamase)
SI	specific intensity
SNP	single nucleotide polymorphism
SSC	sodium chloride sodium citrate buffer
SSCP	single strand conformational polymorphism
ssDNA	single stranded DNA
SSPE	sodium chloride sodium phosphate EDTA buffer
STR	short tandem repeats
TAE	Tris acetate EDTA buffer
TE	Tris EDTA buffer
TEM	Temoniera (name of beta-lactamase)
TLA	name of beta-lactamase
T <sub>m</sub>	melting temperature
TPase	transpeptidase
Tris	Tris-(hydroxymethyl) aminomethan
U	unit
UK	United Kingdom
US	United States
UV	ultra violet
VEB	name of beta-lactamase
WT	wild type

### 6.2 Acknowledgements

I would like to thank Prof. Rolf D. Schmid for providing this interesting project and the opportunity to work in his institute with an excellent equipment, as well as for his help and motivational support during the whole time.

A special thanks goes to my supervisor PD Dr. Till T. Bachmann for my introduction into the subject, his untiring support, scientific advice and help for writing this thesis and publications, as well as the management of an inspiring and agreeable working group.

I would also like to thank Beate Rössle-Lorch for proofreading, as well as scientific discussions, her readiness to help and good work together.

I thank Dirk Leinberger for the agreeable work together, discussions and his support for creating some of the images displayed in this thesis.

A special thanks goes also to all the present and former lab members, with whom I had the opportunity to work: Dr. Xiao Lei Yu, Dr. Holger Schulze, Jutta Secker, Marco Hofmann, Susanne Münch, Carolina Soekmadji, Kristina Knösche, Timo Barl, Katja Kurr, Dr. Flaubert Mbeunkui, Stefanie Häfele. They were always helpful, ready to give good advice and made my stay in the lab an enjoyable experience.

I would like to thank Dr. Satoshi Ezaki for the introduction into the subject and the work preceding this study, which paved the way for the development of the here presented arrays.

I also want to thank Christina Onaca, whose work accomplished within the scope of a Studienarbeit delivered some data for this thesis and Marlies Fischer for an agreeable time of work together during her Studienarbeit.

This work was done in cooperation with academic and industry partners. Therefore, I would like to thank Prof. Dr. Cornelius Knabbe, Dr. Milorad Susa and Jan Weile, the coworkers at the Robert-Bosch Hospital in Stuttgart, for performing the phenotypic testing, support of the strain collection and providing advice concerning the clinical microbiology point of view.

My thanks go also to Prof Dr. Witte and coworkers at the Wernigerode branch of the Robert Koch Institute for delivering reference strains and knowledge regarding importance and prevalence of diverse antibiotic resistance traits.

I thank PD Dr. Wolfgang Ludwig and Katharina Fichtl for providing access to a method for the species-specific enrichment of pathogenic bacteria in order to test a combination with the resistance arrays.

I thank the industry partner Eppendorf AG, who supported this work with technical equipment and promotes the transfer of the developments to a marketable format.

I also thank Maya Rubtsova from the National Research Center for Antibiotics in Moscow, Russia for her work on the CTX-M-array, which is an important step for the development of a complete ESBL-chip.

Since this thesis was accomplished at the Insitute of Technical Biochemistry within the scope of the GenoMik (Genome research on microorganisms) project, I would like to thank the BMBF for funding this work.

Furthermore, I would like to thank my parents and my husband Thomas for their irreplaceable help, patience and support during my whole time of studies.

### **6.3 Curriculum Vitae**

Surname: Grimm, née Jung  
First names: Verena, Ulrike  
Date of Birth: 21 November 1975  
Place of Birth: Herten in Westfalen  
Marital status: married  
Nationality: German

#### **Education/Studies**

- Nov. 01 - Oct. 05    **Doctorate**  
***Institute of Technical Biochemistry,  
University of Stuttgart, Prof. R. D. Schmid***  
Development of a diagnostic microarray for the rapid detection of Extended Spectrum Beta-Lactamases for the use in clinical microbiology
- Jan. 01 - Sept. 01    **Diplomarbeit**  
***Department of Microbiology and Immunology,  
University of Michigan USA, Prof. M. Imperiale***  
Development of Adeno-Associated Virus Vectors for gene therapy of the nervous system
- Sept. 98 - Sept. 01    **Preparation of a trinational diploma in Biotechnology**  
***at the Ecole Supérieure de Biotechnologie de Strasbourg***  
Degree: Diplôm d'Ingénieur en Biotechnologie,  
Diplôm Biotechnologin  
***conferred by the European Confederation of the  
University Louis Pasteur in Strasbourg (France),  
University of Basel (Switzerland), Freiburg and Karlsruhe  
(Germany)***
- Sept. 95 - May 98    **Vordiplom in Chemistry**  
***University of Karlsruhe***
- Sept. 86 - Jun. 95    **Abitur**  
***Städtisches Gymnasium Herten, Westfalen***
- Sept. 82 - Jul. 86    **Primary school**  
***Comenius Grundschule in Herten, Westfalen***

#### **6.4 Declaration**

Herewith I declare that the presented work was accomplished independently and only by the use of the specified resources and literature.

Stuttgart, 12 October 2005